MRI MEASURES OF NEURODEGENERATION AS BIOMARKERS OF ALZHEIMER'S DISEASE

Shannon Leigh Risacher

Submitted to the faculty of the University Graduate School
in partial fulfillment of the requirements
for the degree
Doctor of Philosophy
in the Department of Medical Neuroscience,
Indiana University

December 2011

Accepted by the Faculty of Indiana University, in partial fulfillment of the requirements for the degree of Doctor of Philosophy.

Doctoral Committee

Li Shen, PhD, Chair

Martin R. Farlow, MD

Sujuan Gao, PhD

Brenna C. McDonald, PsyD, MBA

November 30, 2011

Andrew J. Saykin, PsyD

Karmen K. Yoder, PhD

Acknowledgements

This work was supported by: the National Institutes of Health (NIH) Clinical and Translational Science Institute (CTSI) Pre-doctoral Training Grant to Shannon L. Risacher (Training Grant TL1 RR025759); NIH grants (R01 AG19771 and R01 CA101318) to Dr. Andrew J. Saykin (AJS); a National Institute on Aging (NIA) Core Supplement to Drs. Bernardino Ghetti and AJS (P30 AG10133-18S1); the Alzheimer's Association (IIRG-99-1653 from the Hedco Foundation to AJS); the Indiana Economic Development Corporation (IEDC #87884 to AJS); NIH/National Center for Research Resources CTSI grants (U54 RR025761 and C06-RR020128); a National Institute of Biomedical Imaging and Bioengineering grant (R03 EB008674) to Dr. Li Shen; and an investigator-initiated grant from Welch Allyn/Blue Highway, Inc (to AJS). In addition, support for education of Ms. Risacher was provided by the Medical Neuroscience Department, the Stark Neurosciences Research Institute, and the Department of Radiology and Imaging Sciences at the Indiana University School of Medicine.

Funding for the Alzheimer's Disease Neuroimaging Initiative (ADNI; Principal Investigator: Michael Weiner), including data collection and sharing, is provided by the National Institutes of Health (NIH grants U01 AG024904 and RC2 AG036535). Additional support for ADNI comes from the National Institute on Aging, the National Institute of Biomedical Imaging and Bioengineering, and generous contributions from the following: Abbott; AstraZeneca AB; Bayer Schering Pharma AG; Bristol-Myers Squibb; Eisai Global Clinical Development; Elan Corporation; Genentech; GE Healthcare; GlaxoSmithKline; Innogenetics; Johnson and Johnson; Eli Lilly and Co.; Medpace; Inc.; Merck and Co., Inc.; Novartis AG; Pfizer Inc.; F. Hoffman-La Roche; Schering-Plough, Synarc, Inc.; and Wyeth; as well as non-profit partners the Alzheimer's Association and Alzheimer's Drug Discovery Foundation, with participation from the U.S. Food and Drug Administration. Private sector contributions to ADNI are facilitated by the Foundation for the National Institutes of Health (www.fnih.org). The grantee organization is the Northern California Institute for Research and Education, and the study is coordinated by the Alzheimer's Disease Cooperative Study at the

University of California, San Diego. ADNI data are disseminated by the Laboratory for Neuro Imaging at the University of California, Los Angeles. This research was also supported by NIH grants P30 AG010129, K01 AG030514, and the Dana Foundation. The National Cell Repository for Alzheimer's Disease (NIH grant U24 AG021886) provided support for DNA and cell line banking and processing for ADNI.

The author gratefully acknowledges the assistance and support of her primary mentor, Andrew J. Saykin, PsyD, as well as the other members of her dissertation committee: Li Shen, PhD, Chair; Martin R. Farlow, MD; Sujuan Gao, PhD; Brenna C. McDonald, PsyD, MBA; and, Karmen K. Yoder, PhD. In addition, the author would like to thank the following individuals for their assistance with the included works and additional support: Daniel S. Albrecht; Vivian Arnold; Laurell A. Beckett, PhD; Kim Campbell; Aaron Cannon; R. Andrew Chambers, MD; Susan K. Conroy; Joshua R. Curtain; Mario Dzemidzic, PhD; Jessica J. Englert, PhD; Hiram Firpi, PhD; Laura A. Flashman, PhD; Bernardino Ghetti, MD; Charles Goodlett, PhD; Danielle J. Harvey, PhD; Christine Herring; Cynthia Hingtgen, MD, PhD; Kelly Holohan; Gary D. Hutchins, PhD; Mark Inlow, PhD; Clifford R. Jack Jr., MD; David Kareken, PhD; Sungeun Kim, PhD; Tamiko R. MaGee, MS; Evan D. Morris, PhD; Richard W. Newman, MS; Kwangsik Nho, PhD; Grant D. Nicol, PhD; Marc D. Normandin, PhD; Darren P. O'Neill; Gerry S. Oxford, PhD; Nadia Paré, PhD; Susan M. Pepin, MD; Heather S. Pixley, MBA; Laura A. Rabin, PhD; Vijay Ramanan; Robert B. Santulli, MD; Eben Schwartz, PhD; Dori Smith; Lindsey Stickans, MS; Jenna M. Sullivan; Shanker Swaminathan; Vanessa Taler, PhD; Fred W. Unvergazt, PhD; Jin Wan; Yang Wang, MD; Michael W. Weiner, MD; John D. West, MS; Heather A. Wishart, PhD; and, Darrell WuDunn, MD, PhD.

The Freesurfer analyses were performed on a 112-node parallel computing environment called Quarry at Indiana University. The author thanks the University Information Technology Services at Indiana University and Randy Heiland, MA, MS for their support. The author also thanks Nick Schmansky, MA, MSc and Bruce Fischl, PhD of Harvard Medical School for assistance with

Freesurfer. The author also gratefully acknowledges the help of the ophthalmology technicians at Indiana University School of Medicine (Linda Morgan, CCRC and Joni Hoop, CCRC, COA) and Dartmouth-Hitchcock Medical Center (Kimberly McQuaid, COMT) for assistance with the FDT exams (Chapter 3); Dr. Katherine Nutter-Upham and Margaret Nordstrom for assistance with cognitive assessment and cohort follow-up (Chapters 2b and 3); and Drs. Edward O'Neil and Greg Gdowski of Blue Highway, LLC, a subsidiary of Welch Allyn, Inc (Chapter 3). In addition, the author thanks all participants and caregivers from the Alzheimer's Disease Neuroimaging Initiative (ADNI), as well as the Memory and Aging Projects in New England and Indiana (Chapters 2b and 3), without whom these studies would not have been possible.

Finally, the author thanks her family and friends for their support, without whom these projects would not have been possible. In particular, the author gratefully acknowledges the support and assistance of Katherine A. Risacher, Martin E. Risacher, Duane M. Klueh, Mary Alice Klueh, Melissa A. Quinn, and Taylor C. Williams.

Informed consent was obtained from all participants in this project. For the ADNI projects (Chapters 1 and 2a), necessary approval was received from Ethical Committees by each of the participating research institutions. Further information about ADNI can be found at www.adni-info.org. For the projects at Dartmouth-Hitchcock Medical Center and Indiana University School of Medicine (Chapters 2b and 3), approval was received from the appropriate Ethical Committees at these two research institutions.

Abstract

Shannon Leigh Risacher

MRI MEASURES OF NEURODEGENERATION AS BIOMARKERS OF ALZHEIMER'S DISEASE

Alzheimer's disease (AD) is the most common age-related neurodegenerative disease. Many researchers believe that an effective AD treatment will prevent the development of disease rather than treat the disease after a diagnosis. Therefore, the development of tools to detect AD-related pathology in early stages is an important goal. In this report, MRI-based markers of neurodegeneration are explored as biomarkers of AD. In the first chapter, the sensitivity of cross-sectional MRI biomarkers to neurodegenerative changes is evaluated in AD patients and in patients with a diagnosis of mild cognitive impairment (MCI), a prodromal stage of AD. The results in Chapter 1 suggest that cross-sectional MRI biomarkers effectively measure neurodegeneration in AD and MCI patients and are sensitive to atrophic changes in patients who convert from MCI to AD up to 1 year before clinical conversion. Chapter 2 investigates longitudinal MRI-based measures of neurodegeneration as biomarkers of AD. In Chapter 2a, measures of brain atrophy rate in a cohort of AD and MCI patients are evaluated; whereas in Chapter 2b, these measures are assessed in a pre-MCI stage, namely older adults with cognitive complaints (CC) but no significant deficits. The results from Chapter 2 suggest that dynamic MRI-

based measures of neurodegeneration are sensitive biomarkers for measuring progressive atrophy associated with the development of AD. In the final chapter, a novel biomarker for AD, visual contrast sensitivity, was evaluated. The results demonstrated contrast sensitivity impairments in AD and MCI patients, as well as slightly in CC participants. Impaired contrast sensitivity was also shown to be significantly associated with known markers of AD, including cognitive impairments and temporal lobe atrophy on MRI-based measures. The results of Chapter 3 support contrast sensitivity as a potential novel biomarker for AD and suggest that future studies are warranted. Overall, the results of this report support MRI-based measures of neurodegeneration as effective biomarkers for AD, even in early clinical and preclinical disease stages. Future therapeutic trials may consider utilizing these measures to evaluate potential treatment efficacy and mechanism of action, as well as for sample enrichment with patients most likely to rapidly progress towards AD.

Li Shen, PhD, Chair

Table of Contents

List of Tables

List of Figures

List of Abbreviations

Aβ	amyloid-beta peptide
$A\beta_{40}$	amyloid-beta peptide, 40 amino acids
$A\beta_{42}$	amyloid-beta peptide, 42 amino acids
AChE	acetylcholinesterase
AD	Alzheimer's disease
AD-C	AD-clinical
AD-P	AD-pathophysiology
ADNI	Alzheimer's Disease Neuroimaging Initiative
ANCOVA	analysis of covariance
ANOVA	analysis of variance
APC	annual(ized) percent change
APOE/ApoE	apolipoprotein E
APOE ε2	apolipoprotein E epsilon 2 allele
APOE ε3	apolipoprotein E epsilon 3 allele
APOE ε4	apolipoprotein E epsilon 4 allele
APOE4+	positive for one or more *APOE* epsilon 4 alleles
APP	amyloid precursor protein
AUC	area under the curve
BL	baseline
BNT	Boston Naming Test
BSI	boundary shift integral
CaMKII	calcium and calmodulin-dependent kinase-II
CC	older adults with cognitive complaints but no cognitive deficits
CC-C	CC to MCI converters
CC-S	participants with a stable CC diagnosis
cdk5	cyclin dependent protein kinase-5
CDR	Clinical Dementia Rating scale
CDR-GL	CDR Global score
CDR-SB	CDR Sum of Boxes
CSF	cerebrospinal fluid

CTSI	Clinical and Translational Science Institute
Cu	copper
CVLT	California Verbal Learning Test-II
CVLT-SD	CVLT short delay recall score
CVLT-LD	CVLT long delay recall score
dB	decibels
DHMC	Dartmouth-Hitchcock Medical Center
DMN	default mode network
DRS	Mattis Dementia Rating Scale-2
DTI	diffusion tensor imaging
DWI	diffusion weighted imaging
EC	entorhinal cortex
ERK	extracellular signal-related kinase
F	female
FAQ	Functional Assessment Questionnaire
FDA	Food and Drug Administration
FDG	fluoro-deoxyglucose
FDR	false discovery rate
FDT	frequency doubling technology
Fe	iron
fMRI	functional magnetic resonance imaging
FSE/TSE	fast spin echo/turbo spin echo
FWE	family-wise error correction
FWHM	full width at half maximum
GDS	Geriatric Depression Scale
GLM	general linear model
GM	grey matter
GMD	grey matter density
GMDens	grey matter density
GMVol	grey matter volume
GM Density	grey matter density

GM Volume	grey matter volume
GSK3	glycogen synthase kinase-3
HC	healthy older adults
Hz	Hertz
ICV	intracranial volume
IDE	insulin-degrading enzyme
IEDC	Indiana Economic Development Corporation
IL-6	interleukin 6
IL-8	interleukin 8
IOP	intraocular pressure
IUSM	Indiana University School of Medicine
k	minimum cluster size (in voxels)
L	left
LGN	lateral geniculate nucleus
LM	Wechsler Memory Scale-III Logical Memory
LOAD	late-onset Alzheimer's disease
LTL	lateral temporal lobe
M	male
MAPK	mitogen-activated protein kinase
MCI	mild cognitive impairment
MCI-C	MCI to probable AD converters
MCI-S	patients with a stable MCI diagnosis
MMSE	Mini-Mental Status Exam
MNI	Montreal Neurologic Institute
mod. VBM	modulated voxel-based morphometry
MP-RAGE	magnetization prepared rapid acquisition gradient echo
MRI	magnetic resonance imaging
MTA	medial temporal atrophy
MTL	medial temporal lobe
NCRR	National Center for Research Resources
NFT	neurofibrillary tangles

NIA	National Institute on Aging
NIBIB	National Institute of Biomedical Imaging and Bioengineering
NIH	National Institutes of Health
NPI-Q	Neuropsychiatric Inventory Questionnaire
NS	not significant
OCT	optical coherence tomography
PET	positron emission tomography
PI	principal investigator
PiB	Pittsburgh Compound B
PS1	presenilin 1
PS2	presenilin 2
PSD95	post-synaptic density 95
QC	quality control
R	right
RAVLT	Rey Auditory Verbal Learning Test
RGC	retinal ganglion cells
ROC	receiver operating characteristic
ROI(s)	region(s) of interest
ROS	reactive oxygen species
SE	standard error of the mean
SPGR	spoiled gradient recalled acquisition
SPM5	Statistical Parametric Mapping 5
TBM	tensor-based morphometry
TE	echo time
TI	inversion time
TL	temporal lobe
TNF-α	tumor necrosis factor alpha
TR	repetition time
URVF	upper right visual field quadrant
unc.	uncorrected for multiple comparisons
VBM	voxel-based morphometry

VF	visual field
VOI(s)	volume(s) of interest
WCST	Wisconsin Card Sorting Task
WM	white matter
WMS-III	Wechsler Memory Scale-III
ZEST	Zippy Estimate of Sequential Testing
Zn	zinc
1.5T	1.5 Tesla
2yr Chg	Two-year change
3.0T	3.0 Tesla

Introduction

Alzheimer's disease (AD) is the most common form of age-related dementia. As of 2000, nearly 25 million individuals world-wide, aged 60 or older, suffered from AD and that number is expected to more than double by 2030 [1]. Age is the primary predictor of AD, so as the proportion of the world population over the age of 65 years continues to grow, the rate of AD will expand rapidly. As of 2000, the annual cost for AD-related treatment and care in the United States was over $100 billion [2]. In addition to the social and economic implications of AD, this devastating disorder robs millions of older adults of their memories, ability to function independently, and ultimately their lives. Currently no treatments effectively target the underlying pathology associated with AD. Effective therapies which ameliorate or prevent the effects of AD would not only provide relief to millions of AD patients and their families, but would also potentially prevent an economic and social crisis which is likely to occur in the upcoming decades if this disease is allowed to grow unchecked.

The most common form of AD is sporadic or late-onset AD (LOAD) which primarily affects people over the age of 65 years. Less than 5% of AD cases are caused by dominantly inherited mutations in three genes, including the amyloid precursor protein (APP) gene, and presenilin 1 and 2 (PS1, PS2) genes [3]. Dominantly inherited or "familial" forms of AD typically show earlier onset (<60 years) than LOAD. Genetic factors are also likely to be important in LOAD. Apolipoprotein E (*APOE*) is the most commonly reported genetic variation associated with LOAD. Patients with an *APOE* epsilon 4 (ε4) allele are predisposed to developing LOAD, with a five-fold increased risk in patients with 1 ε4 allele and an even higher risk in patients with 2 ε4 alleles relative to patients with 2 epsilon 3 (ε3) alleles [3-5]. On the other hand, the *APOE* epsilon 2 (ε2) allele is thought to be protective against the development of AD [6]. Numerous other candidate genes have also been identified for AD (see http://www.alzgene.org for an updated list of candidate genes). Future developments in the genetic basis of LOAD are likely to play an important role in early diagnosis.

Neurobiology and Neuropathology of AD

Both the inherited and sporadic forms of AD feature two neuropathological hallmarks: amyloid plaques and neurofibrillary tangles (NFT). Amyloid plaques are extracellular aggregations of the amyloid-beta (Aβ) peptide that are found throughout the AD brain. Aβ is formed from processing of APP, a transmembrane protein thought to function as a cell surface receptor. Cleavage of APP by β-secretase, followed by γ-secretase, results in the formation of the Aβ peptide, which can be 36 to 42 amino acids in length. The most common forms of Aβ are 40 and 42 amino acids long ($A\beta_{40}$ and $A\beta_{42}$). As levels of Aβ increase in preclinical and clinical AD, the Aβ peptide aggregates into dimers and oligomers as a cross-linked β-sheet, with the $A\beta_{42}$ form most likely to show aggregation. Aβ oligomers are thought to be a major neurotoxic species in the brains of patients with AD [7-9]. Ultimately, Aβ oligomers and soluble fragments become large fibrils, which further aggregate to form insoluble deposits in the extracellular space, including small diffuse plaques and dense core plaques, which are a hallmark of AD neuropathology. Insoluble Aβ plaques may also be neurotoxic, although the mechanisms by which this occurs are still not fully understood.

Aβ is catabolized by a number of enzymes, including insulin-degrading enzyme (IDE), neprilsyn, and endothelin-converting enzyme. Aβ is also cleared by the brain immune cells, including astrocytes and microglia [10-12]. Recent studies suggest that while familial forms of AD show Aβ accumulation due to overproduction, accumulation of Aβ in LOAD may result primarily from imbalanced or ineffective Aβ clearance [13-14]. Interestingly, apolipoprotein E has also been implicated in Aβ metabolism and clearance [15], providing a potential mechanism to explain the significant impact of genetic variation in the *APOE* gene on LOAD likelihood and progression.

NFT result from the hyperphosphorylation of a microtubule-associated protein known as “tau”. In the non-hyperphosphorylated state, tau is involved in axonal transport and promotes assembly and stabilization of microtubules. Once hyperphosphorylated, tau undergoes a conformational change preventing normal binding to microtubules. Microtubules then become destabilized and axonal

transport is impaired, which leads to axonal degeneration, neuron dysfunction and ultimately cell death. In addition, the hyperphosphorylated tau forms insoluble filamentous structures. These hyperphosphorylated tau filaments combine to create paired helical filaments, a key component of the neurofibrillary tangles seen in the brains of patients with AD [16]. The underlying cause of this abnormal hyperphosphorylation is currently unknown, but is likely due to a disruption in the balance between the kinases and phosphatases regulating tau phosphorylation. Some of the kinases known to be involved in the phosphorylation of tau include glycogen synthase kinase-3 (GSK3), cyclin dependent protein kinase-5 (cdk5), calcium and calmodulin-dependent kinase-II (CaMKII), and mitogen-activated protein kinases (MAPK)/extracellular signal-related kinases (ERK) 1 and 2 [16].

The temporal relationship and direct link between amyloid plaques and NFT is not completely elucidated at this time. Current theories suggest that amyloid plaque formation likely precedes NFT, with amyloid accumulation occurring during a long preclinical period lasting years to decades [17]. However, formation and extent of NFT is more strongly associated than amyloid plaque deposition to the neurodegeneration, synaptic loss, and cognitive symptoms seen in AD patients [18-20]. The current framework of AD development suggests that amyloid accumulation initiates a pathological cascade resulting in the formation of NFT [17, 21]. The formation of NFT and toxic Aβ species (e.g., oligomers), as well as the initiation of other apoptotic cascades, leads to widespread neuronal injury and death and thus, the clinical symptoms associated with the disease. Formation of NFT may result from the oxidative stress, inflammatory responses, mitochondrial and metabolic dysregulation, and altered ionic homeostasis that occurs with Aβ accumulation [22-23]. Ultimately, the accumulation of amyloid and the formation of NFT results in widespread changes in cell signaling and neuronal loss throughout the brain.

In addition to amyloid plaques and NFT, other biological processes are potentially important in the pathology of AD, including neuroinflammation, oxidative stress, changes in metal homeostasis, neurogenesis disruption, and

mitochondrial/metabolic dysfunction [10-11, 24-26]. Extensive neuroinflammation is observed throughout the AD brain [10-11, 25]. Activated microglial cells and reactive astrocytes are upregulated, especially around amyloid plaques [10, 25, 27]. In fact, Aβ is known to directly activate microglia through secretion of pro-inflammatory cytokines (e.g., interleukin 6 (IL-6), IL-8, tumor necrosis factor alpha (TNF-α)) and through p44/p42 MAP kinase signaling [25, 28-29]. Activated microglia are thought to be a key factor in the link between Aβ and neurodegeneration in AD, since activated microglia can be toxic to neurons by activation of the complement pathway and release of toxic free radicals [25]. Aβ can also directly activate the complement pathway, resulting in cell phagocytosis and lysis [25, 30].

Oxidative stress is also thought to be a key process in the neuropathology of AD. AD brains show an increased level of oxidized proteins and significant DNA damage, particularly around amyloid plaques and NFT, suggesting extensive release of reactive oxygen species (ROS) [10, 31-33]. Aβ can directly cause oxidative stress by altering calcium homeostasis [10] or through activation of microglial cells as previously discussed. Oxidative stress caused by Aβ through the generation of ROS and reactive nitrogen species can result in widespread cell death from a variety of mechanisms, including impaired glutamate neurotransmission and excitotoxicity, apoptosis, lipid peroxidation, and DNA damage [10, 34-36].

Altered metal homeostasis may also be important in AD pathology, as high levels of copper (Cu), zinc (Zn) and iron (Fe) are observed in the brains of patients with AD [10, 37-38]. Aβ is a metalloprotein with high affinity for Cu, Fe, and Zn [10, 37, 39]. The ability of amyloid plaques to promote ROS has been shown to be dependent on Cu and Fe, suggesting that neurodegeneration associated with oxidative stress in AD might be associated with metal accumulation [10, 40-41]. Furthermore, high levels of Zn, Cu, and Fe promote aggregation of Aβ [39, 42] and the formation of toxic Aβ oligomers [10, 43].

Impaired neurogenesis has also been observed in AD [24, 44-47], which may contribute to the memory deficits observed in the disease (see “Clinical

Symptoms and Diagnosis of AD" section). Aβ is thought to directly alter neurogenesis through the calpain/p35 and cdk5 pathway [24, 46, 48]. Activation of cdk5 may also be involved in tau hyperphosphorylation and destabilization of microtubules [16]. Cdk5 has also been shown to regulate other synaptic proteins, such as post-synaptic density 95 (PSD-95), cadherin, and synapsin [24].

Mitochondrial and metabolic dysfunction has also been implicated in the pathophysiology of AD [26]. AD patients show impaired mitochondrial function, including reduced levels of cytochrome oxidase and Krebs cycle enzymes [26, 49-51]. Reduced levels of cytochrome oxidase and mitochondrial dysfunction are thought to lead to increased release of ROS and additional oxidative stress responses, tau hyperphosphorylation, Aβ accumulation, and increased activation of apoptotic pathways [26, 52-53]. Patients with AD also show altered metabolic function *in vivo* with reduced peak levels of oxygen utilization, reduced levels of insulin in the central nervous system, and decreased brain metabolism at rest [26, 54-58].

The biochemical processes involved in AD development ultimately converge upon widespread cell death and neuronal loss, likely through apoptosis. The direct mechanisms by which amyloid pathology and NFT lead to neurodegeneration are not fully understood. Aβ oligomers may be directly toxic to neurons, possibly through neuroinflammatory processes. Axonal degeneration may also result from disruption of trajectories by amyloid plaques and/or by intracellular breakdown due to NFT. Whatever the mechanism, the "downstream" result of amyloid plaques and NFT is widespread, progressive neuronal cell death resulting in marked brain atrophy. The stages of neurodegeneration in AD are described in detail by Braak and Braak (1993) [59]. The first regions of the brain to show neuronal loss associated with AD are in the medial temporal lobe (MTL), including the entorhinal cortex (EC), hippocampus, amygdala, and parahippocampal cortex. Additionally, extensive degeneration of the cholinergic innervations to the neocortex from the basal nucleus of Mynert and the medial septal nucleus occurs early in the disease process [60]. The next stage of degeneration usually involves neuronal loss in the cerebral cortex, particularly in

the lateral temporal and medial parietal cortices, followed by atrophy of the lateral parietal and frontal lobes. By the time a patient has reached a diagnosis of AD, neurodegeneration is usually found throughout the neocortex and subcortical regions, with significant atrophy of the temporal, parietal and frontal cortices, but relative sparing of the primary occipital cortex and primary sensory-motor regions [59, 61].

Clinical Symptoms and Diagnosis of AD

The earliest clinical symptoms associated with AD are a direct result of the brain regions to first degenerate, namely the MTL. Memory impairments, particularly in the episodic and semantic domains, as well as deficits in language and executive functioning are common symptoms early in the disease course [62]. Patients with mild AD also show significant impairment in daily functioning with disruption or cessation of the ability to perform complex tasks associated with general life (e.g., balancing a checkbook, workplace performance, and social activities). In moderate to severe AD, patients may show an inability to function independently, with difficulties in even simple daily tasks, such as feeding and dressing.

Clinicians and researchers have recently updated the AD diagnostic criteria for use in clinical practice and research [63]. To meet a clinical diagnosis of AD, a patient must meet the following criteria: (1) impairment in two or more cognitive domains (memory, executive function, language, visuospatial, personality/behavioral) beyond that expected for age and educational level as determined through patient or informant report or objective cognitive assessment (given either by treating physician or trained neuropsychologist); (2) cognitive impairment represents a gradual decline from previous levels of functioning; (3) cognitive impairment is severe enough to interfere with the ability to perform work, home and/or social activities; and, (4) cognitive impairment not explained by other etiologies, such as delirium, co-morbid medical conditions or medication usage, and/or a psychiatric disorder. Currently, the diagnosis of AD is made clinically, based on cognition and the relative impact of impairments on daily

activities. However, biomarkers (e.g., cerebrospinal fluid (CSF) protein levels, neuroimaging) may be used to rule out other causes of dementia (e.g., vascular) and to support the AD diagnosis in cases with unclear or atypical presentations.

Attempts to diagnose AD at an earlier stage have led to the development of a clinical syndrome termed “mild cognitive impairment” (MCI) [64-67]. Recently, new criteria for diagnosis of MCI in clinical and research settings have been published [68]. A patient must have the following symptoms to receive a clinical diagnosis of MCI: (1) concern regarding a change in cognition (by the patient, an informant, and/or a skilled clinician); (2) impairment in one or more cognitive domains (memory, executive function, attention, visuospatial, language) greater than expected for age and education level; (3) preservation of independence in functional activities, meaning a patient may show mild problems performing complex functional tasks but they should be able to generally maintain their independence with minimal aid or assistance; and, (4) changes should be sufficiently mild so that there is no significant impairment in occupational or social functioning (i.e., not demented). Currently, biomarkers (e.g., CSF protein levels, neuroimaging) are only used in the diagnosis of MCI in clinical settings to rule out alternative etiologies of cognitive impairment. However, diagnosis of MCI in research settings may include the use of biomarkers to support the underlying cause of the MCI and to predict the type and rate of future disease progression. Patients with MCI typically show deficits in cognition that fall between 1 and 1.5 standard deviations below age and education adjusted and culturally appropriate normative levels [68-69]. The most common presentation of MCI features impairments in memory (amnestic MCI). Executive impairments are also commonly reported and can co-occur with other cognitive deficits (multi-domain MCI). Atypical presentations of MCI are also observed (e.g., visual variant with visuospatial deficits, language variant with speech and language deficits) [68]. Amnestic MCI is widely considered to be a prodromal form of AD, as nearly 10-15% of amnestic MCI patients convert to probable AD each year, relative to only 1-2% of the general elderly population [67].

Recently, researchers and clinicians have been attempting to detect AD-related changes and predict progression even earlier than MCI (e.g., “pre-MCI” or “preclinical AD”). A recent article details a conceptual framework for identifying preclinical AD patients [14]. This framework was designed to categorize and conceptualize the presence of AD pathology in seemingly healthy older adults. In fact, 20-40% of older adults show extensive amyloid pathology with minimal or no clinical AD symptoms [14, 70-72]. In the new framework for preclinical AD identification, older adults with AD pathology are referred to as having “AD-pathophysiology” (AD-P), while patients with clinical AD symptoms (i.e., patients diagnosed with MCI or AD) are referred to as having “AD-clinical” (AD-C). A time-lag of 10-15 years between the initial development of AD-P and the emergence of AD-C is thought to be common. Thus, cognitively healthy participants with AD-P are considered to be at increased risk for progression to AD-C. Using biomarkers to measure the various stages of AD pathophysiology (e.g., amyloid deposition, NFT formation, neurodegeneration), Sperling *et al.* (2011) identified three stages of preclinical AD, including: (1) presence of amyloidosis in the absence of other pathology; (2) presence of amyloidosis and neurodegeneration (or tau pathology) in the absence of any cognitive symptoms; and, (3) presence of amyloidosis, neurodegeneration, and subtle cognitive changes (i.e., cognitive decline and complaints which do not reach clinical criteria for MCI). Future studies will confirm whether these three stages of preclinical AD are ideal for characterizing the early stages of AD and/or progress in the indicated fashion. However, preclinical patients in any of these stages are likely to be at higher risk for future progression to MCI and AD. Other researchers define preclinical AD patients using other characteristics, such as subjective reports of cognitive changes (i.e., cognitive complaints), *APOE* genotype, and/or family history of dementia [73-77]. All of these factors have been shown to be linked with increased risk for future progression to AD [4, 76, 78-80].

Biomarkers of AD

Early detection of AD is an important goal because future treatments will likely target disease prevention or slowing of AD development, rather than reversal of AD related damage. Therefore, these interventions would likely be maximally effective in the prodromal stages of the disease. Sensitive and specific biological markers ("biomarkers") of AD are desperately needed to detect patients in the early stages of AD, effectively monitor and predict disease progression, and provide differential diagnostic information for an accurate diagnosis of AD. Furthermore, biomarkers would be particularly helpful in clinical trials of new pharmaceutical interventions to enrich the sample with patients likely to progress to AD and monitor the outcome of new treatments. Levels of AD-related protein (e.g., levels of $A\beta_{40}$, $A\beta_{42}$, total tau, phosphorylated tau) measured from the CSF are commonly used as biomarkers in AD research [81-83]. Neuroimaging is also an exceptional tool for measuring *in vivo* AD pathophysiology and brain atrophy associated with MCI and AD, as well as for predicting disease progression, even in patients with relatively minor cognitive impairments (e.g., preclinical AD patients) [17, 82, 84-99].

The two types of neuroimaging most commonly used as AD biomarkers include positron emission tomography (PET) and magnetic resonance imaging (MRI). PET uses radiolabeled ligands to measure metabolic and neurochemical processes *in vivo*. In AD research, two types of PET ligands are primarily utilized: (1) [18F] fluoro-deoxyglucose (FDG), which measures brain metabolism and (2) amyloid tracers (e.g., [11C] Pittsburgh Compound B (PiB), [18F] florbetapir), which bind to fibrillar amyloid plaques [100]. Studies with FDG-PET have indicated a consistent pattern of resting hypometabolism in AD patients in the temporoparietal cortex, precuneus and posterior cingulate, and frontal lobes [101-104]. Patients with MCI also show a similar pattern of hypometabolism, the presence and extent of which predicts future disease progression and conversion from MCI to probable AD [105-111]. The hypometabolism measured using FDG-PET is thought to reflect impaired synaptic function and neuronal injury in patients with MCI and AD [102, 112-114].

The development of a PET ligand for specific and sensitive detection of amyloid *in vivo* was a significant advancement in the understanding and detection of AD. The most commonly used ligand to date, [11C]PiB, binds to fibrillar amyloid deposits but not to diffuse amyloid plaques or Aβ oligomers [115-116]. *In vivo* PiB binding has been shown to correlate highly with extent and distribution of Aβ plaques in *post-mortem* tissue [115]. Researchers have observed that PiB often shows a somewhat bimodal distribution, with some participants showing significant PiB binding ("PiB-positive") and others showing little or no PiB binding ("PiB-negative"). Thus, optimal cut-off values were reported and this delineation of participants into PiB-positive and PiB-negative is used in many studies [117-122]. Across PiB studies, more than 90% of AD patients were reported to be PiB-positive, reflecting significant amyloid deposition [100, 120, 122-125]. However, longitudinal studies suggest that patients with AD show minimal increases in PiB over 1-2 years, suggesting that patients diagnosed with AD may have reached a plateau of amyloid accumulation [126-127]. Nearly 60% of MCI patients were also reported to be PiB-positive [117, 120, 122, 125, 128-131]. PiB-positive MCI patients show a higher rate of progression and clinical conversion to AD than PiB-negative MCI patients [118, 132]. At this time it is unclear whether PiB-negative MCI patients reflect AD as the underlying disease or whether they have a non-AD dementia. In any case, PiB-negative patients show much lower conversion from MCI to AD over 1-3 years than PiB-positive MCI patients (8-15% vs. 20-50%, respectively) [118]. Furthermore, 20-40% of cognitively healthy older adults also show amyloid pathology and are PiB-positive [71, 119-122, 127, 133-136]. PiB-positive cognitively healthy older adults progress to MCI and AD at a much higher rate than those who are PiB-negative, suggesting PiB-positive healthy older adults are at an increased risk for the development of AD [121, 137].

The most widely used neuroimaging technique to investigate structural changes and neurodegeneration associated with AD *in vivo* is structural MRI. A number of studies have investigated differences between AD patients, MCI patients and healthy age-matched controls (HC) on measures of global and local

brain volume, tissue morphology, and rate of atrophy using both manually applied and automated techniques. Historically, manually applied techniques were used to extract volumetric and morphometric characteristics, including manual tracing of regions of interest (ROIs), in which an anatomically trained scientist traces a border around a specific brain structure on sequential MRI slices to extract a 3-dimensional representation [138-139], and medial temporal atrophy (MTA) scores, in which a trained neuroradiologist scores the amount of MTL atrophy [140-141]. More recently, automated techniques to extract volumes of interest (VOIs) and cortical thickness values for numerous neocortical regions [142-144], as well as semi-automated whole-brain morphometry techniques, such as voxel-based morphometry (VBM; [145-146]) and others [147-148], which determine the density of grey matter (GM), white matter (WM), and CSF on a voxel-by-voxel basis, have been developed and utilized in studies of brain aging and AD.

MRI estimates of regional volumes, extracted using either manual or automated techniques, show significant brain atrophy in AD and MCI patients, following an anatomical distribution similar to the pattern reported in Braak and Braak [59] according to disease severity [149]. The most commonly reported and most significant differences between AD and MCI patients and HC are in the MTL. Numerous studies have reported that AD patients have significantly smaller whole brain [150], hippocampal [138-139, 151-153], EC [139, 154-157], and amygdalar volumes [158-160], and significantly enlarged ventricles [161-162], particularly in the temporal horn of the lateral ventricle [163], relative to HC. MCI patients tend to have intermediate volumetric estimates between AD patients and HC, supporting this as an intermediate stage between healthy aging and AD [164-170]. AD patients have also been shown to have extensive cortical atrophy throughout the brain, particularly in later stages of the disease. The frontal, parietal, and temporal lobes of AD patients show significantly reduced volume and thickness relative to HC [158, 171-175], while MCI patients have intermediate atrophy in these regions. The occipital lobe and primary sensory-motor regions show minimal atrophy until late in the disease. A number of studies

have also shown that measures of hippocampal and EC volume can correctly classify AD patients and HC with an overall accuracy of between 85-95% [139, 157-158, 169, 176-179] and MCI patients and HC with an overall accuracy of between 75-85% [157, 165, 169-170, 180-182].

Similar differences between AD, MCI, and HC are also seen in studies evaluating global and regional tissue morphometry. AD patients show reduced GM density and GM volume in the MTL and throughout the frontal, parietal and lateral temporal lobes [117, 183-190]. MCI patients tend to have a more focal GM density reduction in the medial and lateral temporal lobes, particularly in the EC and hippocampus, supporting that the degeneration of these regions occurs early in the disease process [184, 186, 191-193]. This technique has also been shown to effectively monitor progression over the course of three years, showing the expected expansion of atrophy as the disease progresses from MCI to probable AD [194]. Changes in global and local tissue morphometry have also been shown to correctly classify AD patients and HC with an overall accuracy of approximately 85-90% [188, 192] and MCI patients and HC with an overall accuracy of 87% [192].

Longitudinal structural MRI with multiple scan sessions over one or more years have also been collected to evaluate the rate of whole brain and regional atrophy in AD and MCI patients and HC. Numerous studies have shown accelerated whole brain atrophy rates [195-197], as well as faster rates of atrophy in the MTL [176, 195, 197-200], in AD and MCI patients relative to HC. Patients with AD show an approximate annual hippocampal decline of -4.5%, while MCI patients and HC show annual hippocampal declines of approximately -3% and -1%, respectively (for meta-analysis, see [201]). The annualized rates of ventricular enlargement and cortical atrophy in the temporal, parietal and frontal lobes have also been shown to be significantly greater in patients with AD and MCI relative to HC [195, 197, 202-206].

MRI measures of volume, morphometry, and rates of brain atrophy have also shown sensitivity for predicting the course of AD progression. In fact, studies have demonstrated significantly reduced hippocampal and EC volume in patients

destined to convert from MCI to probable AD (MCI-Converters (MCI-C)), up to two years prior to clinical conversion, relative to MCI patients that remain at a stable MCI diagnosis (MCI-Stable (MCI-S)) [155, 166, 168, 202, 207-211]. Additionally, MCI-C show significantly reduced cortical thickness in regions of the MTL, lateral temporal cortex, and parietal cortex relative to MCI-S [212-215]. Techniques assessing global and local tissue morphometry have also shown significantly reduced GM density and GM volume in MCI-C relative to MCI-S [184, 191, 193, 216-217]. Rates of brain atrophy, including annualized whole brain, hippocampal, and EC volume decline, as well as rates of ventricular enlargement, are also accelerated in patients who are progressing from MCI to AD [197, 200, 218-221]. In addition to detecting differences between MCI-C and MCI-S, baseline and rate of hippocampal atrophy have been used to predict MCI to probable AD conversion. Using Cox proportional hazard models, reduced baseline hippocampal volume and increased annual hippocampal atrophy rates accurately predicted MCI to probable AD conversion [166, 208-209, 222-223]. Baseline hippocampal volume also correctly classified MCI-C and MCI-S with an overall accuracy of between 75-90% [156-157, 167, 207, 212, 214].

Advanced structural and functional MRI techniques have also been evaluated as biomarkers of AD, although further research is needed. Diffusion weighted imaging (DWI) and diffusion tensor imaging (DTI) measure the integrity of WM pathways in the brain. Patients with AD and MCI show reduced WM integrity using both DWI and DTI [224-227]. DWI measures may also be sensitive to predicting progression from MCI to probable AD [228]. Functional MRI (fMRI) measures brain activity during a task or at rest by measuring blood flow and blood oxygen levels. fMRI techniques evaluating both task-related brain activation and brain activation during a resting state have been assessed for utility as biomarkers of AD [229]. During memory tasks, patients with AD show reduced brain activation in the hippocampus [230-236], as well as reduced deactivation of the default mode network (DMN) [237-242], a functional brain network that is active during rest and deactivates upon task initiation. Patients with MCI show different brain activation patterns depending on disease severity.

Early MCI patients have increased brain activation in the hippocampus and increased deactivation of the DMN upon initiation of a memory task [230, 237, 241, 243-245]. However, late MCI patients show a more AD-like pattern, with reduced brain activation in the hippocampus during a memory task and reduced deactivation of the DMN [233, 237, 240, 246]. Recent longitudinal studies of patients with MCI demonstrated that increased or “hyperactivation” in the hippocampus during a memory task at baseline was predictive of future clinical decline [247-248]. The observed hippocampal hyperactivation during memory tasks in early MCI patients may reflect compensation for synaptic impairment and/or loss of or altered blood flow and brain oxygen utilization.

Current Project and Significance

Although MRI-based techniques have shown promise as sensitive biomarkers of AD-related neurodegeneration, even in early stages of disease such as MCI and pre-MCI, the majority of previous studies have featured relatively small samples and selective cohorts. Therefore, a conclusive role of MRI-based biomarkers in the detection and prediction of AD has yet to be determined. Furthermore, the role of longitudinal MRI biomarkers has not been comprehensively examined in pre-MCI stages of disease, such as in older adults with cognitive complaints (CC) but no significant cognitive deficits. In Chapters 1 and 2a, the present report aims to evaluate the role of cross-sectional and longitudinal MRI biomarkers in the largest sample of AD, MCI, and HC participants to date, the Alzheimer's Disease Neuroimaging Initiative (ADNI). In Chapter 2b, alterations in cross-sectional and longitudinal MRI atrophy measures in CC participants will be assessed. Overall, the results of Chapters 1 and 2 will provide evidence regarding the sensitivity of MRI-based measures as biomarkers for detection and monitoring of early AD.

In addition to exploring the use of MRI biomarkers in detection and monitoring of neurodegeneration in patients with MCI and AD and older adults with CC, the present study will assess the ability of these measures to predict future clinical progression. Specifically, differences in cross-sectional atrophy and longitudinal atrophy rate between patients who convert from MCI to probable AD and patients with a stable MCI diagnosis will be evaluated in Chapters 1 and 2. In Chapter 2b, the differences in baseline atrophy and two-year annualized atrophy rate between patients who convert from a diagnosis of CC at baseline to a diagnosis of MCI and participants with a stable CC diagnosis will also be assessed. Determining the sensitivity of MRI biomarkers to differences between stable and clinically progressing patients is important for assessing whether these markers could be used in early stages of AD to predict the likelihood and time-course of future clinical decline.

One unique characteristic of the present report is the use of multiple MRI analysis techniques, which will provide a comprehensive assessment of how

various MRI analytic methods perform in AD detection, monitoring, and outcome prediction. Presently, no other reports to our knowledge have directly compared different MRI analysis techniques using a within-subject approach. The results from Chapters 1 and 2 will allow for a direct comparison of the accuracy and sensitivity of various MRI analytic techniques in cross-sectional and longitudinal analyses at various stages of AD progression.

Finally, the determination of novel biomarkers of AD is essential for understanding the biological mechanisms associated with AD and to assist with improved detection, monitoring, and prediction of clinical progression. In order to properly evaluate whether a new tool is more effective than previous biomarkers and/or has an “added benefit” to known diagnostic assessments, analyses of the relative sensitivity and predictive ability of the novel biomarker alone and in combination with other biomarkers (e.g., MRI) is needed. Chapter 3 of the present study will evaluate a novel biomarker for AD, visual contrast sensitivity. In addition, the relationships between this novel biomarker and cognitive performance, as well as between contrast sensitivity and MRI-based measures of AD neurodegeneration, will be assessed. Results from these analyses will provide useful information about the role of the novel measure as an AD biomarker, as well as how the novel biomarker is associated with a known AD biomarker, neurodegeneration assessed by MRI.

Understanding the ability of MRI measures and/or any novel biomarker of AD (i.e., visual contrast sensitivity) to detect and monitor neurodegeneration and/or other AD-related pathology in patients with MCI and AD will be important for determining whether these measures would be useful in therapeutic trials and/or clinical diagnosis. Markers that can reliably measure AD-related neurodegeneration could be used as outcome measures to evaluate the functional mechanism of a target treatment (i.e., neuronal viability/degeneration) and to determine the efficacy of therapeutic interventions designed to reduce AD-related neurodegeneration. In addition, biomarkers that can identify patients with significant AD pathology could be used in clinical trials to enrich the patient group with individuals that most reflect the targeted pathological stage of disease.

Finally, biomarkers that are sensitive to disease pathology and show effective differential diagnostic utility could improve clinical diagnosis of AD by providing additional support to diagnoses suggested by clinical and psychometric data.

Many researchers and clinicians currently believe that an effective treatment for AD will likely involve prevention of disease rather than amelioration of the pathology once a patient already has an AD diagnosis. In order to test target therapeutics for effective prevention of AD, biomarkers are needed that accurately predict future clinical progression to AD in patients with mild or no cognitive symptoms. In addition, once an effective treatment to prevent AD is discovered, clinicians must be able to routinely test for and accurately detect patients likely to progress to AD to whom this treatment should be administered. Therefore, biomarkers that reliably and accurately predict future progression to AD in patients at early clinical stages or even preclinical stages are essential.

This report features a comprehensive assessment of the sensitivity of MRI measures for detecting and monitoring neurodegeneration in patients with MCI and AD. In addition, the ability of these measures to identify differences in early disease stages between patients who subsequently clinically progress and those who are stable will be evaluated. Finally, visual contrast sensitivity will be assessed as a novel biomarker of AD. The results of these studies will provide needed evidence to support the use of MRI biomarkers, and potentially visual contrast sensitivity, in therapeutic trials and clinical practice for detection and longitudinal monitoring of neurodegeneration and other pathology associated with AD, as well as prediction of future clinical decline.

Chapter 1: Cross-sectional MRI Biomarkers of AD

This chapter explores the use of MRI biomarkers from a scan at a single visit to detect differences between patients with AD and MCI and healthy older adults (HC) in the extent and pattern of neurodegeneration. In addition, the sensitivity of baseline MRI measures to detect atrophic changes in patients destined to progress from MCI to probable AD is assessed. Data from participants in the Alzheimer's Disease Neuroimaging Initiative (ADNI) is used in this section. Two widely-used and publically available MRI analysis techniques are utilized to analyze the 1.5 Tesla baseline structural MR images, including: (1) voxel-based morphometry (VBM), which measures the density of grey matter (GM), white matter (WM), and cerebrospinal fluid (CSF) across the brain on a voxel-wise basis; and, (2) automated parcellation (Freesurfer version 4), which automatically generates volumetric and cortical thickness estimates for more than 100 regions across the brain.

The results of these analyses indicate that cross-sectional MRI measures, particularly measures of medial and lateral temporal lobe atrophy, are useful biomarkers for the detection of neurodegeneration in patients with MCI and AD. In addition, baseline MRI biomarkers are sensitive to differences between patients who subsequently convert from MCI to probable AD over the following year and patients with a stable MCI diagnosis. In fact, patients who progressed from MCI to probable AD show nearly equivalent hippocampal and medial temporal lobe (MTL) atrophy to AD patients, up to one year before clinical conversion. This result suggests that MRI measures of neurodegeneration may precede the clinical AD diagnosis by up to one year. In summary, this article, which was published in *Current Alzheimer Research* in 2009 [213], supports cross-sectional MRI measures as sensitive biomarkers for detecting AD-related neurodegeneration and predicting progression from MCI to probable AD.

Introduction

Alzheimer's disease (AD) is the most common neurodegenerative illness associated with aging, accounting for 60-70% of age-related dementia cases. In 2000, approximately 25 million people over the age of 60 were diagnosed with dementia worldwide, and the number afflicted is expected to reach over 80 million by 2040 [1, 249]. Earlier diagnosis of AD is widely considered to be an important goal for researchers. Characterization of the earliest known clinical signs has led to the development of the classification of mild cognitive impairment (MCI), which is thought to be a transitional stage between normal aging and the development of AD [64]. Patients with MCI, specifically those with primary memory deficits or "amnestic MCI", have a significantly higher likelihood to progress to probable AD, with a conversion rate of 10-15% per year [67]. Therefore, MCI represents an important clinical group in which to study longitudinal changes associated with the development of AD. The detection of subtle changes in brain structure associated with disease progression and the development of tools to detect those who are most likely to convert from MCI to probable AD is an important goal.

The Alzheimer's Disease Neuroimaging Initiative (ADNI) is a five-year public-private partnership to test whether serial magnetic resonance imaging (MRI), positron emission tomography (PET), other biological markers, and clinical and neuropsychological assessment can be combined to measure the progression of amnestic MCI and early probable AD [250-252]. One of the major goals of ADNI is to assess selected neuroimaging and analysis techniques for sensitivity and specificity for both cross-sectional diagnostic group classification and longitudinal progression of MCI and AD. A powerful technique for analyzing high resolution structural MRI data is voxel-based morphometry (VBM), which allows specific tissue classes (i.e., grey matter (GM), white matter (WM), or CSF) to be analyzed in an automated and unbiased manner [145-146, 253]. VBM analyses, particularly comparisons of GM density between groups, have been used to examine diagnostic group differences in both cross-sectional and longitudinal studies of brain aging and AD [77, 117, 183-185, 187-194, 216-217,

254-258]. In fact, VBM has been shown to accurately classify controls and AD patients and to predict conversion from MCI to AD and rate of progression in studies of brain aging [184, 191, 193, 216-217, 257]. However, the small sample sizes in these studies and minimal longitudinal monitoring has prevented VBM from being established as a conclusive biomarker for MCI to probable AD conversion.

Regions of interest (ROIs) and volumes of interest (VOIs) have also been effective in measuring local atrophy associated with AD and MCI and longitudinal monitoring of neurodegeneration in studies of brain aging. Numerous studies using manually defined ROIs have found that local hippocampal and total brain volume are significantly reduced in AD and MCI patients relative to healthy older adults [77, 81-82, 92, 117, 139, 156, 162, 167, 192, 197, 202, 208-210, 219-220, 254, 259-260]. Rates and amount of hippocampal, medial temporal lobe (MTL), and total brain atrophy have also been shown to correlate with MCI to AD conversion [81-82, 92, 140, 166, 197, 208-209, 211, 219, 223, 259-262]. Recently, automated methods for extraction of specific regional volumes have been developed and found to provide similar reliability as manually traced ROIs in AD [143, 263-265]. Automated parcellation methods have also demonstrated reliable cortical thickness value estimations and decreased cortical thickness in AD [143, 266].

The goal of the present study was to perform group comparisons using the 1.5T T1-weighted structural scans obtained from ADNI participants at baseline. Using VBM as implemented in SPM5 (http://www.fil.ion.ucl.ac.uk/spm/), we examined cross-sectional GM differences between groups stratified by baseline diagnosis and one-year conversion from MCI to probable AD. Study groups included participants diagnosed with AD at the screening, baseline, 6-, and one-year follow-up visits (AD), participants designated as healthy age-matched controls at all four visits (HC), participants who were diagnosed with MCI at all four visits (MCI-Stable (MCI-S)), and participants who were diagnosed with MCI at baseline and converted from MCI to probable AD within the first year (MCI-Converters (MCI-C)). We extracted bilateral hippocampal GM density values,

hippocampal and amygdalar volumes, and entorhinal cortex, temporal lobe, and parietal lobe cortical thickness values for between-group comparisons. We hypothesized that patients with AD would show extensive GM reduction in medial and lateral temporal lobes and other neocortical regions, and that both of the MCI groups would demonstrate focal reduction in MTL structures compared to HC. We also hypothesized that MCI participants who converted to AD within one year would show a more extensive pattern of global GM reduction relative to HC, particularly in regions of the MTL, than participants with a stable diagnosis of MCI, but a less extensive pattern than AD participants. We also predicted that MCI-C would show greater MTL and neocortical GM density reductions relative to MCI-S participants. Finally, we investigated whether local hippocampal GM density and volume, amygdalar volume, and entorhinal, temporal, and parietal cortical thickness values would reflect the same pattern of group differences, and the relative ability of these MRI metrics to detect differences between MCI-C and MCI-S groups.

Methods

ADNI

ADNI was launched in 2004 by the National Institute on Aging (NIA), the National Institute of Biomedical Imaging and Bioengineering (NIBIB), the Food and Drug Administration (FDA), private pharmaceutical companies, and nonprofit organizations. More than 800 participants, ages 55-90, have been recruited from 59 sites across the U.S. and Canada to be followed for 2-3 years. The primary goal of ADNI is to determine whether serial magnetic resonance imaging (MRI), positron emission tomography (PET), other biological markers, and clinical and neuropsychological assessment can accurately measure the progression of MCI and early AD. The identification of specific biomarkers of early AD and disease progression will provide useful tools for researchers and clinicians in both the diagnosis of early AD and in the development, assessment and monitoring of new treatments. For additional information about ADNI, see www.adni-info.org.

MRI Scans

Baseline 1.5T MRI scans from 820 participants were downloaded from the ADNI public website (http://www.loni. ucla.edu/ADNI/) onto local servers at Indiana University School of Medicine between January and April 2008. The downloaded data initially included baseline scans from 229 HC, 403 patients with MCI, and 188 patients with AD. Complete details regarding participant exclusion and categorization are provided in Figure 1. Scan data were acquired on 1.5T GE, Philips, and Siemens MRI scanners using a magnetization prepared rapid acquisition gradient echo (MP-RAGE) sequence that was selected and tested by the MRI Core of the ADNI consortium [250]. Briefly, two high-resolution T1-weighted MRI scans were collected for each participant using a sagittal 3D MP-RAGE sequence with an approximate TR = 2400ms, minimum full TE, approximate TI = 1000ms, and approximate flip angle of 8 degrees (scan parameters vary between sites, scanner platforms, and software versions). Scans were collected with a 24cm field of view and an acquisition matrix of 192 x 192 x 166 (x, y, z dimensions), to yield a standard voxel size of 1.25 x 1.25 x 1.2 mm. Images were then reconstructed to give a 256 x 256 x 166 matrix and voxel size of approximately 1 x 1 x 1.2 mm. Additional scans included prescan and scout sequences as indicated by scanner manufacturer, axial proton density T2 dual contrast FSE/TSE, and sagittal B1-calibration scans as needed. Further details regarding the scan protocol can be found in Jack *et al.* (2008) [250] and at www.adni-info.org.

Scans were collected at either screening (n=845) or baseline visits (n=184) between August 2005 and October 2007. If scans existed from both sessions for a single participant, the scan from the screening visit was used. Details of the ADNI design, participant recruitment, clinical testing, and imaging methods, have been published previously [250-252] and at www.adni-info.org.

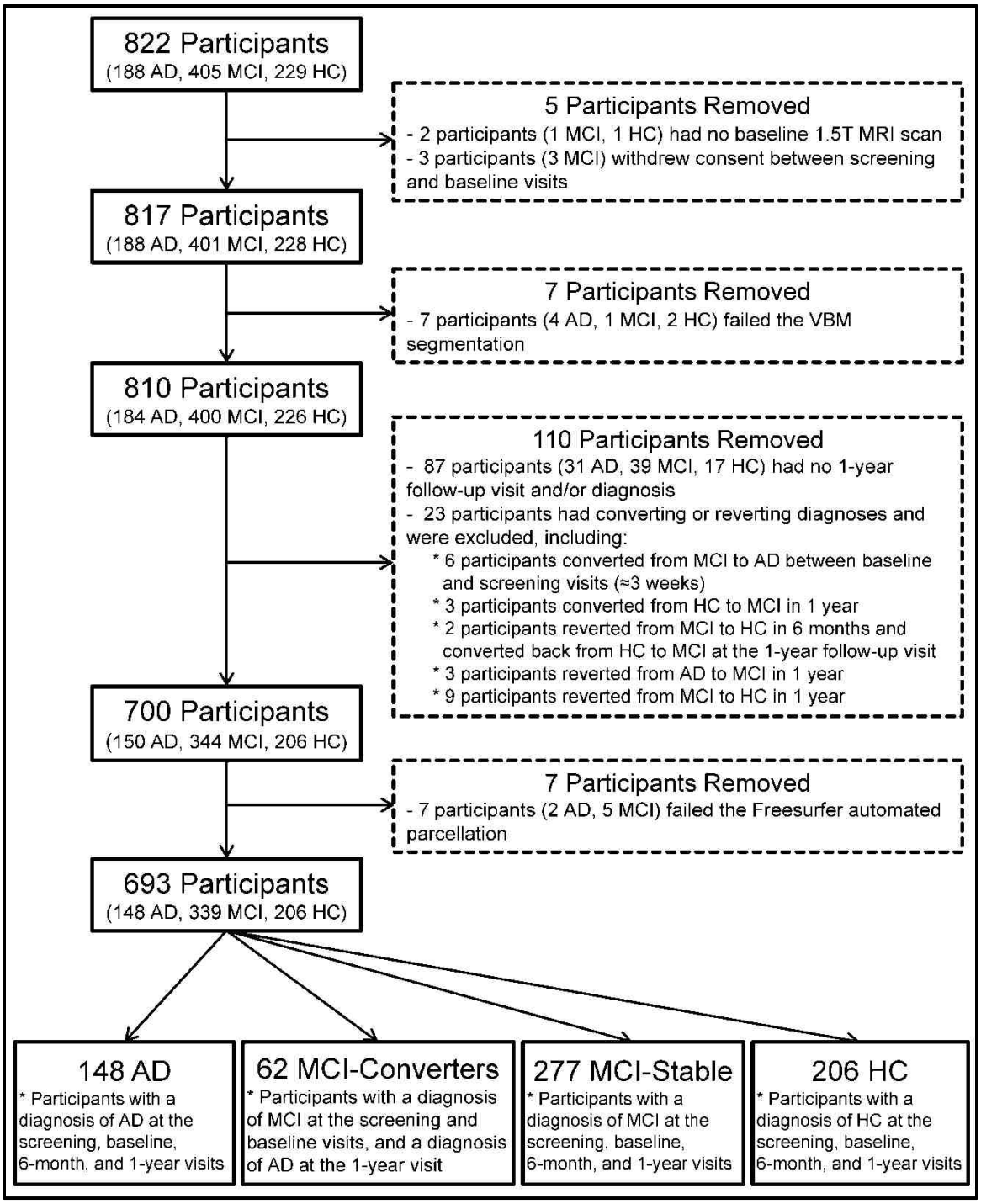

Figure 1. Flowchart of Participant Pool Selection with Group Exclusion and Inclusion Criteria

Image Processing

VBM: Analysis was performed using previously described methods [145-146, 253], as implemented in SPM5 (http://www.fil.ion.ucl.ac.uk/spm/). Briefly, scans were converted from DICOM to NIfTI format, co-registered to a standard T1-weighted template image, bias corrected, and segmented into GM, WM, and CSF compartments using standard SPM5 templates. GM maps were then normalized to Montreal Neurologic Institute (MNI) atlas space as 1 x 1 x 1 mm voxels and smoothed using a 10 mm FWHM Gaussian kernel. In cases where the first MP-RAGE scan could not be successfully segmented we attempted to use the second MP-RAGE. This was successful for only 1 of 8 cases.

Region of Interest: A hippocampal ROI template was created by averaging manual tracings of the left and right hippocampi from an independent sample of 40 HC participants enrolled in a study of brain aging and MCI at Dartmouth Medical School [77, 267]. These hippocampal ROIs were used to extract GM density values from smoothed, unmodulated normalized and modulated normalized GM maps for the ADNI cohort.

Automated Parcellation: VOIs, including bilateral hippocampi and amygdalar nuclei, were extracted using Freesurfer version 4 [142-144, 268-270]. Freesurfer was also used to extract cortical thickness values from the left and right entorhinal cortex, inferior, middle, and superior temporal gyri, inferior parietal gyrus, and precuneus.

The final sample reported here passed site, ADNI MRI Core, and our internal quality control, and did not fail any step of the processing pipeline (Figure 1).

Demographic Data

Demographic information, apolipoprotein E (*APOE*) ε4 genotype, neuropsychological test scores, and diagnosis were downloaded from the ADNI clinical data repository (https://www.loni.ucla.edu/ADNI/Data/ADCS_Download.jsp). The “10-27-08” version of the ADNI clinical database was used for all analyses. Participants

were classified into groups based on screening, baseline, 6-month, and one-year diagnoses as reported in the diagnosis and conversion/reversion database.

VBM Statistical Analyses

Statistical analyses were performed on a voxel-by-voxel basis using a general linear model (GLM) approach implemented in SPM5. A false discovery rate (FDR) adjustment was used to control for multiple comparisons, and a minimum cluster size (k) of 27 voxels was required for significance. Age, gender, years of education, handedness, and total intracranial volume (ICV) were included as covariates, and an explicit GM mask was used to restrict analyses to GM regions. A one-way ANOVA was performed to compare the smoothed, unmodulated normalized GM maps between groups to determine the effects of diagnosis and one-year conversion from MCI to probable AD on GM density. The initial comparison was done using the entire available sample of 693 participants. A second comparison was completed using the same methods but with sub-groups of matched participants to correct for unequal group sizes (n=248; 62 in each group). Matching was done on a case by case basis using the best available match on age, gender, education, and handedness, while preserving the relative proportion of *APOE* ε4 positive participants within each sub-group. After matching there were no significant group differences in age, gender, education, or handedness. Finally, a third set of analyses were performed with the full available sample of 693 participants, adding a volume preserving modulation step to the VBM method, yielding an assessment of local GM volume differences instead of GM density.

Other Statistical Analyses

Mean left and right hippocampal GM density, hippocampal and amygdalar volumes, and cortical thickness values for all 693 participants were compared between groups using a one-way multivariate ANCOVA in SPSS (version 16.0.1). Age, gender, education, handedness, and total ICV were included as covariates in all ROI, VOI, and cortical thickness comparisons. One-way

ANCOVA and chi-square tests were used to determine between-group differences in age, gender distribution, *APOE* ε4 genotype, education, handedness distribution, primary language distribution, and baseline global, functional, behavioral, neurological, neuropsychiatric, and neuropsychological test scores. Post-hoc pairwise comparisons were performed for all ANCOVA analyses using a Bonferroni correction for multiple comparisons. All graphs were created using SigmaPlot (version 10.0).

Effect sizes for the comparison between MCI-C and MCI-S participants were also calculated for selected imaging biomarkers, including bilateral mean hippocampal GM density and GM volume from the VBM images, bilateral mean hippocampal, amygdalar, accumbens, ventral dorsal column, inferior lateral ventricle, lateral ventricle, cerebral cortex, and cerebral white matter volumes extracted using Freesurfer, and bilateral mean cortical thickness values from the entorhinal cortex, inferior, middle, and superior temporal gyri, inferior parietal gyrus, and precuneus, which were also extracted using Freesurfer. These values were assessed due to significant differences between MCI-C and MCI-S groups upon post-hoc pairwise comparisons ($p<0.05$). Left and right adjusted means for each imaging measure, adjusted for age, gender, education, handedness, and ICV, were averaged to give a bilateral estimate, and used to calculate effect sizes (Cohen's d) in SPSS and Microsoft Excel (version 2007).

Results

Sample Characteristics

Demographic information and mean baseline test scores for all groups are presented in Table 1. Mean participant age and handedness distribution did not differ across groups. Years of education and percent of participants with either one or two *APOE* ε4 alleles (APOE4+) were significantly different among diagnosis groups (both $p<0.001$). AD participants showed significantly fewer years of education than either HC ($p<0.001$) or MCI-S ($p=0.003$) participants. Years of education did not differ significantly between any other groups in post-

hoc pairwise comparisons. As expected, the HC group had a lower percentage of APOE4+ participants than any of the clinical groups, while the AD group had the highest percentage of APOE4+ participants. The MCI-S and MCI-C groups had different proportions of APOE4+ participants, with the MCI-C group showing a higher percentage of APOE4+ participants than the MCI-S group.

Neuropsychiatric test results, including scores from the Geriatric Depression Scale (GDS) [271] and Neuropsychiatric Inventory Questionnaire (NPI-Q) [272], were significantly different among groups (both $p<0.001$). HC participants showed significantly fewer depressive symptoms than either AD or MCI-S participants (both $p<0.001$), and had a lower mean score on the NPI-Q than the AD, MCI-S, and MCI-C groups (all $p<0.001$). AD participants also had a significantly higher mean NPI-Q score than the MCI-S ($p<0.001$) and MCI-C ($p=0.008$) groups. No significant differences in mean GDS scores were found between the MCI-S, MCI-C, and AD groups. No group showed clinically meaningful levels of depressive symptoms. Ischemic events and/or risk were not significantly different between groups as assessed by the Modified Hachinski scale [273].

As expected, clinical test scores (Mini-Mental Status Exam (MMSE) total score [274-275], Clinical Dementia Rating Scale (CDR) Global score (CDR-GL) and Sum of Boxes score (CDR-SB) [276], and the Functional Assessment Questionnaire (FAQ) total score [277]) varied significantly among groups (all $p<0.001$). Post-hoc pairwise comparisons showed a similar pattern for the MMSE, CDR-GL, and CDR-SB. HC participants had significantly higher MMSE and lower CDR scores relative to all other groups (all $p<0.001$). Additionally, MCI-S and MCI-C participants showed significantly higher MMSE and lower CDR scores compared to AD participants (all $p<0.001$), but did not differ from one another on these assessments. Mean FAQ total scores were significantly different across groups and in all post-hoc pairwise comparisons (all $p<0.001$).

Neuropsychological scores from the Rey Auditory Verbal Learning Test (RAVLT) [278], Boston Naming Test (BNT) [279], and category verbal fluency tests (Fluency-Animals, Fluency-Vegetables) [280] also showed significant

differences among groups (all $p<0.001$). However, these assessments showed a different pattern in pairwise comparisons than the MMSE, CDR-GL, and FAQ. MCI-C and AD participants showed similar scores on the learning and verbal neuropsychological tests, with no significant differences in post-hoc comparisons on RAVLT measures, BNT, or verbal fluency tests. As expected, all of the clinical groups performed below HC participants for RAVLT, BNT, and verbal fluency measures (all $p<0.001$). MCI-S participants also had significantly higher scores on all RAVLT measures and Fluency-Vegetables than both the AD and MCI-C groups (all $p<0.001$). Finally, MCI-S participants had significantly higher scores than AD participants but not MCI-C on Fluency-Animals and BNT (both $p<0.001$).

	AD (n=148)	MCI-C (n=62)	MCI-S (n=277)	HC (n=206)	ANOVA p-value	Post-hoc Comparisons (at p<0.01)
Age (years)	75.4 (0.6)	74.3 (0.9)	75.1 (0.4)	76.0 (0.5)	NS	No pairs significant
Gender (M, F)	77, 71	36, 26	178, 99	107, 99	0.02	MCI-S>HC
Education (years)	14.8 (0.2)	15.2 (0.4)	15.8 (0.2)	16.1 (0.2)	<0.001	HC, MCI-S>AD
Handedness (R, L)	141, 7	57, 5	253, 24	189, 17	NS	No pairs significant
% English Speaking	98.7%	98.4%	97.5%	99.0%	NS	No pairs significant
% *APOE* ε4 Positive (1 or 2 alleles)	65.5%	59.7%	53.1%	27.2%	<0.001	AD, MCI-C, MCI-S>HC
MMSE[e]	23.5 (0.1)	26.7 (0.2)	27.1 (0.1)	29.1 (0.1)	<0.001	HC>all[f]; MCI-S, MCI-C>AD
CDR-GL[e]	0.75 (0.01)	0.50 (0.02)	0.50 (0.01)	0.00 (0.01)	<0.001	AD>all[g]; MCI-S, MCI-C>HC
CDR-SB[e]	4.3 (0.1)	1.9 (0.1)	1.5 (0.1)	0.3 (0.7)	<0.001	AD>all[g]; MCI-S, MCI-C>HC
FAQ[a,e]	13.0 (0.4)	6.4 (0.5)	3.2 (0.3)	0.1 (0.3)	<0.001	All pairs significant
Geriatric Depression Scale[e]	1.6 (0.1)	1.3 (0.2)	1.6 (0.1)	0.8 (0.1)	<0.001	AD, MCI-S>HC
NPI-Q[e]	3.5 (0.2)	2.2 (0.3)	1.7 (0.2)	0.4 (0.2)	<0.001	AD>all[g]; MCI-S, MCI-C>HC
Modified Hachinski[e]	0.64 (0.06)	0.63 (0.09)	0.65 (0.04)	0.57 (0.05)	NS	No pairs significant
RAVLT (1-5)[b,e]	23.5 (0.7)	26.2 (1.1)	31.9 (0.5)	42.5 (0.6)	<0.001	HC>all[f]; MCI-S>MCI-C, AD
RAVLT 30min Recall[c,e]	0.8 (0.3)	1.2 (0.4)	3.1 (0.2)	7.5 (0.2)	<0.001	HC>all[f]; MCI-S>MCI-C, AD
RAVLT 30min Recognition[c,e]	7.4 (0.3)	8.1 (0.4)	10.0 (0.2)	13.0 (0.2)	<0.001	HC>all[f]; MCI-S>MCI-C, AD
Boston Naming Test[d,e]	22.8 (0.3)	24.4 (0.5)	25.5 (0.2)	27.9 (0.3)	<0.001	HC>all[f]; MCI-S>AD
Fluency - Animals[e]	12.7 (0.4)	14.3 (0.6)	16.2 (0.3)	20.1 (0.3)	<0.001	HC>all[f]; MCI-S>AD
Fluency - Vegetables[e]	7.8 (0.3)	9.3 (0.4)	11.2 (0.2)	14.7 (0.2)	<0.001	HC>all[f]; MCI-S>MCI-C, AD
Total Intracranial Volume (ICV)[e]	1607159.5 (14004.6)	1598192.9 (21470.1)	1597844.8 (10181.0)	1576429.8 (11855.6)	<0.001	No pairs significant

[a] 3 MCI-S participants removed due to incomplete scores

[b] 7 participants removed due to incomplete scores (3 AD, 4 HC)

[c] 1 HC participant removed due to an incomplete score

[d] 3 participants removed due to incomplete scores (1 AD, 1 MCI-S, 1 HC)

[e] Covaried for age, education, gender, and handedness

[f] HC>all is HC>MCI-S, MCI-C, AD

[g] AD>all is AD>MCI-S, MCI-C, HC

(Note: greater scores on these measures (CDR, FAQ, GDS, NPI-Q, and Modified Hachinski) signify more impairment)

Table 1. ADNI Participants at Baseline (Adjusted Mean (SE))

VBM Group Comparisons by Baseline Diagnosis and One-Year Conversion Status

All 693 participants were included in the initial VBM analyses. A one-way ANCOVA indicated striking between-group differences in smoothed, unmodulated normalized GM maps (Figures 2 and 3; unless noted, all differences are $p<0.005$ (FDR)). AD participants showed reduced density in nearly all GM regions compared to the HC group, with the maximum global difference in the left hippocampus (Figure 2A, HC>AD). Surface renderings of the comparison between the HC and AD groups showed that the GM density of nearly the entire cortical surface is significantly lower in AD (Figure 2B, HC>AD), including significant differences in the temporal, frontal and parietal lobes. MCI-C also showed reduced GM density compared to HC, with a global maximum in the left hippocampus (Figure 2C, HC>MCI-Converters). The pattern of significant voxels in the comparison between HC and MCI-C was very similar to that seen in the HC>AD comparison, both in subcortical regions and on the cortical surface (Figure 2D, HC>MCI-Converters). Selected sections (Figure 2E, HC>MCI-Stable) show a more focal distribution of differences in the comparison of GM maps from MCI-S and HC participants. MCI-S participants showed reduced GM density in focal bilateral MTL regions relative to HC, with a global maximum in the right parahippocampal gyrus and additional local maxima in bilateral amygdalar and hippocampal regions. Surface renderings reflect the focal distribution of significant voxels in the HC>MCI-S contrast (Figure 2F, HC>MCI-Stable), with differences localized primarily in the temporal and frontal lobes.

A widespread pattern of significant voxels was also detected in the comparison between the MCI-S and AD groups. MCI-S participants showed significantly higher GM density than AD in the MTL, including a global maximum difference in the left hippocampus (Figure 3A, MCI-Stable>AD) and additional local maxima in bilateral amygdalar and hippocampal regions. The extensive pattern of GM differences between MCI-S and AD participants is further reflected in the surface renderings, with AD participants having significant GM reductions on nearly the entire cortical surface relative to MCI-S participants (Figure 3B,

MCI-Stable>AD). A more focal pattern was observed when comparing MCI groups. MCI-C had significantly reduced GM density relative to MCI-S participants in bilateral MTL regions, with a global maximum in the right insula and additional local maxima in bilateral amygdalar and hippocampal regions (Figure 3C, MCI-Stable>MCI-Converters). Surface renderings of the comparison between the MCI-S and MCI-C groups also show a focal pattern of GM differences in the frontal and temporal lobes (Figure 3D, MCI-Stable>MCI-Converters). No significant voxels were found in the comparison between GM density maps from MCI-C and AD participants (Figure 3, MCI-Converters>AD). At a lower statistical threshold ($p<0.001$ (uncorrected)), AD participants showed reduced GM density in focal regions of the posterior parietal and occipital lobes relative to MCI-C (*data not shown*).

Similar contrasts were performed using matched participants in equal sized groups to control for power as a function of group size. This comparison resulted in a similar pattern of between-group differences as seen using the full sample but at a lower statistical threshold (*data not shown*). Results from comparisons between groups using modulated normalized GM maps from the full sample were also similar to those using unmodulated images (*data not shown*).

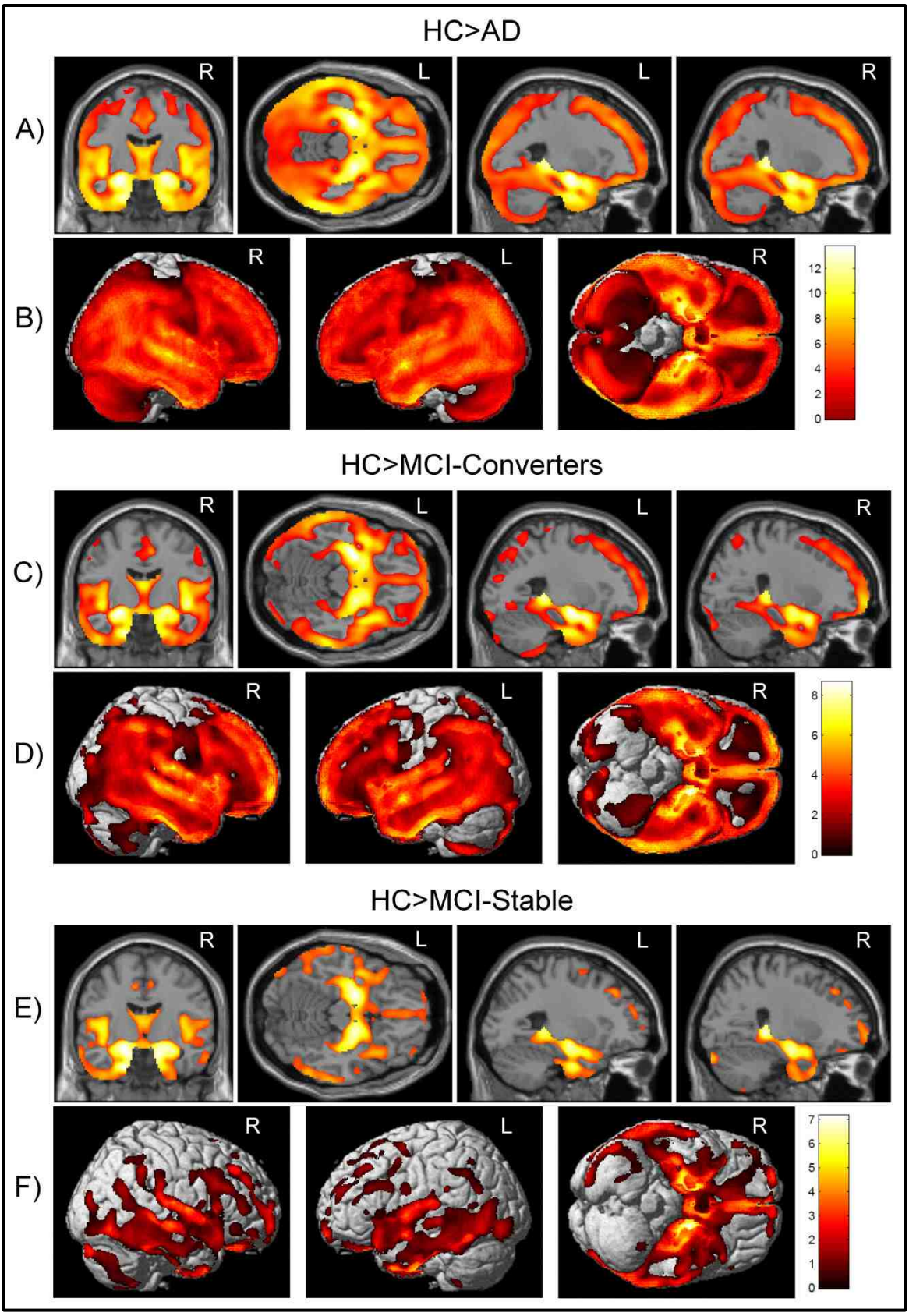
HC>AD
A)
R
L
L
R
B)
R
L
R
12
10
8
6
4
2
0
HC>MCI-Converters
C)
R
L
L
R
D)
R
L
R
8
6
4
2
0
HC>MCI-Stable
E)
R
L
L
R
F)
R
L
R
7
6
5
4
3
2
1
0

Figure 2. Comparisons of GM Density Maps between Healthy Control Participants and Patient Groups using a One-way ANCOVA

Selected slices (A) and surface renderings (B) of regions where HC>AD. Selected slices (C) and surface renderings (D) of regions where HC>MCI-C. Selected slices (E) and surface renderings (F) of regions where HC>MCI-S. All comparisons are displayed at a threshold of $p<0.005$ (FDR), minimum cluster size (k) = 27. Age, gender, years of education, handedness and ICV were included as covariates in all comparisons. Reverse comparisons showed no significant voxels at the established threshold. Selected sections for (A), (C), and (E) include left to right MNI coordinates: (0, -9, 0, coronal), (0, -23, -16, axial), (-26, -10, -15, sagittal), and (26, -10, -15, sagittal).

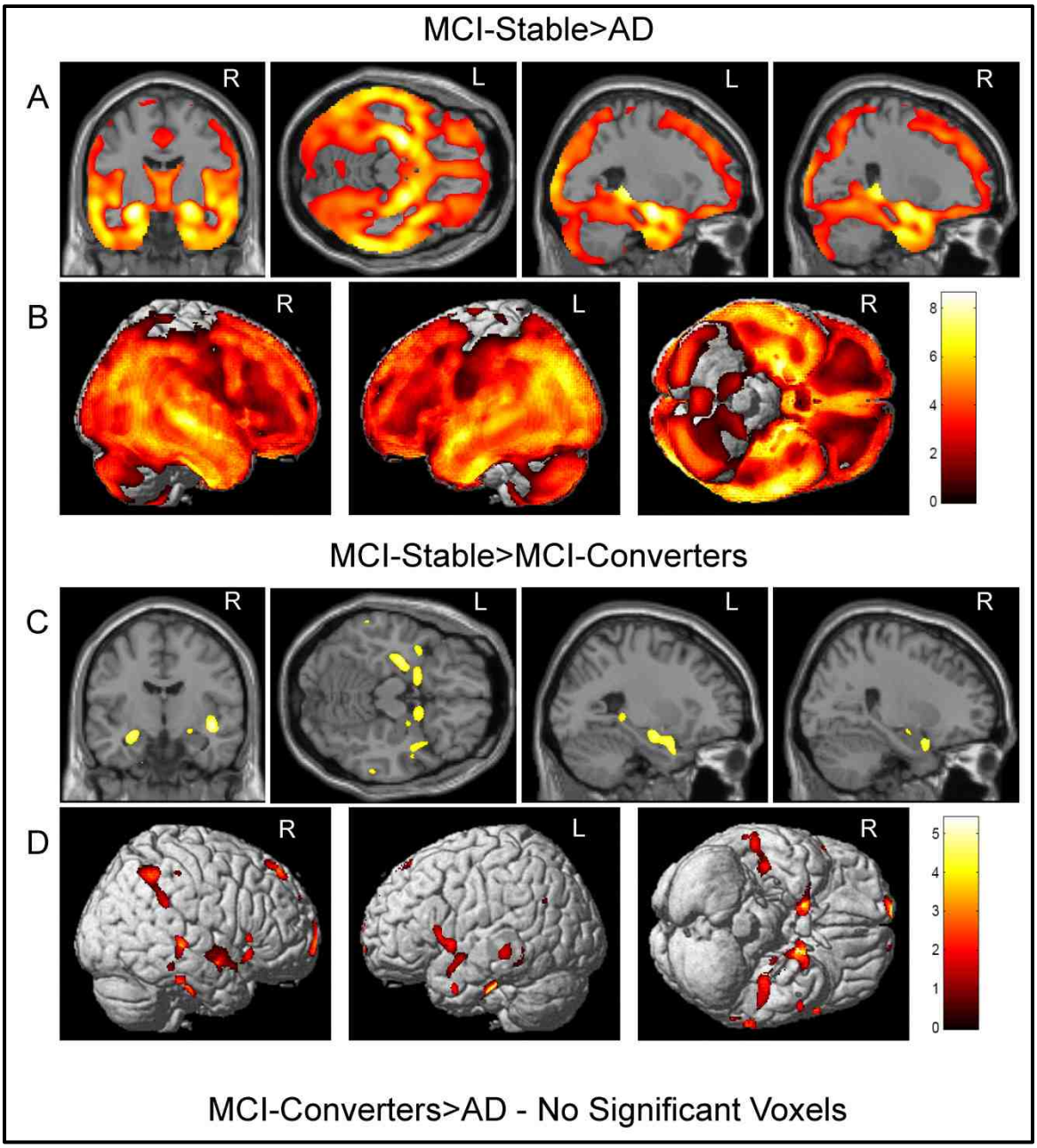

Figure 3. Comparisons of GM Density Maps between Patient Groups by Baseline Diagnosis and One-Year Conversion Status using a One-way ANCOVA

Selected slices (A) and surface renderings (B) of regions where MCI-S> AD. Selected slices (C) and surface renderings (D) of regions where MCI-S> MCI-C. No significant voxels were found in the comparison between MCI-C and AD participants. Using a more lenient statistical threshold, differences were apparent in the posterior

parietal and occipital lobes for MCI-C>AD (*data not shown*). All comparisons are displayed at a threshold of $p<0.005$ (FDR), minimum cluster size (k) = 27 voxels. Age, gender, years of education, handedness and ICV were included as covariates in all comparisons. Reverse comparisons showed no significant voxels at the established threshold. Selected sections for (A) and (C) include left to right MNI coordinates: (0, -9, 0, coronal), (0, -23, -16, axial), (-26, -10, -15, sagittal), and (26, -10, -15, sagittal).

ROI Grey Matter Density Comparisons

Mean left and right hippocampal GM density values from the smoothed, unmodulated normalized GM maps of all 693 participants were extracted as described above. GM density was significantly different among all groups for both the left and right hippocampi (Figure 4A, both $p<0.001$). In post-hoc pairwise comparisons, HC participants showed significantly greater hippocampal GM density bilaterally relative to all other groups (all $p<0.001$). MCI-C had significantly reduced local GM density relative to MCI-S participants in both the left ($p=0.001$) and right ($p=0.034$) hippocampi, as did AD participants ($p<0.001$, bilaterally). Hippocampal GM density did not differ significantly between AD participants and MCI-C. Analyses using smoothed, modulated normalized GM maps showed a similar pattern of results to those using unmodulated images (*data not shown*).

Freesurfer-Derived VOI and Cortical Thickness Comparisons

Bilateral hippocampal and amygdalar volumes and cortical thickness values from the entorhinal cortex, inferior, middle, and superior temporal gyri, inferior parietal gyrus and precuneus were extracted from all 693 participants as described above. Comparisons of mean bilateral hippocampal (Figure 4B) and amygdalar (Figure 4C) volumes and entorhinal cortex thickness (Figure 4D) were significant across all groups (all $p<0.001$), and show similar results to hippocampal GM density in pairwise comparisons. All of the clinical groups (AD, MCI-C, MCI-S) had decreased bilateral hippocampal and amygdalar volumes and entorhinal cortex thickness compared to HC (all $p<0.001$). MCI-C also showed significant reductions relative to MCI-S participants, including reduced bilateral hippocampal volumes (both $p<0.001$), bilateral amygdalar volumes ($p<0.001$ left, $p=0.01$ right), and thinner bilateral entorhinal cortex ($p=0.006$ left, $p<0.001$ right). AD participants also had significant reductions in bilateral hippocampal and amygdalar volumes and entorhinal cortex thickness relative to MCI-S participants (all $p<0.001$). However, MCI-C and AD participants showed

no significant differences in any of the MTL measures (hippocampal and amygdalar volume or entorhinal cortex thickness).

Mean cortical thickness values from lateral temporal cortices were also significantly different across groups (Figure 5, $p<0.001$). Similar to other ROI and VOI comparisons, HC participants had significantly greater bilateral inferior (Figure 5A), middle (Figure 5B) and superior (Figure 5C) temporal gyrus cortical thickness relative to all other groups in post-hoc pairwise comparisons (all $p<0.001$). MCI-C had significant cortical thinning bilaterally relative to MCI-S participants in the inferior (both $p<0.001$), middle ($p<0.001$ left, $p=0.001$ right), and superior ($p=0.003$ left, $p=0.002$ right) temporal gyri. AD participants also had significantly thinner bilateral inferior, middle, and superior temporal gyri relative to MCI-S participants (all $p<0.001$). MCI-C and AD participants showed no difference in temporal gyri cortical thicknesses.

Parietal lobe cortical thickness values also showed significant differences across all groups, specifically in the inferior parietal gyrus (Figure 6A, $p<0.001$) and precuneus (Figure 6B, $p<0.001$). Post-hoc pairwise comparisons showed similar patterns as those of other imaging biomarkers. HC participants had significantly greater cortical thickness in bilateral inferior parietal gyrus and precuneus relative to all other groups (all $p<0.001$). AD participants had significantly reduced cortical thickness in bilateral inferior parietal and precuneus regions relative to MCI-S participants (both $p<0.001$), as did MCI-C (inferior parietal gyrus $p=0.006$ left, $p=0.009$ right; precuneus $p=0.012$ left, $p=0.013$ right). MCI-C and AD participants showed no significant differences in either inferior parietal gyrus or precuneus cortical thickness values.

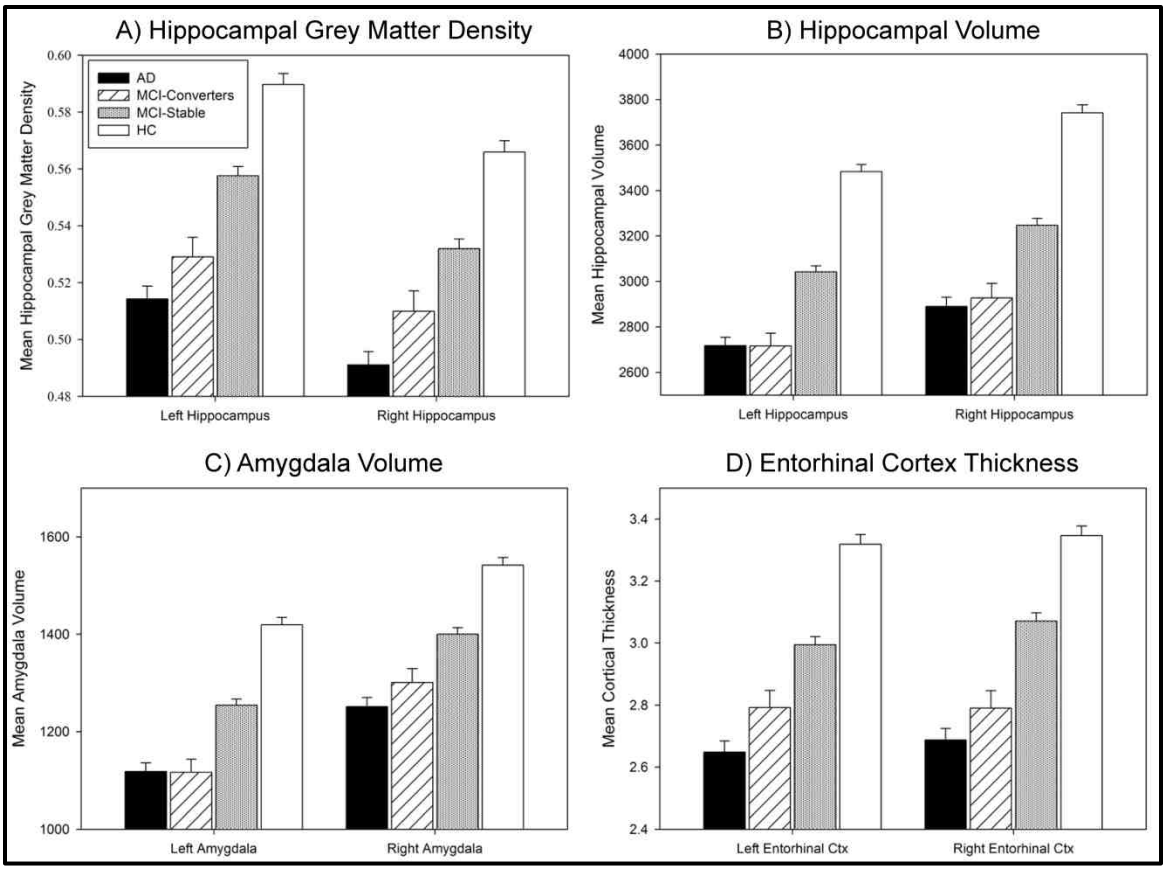

Figure 4. Comparison of Medial Temporal Lobe GM Density, Volume, and Cortical Thickness Values among Groups

Hippocampal GM density values (A) were extracted from the unmodulated VBM GM maps using standard left and right hippocampal ROIs traced on an independent sample of 40 HC participants [77, 267]. Bilateral hippocampal (B) and amygdalar (C) volume estimates and entorhinal cortex thickness values (D) were extracted using automated parcellation. The comparisons of all four measures show a significant difference (all $p<0.001$) across all groups. In post-hoc pairwise comparisons, hippocampal GM density, hippocampal and amygdalar volumes, and entorhinal cortex thickness show significant differences between HC and all clinical groups (all $p<0.001$) bilaterally and MCI-S and AD groups (all $p<0.001$) bilaterally. Furthermore, MCI-S and MCI-C groups show significant differences in GM density and volume in the left (GM density (A), $p=0.001$; volume (B), $p<0.001$) and right (GM density (A), $p=0.034$; volume (B), $p<0.001$) hippocampi, as well as significant differences in left ($p<0.001$) and right amygdalar volumes ($p=0.01$). MCI-C also showed significantly thinner entorhinal cortices

than MCI-S participants on both the left ($p=0.006$) and right ($p<0.001$). No significant differences were found in hippocampal GM density, hippocampal or amygdalar volumes, or entorhinal cortex thickness values between MCI-C and AD groups. Group mean values (+/- SE) adjusted for age, gender, years of education, handedness, and total ICV are displayed.

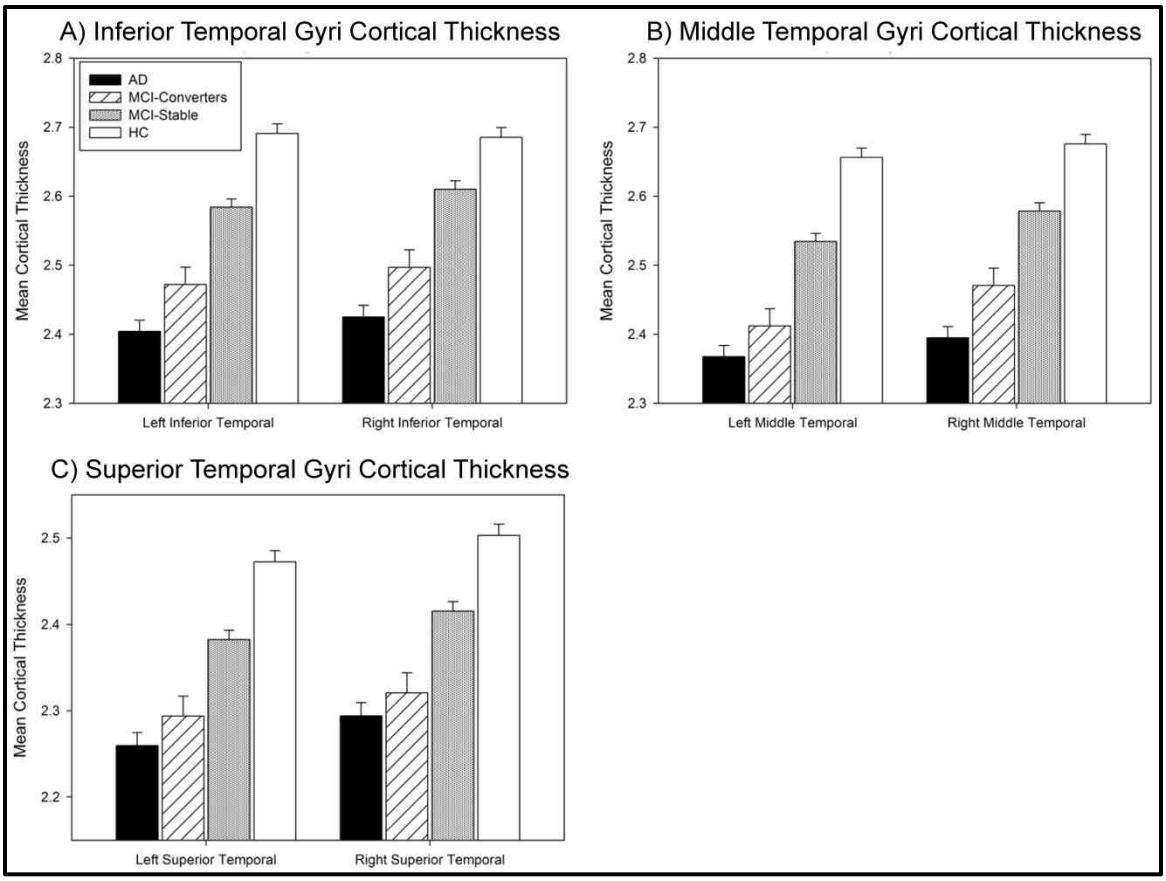

Figure 5. Differences in Temporal Lobe Cortical Thickness Values Extracted using Automated Parcellation by Group

Comparisons between cortical thickness values from three regions of the temporal lobe, including the left and right inferior (A), middle (B), and superior (C) temporal gyri, demonstrated significant differences (all $p<0.001$) across all groups. Post-hoc pairwise comparisons demonstrated significantly greater cortical thickness values for all temporal gyri bilaterally in HC relative to all other groups (all $p<0.001$), as well as in MCI-S participants relative to AD patients (all $p<0.001$). MCI-C showed significantly thinner cortices in the bilateral inferior temporal gyri (both $p<0.001$), left ($p<0.001$) and right ($p=0.001$) middle temporal gyri, and left ($p=0.003$) and right ($p=0.002$) superior temporal gyri relative to MCI-S participants. Cortical thickness values from bilateral inferior, middle, and superior temporal gyri were not significantly different between the MCI-C and AD groups. Group mean values (+/- SE) adjusted for age, gender, years of education, handedness, and total ICV are displayed.

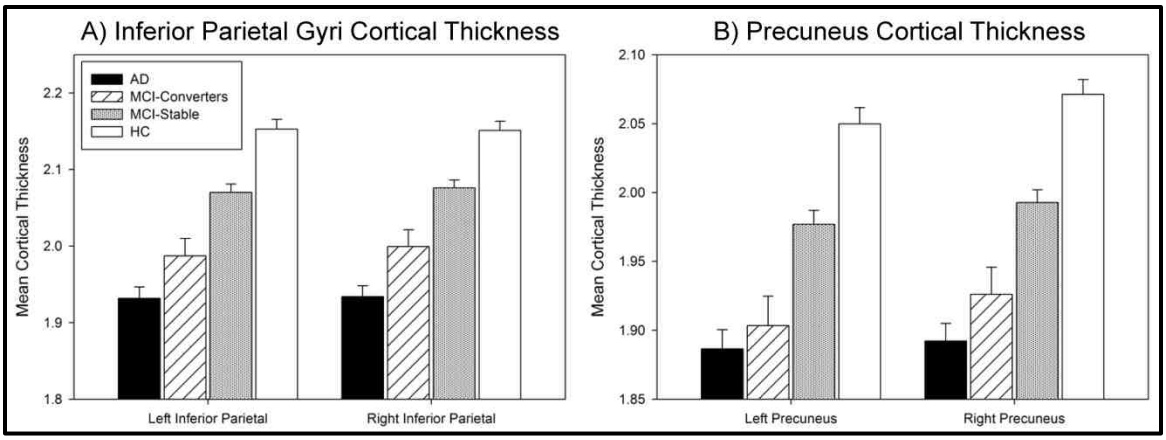

Figure 6. Differences by Group in Parietal Lobe Cortical Thickness Values Extracted using Automated Parcellation

Cortical thickness values from the inferior parietal gyrus (A) and precuneus (B) showed significant differences among groups ($p<0.001$). Post-hoc pairwise comparisons showed significantly greater cortical thickness values in the bilateral inferior parietal gyri and precuneus in HC relative to all clinical groups (all $p<0.001$), as well as in MCI-S participants relative to AD patients (both $p<0.001$). In addition, MCI-S participants showed significantly greater thickness values in the left ($p=0.006$) and right ($p=0.009$) inferior parietal gyri and left ($p=0.012$) and right ($p=0.013$) precuneus than MCI-C. No significant differences were found between MCI-C and AD groups in any region. Group mean values (+/- SE) adjusted for age, gender, years of education, handedness, and total ICV are displayed.

Effect Sizes of Imaging Biomarkers

Imaging metrics with the 20 largest effect sizes are shown in Figure 7. Effect sizes of selected imaging biomarkers extracted using both unmodulated and modulated VBM GM maps and automated parcellation for the comparison of MCI-C versus MCI-S participants were calculated. Large effect sizes were observed for in medial and lateral temporal lobe and parietal lobe ROIs (Figure 7). Bilateral mean hippocampal volume had the highest effect size, with a Cohen's d of 0.603. Cortical thickness values from the inferior and middle temporal gyri, as well as the entorhinal cortex, also showed strong effect sizes, with Cohen's d values of 0.535, 0.529, and 0.493, respectively. Amygdalar volume (Cohen's d=0.478), superior temporal cortical thickness (Cohen's d=0.448), inferior parietal cortical thickness (Cohen's d=0.417), precuneus cortical thickness (Cohen's d=0.408), and hippocampal GM density (Cohen's d=0.408) also showed high effect sizes.

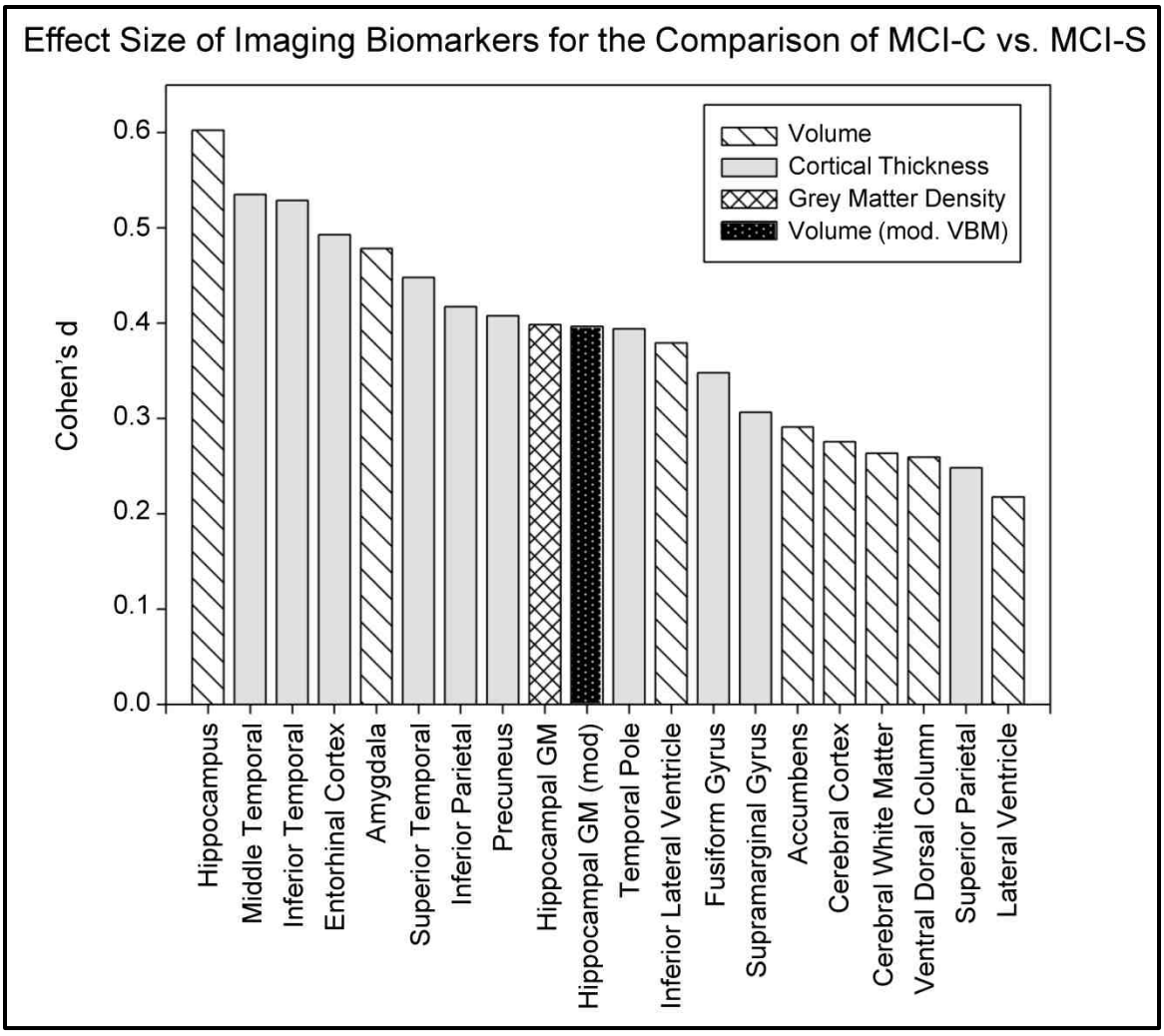

Figure 7. Effect Sizes of Selected Imaging Biomarkers for the Comparison between MCI-Stable and MCI-Converter Groups

GM density, volume, and cortical thickness estimates were extracted using VBM and automated parcellation and compared between MCI sub-groups based on one-year MCI to probable AD conversion status. Effect sizes (Cohen's d) for the comparison between MCI-S and MCI-C groups showed that measures of temporal lobe atrophy, including hippocampal and amygdalar volume and cortical thickness values from the entorhinal cortex and inferior, middle, and superior temporal gyri, provided the greatest difference. Bilateral mean values from target ROIs adjusted for age, gender, education, handedness, and total ICV were used to calculate effect size.

Discussion

We examined baseline 1.5T T1-weighted MRI scans from 693 participants in the ADNI cohort to (1) characterize initial differences between the AD, MCI, and HC groups and (2) detect anatomic features associated with imminent conversion from MCI to probable AD within one year (MCI-C). We hypothesized that cross-sectional baseline differences would be consistent with the well-established progression of neurodegeneration from MTL structures to neocortical involvement, and that those individuals with MCI who are about to convert to AD will appear more similar to AD prior to conversion than those MCI patients who remain stable for at least one additional year. Publically available and widely used semi-automated image analysis methodologies (VBM in SPM5, automated parcellation in Freesurfer) were employed to assess these hypotheses.

Several key conclusions can be drawn from the obtained results. First, the overall pattern of structural MRI changes in MCI and AD patients observed at baseline in the ADNI cohort is similar to prior findings in other, typically smaller and less intensively characterized samples [77, 81-82, 92, 117, 139, 156, 162, 167, 171, 183-185, 187-191, 202, 208-209, 216, 219, 223, 254-256, 258, 260, 263, 266]. Second, MCI-C are distinguishable at baseline from individuals with MCI who will not show significant clinical progression over the next year (MCI-S). Third, MCI-C show significantly greater global and MTL atrophy than MCI-S participants, a pattern previously reported in earlier studies with smaller samples [81-82, 92, 156, 167, 184, 191, 193-194, 197, 207-210, 216-217, 219-220, 222, 257, 260]. Fourth, MCI-C show a neurodegenerative profile more similar to that seen in AD patients than that seen in stable MCI patients. In fact, the MCI-C group demonstrated a pattern of atrophic changes nearly equivalent to those of the AD group up to a year before meeting clinical criteria for probable AD. Finally, a comparison of effect sizes of MRI metrics for the contrast between the MCI-C and MCI-S groups indicated that degree of neurodegeneration of MTL structures is the best antecedent MRI marker of imminent conversion, with decreased hippocampal volume (left more than right) being the most robust structural MRI feature.

There are several aspects to these results and analyses that warrant comment. This report is among the first, in the fully enrolled ADNI cohort, to assess group differences between AD, MCI, and controls at baseline, as well as to examine antecedent imaging predictors of future change in clinical status (i.e., conversion to probable AD by patients with amnestic MCI). Our comparisons of the three baseline diagnostic groups using VBM are similar to previous reports using alternative methods to compare global atrophy between AD, MCI, and HC participants in the ADNI cohort [148, 281-282]. One recent study from Hua *et al.* [148] found significant MTL atrophy in both AD and MCI participants in the ADNI cohort using tensor-based morphometry (TBM), similar to our results using VBM. Furthermore, our results using the one-year MCI to AD converter population from the ADNI cohort provided congruent results with those of Hua *et al.* (2008), in which temporal lobe atrophy as assessed using TBM correlated with MCI to AD conversion in a subset of the ADNI MCI to probable AD converters (n=40) [148]. A recent study using another imaging analysis technique (RAVENS) also found a similar pattern of distinctive atrophy in MCI-C relative to MCI-S participants in a sub-sample (27 MCI-C, 76 MCI-S) of the ADNI cohort, which could be used to predict MCI to probable AD conversion using a pattern classification technique [282]. In the present study, we were able to substantially extend the results of earlier partial cohort analyses by including the largest possible set of ADNI participants with usable data, since one-year outcomes were only recently completed. Further, our multi-method approach included VBM-based analyses of GM density and GM volume and Freesurfer-derived ROI analyses of volume and cortical thickness, which together provide a more detailed picture of anatomical differences among groups.

Studies employing VBM methods differ with regard to including a volume conserving step referred to as “modulation” [145-146, 253]. Briefly, unmodulated GM maps are typically interpreted as indicating differences in GM density or concentration. By contrast, VBM performed with modulated GM maps are interpreted as local GM volume estimates. At present there is no strong consensus in the literature regarding which approach is more appropriate for a

given application. Furthermore, the pathophysiological significance of differences detected by one method versus the other has not been conclusively determined. Our primary VBM analyses were performed without modulation. We then repeated the analyses with the modulation step for comparison, and found highly similar patterns of GM differences between groups (Figures 2 and 3, modulated data not shown). Specifically, the overall pattern of GM reduction for all patient groups (AD, MCI-C, MCI-S) compared to HC participants remained significant using both VBM methods, with the greatest differences remaining in bilateral MTL. Similarly, the pattern for MCI-C relative to the MCI-S participants was largely unaffected by analytic methodology. Analysis of GM values extracted from left, right and combined hippocampal ROIs defined in an independent cohort of healthy older adult controls [77, 267] showed similar group differences, and the effect size for MCI-C versus MCI-S participants was nearly identical (Figure 7). Overall, inclusion of a volume conserving modulation step in the VBM analyses had little influence on the pattern or magnitude of group differences. This may in part be related to our inclusion of intracranial volume as a covariate in all analyses. To eliminate the possibility of bias due to markedly unequal group sizes when comparing MCI-C and MCI-S participants, we repeated the main VBM analyses on four matched groups of equal size. Despite slightly attenuated power to detect group differences, the additional matched group analyses did not alter the overall pattern of results (*data not shown*).

The second major approach to assess morphological changes in AD and MCI patients relative to HC entailed examining Freesurfer parcellation derived ROIs, selected on the basis of their status as important regions for AD pathology. Group differences were evaluated for left, right and combined hippocampal volume and GM density, additional MTL ROIs, and regional cortical thickness estimates. Significant differences between groups were found in hippocampal, amygdalar, and other MTL regions, as well as widespread neocortical regions. These results are consistent with prior ROI and VOI studies in AD and MCI, in which hippocampal volumes [77, 81-82, 92, 117, 139, 156, 166, 202, 208-210, 219, 223, 263, 283], hippocampal GM density [77, 190, 192], and other regions

[81-82, 92, 139-140, 156, 162, 167, 189-190, 202, 207-209, 211, 222, 260-261], were found to be significantly decreased relative to HC. As in our VBM results, ROI measures indicated that participants who convert from MCI to AD within one year show significant baseline atrophy relative to MCI participants who remain clinically stable, and also have a generally equivalent degree of atrophy at baseline to AD participants. Decreased hippocampal GM density and volume, amygdalar volume, and cortical thickness in the entorhinal cortex, inferior, middle, and superior temporal gyri, inferior parietal gyrus, and precuneus reflect the antecedent structural characteristics of neurodegeneration in MCI-C compared to individuals with MCI who remained clinically stable for at least a year. Similar to the global atrophy detected using VBM, local measures of volume and cortical thickness detected significant degeneration in MCI-C up to one year prior to the point at which they meet clinical criteria for an AD diagnosis, suggesting an accelerated amount and rate of neuropathological changes in these individuals which is not well captured by the MCI diagnosis alone. Furthermore, these results, obtained from assessment of the largest group of one-year conversion from MCI to probable AD to date, extend the findings of previous smaller studies which have reported local atrophy in MCI to AD converters using measures of hippocampal, amygdalar, entorhinal cortex, and other MTL volume estimates [81-82, 92, 140, 167, 184, 191, 193, 207-210, 216-217, 219, 222, 257, 259-260, 284].

Taken together, the present findings support the use of structural MRI as a biomarker for assessing prodromal and early AD-related neurodegenerative changes. An important implication of the analyses performed in this report is that although many regions and measurements are sensitive to early AD pathology, MRI markers have differential sensitivities for detection of those individuals who are at greatest risk for short-term progression to probable AD. The MRI measures with the largest effect sizes (far left, Figure 7) for MCI-C versus MCI-S contrasts appear to be important biomarker candidates for prediction of MCI to AD conversion. Previous studies have investigated the use of MTL density and volume in the prediction of MCI to AD conversion, with some reports finding

significantly greater sensitivity and specificity achieved by adding imaging biomarkers to clinical test prediction algorithms, while others suggested minimal utility of including additional imaging variables [81-82, 92, 166-167, 207-209, 211, 214, 220, 222, 259-261, 283]. However, the majority of these studies included modest participant pools and manually drawn ROIs. The time-consuming nature of manual ROI tracing limits the utility of these endpoints as biomarkers in studies with large numbers of participants, as well as in routine clinical settings. Automated or semi-automated extraction of volume and cortical thickness values from ROIs in the MTL requires minimal manual intervention. The largely automated nature and wide availability and use of this and other methods (e.g., [263, 285]) in assessing local and global atrophy will facilitate incorporation of these measures as key variables in pharmacological efficacy and neuroprotection trials.

A limitation of the present report is the inclusion of only baseline scans in characterizing anatomic changes. Additional information, including changes in imaging measures over time and rate of atrophy, has been shown to be useful in assessing and accurately predicting rapid conversion [197, 220]. As a cross-sectional assessment of structural neuroimaging measures, the present study does not capture the dynamic atrophic processes associated with MCI to AD conversion. Future studies assessing multiple timepoints, including two and three year MCI to AD conversion patterns, will be needed to determine the diagnostic and predictive value of dynamic measures of global and local atrophy. Furthermore, the current participant pool includes 182 participants diagnosed with MCI at baseline who were on AD-indicated medications during the first year of the study. Pharmacological treatments, such as AChE inhibitors and memantine, have been shown to reduce or delay MCI to AD conversion [286-290]. The impact of medications was not assessed in the current study. Future studies should focus on including this variable in predicting and assessing conversion from MCI to AD. Another limitation of this report is the inclusion of only structural imaging. It is possible that FDG PET, obtained on approximately half of the ADNI cohort, could enhance the detection and characterization of

antecedent AD-related changes alone or in combination with MRI and other measures. Targeted molecular PET imaging for amyloid deposition with [11C]PiB is also being investigated in a smaller add-on study in the ADNI cohort [136]. Future studies will undoubtedly clarify the contribution of FDG and PiB PET to understanding early changes and predicting clinical trajectory of patients progressing towards AD. Finally, the role of genetic factors was only considered to a limited degree in the present study by evaluating the distribution of *APOE* ε4 genotype in the sample. A genome-wide association study employing a high density microarray with over 620,000 single nucleotide polymorphisms is underway by the ADNI Genetics Working Group and these forthcoming results will permit inclusion of data on individual differences in important biological pathways in predictive models.

In summary, a major goal of ADNI is to identify imaging biomarkers that could be used for early detection and prediction of longitudinal changes in MCI and AD. Two semi-automated, widely used and publically available image analysis methods (VBM, automated parcellation) revealed significant global and local atrophy in AD and MCI patients in a large sample from the ADNI cohort at baseline relative to HC. These techniques were also successful at detecting differences at baseline between participants who would convert from MCI to AD within one year and those who would remain stable with a diagnosis of MCI for at least one year. The results of these analyses suggest that VBM and automated parcellation are useful tools for characterization of atrophy in MCI and AD and prediction of disease course. Employed with repeated scans for longitudinal monitoring of brain degeneration, these methods may be useful for clinical trials in MCI and AD. With further refinement, MRI coupled with advanced image analysis approaches appears to have potential for individualized prediction of risk of progression and enhancement of clinical trials by including those at greatest risk of conversion.

Funding

Data collection and sharing was funded by the Alzheimer's Disease Neuroimaging Initiative (ADNI; Principal Investigator: Michael Weiner; NIH grant U01 AG024904). ADNI is funded by the National Institute on Aging (NIA), the National Institute of Biomedical Imaging and Bioengineering (NIBIB), and through generous contribution from the following: Pfizer Inc.; Wyeth Research; Bristol-Myers Squibb; Eli Lilly and Company; GlaxoSmithKline; Merck & Co. Inc.; AstraZeneca AB; Novartis Pharmaceuticals Corporation; the Alzheimer's Association; Eisai Global Clinical Development; Elan Corporation plc; Forest Laboratories; and the Institute for the Study of Aging, with participation by the U.S. Food and Drug Administration. Industry partnerships are coordinated through the Foundation for the National Institutes of Health. The grantee organization is the Northern California Institute for Research and Education, and the study is coordinated by the Alzheimer's Disease Cooperative Study at the University of California, San Diego. ADNI data are disseminated by the Laboratory of Neuro Imaging at the University of California, Los Angeles.

Data analysis was supported in part by the following grants from the National Institutes of Health: NIA R01 AG19771 to AJS and P30 AG10133 to Bernardino Ghetti, MD and NIBIB R03 EB008674 to LS, and by the Indiana Economic Development Corporation (IEDC #87884 to AJS).

Acknowledgments

The authors thank Aaron Cannon of Brigham Young University, Sungeun Kim, PhD of Indiana University School of Medicine, Nick Schmansky, MA, MSc and Bruce Fischl, PhD of Harvard Medical School, and Randy Heiland, MA, MS of Indiana University for their help. We also thank Bernardino Ghetti, MD, Guest Editor and organizer of the Indiana Alzheimer Disease Center MCI Symposium in which initial results were presented.

Chapter 2a: Longitudinal MRI Biomarkers in Patients with AD, MCI, and HC

This chapter explores the use of MRI biomarkers from two scans collected at repeated visits which were approximately one year apart. The goal was to detect differences in the rate of brain atrophy between patients with AD and MCI and healthy older adults (HC). In addition, we explored whether rates of atrophy in selected MRI biomarkers can sensitively monitor progression from MCI to probable AD. 1.5 Tesla MRI scans from the baseline and one-year follow-up visits for participants from the Alzheimer's Disease Neuroimaging Initiative (ADNI) were used in this analysis. Multiple MRI analytic techniques, including VBM, automated parcellation (Freesurfer version 4), and an additional region of interest (ROI) extraction technique (MarsBaR), were used to evaluate dynamic changes in brain structure and atrophy rates in target regions.

The results of this study indicate that longitudinal MRI measures of brain atrophy rate are useful biomarkers for measuring the progression of neurodegeneration in patients with MCI and AD, as well as distinguishing MCI patients who progress to probable AD (MCI-Converters (MCI-C)) from those who have a stable diagnosis of MCI (MCI-Stable (MCI-S)) over one year. In addition, rates of hippocampal volume and grey matter loss are sensitive measures for differentiating AD and MCI patients from HC, as well as MCI-C from MCI-S. The sensitivity of these measures as endpoints for drug trials is assessed by calculating the needed sample sizes for each measure to detect a 25% reduction in atrophy rate. Using the most sensitive brain atrophy measures, only 100-150 participants would be needed to detect significant 1-year changes in patients with MCI and AD. The impact of apolipoprotein E (*APOE*) genotype on brain atrophy rate is assessed, as the presence of an *APOE* ε4 allele is the most significant genetic risk factor for late-onset AD. Patients with an *APOE* ε4 allele show higher rates of brain atrophy in the medial temporal lobe than patients without an *APOE* ε4 allele in all diagnostic groups. In summary, this article, which was published in *Neurobiology of Aging* in 2010 [291], supports the use of MRI measures of brain atrophy rate as biomarkers for AD.

Introduction

Alzheimer's disease (AD) is the most common age-related neurodegenerative disease, affecting nearly 25 million people worldwide, a number expected to triple in the next 50 years [1, 249]. Patients with AD show significant impairment in multiple cognitive domains, including deficits in memory and executive functioning. Progress in the early clinical diagnosis of AD has led to the characterization of a prodromal syndrome featuring relatively isolated memory deficits termed "amnestic mild cognitive impairment" (MCI) [292-293]. Amnestic MCI is conceptualized as a preliminary stage of AD-associated pathology with the majority of patients eventually progressing to AD at a rate of approximately 10-15% per year [67, 294].

The increasing recognition that early diagnosis and therapeutic intervention will be necessary to prevent the development of AD underscores the need to develop sensitive and specific biomarkers for detecting and monitoring MCI and AD. Structural magnetic resonance imaging (MRI) has shown significant promise as a biomarker to detect early MCI and AD-associated neurodegenerative changes, as well as to predict the rate of disease progression [82, 93, 166]. Cross-sectional studies evaluating the utility of structural MRI in detecting neurodegeneration have identified significant brain atrophy in patients with MCI and AD, particularly in regions of the medial temporal lobe (MTL), using regional volumetric extraction tools such as manual tracing of regions of interest (ROIs) [77, 82, 138, 155-157, 165, 168-169], and more recently automated segmentation and parcellation of target regions [143, 173, 213, 263, 266]. Other semi-automated tools which provide three-dimensional mapping of brain morphology, including voxel-based morphometry (VBM), tensor-based morphometry (TBM) and related techniques have also identified significant global and local tissue changes in patients with MCI and AD, including decreased whole brain, hippocampal, and temporal lobar grey matter (GM) density [77, 117, 185-187, 189, 192, 258]. Structural MRI techniques have also been shown to provide sensitive prediction of disease progression. Hippocampal volume and GM density, as well as measures of MTL volume and cortical thickness, have been

identified as sensitive biomarkers for predicting conversion from MCI to probable AD [166, 184, 193, 209, 211, 213, 216, 257, 284].

Longitudinal monitoring of atrophy rate using MRI measures has also proven sensitive to AD-related changes. Increased rates of whole brain and MTL atrophy in patients with MCI and AD relative to healthy elderly controls (HC) are routinely reported in studies of brain aging and dementia ([for recent review, see 87]). Manual tracing or automated ROI techniques and analysis of deformation fields reflecting brain shrinkage are the most commonly employed methods for evaluating longitudinal changes in global and regional volume, particularly in the MTL. Previous studies have reported rates of hippocampal annual decline of -4.5% in patients with AD and -3% in patients with MCI in contrast to -1% in HC ([for meta-analysis see 201]). Furthermore, increased atrophy rates can predict future clinical decline, including MCI to probable AD conversion [197, 200, 218-220, 295]. Patients who convert from MCI to probable AD show higher rates of hippocampal atrophy compared to patients with a stable diagnosis of MCI, reported as -3.5% and -2.2%, respectively [197, 219].

Genetic factors play a significant role in the development and progression of MCI and AD. Genetic variation in the apolipoprotein E gene (*APOE*) is the most commonly reported genetic risk factor associated with late-onset AD, with the presence of a single ε4 allele conferring a 2-fold or 3-fold increased risk of developing AD and two ε4 alleles associated with nearly an 11-fold increased risk [3, 296-297]. In addition to an increased risk of AD, the presence of an ε4 allele has been associated with imaging markers of neurodegeneration. Significantly greater cross-sectional hippocampal atrophy and an increased rate of hippocampal and whole brain atrophy in ε4 carriers has been reported in non-demented individuals, as well as in MCI and AD patients in some studies [223, 256, 298-305], but not in others [306-307].

The Alzheimer's Disease Neuroimaging Initiative (ADNI) is a five-year consortium study designed to assess the utility of various biomarkers for detecting early changes associated with MCI and AD and predicting disease course over time. Target biomarkers collected as part of ADNI include

longitudinal structural MRI and positron emission tomography (PET) scans, genetic factors, psychometric scores, CSF markers, and other variables. A number of studies utilizing MRI data from this cohort have been published recently. Using both ROI and three-dimensional mapping techniques the expected differences in structural MRI markers have been found between diagnostic (AD, MCI, HC) groups at baseline assessment, including atrophy in hippocampal and other MTL regions and enlarged ventricles in patients with AD and MCI [213, 281, 308-314]. Hippocampal volume has also been found to be sensitive and specific for predicting one-year conversion from MCI to probable AD [213, 282, 309, 311-312, 315-316]. MRI studies of the ADNI cohort have also examined longitudinal change in brain volumes using ROI and whole-brain structural change techniques (e.g., Jacobian determinants, boundary shift integral), and have detected differences in annual change in whole brain volume, hippocampal volume, and ventricular volume as a function of baseline diagnostic group (AD, MCI, HC) [127, 282, 304-305, 311, 316-323] and of *APOE* ε4 genotype [303-305, 311]. Several studies have reported larger declines in whole brain and regional volumes as well as larger ventricular volume increases in MCI to AD converters than MCI non-converters [282, 311, 317, 322].

In order to better evaluate the effectiveness of future disease modifying therapeutics, biomarkers of disease state and progression are likely to be more sensitive and reliable than clinical measures, which may be highly variable within and between participants. When designing clinical trials, an important consideration is the sample size needed to detect a therapeutic effect that is both statistically significant and clinically meaningful in a target biomarker with 80% or 90% power. Several previous studies in the ADNI cohort have calculated the relative sample size needed to detect a hypothetical treatment-induced 25% reduction in brain atrophy for various regional MRI markers and have suggested that to achieve 80% power approximately 35-100 AD and 100-200 MCI participants are required [311, 318, 320-321].

Despite the extensive MRI analyses in AD and MCI, prior studies have not directly compared the relative sensitivity of longitudinal changes in GM density

and volume, cortical thickness and ROI volumes in relation to changes in clinical status. In ADNI, longitudinal studies have primarily focused on baseline diagnostic groups rather than one-year clinical conversion status. The present study was designed to compare the annual percent change (APC) of different types of structural MRI markers among groups defined by baseline diagnosis and one-year MCI to probable AD conversion status using the final one-year sample. We hypothesized that patients with more advanced clinical indicators of disease progression, particularly AD and MCI to probable AD converter participants, would show significantly greater APC in major structural MRI markers. We also evaluated the relative sensitivity of these markers to progression of atrophy over time. Because of the important implications for design of future therapeutic trials of disease modifying agents, we also calculated the sample size needed to detect a 25% reduction in atrophy rate for selected markers. We hypothesized that the MTL atrophy rates would constitute the most sensitive regional markers of progression and therefore require the smallest potential sample sizes. Prior ADNI reports have not evaluated the sample size needed for trials in rapidly progressing MCI participants compared to stable MCI participants, an important distinction for trial design. Additionally, previous reports have focused primarily on sample sizes needed for MRI markers that were extracted using a single technique. In the present study, we compared GM density and volume, cortical thickness and ROI volumetric markers. Finally, we assessed the impact of *APOE* genotype on the APC in several key target regions, which to date has not been examined in patients who converted from MCI to probable AD the ADNI cohort to our knowledge. We hypothesized that the presence of an ε4 allele would increase the annual rate of decline in selected MRI markers of MTL integrity.

Methods

ADNI

ADNI is a consortium study initiated in 2004 by the National Institute on Aging (NIA), the National Institute of Biomedical Imaging and Bioengineering

(NIBIB), the Food and Drug Administration (FDA), private pharmaceutical companies, and non-profit organizations. More than 800 participants age 55-90 have been recruited from 59 sites across the U.S. and Canada to be followed for 2-3 years, with repeated structural MRI and PET scans and functional, psychological, and psychometric test data collected every 6 or 12 months. For additional information about ADNI, see www.adni-info.org and Mueller *et al.* (2005a, 2005b) [251-252].

MRI Scans

Raw baseline 1.5T MRI scans from 820 participants were downloaded from the ADNI public website (http://www.loni.ucla.edu/ADNI/) onto local servers at Indiana University School of Medicine between January and April 2008 and processed using Freesurfer and VBM implemented in SPM5 as previously described [213]. All available 1.5T MP-RAGE scans collected at the one-year follow-up visit were also downloaded for all participants (n=693) as of June 2009. A minimum of two MP-RAGE images were acquired at each timepoint for each participant, using a standard MP-RAGE protocol that was selected and tested by ADNI [250].

Participants were only included in the present analysis if their baseline and one-year MRI scans were successfully preprocessed. Four participants failed Freesurfer processing and were not included in any analyses. 30 additional participants were excluded from only the VBM analyses due to failed processing of scans from either the baseline or one-year visit. Participants who did not have either baseline (n=2) or one-year (n=124) scans were also excluded. Included participants (n=673 for Freesurfer analyses, n=643 for VBM analyses) were divided into groups by baseline and one-year clinical diagnosis and one-year MCI to probable AD conversion status, resulting in 4 groups: (1) participants with a stable AD diagnosis for the first year of the study (AD; n=152 for Freesurfer analyses, n=143 for VBM analyses); (2) participants with an MCI diagnosis at baseline who converted to a diagnosis of probable AD at either the 6-month or one-year visit (MCI-Converters (MCI-C); n=60 for Freesurfer analyses, n=57 for

VBM analyses); (3) participants with a stable diagnosis of MCI over the first year of the study (MCI-Stable (MCI-S); n=261 for Freesurfer analyses, n=253 for VBM analyses); (4) participants with a stable designation of healthy control for the first year of the study (HC; n=200 for Freesurfer analyses, n=190 for VBM analyses). Participants who showed other forms of conversion, reversion, or otherwise unstable diagnostic designation were excluded (e.g., conversion from HC to MCI at the 6-month visit, followed by a reversion from MCI to HC at the one-year visit, etc.; n=16). Details of the ADNI design, participant recruitment, clinical testing, and additional methods have been published previously [251-252, 259, 324] and at www.adni-info.org.

Demographic and Clinical Data

Demographic information, *APOE* genotype, neuropsychological test scores, and diagnosis information for all analyzed visits were downloaded from the ADNI clinical data repository (https://www.loni.ucla.edu/ADNI/Data/ADCS_Download.jsp). The “8-09-09” version of the ADNI clinical database was used for all analyses. By this time all one-year clinical and scan data were complete. Participants were classified into groups based on baseline and one-year diagnoses as reported in the conversion/reversion database.

In order to evaluate the impact of *APOE* genotype on annual rate of atrophy, we also classified participants by the presence or absence of an *APOE* ε4 allele. Given the unknown impact of having an ε2ε4 genotype (i.e., possessing a potential protective allele (ε2) and a risk allele (ε4) for AD), we chose to run analyses both including and excluding the ε2ε4 participants (n=13; 3 AD, 7 MCI-S, 3 HC). We found similar results from the two comparisons (*data not shown*), and thus, chose to use the largest available sample in the results presented in this report. For the evaluation of hippocampal volume and EC thickness, 673 participants were included: 99 AD, 35 MCI-C, 143 MCI-S, and 56 HC who were *APOE* ε4 positive (ε2ε4, ε3ε4 or ε4ε4 genotypes) and 53 AD, 25 MCI-C, 118 MCI-S, and 144 HC who were *APOE* ε4 negative (ε2ε2, ε2ε3, or ε3ε3

genotypes). 30 participants were excluded due to failed VBM processing, as previously described. Thus, the analysis of the effect of *APOE* ε4 genotype on bilateral mean hippocampal GM density and volume included the following participants (n=643): 95 AD, 34 MCI-C, 142 MCI-S, and 53 HC who were *APOE* ε4 positive and 48 AD, 23 MCI-C, 111 MCI-S, and 137 HC who were *APOE* ε4 negative.

Image Processing

VBM: Scans were processed with VBM in SPM5 (http://www.fil.ion.ucl.ac.uk/spm/), using previously described methods [145-146, 253]. Briefly, after conversion from DICOM to NIfTI, both baseline MP-RAGE scans were aligned to the T1-weighted template and both one-year scans were co-registered to the first T1-template aligned baseline scan. After alignment, all scans were bias corrected and segmented into GM, WM, and CSF compartments using standard SPM5 templates. GM maps were normalized to MNI atlas space as 1 x 1 x 1 mm voxels and smoothed using a 10 mm FWHM Gaussian kernel. Both modulated and unmodulated GM maps were generated. In order to maximize signal and minimize variability in the imaging markers, we chose to create a mean GM image of the two independent MP-RAGE-derived GM maps using SPM5. These mean GM maps were then employed in all subsequent VBM analyses. This process was completed for both unmodulated and modulated normalized GM maps at each timepoint (baseline and one-year), yielding a mean GM density image and a mean GM volume image, respectively.

Regions of Interest (ROIs): A hippocampal ROI template was created by manual tracing of the left and right hippocampi in an independent sample of 40 HC participants enrolled in a study of brain aging and MCI [77, 267, 270]. Hippocampal GM density and GM volume values were extracted from baseline and one-year mean GM maps from VBM, as previously described [213]. Additionally, mean GM density and mean GM volume were extracted from 90 cortical and 26 cerebellar regions using MarsBaR ROI templates [325]. Mean lobar measures from MarsBaR regions were calculated from target ROIs as

follows: mean frontal lobe is the mean of GM density values from inferior frontal operculum and triangularis, inferior, medial, middle and superior orbital frontal, middle and superior frontal, and medial superior frontal regions; mean parietal lobe is the mean of inferior and superior parietal, angular gyrus, supramarginal gyrus, and precuneus GM density values; and mean temporal lobe value is the mean of GM density values from the amygdala and hippocampus, middle and superior temporal pole, inferior, middle and superior temporal gyri, and fusiform, Heschl's, lingual, olfactory, and parahippocampal gyri.

Automated Parcellation: Bilateral volumetric and cortical thickness estimates from the baseline and one-year scans were extracted using Freesurfer version 4 [142-144, 268, 270], as previously described [213]. Each baseline and one-year scan was processed independently. The final extracted values were then used to calculate a mean volume or cortical thickness for each region for both the baseline and one-year visits. Mean lobar cortical thickness measures were calculated from selected ROI mean cortical thicknesses from Freesurfer as follows: mean frontal lobe was the mean of caudal midfrontal, rostral midfrontal, lateral orbitofrontal, medial orbitofrontal, and superior frontal gyri, pars opercularis, oribitalis, and triangularis, and frontal pole thicknesses; mean parietal lobe was the mean of inferior parietal, superior parietal and supramarginal gyri, and precuneus thicknesses; and mean temporal lobe was the mean of the fusiform, lingual, parahippocampal, inferior temporal, middle temporal, and lateral temporal gyri, as well as temporal and transverse temporal pole thicknesses. Baseline total intracranial volume (ICV), which was used in most subsequent analyses as a covariate, was also generated using Freesurfer.

VBM Statistical Analysis

A two-way ANCOVA assessing time and group membership (AD, MCI-C, MCI-S, HC) was performed to compare the change in GM density over one year between groups using the smoothed, unmodulated normalized mean GM maps. Statistical analyses were performed on a voxel-by-voxel basis using a general linear model (GLM) approach implemented in SPM5. A threshold of $p<0.0001$

(uncorrected for multiple comparisons) and minimum cluster size (k) of 27 voxels was considered significant. We chose to show the VBM comparison images at this threshold ($p<0.0001$ unc.) for display purposes although all comparisons survive $p<0.05$ with a false discovery rate (FDR) correction for multiple comparisons and have at least 1 cluster which survives $p<0.01$ with a family-wise error (FWE) multiple comparison correction. Baseline age, gender, years of education, handedness, and baseline mean total intracranial volume (ICV) were included as covariates, and an explicit GM mask was used to restrict analyses to GM regions.

Other Statistical Analyses

Annual percent change (APC) estimates were calculated using mean values from left and right ROIs from baseline and one-year scans for each participant using the following equation:

$$\textit{Annual percent change (APC)} = \frac{\textit{(one-year ROI estimate – baseline ROI estimate)}}{\textit{baseline ROI estimate}} \Big/ \textit{(Time (in years) between baseline and one-year visits)}$$

A one-way multivariate ANCOVA was used to assess differences in APC between groups. Baseline age, gender, education, handedness, and baseline mean ICV were included as covariates. Post-hoc pairwise comparisons with a Bonferroni adjustment for multiple comparisons were used to assess differences between individual group pairs. One-way ANCOVA and chi-square tests were used to determine group differences in demographic variables, as well as baseline values and annual change of psychometric test scores. Baseline age, gender, years of education, and handedness were included as covariates where appropriate. SPSS (version 17.0.2) was used for all statistical analyses.

The sample size needed to detect a 25% reduction in atrophy rate (two-sided t-test; $\alpha=0.05$) with 80% or 90% power was also calculated using Microsoft Excel 2007 for the absolute change over one year of all target variables in all four groups. Only participants with values for all analyzed regions were included in

these calculations (n=643; 143 AD, 57 MCI-C, 253 MCI-S, 190 HC). Sample size was calculated using the following equation:

$$n = \frac{2\sigma^2 (z_{1-\alpha/2} + z_{power})^2}{(0.25\,\beta)^2}$$

where n is the target sample size, $\alpha = 0.05$, β is the mean absolute change in a target ROI adjusted for baseline age, gender, education, handedness and baseline ICV, σ is the standard deviation of the measure, and z_a is the value from the standard distribution for 80% or 90% power [318, 321, 326].

Effect sizes for the comparisons between pairs of diagnostic groups were also calculated for bilateral mean APC and baseline values of selected imaging markers. Left and right adjusted means, covaried for baseline age, gender, education, handedness, and baseline mean ICV, were averaged to yield a bilateral estimate. These bilateral mean values were then used to calculate the effect size (Cohen's d) between group pairs for all imaging measures in Microsoft Excel 2007 using the following equation:

$$d = \frac{(M_1 - M_2)}{\sqrt{[(\sigma_1^2 + \sigma_2^2) / 2]}}$$

where, for the target biomarker, M_1 = mean value for group 1, M_2 = mean value for group 2, σ_1 = standard deviation for group 1, and σ_2 = standard deviation for group 2 [327]. In order to accurately compare the resulting effect sizes, only participants with values for all analyzed regions were included in this comparison (n=643; 143 AD, 57 MCI-C, 253 MCI-S, 190 HC).

Finally, a two-way ANCOVA was used to assess the impact of diagnostic group and *APOE* ε4 genotype on the most sensitive imaging phenotypes as determined by effect size in the comparison of MCI-C and MCI-S participants, namely the APC in bilateral mean hippocampal GM density and GM volume, hippocampal total volume, and EC thickness. Additionally, two-sample t-tests were used to evaluate the influence of *APOE* ε4 genotype within each of the 4 diagnostic groups on MTL change measures. Age, gender, education,

handedness, and baseline ICV were included as covariates in all analyses. All graphs were created using SigmaPlot (version 10.0).

Results

Group Characteristics and Change in Psychometric Scores

Demographic information and the baseline values and change over the first year in selected psychometric scores are found in Table 2. Significant differences were demonstrated in education level ($F=6.53$, $p<0.001$) and *APOE* genotype (percentage positive for 1or 2 ε4 alleles; $\chi^2=56.64$, $p<0.001$). Post-hoc tests indicated significant differences between HC and all patient groups (all $p<0.05$). Expected differences between groups in psychometric test scores were found to be significant for both baseline scores and annual change in scores on the Clinical Dementia Rating Scale Sum of Boxes score (CDR-SB; baseline, $F=532.91$, $p<0.001$; annual change, $F=21.42$, $p<0.001$), Mini-Mental Status Exam (MMSE; baseline, $F=342.97$, $p<0.001$; annual change, $F=23.14$, $p<0.001$), and Rey Auditory Verbal Learning Test (RAVLT; baseline, $F=193.85$, $p<0.001$; annual change, $F=8.02$, $p<0.001$). Post-hoc paired comparisons between groups also indicated significant differences in both baseline values and annual change as shown in Table 2. No significant difference among groups was detected in baseline or one-year age, gender distribution, handedness distribution, or baseline mean total intracranial volume (ICV).

	AD (n=152)	MCI-C (n=60)	MCI-S (n=261)	HC (n=200)	ANOVA p-value	Significant Post-hoc Comparisons (p<0.05)
Baseline Age	75.33 (0.5)	74.04 (0.9)	75.07 (0.4)	75.95 (0.5)	NS	none
One-Year Visit Age	76.41 (0.5)	75.11 (0.9)	76.15 (0.4)	77.04 (0.5)	NS	none
Education	14.82 (0.2)	15.15 (0.4)	15.89 (0.2)	16.08 (0.2)	<0.001	HC, MCI-S>AD
Gender (M, F)	80, 72	35, 25	166, 95	105, 95	0.06	MCI-S vs. AD, HC
Handedness (R, L)	144, 8	55, 5	239, 22	185, 15	NS	none
APOE Genotype (% APOE4+)	65.13%	58.33%	54.79%	28.00%	<0.001	AD, MCI-C, MCI-S>HC
Baseline CDR-SB[e]	4.18 (0.1)	2.00 (0.1)	1.52 (0.1)	0.02 (0.1)	<0.001	AD>MCI-C>MCI-S>HC
One-Year Change in CDR-SB[a,e]	+2.13 (0.1)	+2.64 (0.2)	+1.26 (0.1)	+1.1 (0.1)	<0.001	AD, MCI-C>MCI-S, HC
Baseline MMSE[e]	23.53 (0.1)	26.58 (0.2)	27.11 (0.1)	29.11 (0.1)	<0.001	HC>MCI-S, MCI-C >AD
One-Year Change in MMSE[b,e]	-1.88 (0.7)	-2.56 (0.4)	-0.35 (0.2)	0.00 (0.2)	<0.001	HC, MCI-S>MCI-C, AD
Baseline RAVLT[c,e]	23.25 (0.7)	26.20 (1.1)	32.00 (0.5)	43.65 (0.6)	<0.001	HC>MCI-S>MCI-C, AD
One-Year Change in RAVLT[d,e]	-2.91 (0.5)	-2.68 (0.8)	-0.81 (0.4)	+0.3 (0.5)	<0.001	HC>MCI-C, AD; MCI-S>AD
Baseline ICV	1552677.32 (13807.5)	1566297.83 (21976.7)	1570616.06 (10537.0)	1534944.90 (12037.1)	NS	none

Data are given as mean (standard error of the mean) or *n*.

Key: AD = Alzheimer's disease; CDR-SB = Clinical Dementia Rating Scale Sum of Boxes score; F = female; HC = healthy control; ICV = total intracranial volume; L = left; M = male; MCI-C = converters from mild cognitive impairment to probable AD; MCI-S = mild cognitive impairment-stable; MMSE = Mini-Mental Status Exam; NS = nonsignificant; R = right, RAVLT = Rey Auditory Verbal Learning Test.

[a] 7 participants missing data (2 AD, 1 MCI-S, 4 HC)

[b] 2 participants missing data (1 MCI-S, 1 HC)

[c] 3 participants missing data (1 AD, 2 HC)

[d] 14 participants missing data (8 AD, 3 MCI-S, 3 HC)

[e] Baseline age, gender, education, and handedness

Table 2. Demographic Information and Baseline and One-Year Change in Neuropsychological Test Scores for ADNI Participants (Adjusted Mean (SE))

VBM Comparisons

AD participants showed greater one-year decline in global GM density than HC (Figure 8A) and MCI-S participants (Figure 8D) in widespread regions of the brain, including bilateral medial and lateral temporal lobes, frontal lobes, and parietal lobes, with maximal the differences of both comparisons found in the left MTL for both comparisons (global peaks). MCI-C participants also showed greater decline in global GM density relative to HC (Figure 8B) in bilateral medial and lateral temporal lobes. This difference between MCI-C and HC was maximal in the left MTL (global peak). Differences in one-year decline in bilateral hippocampal GM density were also detected between HC and MCI-S participants, with MCI-S showing greater decline in focal clusters of the bilateral medial and lateral temporal lobes than HC (Figure 8C). MCI-C also showed greater 1-year decline in bilateral medial and lateral temporal lobes GM density than MCI-S (Figure 8E). Finally, greater one-year decline in global GM density was detected for AD participants relative to MCI-C in a small cluster of voxels in the anterior parietal lobe/posterior frontal lobe (Figure 8F). All comparisons were significant above a threshold of $p<0.0001$ (uncorrected for multiple comparisons) and a minimum cluster size (k) of 27 voxels.

Target Region Comparisons

Results from regional assessments of GM density and GM volume, as well as cortical thickness and volumetric measures, show a similar magnitude and anatomical pattern of decline over one year by group as seen in the results from the VBM comparisons. The APC values for all selected ROIs, including hippocampal GM density and GM volume extracted using two ROI methods [77, 267, 270, 325], hippocampal volume, entorhinal cortex (EC) thickness and mean lobar thickness values extracted using Freesurfer [142-144, 268], and mean lobar GM density and GM volume extracted using MarsBaR ROIs [325] are found in Table 3 and Figures 9-11. All APC values were significantly different across groups ($p<0.001$). Significant post-hoc paired comparisons using a Bonferroni correction are indicated in Table 3.

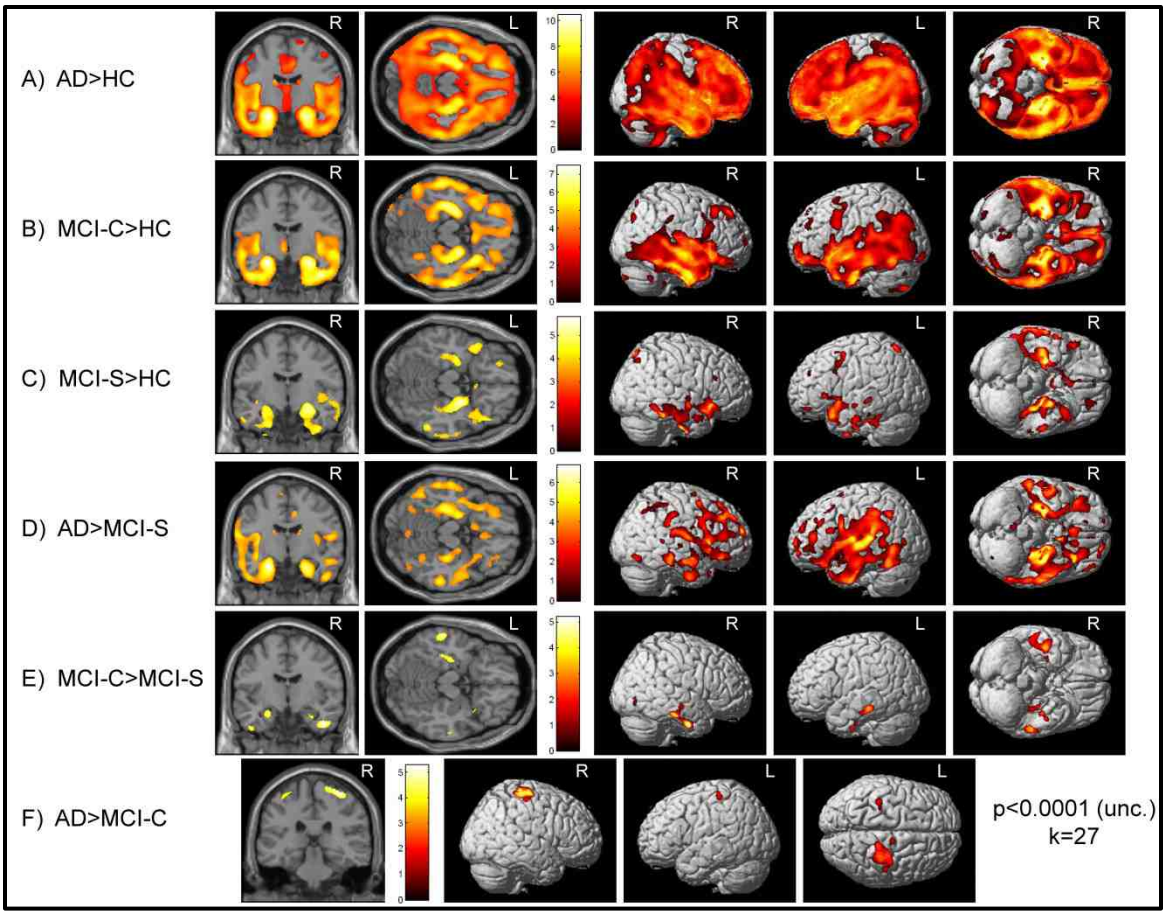

Figure 8. Group Differences in Global Reductions in Grey Matter (GM) Density over One Year in the ADNI Cohort

Comparisons between groups in the reduction in GM density from baseline to one-year in the ADNI cohort demonstrate significantly greater annual atrophy in patients relative to HC (n=643*; 143 AD, 57 MCI-C, 253 MCI-S, 190 HC). All comparisons of the interaction of time x diagnosis group are displayed at a threshold of $p<0.0001$ (uncorrected for multiple comparisons) with a minimum cluster size (k) = 27 voxels. Reverse comparisons showed no significant clusters at the established threshold. Cross-sections in (A-E) are (0, -9, 0, coronal) and (0, -23, -16, axial), left to right. Cross-section in (F) is (34, -29, 64, coronal). (*30 participants removed from comparisons due to failed image processing)

		AD (n=152)	MCI-C (n=60)	MCI-S (n=261)	HC (n=200)	ANOVA p-value	Significant Post-hoc Comparisons (p<0.05)
Hippocampal GM Density (Independent ROI)[a,b]	L	-4.50 (0.2)	-3.94 (0.4)	-2.09 (0.2)	-0.86 (0.2)	<0.001	HC>MCI-S>MCI-C, AD
	R	-4.50 (0.2)	-3.82 (0.4)	-2.23 (0.2)	-0.84 (0.2)	<0.001	HC>MCI-S>MCI-C, AD
Hippocampal GM Density (MarsBaR)[a,b]	L	-4.57 (0.2)	-4.02 (0.4)	-2.16 (0.2)	-0.97 (0.2)	<0.001	HC>MCI-S>MCI-C, AD
	R	-4.62 (0.2)	-4.05 (0.4)	-2.33 (0.2)	-0.85 (0.2)	<0.001	HC>MCI-S>MCI-C, AD
Hippocampal GM Volume (Independent ROI)[a,b]	L	-4.69 (0.2)	-4.58 (0.4)	-2.12 (0.2)	-1.17 (0.2)	<0.001	HC>MCI-S>MCI-C, AD
	R	-4.71 (0.2)	-4.33 (0.4)	-2.31 (0.2)	-1.09 (0.2)	<0.001	HC>MCI-S>MCI-C, AD
Hippocampal GM Volume (MarsBaR)[a,b]	L	-4.66 (0.2)	-4.55 (0.4)	-2.14 (0.2)	-2.24 (0.2)	<0.001	HC>MCI-S>MCI-C, AD
	R	-4.85 (0.3)	-4.55 (0.4)	-2.39 (0.2)	-1.07 (0.2)	<0.001	HC>MCI-S>MCI-C, AD
Hippocampal Volume (FreeSurfer)[b]	L	-4.12 (0.3)	-4.20 (0.5)	-2.55 (0.2)	-0.92 (0.3)	<0.001	HC>MCI-S>MCI-C, AD
	R	-3.76 (0.3)	-3.99 (0.5)	-2.74 (0.2)	-1.31 (0.3)	<0.001	HC>MCI-S, MCI-C, AD
EC Thickness (Freesurfer)[b]	L	-4.84 (0.5)	-6.08 (0.8)	-2.49 (0.4)	-0.76 (0.4)	<0.001	HC>MCI-S>MCI-C, AD
	R	-4.49 (0.5)	-3.86 (0.8)	-2.16 (0.4)	-0.69 (0.4)	<0.001	HC>MCI-C, AD; MCI-S>AD
Mean Frontal Cortical Thickness (Freesurfer)[b]	L	-1.57 (0.3)	-2.29 (0.4)	-0.94 (0.2)	-0.40 (0.2)	<0.001	HC, MCI-S>MCI-C; HC>AD
	R	-1.36 (0.2)	-1.91 (0.4)	-0.78 (0.2)	-0.56 (0.2)	<0.001	HC>MCI-C
Mean Parietal Cortical Thickness (Freesurfer)[b]	L	-2.14 (0.3)	-2.22 (0.4)	-1.17 (0.2)	-0.58 (0.2)	<0.001	HC>MCI-C, AD; MCI-S>AD
	R	-2.18 (0.3)	-2.28 (0.4)	-0.98 (0.2)	-0.60 (0.2)	<0.001	HC, MCI-S>MCI-C, AD
Mean Temporal Cortical Thickness (Freesurfer)[b]	L	-2.45 (0.2)	-3.11 (0.4)	-0.96 (0.2)	-0.62 (0.2)	<0.001	HC, MCI-S>MCI-C, AD
	R	-2.46 (0.2)	-2.81 (0.4)	-1.05 (0.2)	-0.49 (0.2)	<0.001	HC, MCI-S>MCI-C, AD
Mean Frontal GM Density (MarsBaR)[a,b]	L	-3.02 (0.2)	-2.47 (0.4)	-1.48 (0.2)	-0.65 (0.2)	<0.001	HC>MCI-S>AD; HC>MCI-C
	R	-2.91 (0.2)	-2.25 (0.4)	-1.37 (0.2)	-0.59 (0.2)	<0.001	HC>MCI-S>AD; HC>MCI-C
Mean Frontal GM Volume (MarsBaR)[a,b]	L	-2.92 (0.2)	-2.59 (0.6)	-1.46 (0.2)	-0.86 (0.2)	<0.001	HC, MCI-S>MCI-C, AD
	R	-2.84 (0.2)	-2.37 (0.4)	-1.36 (0.2)	-0.86 (0.2)	<0.001	HC>MCI-S>AD; HC>MCI-C
Mean Parietal GM Density (MarsBaR)[a,b]	L	-3.21 (0.3)	-2.40 (0.5)	-1.53 (0.2)	-0.51 (0.3)	<0.001	HC>MCI-S>AD; HC>MCI-C
	R	-3.02 (0.3)	-1.95 (0.5)	-1.41 (0.2)	-0.55 (0.3)	<0.001	HC, MCI-S>AD
Mean Parietal GM Volume (MarsBaR)[a,b]	L	-3.60 (0.3)	-2.71 (0.4)	-1.76 (0.2)	-0.90 (0.2)	<0.001	HC>MCI-S>AD; HC>MCI-C
	R	-3.64 (0.3)	-2.45 (0.5)	-1.51 (0.2)	-0.76 (0.3)	<0.001	HC>MCI-S>AD; HC>MCI-C
Mean Temporal GM Density (MarsBaR)[a,b]	L	-3.33 (0.2)	-2.81 (0.3)	-1.63 (0.1)	-0.76 (0.2)	<0.001	HC>MCI-S>MCI-C, AD
	R	-3.04 (0.2)	-2.66 (0.3)	-1.59 (0.1)	-0.65 (0.2)	<0.001	HC>MCI-S>MCI-C, AD
Mean Temporal GM Volume (MarsBaR)[a,b]	L	-3.32 (0.2)	-3.30 (0.3)	-1.52 (0.2)	-0.89 (0.2)	<0.001	HC>MCI-S>MCI-C, AD
	R	-3.14 (0.2)	-3.00 (0.3)	-1.52 (0.2)	-0.73 (0.2)	<0.001	HC>MCI-S>MCI-C, AD

[a] 30 participants excluded because of failed processing (9 AD, 3 MCI-C, 9 MCI-S, 9 HC)

[b] Covaried for baseline age, gender, education, handedness, and baseline ICV

Table 3. APC of Selected Imaging Biomarkers in the ADNI Cohort (Adjusted Mean (SE))

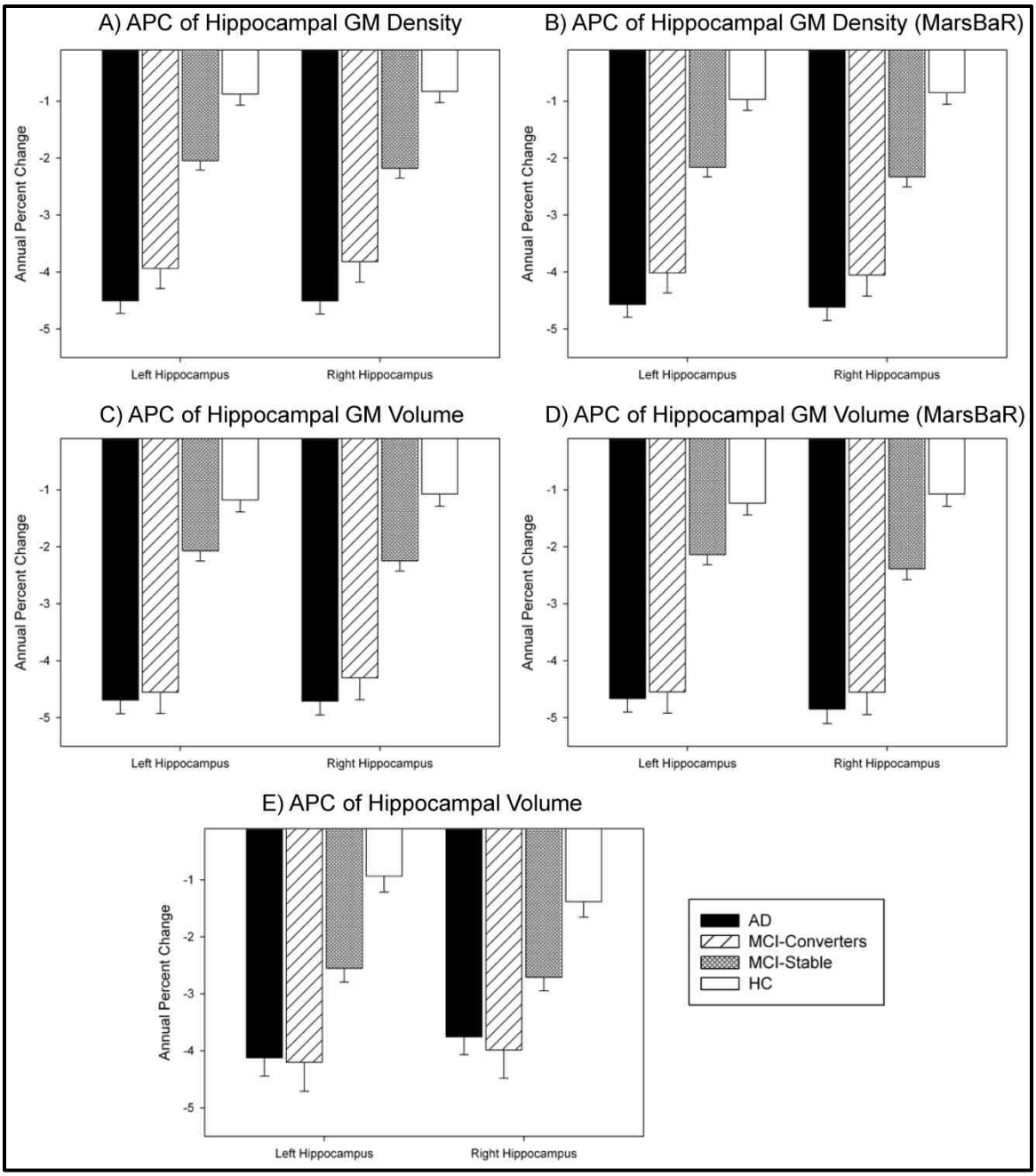

Figure 9. APC in Selected MTL Imaging Biomarkers

Plots of the mean APC in (A, B) hippocampal GM density and (C, D) GM volume extracted using left and right hippocampal ROIs extracted using a template derived on an independent sample of 40 healthy elderly controls [77, 267, 270] (A and C) and from MarsBaR (B and D) (n=643*; 143 AD, 57 MCI-C, 253 MCI-S, 190 HC). APC in hippocampal GM density and GM volume was significantly different among groups with AD and MCI-C participants showing greater faster atrophy rates than MCI-S and HC.

The APC in (E) hippocampal volume (n=673; 152 AD, 60 MCI-C, 261 MCI-S, 200 HC) extracted using Freesurfer showed a similar trend. See Table 3 for post-hoc comparison results. (*30 participants removed from comparisons due to failed image processing; group mean APC values (+/-SE) adjusted for baseline age, gender, education, handedness, and baseline total ICV are displayed)

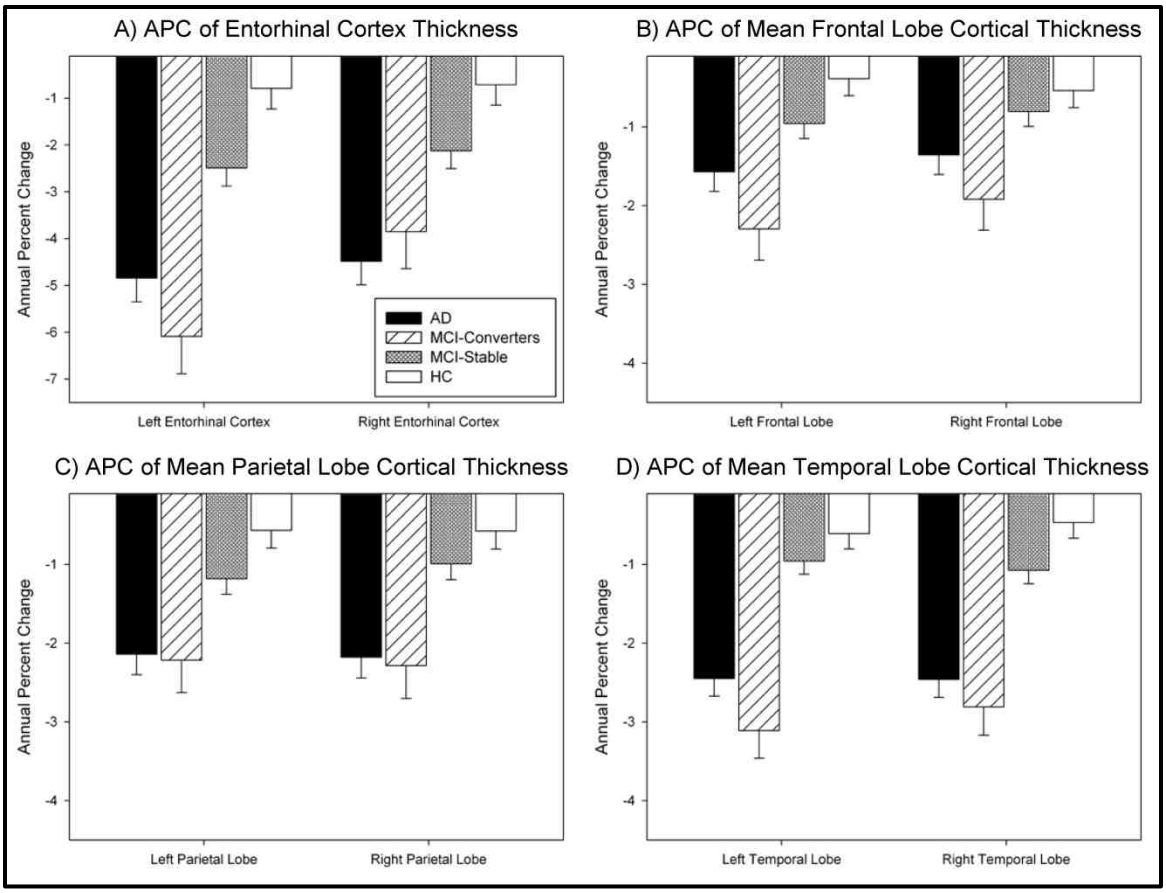

Figure 10. APC in Entorhinal Cortex and Mean Frontal, Parietal, and Temporal Lobe Cortical Thickness

APC in (A) entorhinal cortex thickness, and mean (B) frontal, (C) parietal, and (D) temporal lobar cortical thickness are significantly different across groups. See Table 3 for the results of post-hoc comparisons. (n=673; 152 AD, 60 MCI-C, 261 MCI-S, 200 HC; group mean APC values (+/-SE) adjusted for baseline age, gender, education, handedness, and baseline total ICV are displayed)

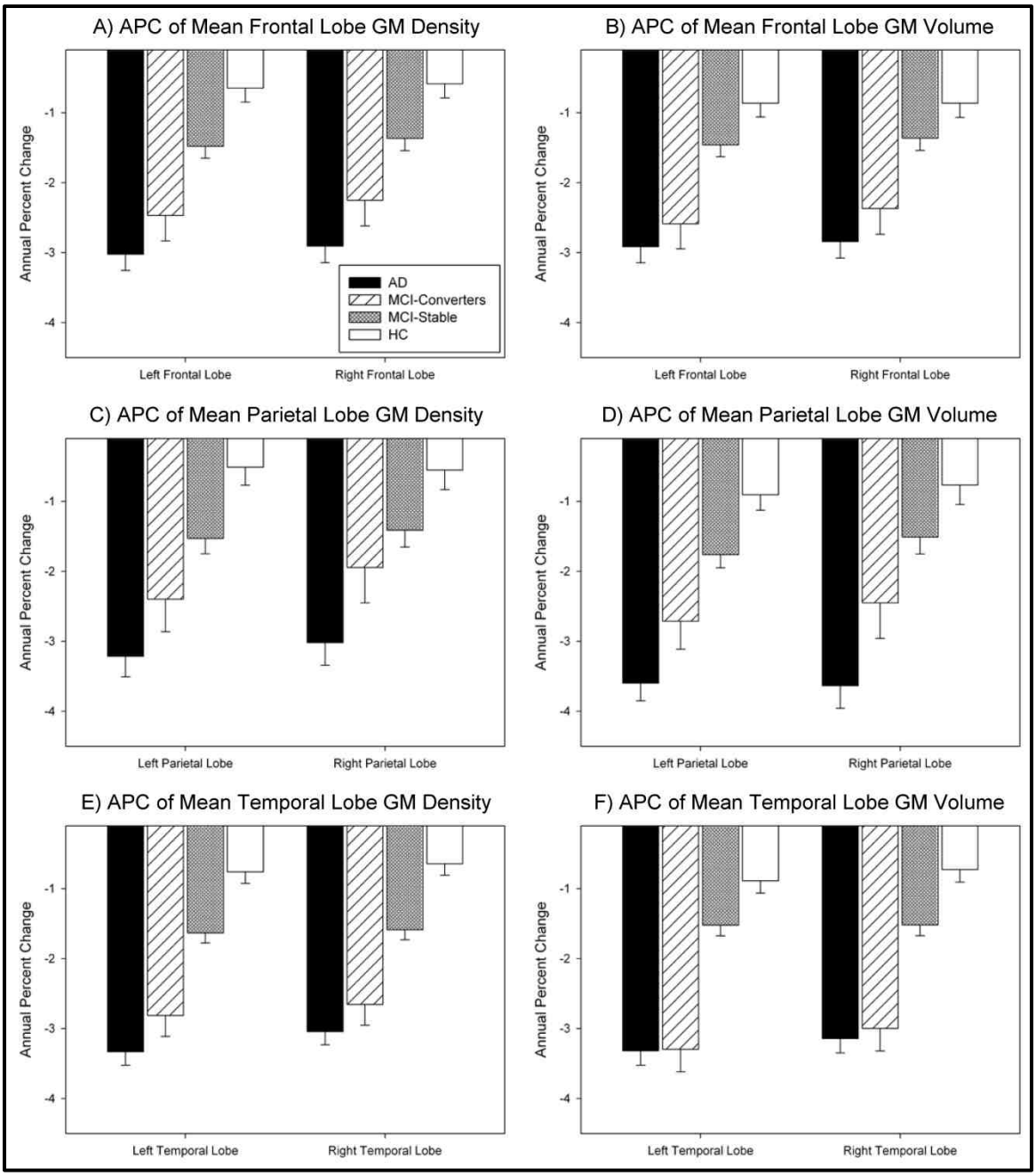

Figure 11. APC in Mean Frontal, Parietal, and Temporal Lobe GM Density and GM Volume

The APC in mean frontal lobe (A) GM density and (B) GM volume, mean parietal lobe (C) GM density and (D) GM volume, and mean temporal lobe (E) GM density and (F) GM volume are significantly different across groups. See Table 3 for results from post-hoc comparisons. (n=643*; 143 AD, 57 MCI-C, 253 MCI-S, 190 HC; *30

participants removed due to failed image processing; group mean APC values (+/-SE) adjusted for baseline age, gender, education, handedness, and baseline total ICV are displayed)

Sample Sizes

The sample size needed to detect a 25% reduction in 1-year change in MRI biomarkers was calculated for 80% or 90% power and a type I error (α) of $p<0.05$ for significant regions from the ANCOVA analysis (Table 4). Mean bilateral hippocampal GM density and GM volume estimates measured using either the independent sample or MarsBaR ROIs would require the smallest sample size to detect the desired reduction for all of the target groups. Other relatively sensitive ROIs for detecting a reduction in regional brain atrophy include hippocampal volume extracted using Freesurfer, mean temporal lobar GM density and GM volume, mean temporal lobe cortical thickness (MCI-C only), and mean frontal lobar GM density and GM volume. A full list of sample sizes needed to detect a 25% decline in brain atrophy at either 80% or 90% power for selected ROIs is found in Table 4.

	AD		MCI-C		MCI-S		HC	
Power:	0.8	0.9	0.8	0.9	0.8	0.9	0.8	0.9
Hippocampal GM Density (Independent ROI)	134	180	95	128	307	411	1243	1665
Hippocampal GM Density (MarsBaR ROI)	129	173	96	129	290	388	1204	1612
Hippocampal GM Volume (Independent ROI)	133	178	77	103	400	535	745	998
Hippocampal GM Volume (MarsBaR ROI)	135	181	74	100	378	507	767	1028
Hippocampal Volume (Freesurfer)	242	324	129	173	452	606	1136	1521
EC Thickness (Freesurfer)	328	439	214	286	1156	1548	7948	10648
Mean Frontal Lobe Cortical Thickness (Freesurfer)	1037	1389	369	494	2488	3333	4727	6333
Mean Parietal Lobe Cortical Thickness (Freesurfer)	629	842	515	689	1848	2475	3142	4209
Mean Temp. Lobe Cortical Thickness (Freesurfer)	403	539	121	162	1405	1882	3031	4061
Mean Frontal Lobe GM Density (MarsBaR ROIs)	284	381	222	297	788	1056	3682	4932
Mean Frontal Lobe GM Volume (MarsBaR ROIs)	280	376	263	353	856	1147	1475	1976
Mean Parietal Lobe GM Density (MarsBaR ROIs)	384	514	373	499	1437	1925	7260	9726
Mean Parietal Lobe GM Volume (MarsBaR ROIs)	238	319	315	422	976	1308	1977	2649
Mean Temp. Lobe GM Density (MarsBaR ROIs)	157	210	129	173	456	610	1850	2479
Mean Temp. Lobe GM Volume (MarsBaR ROIs)	158	212	100	134	646	866	1427	1911

Table 4. Sample Sizes Needed to Detect 25% Reduction in One-Year Change in Selected MRI Biomarkers

Effect Sizes

In order to effectively compare the relative sensitivity of MRI markers to distinguish between groups, we calculated the effect size for all available baseline and APC ROIs from VBM and Freesurfer for each group pair. Effect sizes for the comparison of AD and HC participants and MCI-C and MCI-S participants are found in Figure 12, while those for other pairs (MCI-C vs. HC; MCI-S vs. HC; AD vs. MCI-S; AD vs. MCI-C) are found in Figure 13. Baseline medial temporal lobe biomarkers, including EC thickness, hippocampal volume, and middle temporal gyri cortical thickness measures, had the highest effect sizes for the comparison of AD vs. HC (Figure 12A), with Cohen's d values of 1.846, 1.628, and 1.579, respectively. The APC in hippocampal GM density extracted using the MarsBaR ROIs had the highest effect size of the APC measures for AD vs. HC with a Cohen's d of 1.308.

Measures with maximal effect sizes for the comparison of MCI-C and MCI-S participants included APC in hippocampal GM volume (Figure 12B; independent sample ROI, Cohen's d=0.853; MarsBaR ROI, Cohen's d=0.852), APC in inferior temporal gyri GM volume (Cohen's d=0.842), and APC in mean temporal lobe GM volume (Cohen's d=0.830). Medial temporal lobe ROIs also had high effect sizes for some of the other comparisons with baseline hippocampal volume showing the highest effect sizes for MCI-C vs. HC (Figure 13A, Cohen's d=1.652) and MCI-S vs. HC (Figure 13B, Cohen's d=0.958), and baseline middle temporal gyri thickness having the highest effect size for AD vs. MCI-S (Figure 13C, Cohen's d=0.890). APC in superior parietal gyri GM volume demonstrated the highest effect size for AD vs. MCI-C with a Cohen's d of 0.456 (Figure 13D).

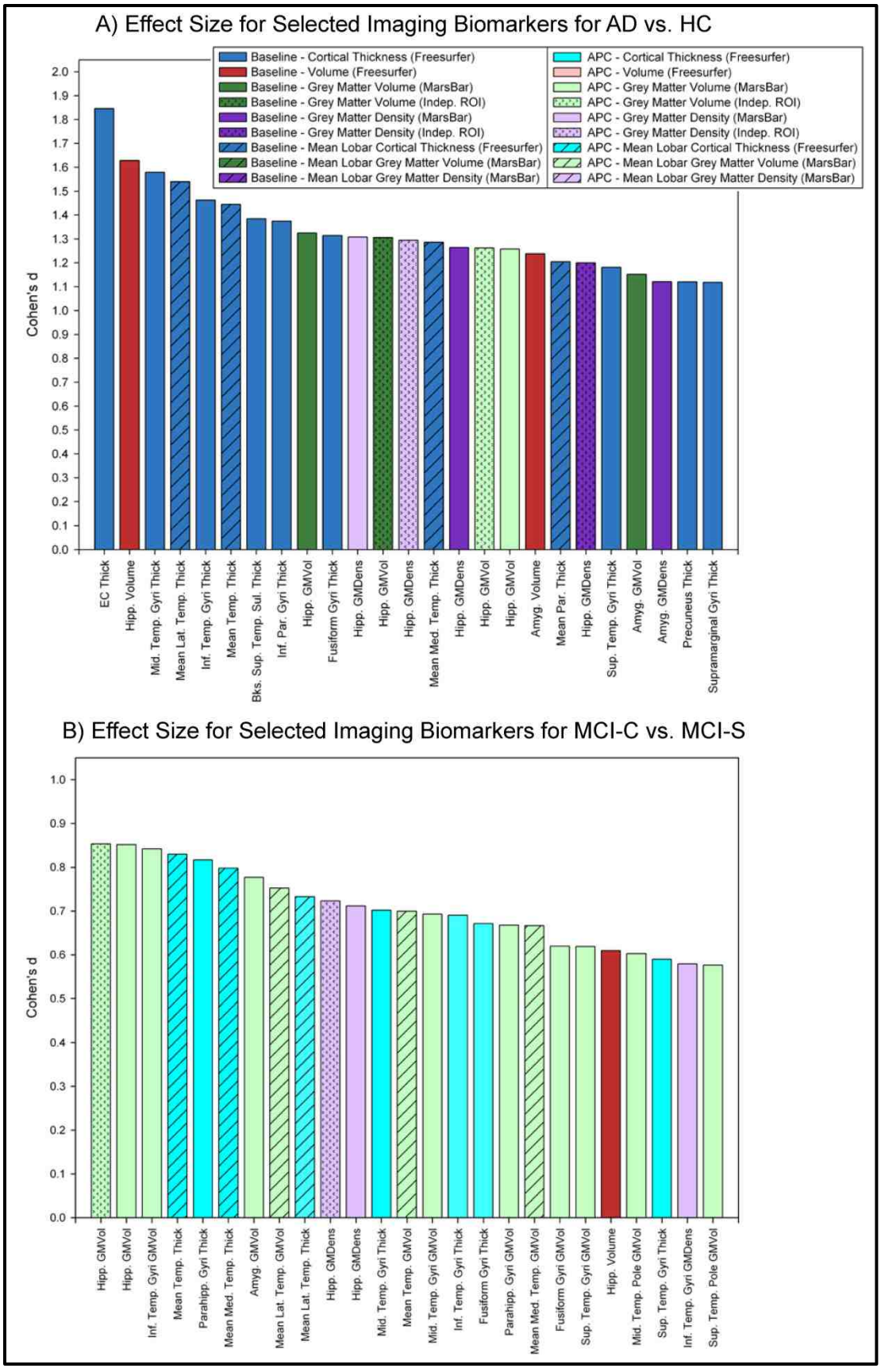
A) Effect Size for Selected Imaging Biomarkers for AD vs. HC
Baseline - Cortical Thickness (Freesurfer)
Baseline - Volume (Freesurfer)
Baseline - Grey Matter Volume (MarsBar)
Baseline - Grey Matter Volume (Indep. ROI)
Baseline - Grey Matter Density (MarsBar)
Baseline - Grey Matter Density (Indep. ROI)
Baseline - Mean Lobar Cortical Thickness (Freesurfer)
Baseline - Mean Lobar Grey Matter Volume (MarsBar)
Baseline - Mean Lobar Grey Matter Density (MarsBar)
APC - Cortical Thickness (Freesurfer)
APC - Volume (Freesurfer)
APC - Grey Matter Volume (MarsBar)
APC - Grey Matter Volume (Indep. ROI)
APC - Grey Matter Density (MarsBar)
APC - Grey Matter Density (Indep. ROI)
APC - Mean Lobar Cortical Thickness (Freesurfer)
APC - Mean Lobar Grey Matter Volume (MarsBar)
APC - Mean Lobar Grey Matter Density (MarsBar)
Cohen's d
EC Thick
Hipp. Volume
Mid. Temp. Gyri Thick
Mean Lat. Temp. Thick
Inf. Temp. Gyri Thick
Mean Temp. Thick
Bks. Sup. Temp. Sul. Thick
Inf. Par. Gyri Thick
Hipp. GMVol
Fusiform Gyri Thick
Hipp. GMDens
Hipp. GMVol
Hipp. GMDens
Mean Med. Temp. Thick
Hipp. GMDens
Hipp. GMVol
Hipp. GMVol
Amyg. Volume
Mean Par. Thick
Hipp. GMDens
Sup. Temp. Gyri Thick
Amyg. GMVol
Amyg. GMDens
Precuneus Thick
Supramarginal Gyri Thick
B) Effect Size for Selected Imaging Biomarkers for MCI-C vs. MCI-S
Cohen's d
Hipp. GMVol
Hipp. GMVol
Inf. Temp. Gyri GMVol
Mean Temp. Thick
Parahipp. Gyri Thick
Mean Med. Temp. Thick
Amyg. GMVol
Mean Lat. Temp. GMVol
Mean Lat. Temp. Thick
Hipp. GMDens
Hipp. GMDens
Mid. Temp. Gyri Thick
Mean Temp. GMVol
Mid. Temp. Gyri GMVol
Inf. Temp. Gyri Thick
Fusiform Gyri Thick
Parahipp. Gyri GMVol
Mean Med. Temp. GMVol
Fusiform Gyri GMVol
Sup. Temp. Gyri GMVol
Hipp. Volume
Mid. Temp. Pole GMVol
Sup. Temp. Gyri Thick
Inf. Temp. Gyri GMDens
Sup. Temp. Pole GMVol

Figure 12. Effect Sizes of Selected Imaging Biomarkers for Comparisons between AD and HC and MCI-C and MCI-S

The effect sizes for baseline and APC values for the comparison of (A) AD and HC participants and (B) MCI-C and MCI-S participants are shown. Baseline MTL regions had the greatest effect sizes when comparing AD and HC, while APC in MTL regions demonstrated the greatest effect sizes in the MCI-C vs. MCI-S comparison. (n=643*; 143 AD, 57 MCI-C, 253 MCI-S, 190 HC; *30 participants removed due to failed image processing; effect sizes are calculated from bilateral mean values of target ROIs adjusted for baseline age, gender, education, handedness, and baseline total ICV)

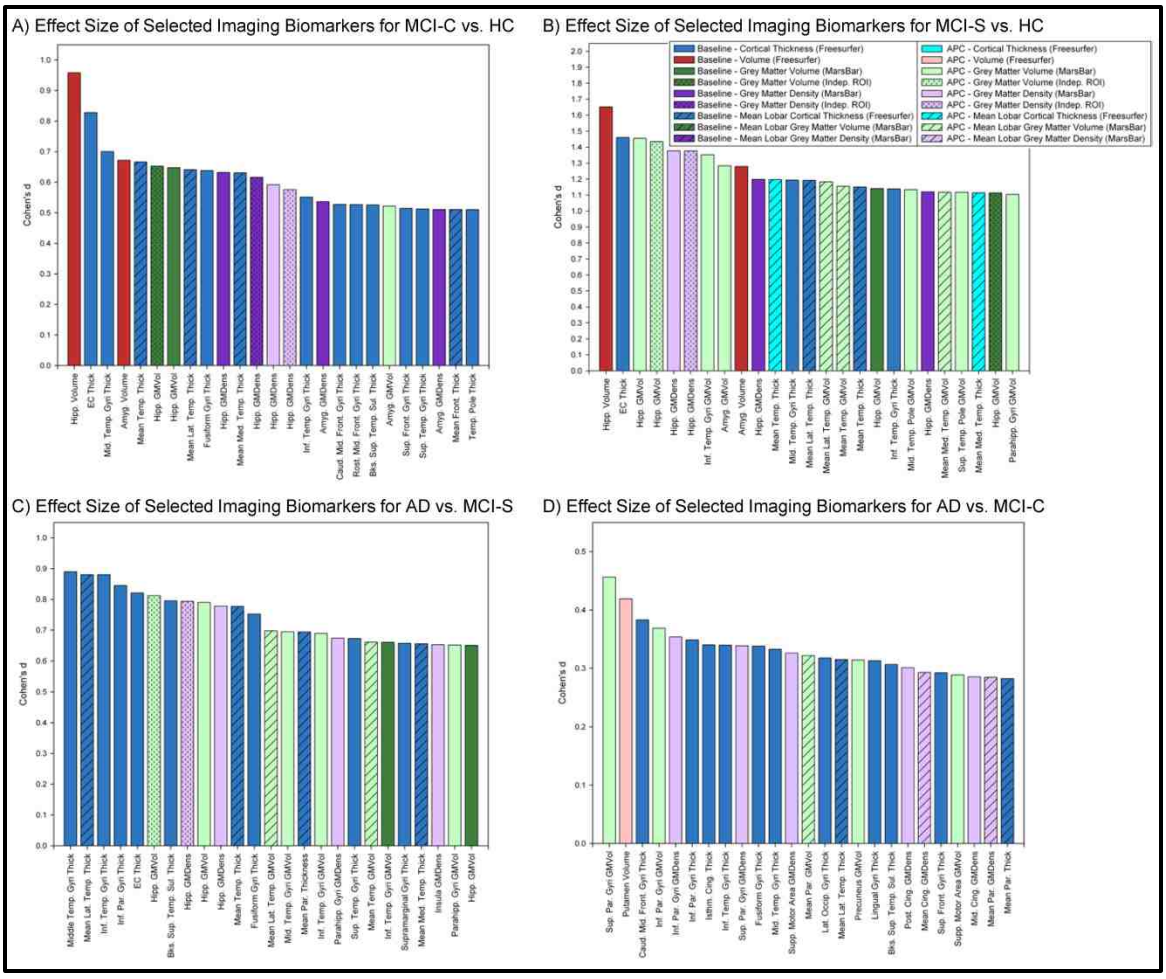

Figure 13. Effect Sizes of Selected Imaging Biomarkers for Comparisons of MCI-C vs. HC, MCI-S vs. HC, AD vs. MCI-S, and AD vs. MCI-C

The effect sizes for baseline and APC values for the comparison of (A) MCI-C vs. HC participants, (B) MCI-S vs. HC participants, (C) AD vs. MCI-S participants, and (D) AD vs. MCI-C participants are shown. (n=643*; 143 AD, 57 MCI-C, 253 MCI-S, 190 HC; *30 participants removed due to failed image processing; effect sizes are calculated from bilateral mean values of target ROIs adjusted for baseline age, gender, education, handedness, and baseline total ICV)

Influence of *APOE* ε4 Genotype

Participants with one or more *APOE* ε4 alleles showed increased atrophy rates in all evaluated measures, including hippocampal GM density ($p=0.001$, Figure 14A), hippocampal GM volume ($p<0.001$; Figure 14B), hippocampal volume ($p=0.001$; Figure 14C), and EC thickness ($p=0.003$; Figure 14D). Additionally, a significant interaction between diagnosis group and *APOE* ε4 genotype was observed for the APC in EC thickness ($p=0.029$). Subsequent analyses within diagnostic group demonstrated that for AD patients *APOE* ε4 carriers showed greater decline in hippocampal GM volume ($p=0.031$) and EC thickness ($p=0.002$). For MCI-C, *APOE* ε4 positive participants also showed greater rate of atrophy in hippocampal GM density ($p=0.031$) and GM volume ($p=0.001$). For the MCI-S group, the atrophy rate in all evaluated regions was greater in *APOE* ε4 positive than negative participants, including APCs for hippocampal GM density ($p=0.004$), hippocampal GM volume ($p<0.001$), hippocampal volume ($p=0.006$), and EC thickness ($p=0.004$). Finally, *APOE* ε4 positive HC participants showed a significantly greater APC in hippocampal volume than those who were *APOE* ε4 negative ($p=0.004$).

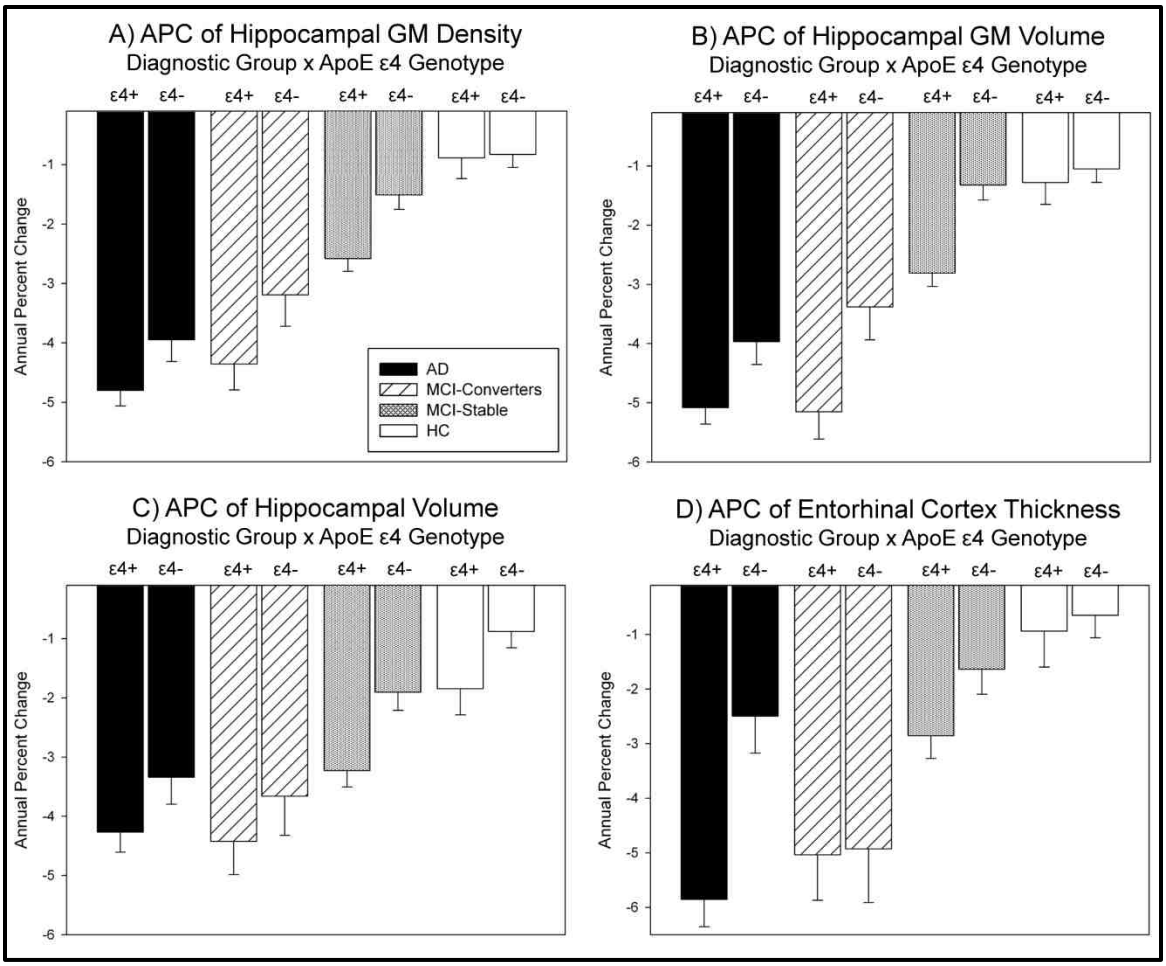

Figure 14. Impact of *APOE* ε4 Genotype on APC in Selected MTL Measures

The APC in bilateral mean hippocampal (A) GM density and (B) GM volume (n=643*; 143 AD, 57 MCI-C, 253 MCI-S, 190 HC), extracted using an independent sample of 40 healthy elderly controls [77, 267, 270], as well as (C) hippocampal volume, and (D) EC thickness extracted using automated parcellation (n=673; 152 AD, 60 MCI-C, 261 MCI-S, 200 HC) show a significant effect of both diagnostic group and *APOE* ε4 genotype. (*30 participants removed due to failed image processing; group mean (+/- SE) APC values adjusted for baseline age, gender, education, handedness, and baseline total ICV are displayed)

Discussion

Our main goal was to assess a detailed panel of longitudinal MRI atrophy markers in the ADNI cohort, including in patients with probable AD, MCI to probable AD converters (within one year), stable MCI (over one year) and healthy control participants. Our main findings were that AD and MCI-C groups had a significantly higher rate of annual decline than MCI-S and HC participants in global and hippocampal GM density and GM volume, hippocampal total volume, EC thickness, and mean frontal, parietal and temporal lobar GM density, GM volume and cortical thickness measures. Sample size calculations indicated that hippocampal GM density and GM volume required the smallest samples to detect a 25% reduction in rate of regional brain atrophy. Finally, effect size estimates indicated that dynamic measures, including APC in MTL volumes and cortical thickness, showed the greatest difference between MCI-C and MCI-S participants. However, baseline hippocampal volume and GM density, as well as baseline temporal lobe cortical thickness measures, demonstrated the greatest effect size when comparing AD and HC participants. This pattern suggests that different structural MRI markers may have differential utility as a function of stage of disease and/or role within a clinical trial. Where hippocampal volume and GM density are powerful tools for assessing baseline neurodegeneration, annual change rate in MTL volumes and cortical thickness may be most useful for comparing stable vs. rapidly progressing individuals, and may be the best choice for surrogate markers in trials of disease modifying agents.

Our estimates of APC in hippocampal volume, including -3.95% for AD patients, -4.10% for MCI-C participants, -2.65% for MCI-S participants, and -1.12% for HC, were similar to estimates from previous reports in the ADNI cohort, as well as other samples (Table 3; [201]). These results demonstrate a significantly accelerated rate of brain atrophy in participants diagnosed with AD, as well as those who show rapid clinical decline from MCI to probable AD. Participants who show stable clinical diagnoses (both MCI and HC) also show relatively stable brain volume and cortical thickness measures, as well as minimal change in psychometric variables (Table 2).

We examined the influence of *APOE* ε4 genotype on annual atrophy rate in selected MTL MRI markers given the mixed prior findings, including significant effects of *APOE* on brain atrophy in some reports [300-301], whereas others found no effect [306-307]. In the present study, we observed a modest but significant effect of *APOE* ε4 genotype on annualized hippocampal and EC atrophy rates. This effect was maximal in MCI-S participants, with ε4 positive participants demonstrating significantly greater APC in all measures evaluated. However, the effect of *APOE* genotype in AD and MCI-C groups was only observed on some measures, suggesting a more moderate yet still detectable effect of genotype. Finally, *APOE* ε4 positive HC participants showed a faster rate of atrophy relative to ε4 negative participants only on hippocampal volume. Our results support the complicated nature of the relationship between *APOE* genotype and MRI markers of neurodegeneration and suggest that the magnitude of the effect may differ by diagnostic stage, as has been previously reported in the ADNI cohort [305, 311]. Future studies will further characterize the impact of *APOE*, as well as that of variation in other candidate genes, on MRI and other ADNI biomarkers, which may assist in elucidating the role of genetic factors in the neuropathology of AD [328].

This report adds to the body of research demonstrating the utility of MRI metrics in detecting and monitoring atrophy associated with AD and MCI, and extends prior research by focusing on identifying differences between rapidly declining MCI to probable AD converters and individuals with a relatively stable MCI diagnosis. Reports in other smaller samples have led to similar conclusions regarding the utility of MRI measures of global and local brain volume, cortical thickness, and morphometry in detecting and monitoring brain atrophy associated with AD and MCI [195-197, 199-200, 204, 206, 218-220, 295, 329]. As previously reported in the ADNI sample, baseline values of hippocampal GM density and volume, amygdalar volume, EC thickness, and temporal and parietal lobe cortical thickness measures are significantly different between MCI-C and MCI-S participants [213]. In fact, MCI-C and AD participants show nearly equivalent atrophy at baseline, up to one year prior to equivalent clinical

diagnoses, indicating that MRI can serve as an antecedent biomarker. Measures of annual decline provide further evidence that MCI to AD converters have characteristic cross-sectional and longitudinal brain atrophy more similar to AD patients than to stable MCI patients. The different longitudinal phenotypes warrant investigation and may be useful in examining genetic variation associated with rate of decline [300, 330].

Our results are generally consistent with previous reports using subsets of the ADNI cohort and alternative methods. Four studies employed Freesurfer based ROI techniques to estimate APC in selected cortical and subcortical regions and reported similar APC values and differences between diagnostic groups as those observed in the present analysis [316, 319-320, 323]. Furthermore, two of these studies divided the MCI group by baseline CDR-SB [323] and by atrophy pattern (AD-like vs. HC-like, [316]) and showed variability of APC values within the MCI group similar to that seen in the present report between MCI-C and MCI-S participants. Two studies used various hippocampal ROIs and reported significantly greater APC in hippocampal volume in AD participants relative to MCI and HC participants [304-305]. Two studies examined changes in ventricular volume, demonstrating greater rates of ventricular enlargement in AD and MCI participants relative to HC, as well as greater ventricular enlargement in participants who converted from MCI to probable AD within the first 6 months of the study relative to stable MCI patients [127, 311]. Three additional studies employed tensor-based morphometry (TBM) and Jacobian maps to investigate whole brain and temporal lobe atrophy rates and found a similar pattern of differences between participants as seen in the present study [318, 321-322]. One of these studies also reported a higher rate of atrophy in MCI-C relative to MCI-S participants, albeit in a significantly smaller sample (7 MCI-C and 32 MCI-S) than used in the present analysis [322]. Misra *et al*. (2009) also reported significant differences in atrophy rate between MCI-C and MCI-S participants using a VBM-like technique (RAVENS), although differences were limited to periventricular WM and the temporal horn [282]. Finally, another study used a boundary shift integral (BSI) technique to evaluate annual rates of whole

brain atrophy and ventricular enlargement [317]. This study reported greater annual rates of whole brain atrophy and ventricular enlargement in AD participants relative to MCI and HC participants, as well as in MCI-C relative to MCI-S participants. In fact, Evans *et al.* (2009) noted that MCI-C demonstrated nearly equivalent rates of atrophy as seen in the AD participants, similar to the pattern reported in the present study. Overall, the results of the present study extend this line of research by providing one of the first direct comparisons of annual atrophy rates for an ensemble of state-of-the-art MRI morphometric, volumetric, and cortical thickness variables in the ADNI cohort, particularly focusing on participants who converted from MCI to AD within the first year of the study.

There are several limitations of the present study. First, we were unable to account for some other variables which may have impacted the results. Since ADNI is an observational study, many participants were taking a number of medications prescribed for AD or other conditions that could have affected the results. Additionally, differences in disease severity beyond clinical diagnostic classification (i.e., AD, MCI, or HC) were not considered in the present analyses. Although diagnostic classification and conversion status incorporate information from psychometric performance, the present report does not explicitly examine the relationship between changes in MRI variables and changes in psychometric performance. Secondly, the inclusion of only two timepoints separated by approximately one year in the present study limited the specificity and accuracy of the APC estimations. One of the major advantages of the ADNI project is the extensive longitudinal data collection. Therefore, as full datasets from the two-year and three-year timepoints become available, we plan to expand our analysis of annual atrophy rates in patients with AD, MCI-C, MCI-S, and healthy older adults. Furthermore, we will employ more advanced statistical modeling to compare the atrophy rates between MCI-C from several timepoints. With 3 or more timepoints any potential non-linearities in longitudinal decline can be detected. Finally, this study was limited by the nature of the methods employed to measure atrophy. Specifically, some variability in segmentation and extraction

of ROIs is likely, based on the interaction between scan quality or other properties and specific image processing algorithms, which may have resulted in variation in the accuracy of the annual change estimates. However, the largely automated methodology employed in these analyses provides for little or none of the rater bias which is inherent in manually directed tools of volume extraction. Furthermore, other analysis techniques (e.g., TBM, BSI) may provide additional and complementary information to that extracted in the present study using VBM and automated parcellation. Although a comprehensive and direct comparison of the relative sensitivity and specificity of target MRI-based atrophy measures extracted using different methods has not been completed to our knowledge, ADNI provides an ideal cohort for investigating this issue.

In summary, these results used a combination of analysis methods to confirm that MRI based morphometric markers detect higher rates of brain atrophy in patients with AD and MCI compared to controls and are highly sensitive to clinical progression with one year. Measures of GM density change within medial and lateral temporal regions have been employed less than volumetric measures to date but appear particularly promising and complementary to more standard measures such as hippocampal volumetry. The sensitivity of automated and unbiased methods for detecting differences in rate of neurodegenerative changes encourages their use in clinical trials of disease modifying agents and in prevention trials.

Acknowledgments

Data collection and sharing for this project was funded by the Alzheimer's Disease Neuroimaging Initiative (ADNI) (National Institutes of Health Grants U01 AG024904 and RC2 AG036535, PI: Michael W. Weiner, MD). ADNI is funded by the National Institute on Aging, the National Institute of Biomedical Imaging and Bioengineering, and through generous contributions from the following: Abbott; AstraZeneca AB; Bayer Schering Pharma AG; Bristol-Myers Squibb; Eisai Global Clinical Development; Elan Corporation; Genentech; GE Healthcare; GlaxoSmithKline; Innogenetics; Johnson and Johnson; Eli Lilly and Co.;

Medpace, Inc.; Merck and Co., Inc.; Novartis AG; Pfizer Inc.; F. Hoffman-La Roche; Schering-Plough; Synarc, Inc.; and Wyeth; as well as non-profit partners the Alzheimer's Association and Alzheimer's Drug Discovery Foundation; with participation from the U.S. Food and Drug Administration. Private sector contributions to ADNI are facilitated by the Foundation for the National Institutes of Health (www.fnih.org). The grantee organization is the Northern California Institute for Research and Education, and the study is coordinated by the Alzheimer's Disease Cooperative Study at the University of California, San Diego. ADNI data are disseminated by the Laboratory for Neuro Imaging at the University of California, Los Angeles. This research was also supported by NIH grants P30 AG010129, K01 AG030514, and the Dana Foundation. The National Cell Repository for Alzheimer's Disease (NIH grant U24 AG021886) provided support for DNA and cell line banking and processing for ADNI.

Data analysis was supported in part by the following grants from the National Institutes of Health: NIA R01 AG19771 to AJS and P30 AG10133-18S1 to B. Ghetti and AJS, and NIBIB R03 EB008674 to LS; and by the Indiana Economic Development Corporation (IEDC #87884 to AJS). The Freesurfer analyses were performed on a 112-node parallel computing environment called Quarry at Indiana University. We thank the University Information Technology Services at Indiana University and Randy Heiland, MA, MS for their support.

Informed consent was obtained from all ADNI participants and necessary approval was received from Ethical Committees by each of the participating research institutions. Further information about ADNI can be found in Jack *et al.* (2008), Mueller *et al.* (2005a, 2005b) [250-251, 324], and at www.adni-info.org.

Chapter 2b: Longitudinal MRI Biomarkers in a pre-MCI Stage

The next chapter evaluates the use of cross-sectional and longitudinal MRI measures of neurodegeneration in a pre-MCI stage, namely older adults with cognitive complaints (CC) but without significant cognitive impairment. For this report, data from a cohort of older adults in a longitudinal study on neuroimaging and brain aging at Dartmouth Medical School (PI: Dr. Andrew Saykin) were analyzed. Longitudinal MRI, clinical, and neuropsychological test data from two visits, with the follow-up visit approximately two years after the initial visit, were assessed. Participants included patients with a stable diagnosis of probable AD, patients with a diagnosis of MCI at baseline who converted to probable AD (MCI-Converters (MCI-C)), patients with a stable diagnosis of MCI (MCI-Stable (MCI-S)), older adults with cognitive complaints but no significant cognitive deficits at baseline who converted to a diagnosis of MCI (CC-Converters (CC-C)), older adults with cognitive complaints who were stable (CC-Stable (CC-S)), and stable healthy older controls without significant cognitive complaints (HC). MRI scans were analyzed using the methods discussed in Chapters 1 and 2a, including regional grey matter (GM) density and volume data from voxel-based morphometry (VBM) and MarsBaR regions of interest (ROIs) and regional volumetric and cortical thickness data from automated parcellation (Freesurfer version 4). We assessed both baseline and two-year annualized percent change (APC) for selected temporal lobe ROIs. In addition, we calculated the effect sizes of baseline and APC measures for the differences between converters and stable participants (MCI-C vs. MCI-S, CC-C vs. CC-S). Finally, we evaluated the relationship between hippocampal atrophy rate and two-year change in clinical and psychometric performance variables.

We observed significant differences among groups in temporal lobe ROIs both at baseline and in two-year annualized atrophy rate. Similar to the previous reports (Chapters 1 and 2a), patients with MCI and AD show greater cross-sectional atrophy and faster atrophy rates in the temporal lobe than HC. MCI-C show more baseline atrophy and faster annualized atrophy rates than MCI-S, although these differences were not significant (likely due to a small sample

size). The novel findings of the present report concern the CC group. Patients who convert from CC to MCI show slightly more atrophy at baseline and faster rates of atrophy in the temporal lobe relative to those who have a stable CC diagnosis. This is the first report to date to evaluate differences in neuroimaging biomarkers between CC-C and CC-S. We also observed that atrophy rate estimates of medial temporal lobe regions are the most sensitive to differences between converter and stable participants. Finally, there was a significant relationship between two-year change in clinical dementia severity and hippocampal atrophy rate in the full cohort, but not in the sub-group of participants with a CC diagnosis at baseline. However, two-year change in memory performance was significantly associated with hippocampal atrophy rate in both the full cohort and the CC at baseline sub-group.

Introduction

Alzheimer's disease (AD) is the most common age-related neurodegenerative disease, affecting more than 25 million people over the age of 60 [1, 249, 331]. AD is characterized pathologically by the accumulation of extracellular amyloid plaques, intracellular neurofibrillary tangles of hyperphosphorylated tau protein, and progressive and widespread neuronal death and brain atrophy [10-11]. Clinically, patients with AD show significantly impaired cognition in memory and other cognitive domains, resulting in dementia and an inability to perform normal daily activities [63].

AD is thought to develop over years or decades, beginning with the accumulation of amyloid and hyperphosphorylated tau, followed by the widespread neurodegeneration and finally the emergence of the clinical syndrome [17]. The most commonly recognized early clinical stage of AD is mild cognitive impairment (MCI) [68, 293]. Patients with MCI show significantly impaired cognition without significant disruption of activities of daily living [64, 68]. MCI patients with a primary deficit in memory are termed "amnestic MCI" and have a much greater risk of progressing to AD than normal older adults (10-15% annual conversion to probable AD in amnestic MCI vs. 1-2% in healthy older adults) [67].

Recently earlier stages of AD than MCI have been explored, although their definitions differ by research group. Some researchers have focused on cognitively healthy older adults with significant AD neuropathology (i.e., amyloid deposition) and have shown these patients to be a higher risk for progression to MCI and AD [14, 71]. Other researchers define early AD stages and at-risk patients by genetic background (i.e., apolipoprotein E (*APOE*) ε4 status) and/or family history of AD [74, 298, 332-336]. Finally, patients who have significant complaints about their cognition, even in the absence of cognitive deficits, may also represent an early stage of AD. In fact, cognitive complaints have repeatedly been shown to be associated with future cognitive decline in memory and progression to dementia [76, 78-79, 337-341], even in the absence of depression or measurable cognitive impairment at baseline. In addition, older adults with

cognitive complaints (particularly memory complaints) show AD-like neuropathology using neuroimaging, including significant neurodegeneration measured using structural magnetic resonance imaging (MRI) [76-77, 342-345], altered white matter integrity measured using diffusion tensor imaging (DTI) [345], and changes in brain function both at rest and during cognitive tasks using positron emission tomography (PET) [337, 346]. These reports highlight preliminary evidence that preclinical stages of AD exist and are identifiable using biomarkers before the diagnosis of MCI can be made. Additional investigation into the preclinical stages of AD is still needed to further characterize the clinical course of these patients. The identification and understanding of preclinical AD stages is important because effective therapeutic interventions are likely to be maximally effective in the earliest stages of disease.

In the present study, we sought to characterize longitudinal outcomes and associated brain atrophy over two years of euthymic older adults with cognitive complaints (CC), patients with MCI and AD, and healthy older adults without cognitive complaints (HC). We divided our sample by baseline and two-year follow-up diagnoses resulting in six groups, including patients with a stable diagnosis of AD, patients who converted from MCI to probable AD (MCI-Converters (MCI-C)), patients with a stable diagnosis of MCI (MCI-Stable (MCI-S)), participants with a CC diagnosis at baseline who converted to MCI (CC-Converters (CC-C)), participants with a stable diagnosis of CC (CC-Stable (CC-S)), and stable healthy older adults without complaints (HC). In this report, we evaluated: (1) baseline differences among groups in brain atrophy of selected MRI measures of volume and grey matter (GM) density; (2) differences among groups annualized rate of atrophy (annualized percent change (APC)) over two years in selected MRI volumetric and GM density measures; (3) the relative sensitivity measured by effect size (Cohen's d) of baseline and APC measures to differences between converter and stable groups (MCI-C vs. MCI-S, CC-C vs. CC-S); and, (4) the relationship between selected MRI measures of APC and two-year change in clinical dementia severity and memory performance in the entire sample and within all participants with a CC diagnosis at baseline. The

goal of these analyses is to characterize MRI measures of neurodegeneration as biomarkers for AD in participants with cognitive complaints but no cognitive impairment.

Methods

Participants

Participants with baseline and a minimum of two-year follow-up data, including successfully processed structural MRI scans and clinical and neuropsychological test scores, were selected from a cohort of patients with probable AD and MCI, older adults with subjective and informant-verified cognitive complaints (CC), and older adults without cognitive complaints (HC) that has been described previously [77, 344-345, 347-348]. Briefly, participants were recruited for a study on neuroimaging and brain aging from Dartmouth Hitchcock Medical Center and the surrounding community. Participants were initially screened by phone and those meeting criteria underwent a comprehensive protocol of structural and functional MRI scans, diffusion tensor imaging (DTI), clinical interview and extensive neuropsychological testing, and other measures (e.g., blood panel, targeted genetic assessment). Inclusion and exclusion criteria, as well as complete details of clinical and psychometric tests used to characterize cognitive deficits and complaints, have been previously described [77]. All participants included in this report underwent our protocol of neuroimaging and clinical and psychometric testing at least annually, and were therefore seen a minimum of three times over the two-year follow-up period.

For the present analysis, 82 participants were divided into six groups by baseline and two-year follow-up clinical diagnosis, including patients with stable AD over the two-year follow-up period (n=4; AD), patients who converted from MCI to probable AD over the two-year follow-up period (n=5, MCI-Converters (MCI-C)), patients with a stable MCI diagnosis during the two-year follow-up window (n=21, MCI-Stable (MCI-S)), older adults with significant cognitive complaints at the baseline visit who converted to MCI during the two-year follow-

up period (n=4,CC-Converters (CC-C)), older adults with a stable CC diagnosis for the two-year follow-up period (n=19, CC-Stable (CC-S)), and healthy older adults without any significant cognitive complaints at the baseline visit or at any time during the two-year follow-up period (n=29, HC). Any participants who did not fall into these groups (e.g., participants who converted from HC to CC, participants who reverted from AD to MCI, MCI to CC, or CC to HC) were excluded from the present analyses. In addition, any participants with incomplete clinical and/or neuroimaging data were excluded.

Structural Magnetic Resonance Imaging (MRI) Scans

Structural SPGR MRI scans were collected annually for a minimum of two years at Dartmouth-Hitchcock Medical Center using a GE Signa 1.5 Tesla Horizon magnet, as previously described [77]. Scans were processed using voxel-based morphometry (VBM) in SPM5 [145-146, 253] and Freesurfer version 4 [142-144, 268] as described below and in previous reports [213, 270, 291].

VBM: Baseline MRI scans were converted from DICOM to NIfTI format and aligned to a standard T1-weighted template image. All follow-up scans were aligned to the T1-aligned baseline image for each participant. All scans were then segmented with bias correction into grey matter (GM), white matter (WM) and cerebrospinal fluid (CSF) compartments using standard VBM templates in SPM5. Finally, all scans were normalized with and without modulation as 1 x 1 x 1 mm voxels to Montreal Neurologic Institute (MNI) standard space and smoothed with a 10mm FWHM Gaussian kernel. Quality control (QC) of VBM processing was done at each step of the processing and scans which failed segmentation were excluded from all analyses. Unmodulated and modulated normalized GM maps were then used to extract GM density (unmodulated) and GM volume (modulated) estimates for regions of interest (ROIs) using MarsBaR [325].

Automated parcellation: All scans were independently processed using Freesurfer version 4. More than 100 ROIs, including more than 50 volumetric and 50 cortical surface thickness measures, were extracted. In addition, total

intracranial volume (ICV), which was used as a covariate in many subsequent statistical analyses, was generated using Freesurfer.

Annualized Percent Change (APC) Calculations

Atrophy rate in target ROIs was assessed using annualized percent change (APC) calculated using the baseline and two-year follow-up scans as follows. First, estimates for target ROIs from the baseline and two-year follow-up scans generated using Freesurfer and VBM/MarsBaR were extracted. Then, the annualized percent change (APC) was calculated for each measure using the following formula:

$$\textit{Annualized percent change (APC)} = \frac{\dfrac{\textit{(two-year ROI estimate – baseline ROI estimate)}}{\textit{baseline ROI estimate}}}{\textit{(Time (in years) between baseline and two-year visits)}}$$

For all participants, if either the baseline or two-year follow-up scan failed QC then that individual was excluded from all APC analyses (n=4).

Statistical Analyses

Baseline and APC estimates for selected ROIs were compared among groups defined by baseline diagnosis and two-year clinical conversion using an analysis of covariance (ANCOVA). Age at baseline scan, gender, years of education, and baseline total ICV were included as covariates in all analyses. Due to the known relationship of depressive symptoms with cognitive complaints, the analyses were also evaluated with the Geriatric Depression Scale (GDS) total score as a covariate. However, no significant effects of GDS on either baseline or APC in target ROIs were observed (*data not shown*). Therefore, the results presented here do not include GDS total as a covariate. For all ROI analyses, post-hoc comparisons with a Bonferroni correction for multiple comparisons, as implemented in SPSS as an adjusted p-value, were utilized to compare specific group differences.

ROIs known to be sensitive to neurodegeneration associated with AD were evaluated, including hippocampal volume, mean temporal lobe cortical thickness, mean medial temporal lobe cortical thickness, mean lateral temporal lobe cortical thickness, hippocampal GM density and GM volume, mean temporal lobe GM density and GM volume, mean medial temporal lobe GM density and GM volume, and mean lateral temporal lobe GM density and GM volume. Baseline and APC estimates of the mean occipital lobe GM density and GM volume were evaluated as control regions. Participants were excluded from all analyses if the baseline MRI processing did not meet QC standards. Four participants (1 MCI-S, 2 CC-S, 1 HC) were included in the baseline analyses but excluded from APC analyses due to failed QC of two-year follow-up MRI processing. Thus, 82 participants were included in the baseline analyses (4 AD, 5 MCI-C, 21 MCI-S, 4 CC-C, 19 CC-S, 29 HC) and 78 participants were included in the analyses of APC measures (4 AD, 5 MCI-C, 20 MCI-S, 4 CC-C, 16 CC-S, 29 HC).

For the cortical thickness analyses, mean lobar regions included the following Freesurfer-generated ROIs: mean temporal lobe cortical thickness included estimates from the banks of the superior temporal sulcus, entorhinal cortex, fusiform gyrus, lingual gyrus, parahippocampal gyrus, and inferior, middle and superior temporal gyri, as well as the temporal pole and transverse temporal pole; mean medial temporal lobe cortical thickness included estimates from the entorhinal cortex, fusiform gyrus, lingual gyrus, parahippocampal gyrus, temporal pole, and transverse temporal pole; and mean lateral temporal lobe cortical thickness included estimates from the banks of the superior temporal sulcus, and the inferior, middle and superior temporal gyri. For the GM density and GM volume mean lobar estimates, the following VBM/MarsBaR ROIs were included: mean temporal lobe GM density and GM volume included estimates from the amygdala, fusiform gyrus, Heschl's gyrus, hippocampus, lingual gyrus, olfactory gyrus, parahippocampal gyrus, and inferior, middle and superior temporal gyri, as well as the inferior and superior temporal poles; the mean medial temporal lobe GM density and GM volume estimates included the amygdala, fusiform gyrus,

Heschl's gyrus, hippocampus, lingual gyrus, olfactory gyrus, parahippocampal gyrus, and the inferior and superior temporal poles; the mean lateral temporal lobe GM density and GM volume estimates included the inferior, middle and superior temporal gyri; and the mean occipital lobar GM density and GM volume measures included estimates from the calcarine gyrus, cuneus, and the inferior, middle, and superior occipital gyri. No significant lateralized differences were observed so bilateral mean estimates of the selected ROIs were used in all statistical analyses.

An ANCOVA model was also used to assess continuous demographic variables, as well as baseline and two-year change in psychometric performance. Age at baseline visit, gender, and years of education were included as covariates in all statistical models assessing psychometric performance. Post-hoc comparisons with a Bonferroni correction for multiple comparisons were also evaluated for all variables of interest. A chi-square test was used to evaluate differences among groups in dichotomous demographic variables. Clinical and psychometric tests evaluated included: the Clinical Dementia Rating (CDR) Scale Global score (CDR-GL) and Sum of Boxes score (CDR-SB) [276]; the Mini-Mental Status Exam (MMSE) total score [274-275]; the Dementia Rating Scale-2 (DRS) total score [349]; the California Verbal Learning Test-II (CVLT) total score, short delay recall score (CVLT-SD) , and long delay recall score (CVLT-LD) [350-351]; Wechsler Memory Scale-III (WMS-III) Logical Memory (LM) total score and delayed recall score [352-353]; and the Geriatric Depression Scale (GDS) total score [271].

The effect size of all baseline and APC variables for differences between converters and stable participants (MCI-C vs. MCI-S and CC-C vs. CC-S) was calculated using the following formula:

$$d = \frac{(M_1 - M_2)}{\sqrt{[(\sigma_1^2 + \sigma_2^2) / 2]}}$$

where, for the target ROI, M_1 = mean value for group 1, M_2 = mean value for group 2, σ_1 = standard deviation for group 1, and σ_2 = standard deviation for

group 2 [327]. In order to accurately compare the resulting effect sizes, only participants with values for all analyzed regions were included in this comparison (5 MCI-C and 20 MCI-S; 4 CC-C and 16 CC-S).

The relationships between APC in selected MRI variables and two-year change in psychometric performance on selected tests was assessed for the full available sample (n=78) and for only participants with a CC diagnosis at baseline (n=20) using a bivariate Pearson correlation. APC in hippocampal volume and APC in hippocampal GM volume were selected for the correlation analyses since these variables showed the greatest effect size for the comparison of CC-C and CC-S (Figure 19B). Selected psychometric tests included a measure of clinical dementia severity, CDR-SB, and a measure of memory performance, LM total score. Prior to the correlation analysis, selected MRI and psychometric variables were tested for significant association with confounding variables, including age at baseline visit, gender, years of education, and total ICV (MRI variables only). No associations were found (*data not shown*), thus, raw values for APC and two-year change in psychometric performance were entered into the correlation analyses. SPSS (version 19.0) was used for all statistical analyses. All graphs were made in SigmaPlot version 10.

Results

Demographics and Psychometric Performance

Demographic information and baseline and two-year change in clinical dementia severity and selected psychometric test performance are presented in Table 5. No significant differences were observed among groups in age, gender, years of education or *APOE* genotype. Expected significant differences among groups in clinical dementia severity (Global CDR and CDR-SB), global cognition (MMSE total score, DRS total score) and memory performance (CVLT total score, CVLT-SD score, CVLT-LD score, LM total score, LM delayed recall score) were observed (all $p<0.001$). The results of post-hoc comparisons between groups are displayed in Table 5. Generally, post-hoc comparisons show

significantly higher dementia severity and reduced global cognition and memory performance in patients with AD and MCI at baseline relative to CC and HC participants ($p<0.05$). By definition, CC participants do not show significant impairments in psychometric performance relative to HC at baseline. Significant differences among groups in two-year change in clinical dementia severity (Global CDR, CDR-SB), global cognition (MMSE total score, DRS total score) and memory performance (CVLT total score, CVLT-LD score, LM total score, LM delayed recall score) were also observed ($p<0.05$). Result of post-hoc comparisons are shown in Table 5. No significant difference among groups in the two-year change in GDS total score was observed.

	AD (n=4)	MCI-C (n=5)	MCI-S (n=21)	CC-C (n=4)	CC-S (n=18)	HC (n=30)	ANOVA p-value	Significant Post-hoc Comparisons (p<0.05)
BL Age (years)	70.3 (2.9)	71.1 (2.6)	74.6 (1.3)	76.7 (2.9)	72.8 (1.4)	70.8 (1.1)	0.158	n/a
Gender (male, female)	3, 1	1, 4	12, 9	3, 1	6, 12	11, 19	0.203	n/a
Education (years)	14.5 (1.5)	16.0 (1.3)	16.5 (0.6)	17.8 (1.5)	17.2 (0.7)	17.1 (0.5)	0.525	n/a
APOE Genotype (% *APOE* ε4 positive)[1]	100.0%	60.0%	47.4%	50.0%	27.8%	43.3%	0.184	n/a
BL Global CDR[2]	0.8 (0.09)	0.6 (0.08)	0.5 (0.04)	0.5 (0.09)	0.5 (0.04)	0.2 (0.03)	<0.001	AD, MCI-C, MCI-S, CC-C, CC-S>HC; CC-S>AD
BL CDR-SB[2]	3.5 (0.3)	2.1 (0.3)	1.2 (0.1)	1.1 (0.3)	0.8 (0.1)	0.2 (0.1)	<0.001	AD>MCI-C, MCI-S, CC-S>HC; AD>CC-C; MCI-C>MCI-S, CC-S
BL MMSE Total Score[2]	25.0 (0.8)	24.5 (0.7)	27.1 (0.4)	28.8 (0.8)	29.2 (0.4)	28.9 (0.3)	<0.001	HC, CC-S>MCI-S, MCI-C, AD; CC-C>MCI-C, AD; MCI-S>MCI-C
BL DRS Total Score[2]	123.8 (1.7)	133.9 (1.5)	137.5 (0.7)	138.1 (1.7)	141.3 (0.8)	141.0 (0.6)	<0.001	HC, CC-S>MCI-S, MCI-C, AD; CC-C, MCI-S, MCI-C>AD
BL CVLT Total Score[2]	22.1 (3.6)	30.7 (3.0)	31.5 (1.5)	44.0 (3.5)	46.7 (1.6)	47.7 (1.3)	<0.001	HC, CC-S>MCI-S, MCI-C, AD; CC-C>MCI-S, AD
BL CVLT-SD[2]	2.7 (1.1)	3.0 (1.0)	5.3 (0.5)	9.2 (1.1)	10.1 (0.5)	11.3 (0.4)	<0.001	HC, CC-S, CC-C> MCI-S, MCI-C, AD
BL CVLT-LD[2]	0.4 (1.2)	3.8 (1.0)	5.8 (0.5)	8.9 (1.2)	10.7 (0.5)	12.1 (0.4)	<0.001	HC, CC-S>MCI-S, MCI-C, AD; CC-C>MCI-C, AD; MCI-S>AD
BL LM Total Score[2]	26.0 (4.3)	27.8 (3.7)	35.7 (1.9)	45.8 (4.2)	43.6 (2.0)	48.7 (1.5)	<0.001	HC>MCI-S, MCI-C, AD; CC-S, CC-C>MCI-C, AD
BL LM Delayed Recall[2]	10.0 (3.6)	10.5 (3.1)	20.6 (1.6)	24.7 (3.5)	26.5 (1.6)	32.3 (1.3)	<0.001	HC>MCI-S, MCI-C, AD; CC-S>MCI-C, AD
BL GDS Total[2]	9.3 (2.0)	7.9 (1.7)	5.1 (0.9)	8.7 (2.0)	5.8 (0.9)	1.7 (0.7)	<0.001	HC>CC-S, CC-C, MCI-C, AD
2yr Chg in Global CDR[2]	0.4 (0.12)	0.1 (0.11)	0.0 (0.05)	0.0 (0.1)	0.0 (0.05)	0.0 (0.04)	0.02	AD>MCI-S, HC
2yr Chg in CDR-SB[2]	4.0 (0.4)	1.2 (0.3)	0.3 (0.2)	0.6 (0.4)	0.1 (0.2)	-0.1 (0.1)	<0.001	AD>CC-S, CC-C, MCI-S; AD>MCI-C>HC
2yr Chg in MMSE Total Score[2]	-5.1 (1.0)	-0.7 (0.9)	-0.1 (0.2)	-1.4 (1.0)	-0.9 (0.5)	0.0 (0.4)	<0.001	HC, CC-S, MCI-S, MCI-C>AD
2yr Chg in DRS Total Score[2]	-7.1 (2.3)	-2.3 (2.0)	1.5 (1.0)	0.5 (2.3)	-0.4 (1.1)	0.9 (0.8)	0.021	HC, MCI-S>AD
2yr Chg in CVLT Total Score[2]	-6.3 (3.5)	-5.7 (3.0)	5.8 (1.5)	-4.3 (3.4)	2.5 (1.6)	1.8 (1.2)	0.001	MCI-S>MCI-C, AD
2yr Chg in CVLT-SD[2]	-2.0 (1.2)	-0.04 (1.1)	1.0 (0.5)	-1.2 (1.2)	1.3 (0.6)	-0.05 (0.4)	0.061	n/a
2yr Chg in CVLT-LD[2]	-0.01 (1.3)	-2.7 (1.1)	0.4 (0.5)	0.1 (1.2)	1.5 (0.6)	-0.86 (0.4)	0.008	HC>CC-S; CC-S>MCI-C
2yr Chg in LM Total Score[2]	-14.5 (3.9)	-0.8 (3.3)	2.6 (1.7)	-10.6 (3.8)	1.3 (1.8)	1.2 (1.4)	<0.001	CC-C>MCI-S; HC, CC-S, MCI-S>AD
2yr Chg in LM Delayed Recall[2]	-6.9 (3.0)	-2.9 (2.6)	2.8 (1.3)	-2.9 (2.9)	3.5 (1.4)	2.1 (1.1)	0.01	CC-S>AD
2yr Chg in GDS Total[2]	-0.3 (1.3)	-0.3 (1.1)	-1.0 (0.6)	-1.9 (1.3)	-1.6 (0.6)	-0.61 (0.5)	0.696	n/a

[1] 2 participants missing *APOE* genotype data

[2] Baseline age, gender, and years of education included as covariates.

BL = Baseline; 2yr Chg = Two-year Change; *APOE* = apolipoprotein E; CDR = Clinical Dementia Rating Scale; CDR-SB = CDR Sum of Boxes score; MMSE = Mini-Mental Status Exam; DRS = Dementia Rating Scale; BNT = Boston Naming Test; CVLT = California Verbal Learning Test II; CVLT-SD = CVLT Short Delay Recall Score; CVLT-LD = CVLT Long Delay Recall Score; LM = Wechsler Logical Memory Scale; GDS = Geriatric Depression Scale

Table 5. Demographic Information and Baseline and Two-Year Change in Psychometric Performance (Adjusted Mean (SE))

Baseline Differences in Temporal Lobe ROIs

Significant differences among groups were observed in baseline hippocampal volume (Figure 15A, $p<0.001$), mean temporal lobe cortical thickness (Figure 15B, $p=0.01$), hippocampal GM density and GM volume (Figures 15C and 15E, both $p<0.0001$), and mean temporal lobe GM density and GM volume (Figures 15D and 15F, both $p<0.001$). Post-hoc comparisons show greater hippocampal volume, hippocampal GM density and GM volume, as well as mean temporal lobe cortical thickness and GM density in HC, CC-S, and MCI-S relative to AD patients (all $p<0.05$). In addition, MCI-C participants show smaller hippocampal volume and GM volume than HC and CC-S participants, as well as smaller hippocampal GM density relative to HC only (all $p<0.05$). Finally, differences in mean temporal lobe GM volume were observed, with CC-S participants showing greater GM volumes than MCI-C and AD patients and CC-C participants showing greater GM volumes than AD patients only (all $p<0.05$). Although the comparisons did not reach statistical significance, MCI-C participants had reduced hippocampal volume, GM density and GM volume relative to MCI-S participants at baseline. In addition, CC-C participants showed slight but notable reductions in hippocampal volume and GM volume at baseline relative to CC-S participants, although these differences did not reach statistical significance.

Annualized Percent Change in Target ROIs

Significant differences among groups were observed in the APC over two years in hippocampal total volume (Figure 16A, $p=0.002$), GM density (Figure 16B, $p<0.0001$), and GM volume (Figure 16C, $p<0.0001$). Post-hoc comparisons showed a faster atrophy rate in hippocampal GM density and GM volume in AD patients relative to all other groups (all $p<0.05$). In addition, MCI-C showed a greater atrophy rate in hippocampal total volume than CC-S participants, as well as a faster annualized decline in hippocampal GM density and GM volume than HC and CC-S participants (all $p<0.05$). MCI-C participants showed a slightly faster hippocampal atrophy rate than MCI-S participants, although the results did

not reach statistical significance. CC-C participants showed a trend for a greater atrophy rate in total hippocampal volume than CC-S participants (Figure 16A, $p=0.084$) and a notable but non-significant increased decline relative to CC-S in hippocampal GM density and GM volume.

Significant differences across groups were also observed for the APC in mean temporal lobe GM density (Figure 17A, $p=0.005$) and GM volume (Figure 17B, $p<0.001$), mean medial temporal lobe GM density (Figure 17C, $p=0.002$) and GM volume (Figure 17D, $p<0.001$), and mean lateral temporal lobe GM density (Figure 17E, $p=0.04$) and GM volume (Figure 17F, $p<0.001$). Post-hoc comparisons indicated that patients with AD showed faster atrophy rates than HC, CC-S, and MCI-S in mean temporal lobe GM volume and mean lateral temporal lobe GM volume, as well as faster rates of atrophy in mean temporal lobe GM density and mean medial temporal lobe GM density and GM volume relative to HC and CC-S (all $p<0.05$). Additionally, MCI-C showed a more negative APC in mean lateral temporal lobe GM volume relative to CC-S and HC (both $p<0.05$). MCI-C also showed a moderately greater atrophy rate in all evaluated regions relative to MCI-S, although these differences did not reach statistical significance. CC-C showed a slightly faster atrophy rate than CC-S participants in all evaluated regions except for mean lateral temporal lobe GM density, although again these comparisons did not reach statistical significance.

In comparison to the temporal lobe regions, APC in mean occipital lobe GM density (Figure 18A) and GM volume (Figure 18B) was not significantly different between groups ($p>0.05$). However, AD and MCI-C participants showed slightly but not significantly elevated mean occipital lobe GM volume atrophy rates relative to the other groups.

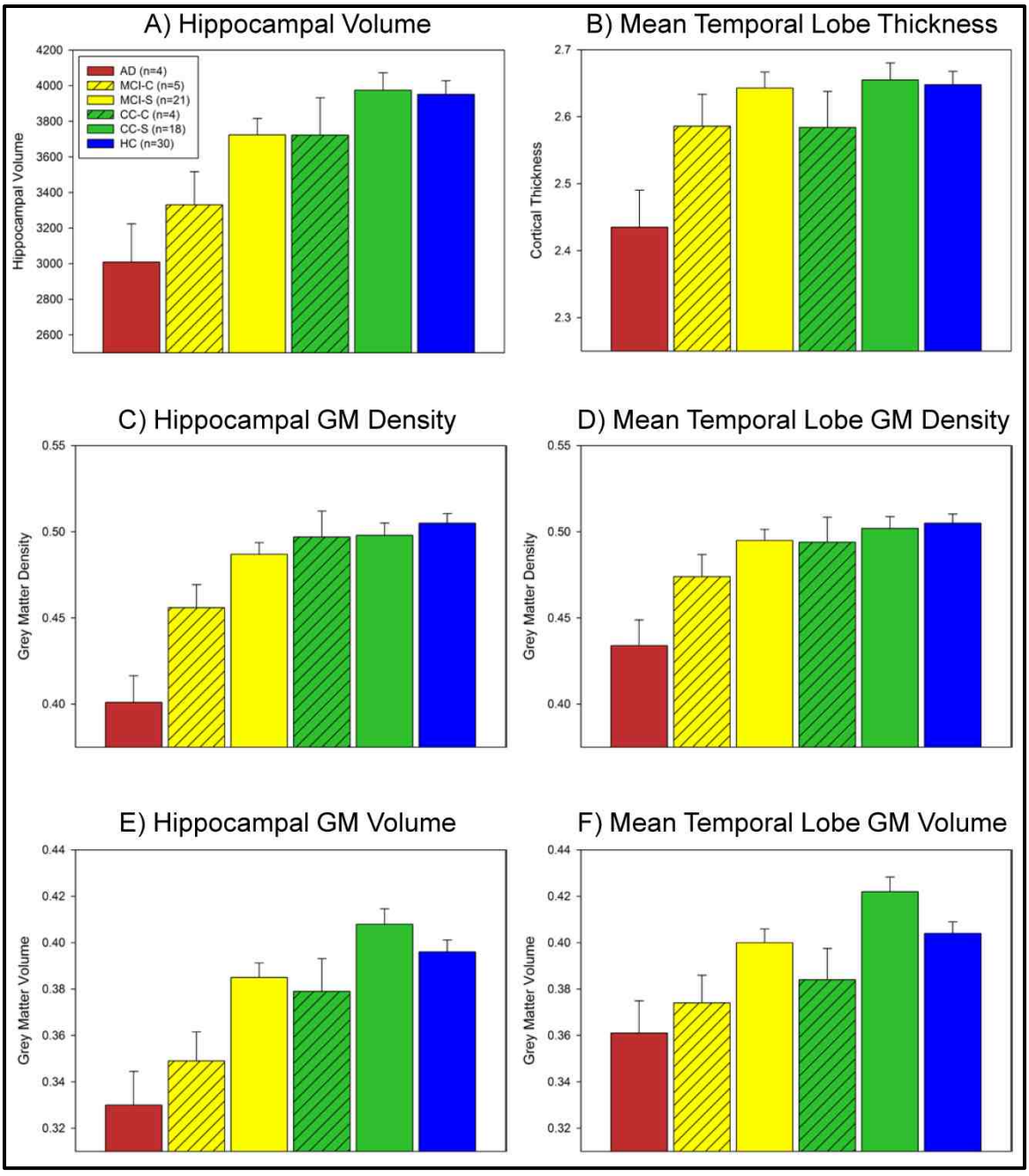

Figure 15. Baseline Differences among Groups in Temporal Lobe Atrophy

Significant differences among groups were observed for baseline (A) hippocampal volume ($p<0.001$), (B) mean temporal lobe cortical thickness ($p=0.01$), (C) hippocampal GM density ($p<0.0001$), (D) mean temporal lobe GM density ($p<0.001$), (E) hippocampal GM volume ($p<0.0001$), and (F) mean temporal lobe GM volume ($p<0.001$). For significant post-hoc comparisons, see the results section. (Group mean

values (+/- SE) adjusted for baseline age, gender, education, and baseline total ICV are displayed)

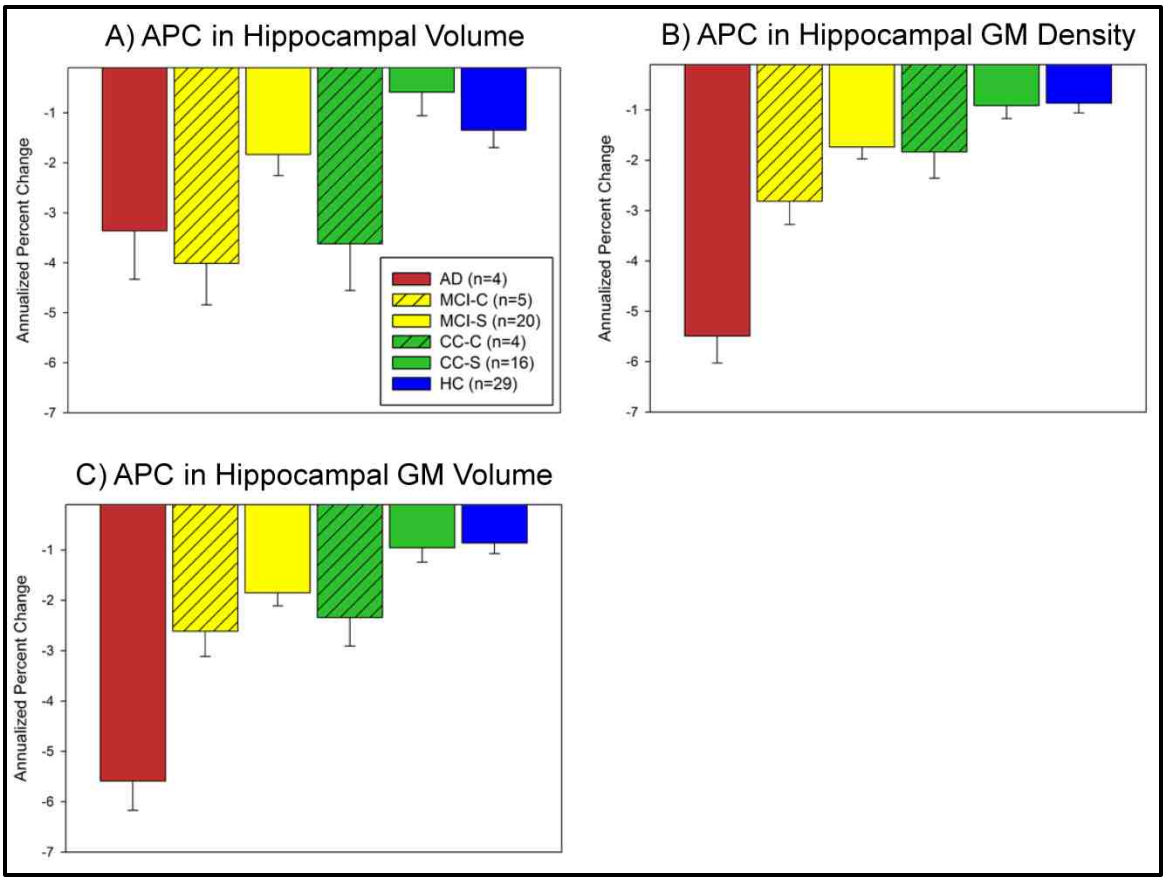

Figure 16. APC in Selected Medial Temporal Lobe ROIs

Significant differences among groups in annualized percent change (APC) over two years in (A) hippocampal volume ($p=0.002$), (B) hippocampal GM density ($p<0.0001$), and (C) hippocampal GM volume ($p<0.0001$). For a complete listing of significant post-hoc comparisons, see the results section. (*Note*: n=78, 4 participants (1 MCI-S, 2 CC-S, 1 HC) from baseline analysis (Table 5, Figure 15) were excluded because of failed two-year follow-up MRI processing; group mean APC values (+/- SE) adjusted for baseline age, gender, education, and baseline total ICV are displayed)

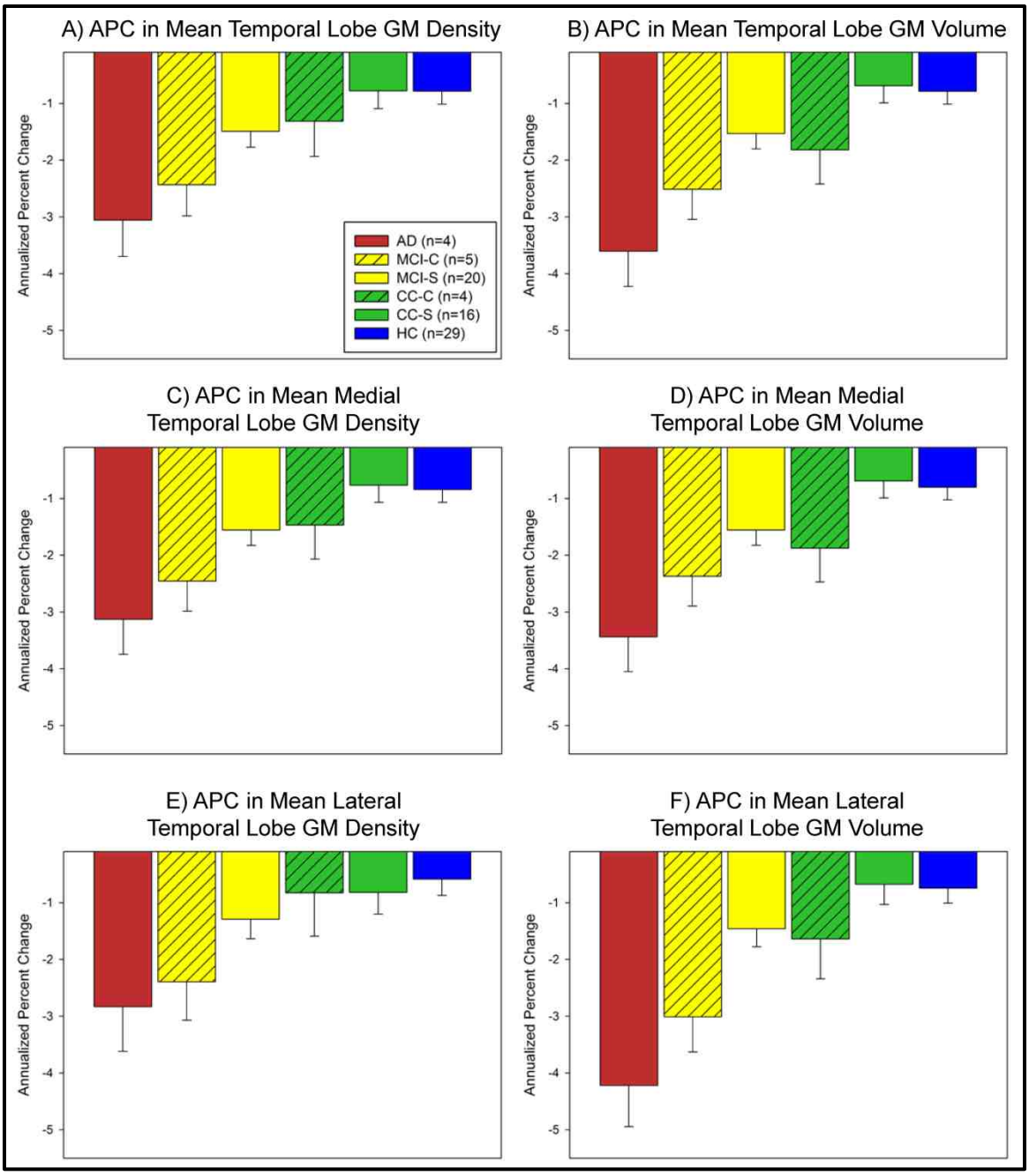

Figure 17. APC in Temporal Lobe GM Density and GM Volume

Significant differences among groups were observed in annualized percent change (APC) in mean temporal lobe (A) GM density ($p=0.005$) and (B) GM volume ($p<0.001$), mean medial temporal (C) GM density ($p=0.002$) and (D) GM volume ($p<0.001$), and mean lateral temporal (E) GM density ($p=0.04$) and (F) GM volume ($p<0.001$). For a complete listing of significant post-hoc comparisons, see the results

section. (*Note*: n=78, 4 participants (1 MCI-S, 2 CC-S, 1 HC) from baseline analysis (Table 5, Figure 15) were excluded because of failed two-year follow-up MRI processing; group mean APC values (+/- SE) adjusted for baseline age, gender, education, and baseline total ICV are displayed)

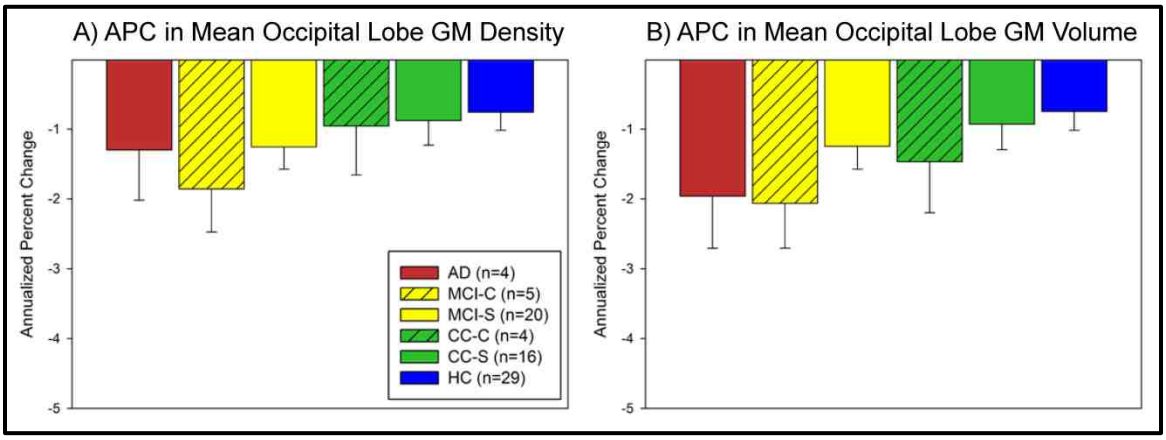

Figure 18. APC in Mean Occipital Lobe GM Density and GM Volume

No significant differences among groups were observed in mean occipital lobe (A) GM density and (B) GM volume. (*Note*: n=78, 4 participants (1 MCI-S, 2 CC-S, 1 HC) from baseline analysis (Table 5, Figure 15) excluded because of failed two-year follow-up MRI processing; group mean APC values (+/- SE) adjusted for baseline age, gender, education, and baseline total ICV are displayed)

Effect Sizes of MRI ROIs for the Comparison between Converters and Stable Participants

Effect sizes for target biomarkers were calculated for the comparisons of MCI-C versus MCI-S and CC-C versus CC-S. The top biomarkers ranked by effect size (Cohen's d) are displayed in Figure 19. APC in mean medial temporal lobe, mean temporal lobe and mean lateral temporal lobe cortical thickness showed the highest effect size for the comparison of MCI-C vs. MCI-S, with Cohen's d values of 1.42, 1.37, and 1.19, respectively (Figure 19A). Longitudinal measures of brain atrophy rate were more sensitive than baseline measures to differences between MCI-C and MCI-S participants, as 12 of the top 15 biomarkers with the highest effect sizes were APC measures. For the comparison of CC-C vs. CC-S, APC in hippocampal volume, hippocampal GM density, and mean temporal lobe GM volume had the greatest effect size, with Cohen's d values of 1.56, 0.81, and 0.79, respectively (Figure 19B). Similar to the comparison between MCI-C and MCI-S, APC measures were slightly more sensitive than baseline measures to the differences between CC-C and CC-S, representing 8 of the top 15 measures with the highest effect sizes.

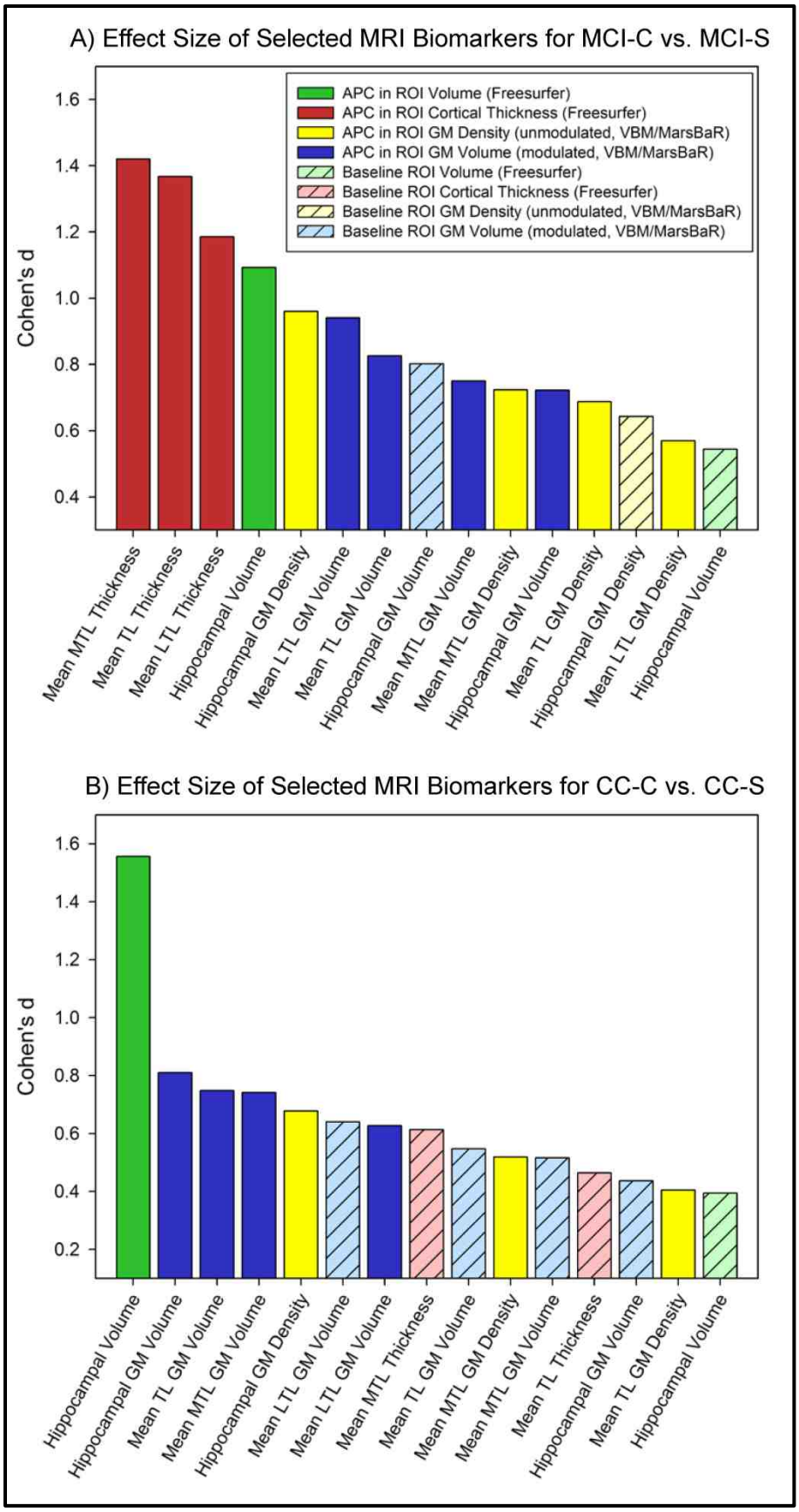
A) Effect Size of Selected MRI Biomarkers for MCI-C vs. MCI-S
Cohen's d
1.6
1.4
1.2
1.0
0.8
0.6
0.4
APC in ROI Volume (Freesurfer)
APC in ROI Cortical Thickness (Freesurfer)
APC in ROI GM Density (unmodulated, VBM/MarsBaR)
APC in ROI GM Volume (modulated, VBM/MarsBaR)
Baseline ROI Volume (Freesurfer)
Baseline ROI Cortical Thickness (Freesurfer)
Baseline ROI GM Density (unmodulated, VBM/MarsBaR)
Baseline ROI GM Volume (modulated, VBM/MarsBaR)
Mean MTL Thickness
Mean TL Thickness
Mean LTL Thickness
Hippocampal Volume
Hippocampal GM Density
Mean LTL GM Volume
Mean TL GM Volume
Hippocampal GM Volume
Mean MTL GM Volume
Mean MTL GM Density
Hippocampal GM Volume
Mean TL GM Density
Hippocampal GM Density
Mean LTL GM Density
Hippocampal Volume
B) Effect Size of Selected MRI Biomarkers for CC-C vs. CC-S
Cohen's d
1.6
1.4
1.2
1.0
0.8
0.6
0.4
0.2
Hippocampal Volume
Hippocampal GM Volume
Mean TL GM Volume
Mean MTL GM Volume
Hippocampal GM Density
Mean LTL GM Volume
Mean LTL GM Volume
Mean MTL Thickness
Mean TL GM Volume
Mean MTL GM Density
Mean MTL GM Volume
Mean TL Thickness
Hippocampal GM Volume
Mean TL GM Density
Hippocampal Volume

Figure 19. Effect Sizes of Selected Imaging Biomarkers for the Comparison of Converters and Stable Participants

Significant effect sizes (Cohen's d) for selected baseline and APC in temporal lobe ROIs for the comparison of (A) MCI-C vs. MCI-S and (B) CC-C vs. CC-S were observed. APC measures are shown in solid colors and baseline measures are shown in light colors with diagonal lines. (n=25 (5 MCI-C, 20 MCI-S) for (A) MCI-C vs. MCI-S and n=20 (4 CC-C, 16 CC-S) for (B) CC-C vs. CC-S for baseline and APC measures due to inclusion of only the participants with successfully processed baseline and two-year follow-up MRI scans; TL=temporal lobe, LTL=lateral temporal lobe, MTL=medial temporal lobe, GM=grey matter; effect sizes are calculated using bilateral mean values of target ROIs adjusted for baseline age, gender, education, and baseline total ICV)

Relationship between Brain Atrophy Rates and Two-Year Change in Dementia Severity and Memory Performance

The relationships between annualized hippocampal atrophy rate (APC in hippocampal volume and hippocampal GM volume) and two-year change in dementia severity and memory performance were evaluated in both the full cohort of available participants (n=78) and in participants with a CC diagnosis at baseline only (n=20; CC-C and CC-S only). A significant association between APC in hippocampal GM volume and two-year change in the CDR-SB was observed in the full cohort (Figure 20A; $r=-0.573$, $p<0.001$), but not in the CC at baseline only sub-sample (Figure 20B; $r=-0.170$, $p>0.05$). A significant association was also observed between APC in hippocampal volume and two-year change in LM total score in both the full sample (Figure 20C; $r=0.276$, $p=0.014$) and the CC at baseline only sub-sample (Figure 20D; $r=0.661$, $p=0.004$).

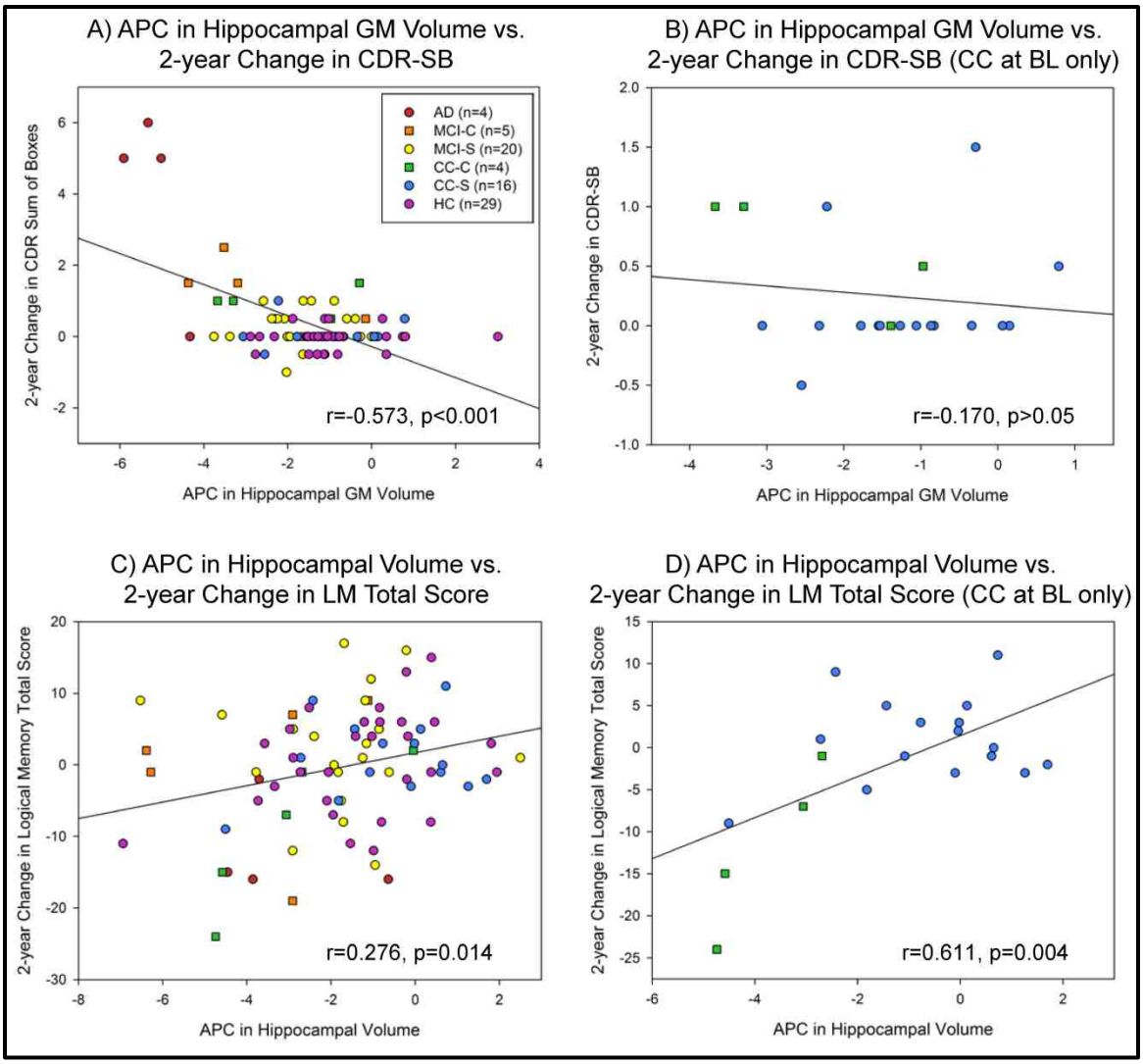

Figure 20. Relationship between Hippocampal Atrophy Rate and Two-Year Change in Psychometric Performance

A significant association between (A) APC in hippocampal GM volume and two-year change in clinical dementia severity (CDR-SB) was observed in the full cohort (r=-0.573, p<0.001), but not in (B) the sub-group of participants with a CC diagnosis at baseline (CC-C and CC-S; r=-0.171, p>0.05). However, significant associations were observed between APC in hippocampal volume and two-year change in memory performance (LM total score) in both the (C) full cohort (r=0.276, p=0.014) and (D) the sub-group of participants with a CC diagnosis at baseline (r=0.611, p=0.004). (n=78 for (A) and (C) and n=20 for (B) and (D) due to inclusion of participants with successfully

processed baseline and two-year follow-up MRI scans only; CDR-SB=CDR Sum of Boxes, LM=WMS-III Logical Memory; GM=grey matter)

Discussion

The present report evaluated MRI biomarkers of AD-related neurodegeneration in a longitudinal study of patients with AD and MCI, older adults with cognitive complaints but no significant cognitive impairment, and healthy older adults with no cognitive complaints. We specifically focused on the sensitivity of MRI measures to detecting differences between patients who clinically declined over the two-year study follow-up period and those who were clinically stable. MRI biomarkers of temporal lobe neurodegeneration showed significant differences among groups both at baseline and in two-year longitudinal annualized atrophy rate. Patients with MCI and AD generally had greater atrophy at baseline and a faster rate of atrophy than CC and HC participants. In addition, patients who demonstrated clinical progression (MCI to AD converters and CC to MCI converters) over the two-year follow-up period showed more baseline atrophy and faster atrophy rates than stable MCI and CC participants. Measures of atrophy rate were more sensitive, as reflected in higher effect sizes, than baseline measures to the differences between MCI-C and MCI-S and between CC-C and CC-S. Finally, the relationship between hippocampal atrophy rate and two-year change in clinical dementia severity was significant across the full sample, but not in the CC at baseline only sub-group. However, the relationship between hippocampal atrophy rate and two-year change in memory performance was significant across the whole cohort and within the CC at baseline only sub-sample.

The significant baseline atrophy and faster atrophy rate observed in patients who convert from MCI to probable AD is similar to findings that have been reported in previous studies [92, 166-167, 207, 213, 219-220, 291]. In addition, the rate of hippocampal atrophy in patients with AD, MCI-C, MCI-S and HC in our sample is similar to previous estimates of annualized decline [201, 219, 291]. However, this is the first report to date to evaluate longitudinal change in patients who convert from CC to MCI relative to stable CC participants. The results suggest that patients with CC show AD-like neurodegenerative patterns at baseline up to two years before clinical symptoms, similar to previous reports

[76-77, 342-345]. Furthermore, a subset of CC participants will progress to MCI each year, with a progression rate in our sample of 5-10% annually. A previous report demonstrated a progression rate of CC participants to MCI and AD of approximately 7-8% annually [78], similar to the rate observed in the present report. In addition, previous reports have indicated that CC participants are more likely than healthy older adults with no cognitive complaints to show cognitive decline, including progression to MCI and AD [79, 337-340, 343, 354], a finding we also observed. The presence of notable differences in MRI measures of neurodegeneration between patients who convert from CC to MCI up to two years before clinical progression and those who have a stable CC diagnosis suggests the AD-like neurodegeneration in these participants may precede the clinical symptoms. In addition, the conversion of patients with CC to a diagnosis of MCI is coupled with a faster rate of brain atrophy in the temporal lobe, including a hippocampal volume loss of more than 3.5% annually.

Similar to previous reports, dynamic measures of atrophy rate appear to be more sensitive than cross-sectional baseline estimates of atrophy to the differences between patients who are clinically progressing and those who are stable [291]. These results suggest that patients who are declining clinically show associated brain degeneration in regions known to degenerate in AD even in early stages of disease (i.e., CC). Furthermore, these results support the utility of MRI biomarkers of neurodegeneration in studies to monitor disease progression and potentially as a marker for treatment effects.

In the present report, an association between hippocampal atrophy rate and two-year change in dementia severity was only detected in the full cohort of participants and not in the sub-set of participants with CC at baseline. This association appears to be primarily driven by the differences between AD patients and all other groups (Figure 20A). Both the full sample and the CC at baseline sub-sample showed a significant association between hippocampal atrophy rate and two-year change in memory performance. However, patients with a CC diagnosis at baseline show a stronger association between hippocampal atrophy rate and two-year change in memory performance than

seen in the full cohort (Figure 20C and 20D). These results suggest that hippocampal atrophy rate is most strongly linked to changes in memory performance in the early stages of AD. In later stages of disease, hippocampal atrophy rate is more strongly associated with the progression of clinical symptoms, including declines in daily functioning and the onset of dementia. These results support the AD biomarker models described in previous reports [14, 17].

A significant limitation of this study is the small sample size, particularly for the AD, MCI-C, and CC-C groups. Future studies in larger cohorts are needed to confirm the present findings. In addition, all AD patients, four MCI-C, and 13 MCI patients were using AD-indicated medication, such as acetylcholinesterase inhibitors and memantine. The presence of medications in a sub-sample of our cohort may have affected the results. We also did not evaluate the impact of *APOE* genotype on MRI measures of brain atrophy and atrophy rate in the present report because of the small sample size. However, *APOE* ε4 status is likely to be an important variable contributing to the extent of baseline atrophy and speed of the longitudinal atrophy rate in all groups, as has been previously observed [291, 299, 305]. Interestingly, the percentage of *APOE* ε4 positive healthy older adults was notably high (>40% *APOE* ε4 positive) relative to what would be expected in a normal population of older adults (~25% *APOE* ε4 positive). The elevated percentage of *APOE* ε4 positive HC participants in this study is potentially due to the fact that healthy older adults with a family history of AD are more likely to participate in AD research in the absence of concerns or symptoms. In fact, 10 of the 14 *APOE* ε4 positive HC participants in this report were positive for a family history of dementia and/or AD. Future studies in expanded samples are needed to evaluate the role of *APOE* ε4 genotype in older adults with cognitive complaints. Finally, the inclusion of other neuroimaging biomarkers (e.g., functional MRI, DTI measures of WM degeneration, positron emission tomography (PET)) may have additional benefits for monitoring clinical decline in this cohort, especially in CC-C participants. Future studies evaluating multiple neuroimaging biomarkers in the prediction and monitoring of patients

with AD and MCI and especially CC patients will be important for determining the validity of these methods for early detection of AD-related neuropathology.

In conclusion, patients who show clinical progression towards AD have greater baseline atrophy, as well as faster rates of atrophy over two years. In fact, patients who convert from either MCI to probable AD or from CC to MCI show greater temporal lobe atrophy and a faster decline in temporal lobe measures up to two years before conversion than stable MCI and stable CC participants, respectively. Measures of annualized atrophy rate in temporal lobe structures appear to be the most sensitive to differences between converting patients and stable patients (MCI-C vs. MCI-S and CC-C vs. CC-S). A greater hippocampal atrophy rate is associated with an increase in clinical dementia severity over two years, as well as a decrease in memory performance. The latter association is particularly strong in the earliest clinical stages of disease (i.e., CC). In summary, older adults with CC appear to have AD-like neurodegeneration up to two years before the emergence of significant cognitive impairment. These results support the premise that the presence of CC in older adults may represent a pre-MCI stage of AD. MRI biomarkers may be sensitive measures to detect and monitor neurodegeneration even in this early stage of disease. Future studies to further evaluate the clinical course of individuals with CC, as well as studies with other AD biomarkers will help elucidate the role of CC in the AD disease continuum.

Acknowledgements

This study was supported in part by: the National Institutes of Health (R01 AG19771 to AJS); Alzheimer's Association (IIRG-99-1653 from the Hedco Foundation to AJS); the Indiana Economic Development Corporation (IEDC 87884 to AJS); National Institute on Aging (NIA) Core Supplement to Drs. B. Ghetti and AJS (P30 AG10133-18S1); a NIH CTSI Pre-doctoral Training Fellowship (Training Grant TL1 RR025759 to SLR); as well as, the NIH/NCRR Indiana Clinical and Translational Sciences Institute (U54 RR025761; C06-RR020128).

The authors gratefully acknowledge the help of Drs. Laura Rabin, Nadia Paré, and Katherine Nutter-Upham, and Margaret Nordstrom for assistance with cognitive assessment and cohort follow-up. We also thank the participants and family members from New England without whom this study would not have been possible.

Chapter 3: Visual Contrast Sensitivity as a Novel Biomarker for AD

The final chapter explores a novel biomarker for AD, visual contrast sensitivity. Contrast sensitivity is the ability to distinguish between dark and light in a static image, and has been shown to be impaired in patients with AD, likely due to degeneration of retinal ganglion cells and/or central neural visual pathways. In this chapter, cross-sectional data from participants in the cohort utilized in Chapter 2b from Dartmouth Medical School, as well as additional participants from the Indiana University School of Medicine, are assessed. Participants included patients with a diagnosis of probable AD, patients with a diagnosis of MCI, older adults with cognitive complaints (CC) but no significant cognitive impairment, and healthy older adults without cognitive complaints (HC). Contrast sensitivity was measured using a standardized tool called frequency doubling technology (FDT-2; Welch Allyn, Inc.). Measure of brain atrophy from MRI scans, as well as clinical and psychometric performance data, were also evaluated. MRI scans were analyzed using VBM and automated parcellation (Freesurfer version 4), as discussed in Chapters 1 and 2. In this study, we first assessed differences in contrast sensitivity performance among groups (AD, MCI, CC, HC). Next, we evaluated the distribution of contrast sensitivity deficits across the visual field. We also estimated the ability of contrast sensitivity measures to accurately classify MCI vs. HC participants. In order to further explore contrast sensitivity as an AD biomarker, we assessed the relationship between contrast sensitivity performance and known markers of AD. We evaluated the relationship between contrast sensitivity measures and performance on a test of general cognition (MMSE total score) and a memory test (CVLT total score and short delay recall score). We also analyzed the relationship between contrast sensitivity measures and grey matter (GM) density on a voxel-wise basis across the whole brain. Finally, we assessed the relationship between contrast sensitivity performance and selected regional brain volumetric and cortical thickness measures.

The results of this study indicated that patients with MCI and AD have significant contrast sensitivity deficits. In addition, patients with CC show

intermediate contrast sensitivity performance between patients with MCI and HC. The contrast sensitivity impairment in patients with MCI and AD appears to be relatively evenly distributed across the visual field (VF) but is most apparent in the upper right VF quadrant. Measures of contrast sensitivity also show a 75-80% overall accuracy in classifying MCI vs. HC participants. Significant associations between measures of contrast sensitivity and both global cognition and memory performance were observed across the full cohort. Furthermore, contrast sensitivity shows a significant association with MRI biomarkers of neurodegeneration. Specifically, impaired contrast sensitivity is associated with reduced GM density in medial temporal lobe, as well as reduced temporal lobe cortical thickness. Overall, the results of this study suggest that visual contrast sensitivity may be a useful biomarker for AD, even in early stages such as MCI and CC.

Introduction

Alzheimer's disease (AD) is the most common form of dementia, affecting more than five million Americans over the age of 65 years [331]. Characterized by memory deficits, cognitive impairment, and dementia, AD is a progressive neurodegenerative disease that evolves over many years, possibly over decades [331, 355]. In addition to cognitive deficits, patients with AD also show alterations in sensory perception, including visual processing [356-358], auditory processing [359-360], and olfaction [361-362]. AD patients show deficits in some types of visual processing, while others are relatively spared. Specifically, patients with AD show deficits in visual contrast sensitivity, color discrimination (lower spectral wavelengths), and motion discrimination, as well as other visual field (VF) deficits [356, 363-367]. Patients with AD also show degeneration in the visual pathway both in the brain and in the retina, including central degeneration of the magnocellular pathway in the lateral geniculate nucleus (LGN) and the visual cortex [368-372], and loss of retinal ganglion cells (RGC) within the retinal nerve fiber layer, respectively [373-380].

Frequency doubling technology (FDT) is a automated tool that can detect contrast sensitivity and VF defects [381-382] and is often used in glaucoma testing [383-384]. This technique utilizes an optical illusion called "frequency doubling," which occurs when an achromatic, low spatial frequency sinusoidal grating undergoes counterphased flickering at high temporal frequency, resulting in an apparent doubling of the spatial frequency of the grating [381-382, 385-386]. Processing of the FDT signal is thought to specifically involve activation in the magnocellular visual pathway and visual association areas [386-387].

In an effort to understand the development of AD and assist with early identification of at-risk individuals, prodromal stages of AD have been defined and extensively studied. Mild cognitive impairment (MCI), a disorder characterized by significant deficits in one or more cognitive domains (typically memory) in the absence of dementia, is the most commonly studied disorder considered to be an early stage of AD [64]. With yearly conversion of 10-15% of MCI patients to probable AD, MCI also represents the most widely accepted pre-

AD stage [67]. In order to identify patients who may progress to AD even before significant cognitive impairments are evident, recent studies have attempted to define earlier stages of AD than MCI using genetic background (i.e., apolipoprotein E ε4 status) [74, 388], family history of AD [333, 336], the presence of extensive Aβ deposition [14], and/or the presence of cognitive complaints [73, 77]. For example, Saykin *et al.* (2006) demonstrated that older adults with cognitive complaints have significant atrophy in AD-related regions (i.e., hippocampus), supporting this classification as a "pre-MCI" stage [77].

The development and evaluation of sensitive and specific biomarkers for the detection and monitoring of AD has become an important goal for many scientists. Neuroimaging and cerebrospinal fluid (CSF) markers are the most commonly used in AD research [17, 82, 86, 88-89, 93]. Structural magnetic resonance imaging (MRI) is an AD biomarker that measures brain structure and tissue morphology [87, 95]. MRI measures have been shown to sensitively measure neurodegeneration associated with AD even in early stages of disease (i.e., MCI and pre-MCI) [98, 139, 213, 310, 313], predictive of future disease progression [92, 166, 213], and useful for monitoring longitudinal decline [197, 201, 291, 389]. As such, structural MRI measures are commonly used in AD research as biomarkers of disease and associated neurodegeneration, as well as in clinical trials for sample enrichment and/or evaluation of treatment efficacy [262, 300].

Alterations in contrast sensitivity have not previously been evaluated in patients with MCI or "pre-MCI" symptoms (e.g., patients with cognitive complaints). Additionally, the relationship of contrast sensitivity measures to other markers of AD pathology, including cognitive deficits and neurodegeneration measured using MRI, has not been established. Therefore, the goals of the present study were: (1) to assess whether AD participants demonstrate the expected deficits in contrast sensitivity using the FDT-2 24-2 VF contrast sensitivity test; (2) to determine the extent to which patients with MCI and older adults with cognitive complaints (CC) show contrast sensitivity deficits relative to healthy older controls (HC); (3) to evaluate how contrast sensitivity

deficits are distributed across the VF; (4) to evaluate the accuracy of contrast sensitivity measures to classify MCI versus HC; (5) to assess the association between contrast sensitivity and cognition; and, (6) to evaluate the relationship between contrast sensitivity measures and a known biomarker of AD, MRI measures of neurodegeneration.

Methods

Participants

107 participants from an ongoing study of aging and cognition at two academic medical centers, Dartmouth-Hitchcock Medical Center (DHMC) and the Indiana University School of Medicine (IUSM), received a comprehensive ophthalmologic examination, including the FDT-2 24-2 VF contrast sensitivity test, as well as an extensive protocol of structural and functional neuroimaging scans, clinical evaluation, and neuropsychological assessment. Of the 107 participants who underwent the ophthalmological examination and FDT-2 testing, 23 participants were excluded, including 10 participants with evidence of glaucoma, 10 participants with comorbid visual problems and health disorders which would significantly affect visual contrast sensitivity (e.g., significant cataracts, poor visual acuity, amblyopia, nystagmus, Graves' disease, significant epiretinal membrane), and three healthy controls who were performance outliers on one or more of the FDT-2 summary variables (mean deviation and/or pattern standard deviation), scoring significantly below the expected performance for their age as determined by an independent sample of healthy participants [390] (<0.5% probability that normal participants would show age-adjusted performance at that level). Consequently, the sample used for analyses reported here includes 84 participants (28 male, 56 female): nine diagnosed with probable Alzheimer's disease (AD; 2 male, 7 female); 27 diagnosed with mild cognitive impairment (MCI; 13 male, 14 female); 19 euthymic individuals with significant cognitive complaints (CC) but normal cognitive performance on psychometric tests (4 male, 15 female); and 29 age-matched healthy controls (HC; 9 male, 20

female). All participants provided written informed consent in accordance with the Declaration of Helsinki via protocols approved by the appropriate Institutional Review Board.

FDT-2 Contrast Sensitivity Threshold Visual Field Test (24-2)

All participants were tested with the standard FDT-2 24-2 VF contrast sensitivity threshold exam protocol which evaluates 55 VF regions in the right eye, followed by 55 regions in the left eye [382]. This test provides a single measure of contrast sensitivity threshold (in decibels (dB)) at each of the 110 VF regions, using a maximum likelihood threshold strategy known as ZEST (Zippy Estimate of Sequential Testing) [391-392]. The 24-2 exam features 24-degree coverage with a stimulus size of five degrees, a spatial frequency of 0.5 cycles per degree, and a temporal frequency of 18Hz [382]. In addition to the threshold values for each VF region, two summary measures of general contrast sensitivity across the entire VF are reported for each eye, including mean deviation and pattern standard deviation. Mean deviation is a measure of the overall contrast sensitivity in each eye, while pattern standard deviation indicates how each of the 55 VF test locations deviates from the expected value from an age-adjusted normative database, after adjustment for any general reduction or enhancement of contrast sensitivity. In addition to the threshold tests, reliability tests were also completed, including assessment of fixation errors, false positive errors, and false negative errors. Fixation errors are tested by a stimulus of 50% contrast in the location of the blind spot (Heijl-Krakau method), which should not be detected if proper fixation is maintained. False positive errors are tested by presenting stimuli at 0% contrast, with any responses to these stimuli considered to be false positive errors. False negative errors are tested by presenting stimuli at 100% contrast, such that no response would be a false negative error [381-382]. In the 24-2 test, 10 fixation error trials, 10 false positive trials, and six false negative trials are included.

Neuropsychological and Clinical Assessments

All participants received a detailed clinical exam, as well as a number of clinical, psychometric, and neuropsychiatric assessments [77]. Measures examined in this study included: the Mini-Mental Status Exam (MMSE) [274-275] and Mattis Dementia Rating Scale-2 (DRS) [349] to assess general cognition; the California Verbal Learning Test-II (CVLT) [350-351] to evaluate memory performance; and the Wisconsin Card Sorting Task (WCST) [393] to determine executive functioning. Cognitive complaints were evaluated using ratings from both from the participant and an informant with a variety of assessments described previously [77]. Clinical diagnoses for all participants were done using group consensus of clinicians and clinically trained research scientists, and the Clinical Dementia Rating Scale (CDR) [276] was used to quantify the severity of clinical symptoms and complaints.

Structural Magnetic Resonance Imaging (MRI)

1.5 Tesla and 3.0 Tesla MP-RAGE structural MRI scans for all available participants were obtained from both sites, as part of a comprehensive neuroimaging protocol, which includes both structural and functional MRI scans. The scans from the DHMC site came from two scanners including a 1.5T GE scanner and a 3.0T GE scanner, due to an upgrade. All structural MRI scans from IUSM were done on a 3.0T Siemens MRI scanner. Structural MRI scans from all participants were processed using two widely used analysis techniques, including voxel-based morphometry (VBM) and automated parcellation (Freesurfer version 4), using methods described previously [213] and briefly below. Five participants (1 MCI, 3 CC, 1 HC) were excluded from all MRI analyses (VBM and automated parcellation) due to a missing MRI scan or failed QC.

VBM: All MP-RAGE scans were converted from DICOM to NIfTI format, aligned to a standard T1-weighted template image, and segmented with bias correction into grey matter (GM), white matter (WM), and cerebrospinal fluid (CSF) compartments using standard templates. The resulting GM images were

then normalized to MNI space using parameters from the segmentation step. SPM5 (http://www.fil.ion.ucl.ac.uk/spm/) was used for all VBM processing. Quality control (QC) was performed on all scans at each processing step by a trained research scientist and scans with poor quality segmentation or other failures were excluded before further analysis.

Automated Parcellation: Freesurfer version 4 was utilized to automatically generate volumetric and cortical thickness estimates for more than 100 regions of interest (ROIs) for each participant with an available MRI scan. Due to the known sensitivity of these measures to AD-related neurodegenerative changes, volumetric values from the medial temporal lobe, as well as cortical thickness values from the temporal, parietal, occipital, and frontal lobes were extracted for use in the present analysis.

VBM Statistical Analyses

A multiple linear regression model was used to evaluate the relationship between selected measures of contrast sensitivity and whole brain GM density on a voxel-wise level. Measures of contrast sensitivity evaluated included mean deviation, pattern standard deviation, and mean contrast threshold in the upper right VF quadrant. An explicit GM mask was applied to limit the statistical analysis to GM regions. In addition, a threshold of $p<0.005$ (uncorrected) and a minimum cluster size (k) of 100 voxels was used for displaying the relationships. Gender, education, MRI scanner type (1.5 Tesla GE, 3.0 Tesla GE, 3.0 Tesla Siemens), and mean intracranial volume (ICV) were used as covariates in all analyses. Age at FDT-2 visit was also included as a covariate in only the analyses using the mean contrast threshold of the upper right VF quadrant.

Other Statistical Analyses

All continuous variables, including demographic information, psychometric performance, visual acuity, intraocular pressure (IOP), and FDT-2 visual contrast sensitivity performance, exam duration, and exam errors were evaluated for the effect of diagnostic group (AD, MCI, CC, HC) using one-way analysis of variance

(ANOVA) or covariance (ANCOVA). FDT-2 performance values for the left and right eye as well as bilateral mean values were evaluated independently. Post-hoc testing with Bonferroni correction for multiple comparisons was used to assess between-group differences. A chi-square test was used to evaluate the effect of diagnostic group on categorical variables (e.g., gender, cataract history). PASW version 18.0.0 (SPSS Inc., Chicago, IL) was used for all statistical analyses. All graphs were created using SigmaPlot (version 10).

Statistical analyses assessing psychometric performance and FDT-2 exam duration, exam errors, and all regional VF contrast sensitivity thresholds included age at visit, gender, and years of education as covariates. Since FDT-2 mean deviation and pattern standard deviation are reported as age-adjusted values, the analyses for these variables included only gender and years of education as covariates. Previous studies have reported an association between the presence of cataracts and/or visual acuity with contrast sensitivity performance [394-396]; however, other studies have suggested these factors may not significantly influence FDT performance [381, 397-398]. We investigated the role of a history of cataracts or cataract surgery and visual acuity (raw and/or corrected) as covariates and found no significant effects (see results). Therefore, the final FDT analyses reported here did not include either cataract history or visual acuity as covariates.

Logistic regression models were used to calculate sensitivity, specificity, and overall accuracy of MCI vs. HC classification using visual contrast sensitivity measures, which were pre-adjusted for appropriate demographic variables and entered individually as independent predictors. Specifically, FDT-2 summary measures (mean deviation, pattern standard deviation) were pre-adjusted for gender and years of education. Visual contrast sensitivity thresholds (single VF regions (1-55) and four VF quadrants for each eye), test duration, and memory performance were pre-adjusted for age at visit, gender, and years of education. Receiver operating characteristic (ROC) curves were then created for the best independent classifiers from the logistic regression model. Finally, the ability of FDT-2 contrast sensitivity performance to improve diagnostic classification

provided by standard psychometric performance was assessed by entering memory performance (CVLT total score, pre-adjusted for age at visit, gender, and years of education) into a logistic regression model as an independent classifier of MCI vs. HC and in combination with the best FDT-2 visual contrast sensitivity classifier. We chose to evaluate only the classification of MCI vs. HC because these groups had relatively balanced number of participants, while the other clinical groups were smaller in size.

In addition to comparing FDT-2 contrast sensitivity results among diagnostic groups, we evaluated the relationship between contrast sensitivity deficits and impairments in global cognition and memory. The relationships between FDT-2 performance (mean deviation in contrast sensitivity; mean contrast sensitivity threshold in the bilateral upper right VF) and clinical performance variables (MMSE total score (general cognition); CVLT total score and short delay recall score (memory performance)) were assessed using a bivariate Pearson correlation. Mean deviation in contrast sensitivity was adjusted for gender and years of education prior to the correlation analysis. Clinical performance scores and mean contrast threshold in the bilateral upper right VF were adjusted for age at visit, gender and years of education prior to the correlation analysis.

Finally, we assessed the relationship between FDT-2 measures of contrast sensitivity with selected MRI biomarkers of neurodegeneration. Specifically, the relationships between contrast sensitivity measures (mean deviation, pattern standard deviation, and mean contrast threshold of the upper right VF quadrant) and mean cortical thickness variables (mean temporal lobe, mean medial temporal lobe, mean frontal lobe, and mean parietal lobe) were evaluated using a bivariate Pearson correlation. All variables were pre-adjusted to remove the effects of nuisance variables, including gender and years of education (all variables), MRI type (1.5T, 3.0T GE, 3.0T Siemens) and total ICV (MRI variables only), and age at visit (MRI variables and mean contrast threshold of the upper right VF quadrant).

Results

Demographics, Ophthalmologic Exam Variables, and Psychometric Performance

Demographic information, selected variables from the ophthalmological exam, and mean psychometric performance are presented in Table 6. Age at visit and years of education differed among groups (both $p<0.05$). Post-hoc analyses indicated that MCI participants were older than CC and HC participants (both $p<0.05$) and HC participants were more educated than AD and MCI participants (both $p<0.05$).

Psychometric performance showed the expected pattern of significant differences among diagnostic groups. Clinical Dementia Rating Scale (CDR) Global score (CDR-GL) and Sum of Boxes score (CDR-SB), Mini-Mental Status Exam (MMSE) total score, Wisconsin Card Sorting Task (WCST) number of categories completed, Dementia Rating Scale-2 (DRS) total score, and California Verbal Learning Test-II (CVLT) total score, short delay recall score (CVLT-SD), and long delay recall score (CVLT-LD), were different among groups (all $p<0.001$). Post-hoc analyses showed significant impairment in patient groups (AD and MCI) relative to HC (see Table 6; all $p<0.05$). By definition, CC participants showed normal mean performance on all psychometric assessments (Table 6). Although AD patients reported more depressive symptoms on the Geriatric Depression Scale (GDS) than HC ($p<0.05$), these scores do not represent a clinically significant level of symptomatology.

Cataract history and visual acuity (raw or corrected) were not different among diagnostic groups (see Table 6). The inclusion of these variables as additional covariates in the assessment of the effect of diagnostic group on FDT-2 performance (presented below) did not change the overall pattern of findings. Therefore, the reported analyses below did not include cataract history or visual acuity as covariates.

	AD (n=9)	MCI (n=27)	CC (n=19)	HC (n=29)	ANOVA p-value	Significant Post-hoc Comparisons (p<0.05)
Age (years)	76.11 (2.3)	77.19 (1.3)	72.00 (1.6)	71.62 (1.3)	0.011	MCI>CC, HC*
Education (years)	14.89 (0.9)	15.74 (0.5)	16.84 (0.7)	17.62 (0.5)	0.028	HC>MCI, AD*
Gender (Male, Female)	2, 7	13, 14	4, 15	9, 20	NS	None
IOP (mmHg) – Right	13.8 (1.0)	13.8 (0.6)	13.4 (0.7)	14.7 (0.5)	NS	None
IOP (mmHg) – Left	14.4 (0.8)	13.3 (0.5)	13.2 (0.6)	14.4 (0.5)	NS	None
Cataracts – Right and/or Left (mild, none/removal)	7, 2	8, 19	7, 12	13, 16	NS	None
Cup-to-Disc Ratio - Right[1]	0.38 (0.05)	0.37 (0.03)	0.34 (0.03)	0.30 (0.02)	NS	None
Cup-to-Disc Ratio - Left[1]	0.36 (0.05)	0.36 (0.03)	0.31 (0.03)	0.30 (0.02)	NS	None
Uncorrected Acuity – Right	20/29.4 (2.8)	20/25.6 (1.6)	20/27.1 (1.9)	20/27.4 (1.6)	NS	None
Uncorrected Acuity – Left	20/31.7 (3.0)	20/26.5 (1.8)	20/27.6 (2.1)	20/26.6 (1.7)	NS	None
Corrected Acuity – Right	20/26.7 (1.8)	20/23.0 (1.0)	20/23.4 (1.2)	20/23.3 (1.0)	NS	None
Corrected Acuity – Left	20/28.3 (2.2)	20/23.9 (1.2)	20/24.2 (1.5)	20/24.5 (1.2)	NS	None
CDR-GL[2,7]	0.93 (0.08)	0.52 (0.05)	0.44 (0.05)	0.07 (0.05)	<0.001	AD>MCI,CC>HC
CDR-SB[2,7]	4.41 (0.4)	1.40 (0.3)	0.89 (0.3)	0.27 (0.2)	<0.001	AD>MCI>HC; AD>CC
MMSE[3,7]	23.95 (0.6)	27.88 (0.3)	28.62 (0.4)	28.85 (0.3)	<0.001	HC, CC, MCI>AD
WCST[4,7]	1.19 (0.5)	2.75 (0.3)	3.55 (0.3)	3.64 (0.2)	<0.001	HC, CC, MCI>AD
CVLT Total[7]	24.83 (3.0)	35.58 (1.8)	50.19 (2.1)	52.57 (1.7)	<0.001	HC, CC>MCI>AD
CVLT-SD[7]	3.03 (0.8)	6.73 (0.5)	11.06 (0.6)	12.17 (0.5)	<0.001	HC, CC>MCI>AD
CVLT-LD[7]	2.42 (0.9)	6.73 (0.5)	11.14 (0.6)	12.52 (0.5)	<0.001	HC, CC>MCI>AD
DRS Total[5,7]	126.52 (2.0)	136.48 (1.2)	138.69 (1.3)	140.78 (1.1)	<0.001	HC, CC, MCI>AD
GDS (15-item)[6,7]	5.62 (1.1)	3.95 (0.7)	2.25 (0.8)	1.50 (0.6)	0.009	AD>HC

* Bonferroni post-hoc correction not included in these comparisons (but in all other post-hoc comparisons)
[1] Missing 14 participants (2 AD, 9 MCI, 3 HC)
[2] Missing 1 AD participant
[3] Missing 1 HC participant
[4] Missing 1 AD participant and 1 MCI participant
[5] Missing 1 AD participant and 1 CC participant
[6] Missing 1 AD participant, 2 MCI participants, and 3 CC participants
[7] Group means are adjusted for selected covariates (age at visit, gender, and years of education)
AD = Alzheimer's disease; MCI = mild cognitive impairment; CC = older adults with cognitive complaints; HC = healthy age-matched controls; ANOVA = analysis of variance; IOP = intraocular pressure; CDR-GL = Clinical Dementia Rating Scale (CDR) Global score; CDR-SB = CDR Sum of Boxes score; MMSE = Mini-Mental Status Exam total score; CVLT = California Verbal Learning Test; CVLT-SD = CVLT short delay recall score; CVLT-LD = CVLT long delay recall score; DRS = Mattis Dementia Rating Scale total score; GDS = Geriatric Depression Scale total score

Table 6. Demographics, Ophthalmologic Exam Variables, and Psychometric Performance (Adjusted Mean (SE))

FDT-2 Exam Duration and Performance Errors

The duration of the FDT-2 exam for both the left and right eyes was different among diagnostic groups (both $p<0.001$; Figure 21A). Post-hoc comparisons indicated that AD patients took longer to complete the exam on average than HC participants for both eyes (both $p<0.001$). Additionally, AD participants had greater mean exam durations than CC participants in both eyes (left (L): $p<0.05$; right (R): $p<0.01$) and MCI participants in the right eye ($p<0.05$). MCI participants also had longer exam durations than HC in both eyes (both $p<0.05$).

Fixation errors and false negative errors did not differ among groups (Figure 21B and 21D). However, false positive errors were different among groups for the left eye only ($p<0.05$; Figure 21C). Post-hoc comparisons indicated more false positive errors in AD patients than in CC and HC participants for the left eye (both $p<0.05$).

FDT-2 Summary Variables

Mean deviation in FDT-2 contrast sensitivity was different among groups in both eyes (both $p<0.0001$; Figure 22A). Post-hoc comparisons demonstrated more impairment in both eyes (lower mean deviation) in AD patients relative to CC (L: $p<0.001$; R: $p<0.01$) and HC (both $p<0.001$). MCI patients also showed lower mean deviation than HC participants in both eyes (L: $p<0.01$; R: $p<0.05$) and CC participants in the left eye ($p<0.05$). CC participants also showed slight impairments in mean deviation relative to HC, with intermediate performance between MCI and HC groups, although the comparisons did not reach statistical significance.

Mean pattern standard deviation in FDT-2 contrast sensitivity also differed among groups in both eyes (both $p<0.001$; Figure 22B). AD patients had more impaired pattern standard deviation in both eyes (larger mean pattern standard deviation value) than CC (L: $p<0.01$; R: $p<0.05$) and HC participants (both $p<0.001$). MCI participants also had significantly greater mean pattern standard deviation than HC in the right eye only ($p<0.05$). Similar to the results for the

mean deviation comparison, CC participants demonstrated slightly elevated mean pattern standard deviation relative to HC in both eyes, but this finding did not reach statistical significance.

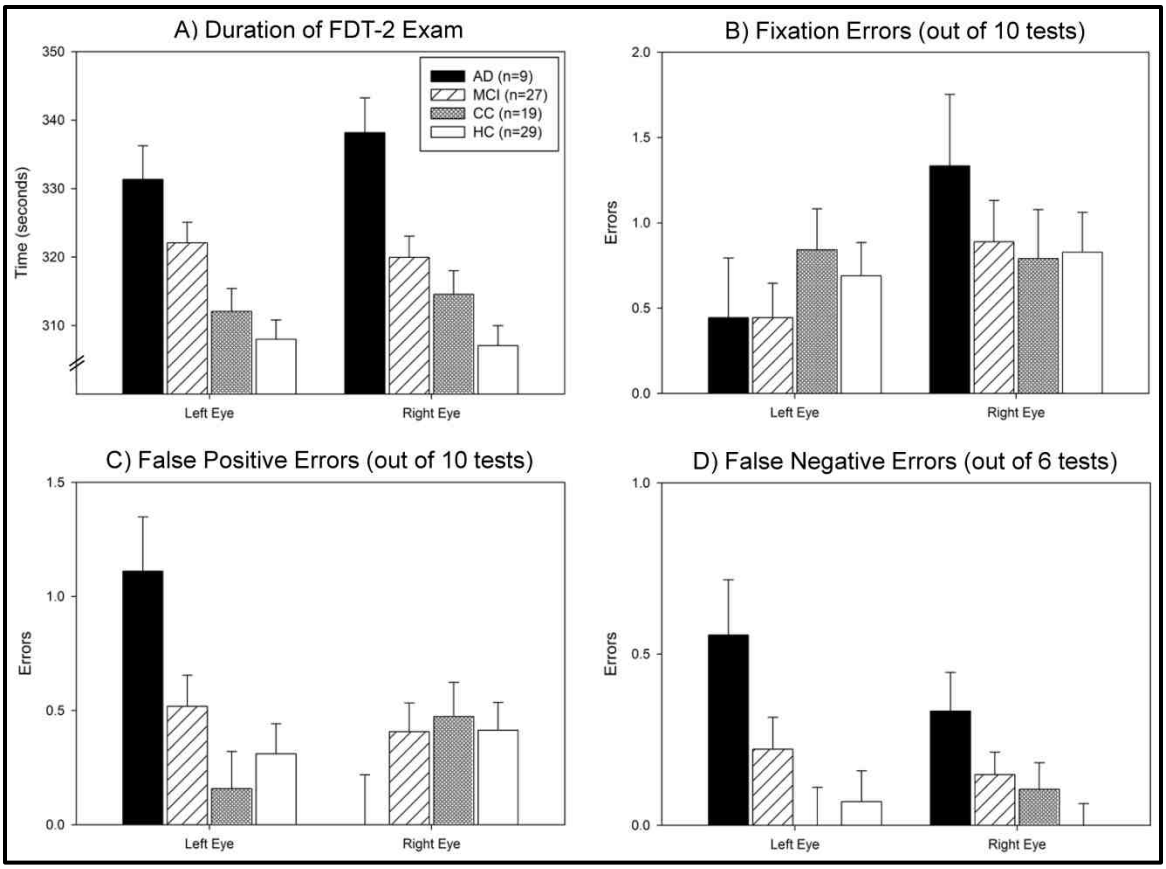

Figure 21. FDT-2 24-2 Exam Duration and Performance Errors

Measures of FDT-2 24-2 test duration (A) and performance errors, including fixation errors (B), false positive errors (C) and false negative errors (D) are shown in Figure 21. Differences among groups were observed in test duration (A) in both eyes (both $p<0.001$), with post-hoc comparisons indicating AD participants take longer to complete the exam on average than CC (L: $p<0.05$, R: $p<0.01$) and HC participants (both $p<0.001$) in both eyes, and MCI in the right eye only ($p<0.05$). MCI participants also took longer to complete the exam than HC participants in both eyes (both $p<0.05$). False positive errors (C) also differed among groups in the left eye only ($p<0.05$), with post-hoc comparisons indicating more false positive errors in AD patients relative to CC and HC (both $p<0.05$). No significant differences across groups in fixation errors (B) and false negative errors (C) were observed. See experimental procedures section for a description of how FDT-2 performance errors are tested. In panel A, bars represent the mean duration (+/- SE) adjusted for age visit, gender, and years of education. In panels B-D, bars represent raw (unadjusted) mean performance errors (+/- SE). However, all

statistical models (panels A-D) included age at visit, gender, and years of education as covariates.

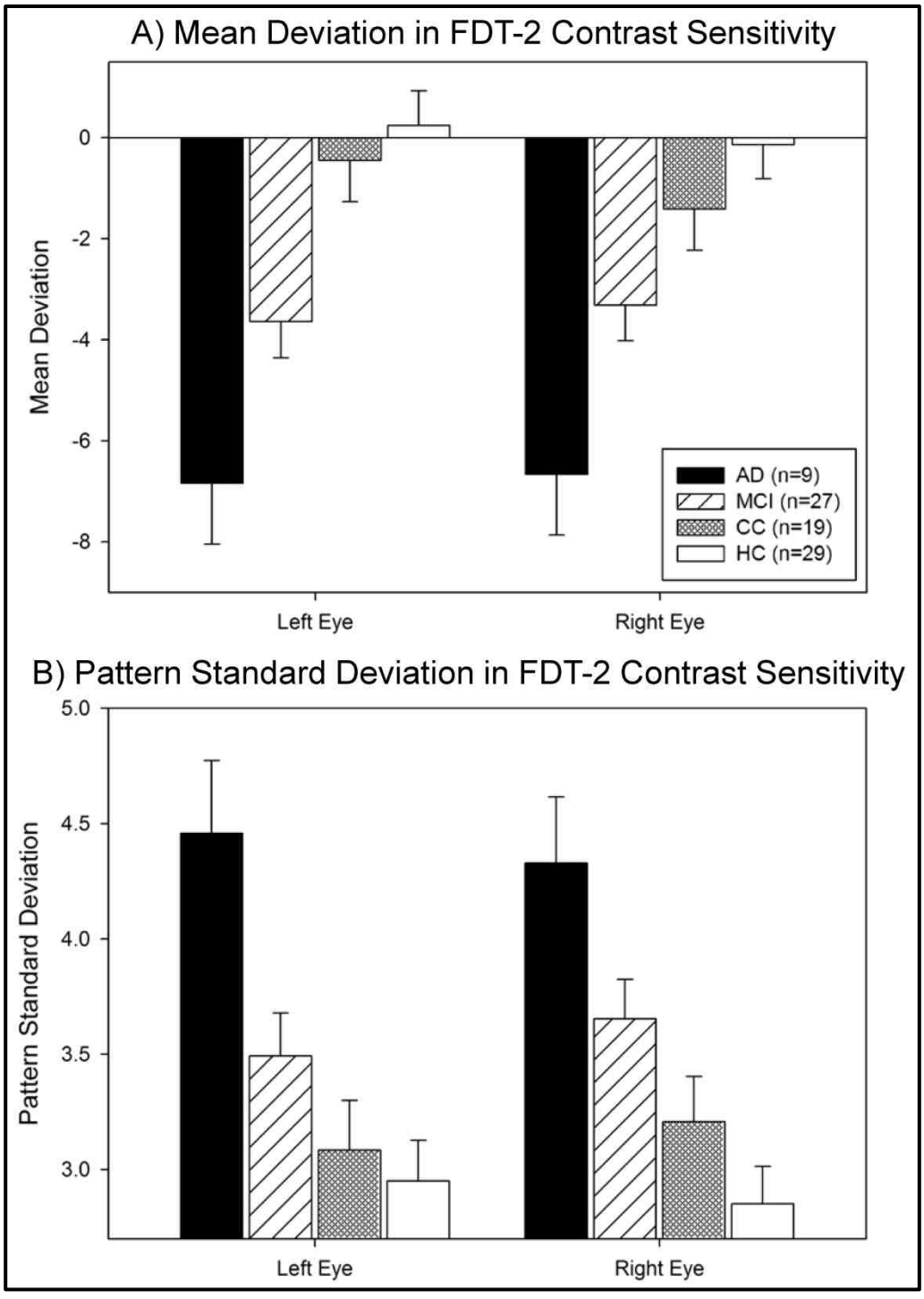

Figure 22. Mean Deviation and Pattern Standard Deviation in Visual Contrast Sensitivity

Summary measures of visual contrast sensitivity performance, including mean deviation (A), which is a measure of general contrast sensitivity performance, and

pattern standard deviation (B), which measures the variability of contrast sensitivity across the VF, were significantly different across groups in both eyes (all $p<0.001$). Post-hoc comparisons indicate that patients with AD show a more impaired mean deviation in both eyes than CC (left (L): $p<0.001$; right (R): $p<0.01$) and HC (both $p<0.001$), as well as a greater pattern standard deviation in both eyes than CC (L: $p<0.01$; R: $p<0.05$) and HC (both $p<0.001$). In addition, MCI patients show a more impaired mean deviation than CC in the left eye only ($p<0.05$) and HC in both eyes (L: $p<0.01$; R: $p<0.05$), as well as a greater pattern standard deviation than HC in the right eye only ($p<0.05$). Bars represent group mean values (+/- SE) adjusted for gender and education.

Regional Contrast Sensitivity Performance across the Visual Field

Contrast sensitivity thresholds in 49 of the 55 VF regions in the left eye (Figure 23A) and 44 of the 55 VF regions in the right eye (Figure 23B) were different among diagnostic groups (see significance values in Figure 23). Post-hoc comparisons indicated that 88 of the 110 VF regions were impaired in AD patients relative to HC, while MCI patients showed significant impairment in 37 of the 110 VF regions relative to HC ($p<0.05$).

Differences among diagnostic groups in mean contrast sensitivity were also detected in the four VF quadrants bilaterally (significance shown in Figure 23C and 23D), with the upper right VF quadrant showing the largest difference among groups in both eyes. Post-hoc comparisons demonstrated impaired mean contrast sensitivity in all VF quadrants of both eyes in AD patients relative to CC (all $p<0.05$) and HC participants (all $p<0.01$), and relative to MCI patients in the upper right VF quadrants of both eyes (both $p<0.05$). MCI patients also demonstrated a reduced mean contrast sensitivity relative to HC in all quadrants of the VF of the left eye (all $p<0.05$) and the upper and lower right VF quadrants of the right eye (both $p<0.05$), as well as an impaired mean contrast sensitivity relative to CC participants in the upper right VF quadrant of the left eye ($p<0.05$).

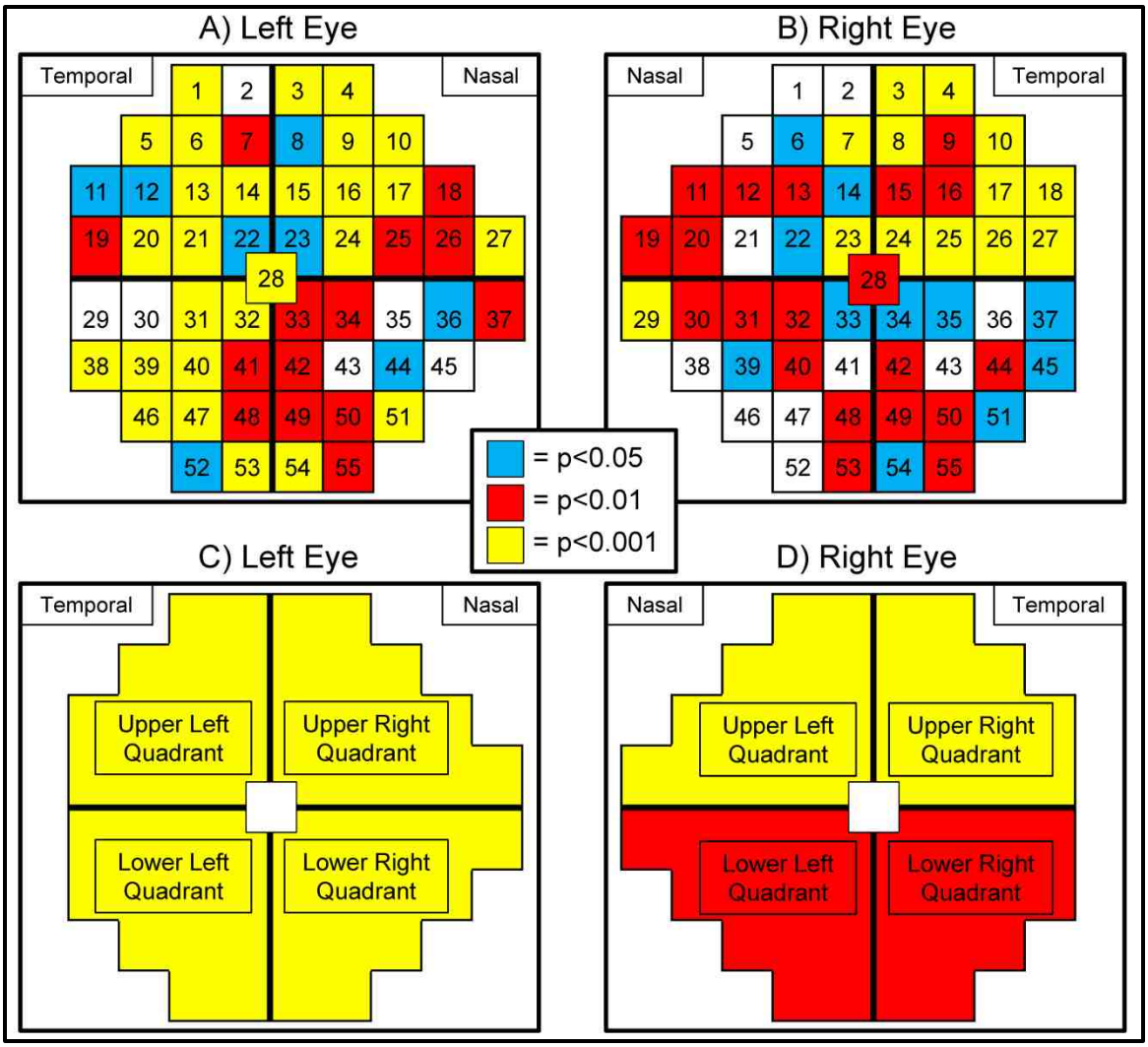

Figure 23. Distribution of Group Differences in FDT-2 Contrast Sensitivity Thresholds across the Visual Field

Significant differences among groups (n=84; 9 AD, 27 MCI, 19 CC, 29 HC) were observed in contrast sensitivity thresholds in 93 of 110 regions across the visual field (VF) in the left (A) and right (B) eyes. In addition to evaluating single regions, mean contrast thresholds for the four VF quadrants within each eye were assessed. All VF quadrants of the left (C) and right (D) eyes were significantly different among diagnostic groups. See text for discussion of between-group differences. All statistical models represented in this figure included age at visit, gender, and years of education as covariates.

Logistic Regression and ROC Curves for Diagnostic Classification of MCI vs. HC

Univariate and multivariate classification capabilities of the FDT-2 variables were examined in a preliminary manner considering the available sample sizes and non-independence of some variables. Logistic regression models demonstrated significant predictive ability of summary and threshold contrast sensitivity variables for classification of MCI patients versus HC. Mean contrast sensitivity threshold in the bilateral lower left VF quadrant was the best MCI vs. HC classifier with 80.4% overall accuracy (specificity=86.2%, sensitivity=74.1%; Figure 24A, area under the curve (AUC)=0.842), while bilateral mean deviation had 75% accuracy (specificity=82.8%, sensitivity=66.7%; Figure 24B, AUC=0.808). Finally, the classification accuracy for MCI vs. HC using a measure of memory performance (CVLT total score) was improved by adding bilateral mean deviation as a second classifier, with CVLT total score alone showing an overall accuracy of 87.5% (specificity=89.7%, sensitivity=85.2%) and CVLT total score and bilateral mean deviation showing an overall accuracy of 94.2% (specificity=93.1%, sensitivity=96.3%).

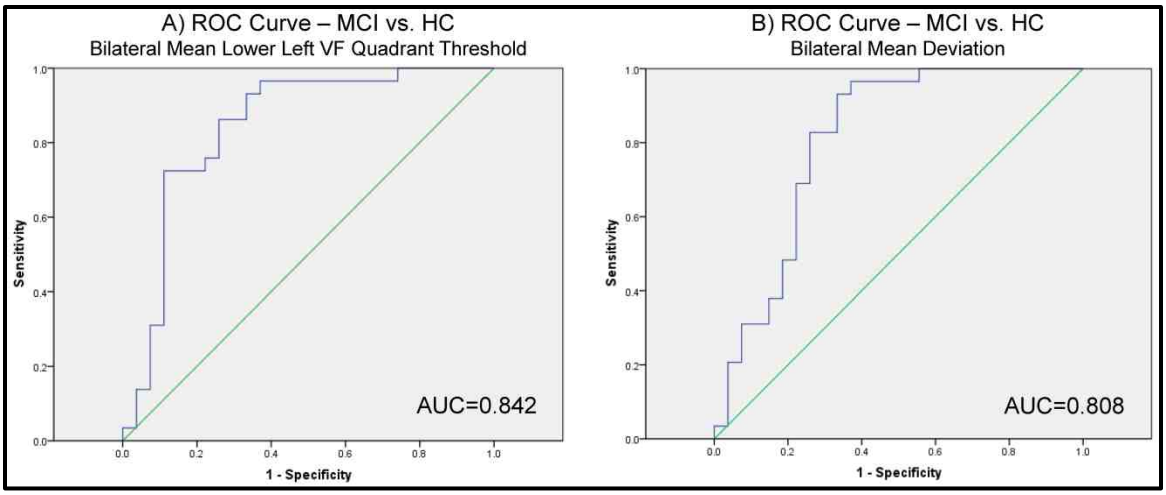

Figure 24. ROC Curves of MCI vs. HC Classification for Selected FDT-2 Measures of Visual Contrast Sensitivity

Visual contrast sensitivity measures effectively classified patients with MCI and HC by diagnostic group (n=56; 27 MCI, 29 HC). The bilateral mean lower left visual field (VF) quadrant contrast threshold (A) was the best classifier of MCI vs. HC. Bilateral mean deviation (B) also successfully classified patients with MCI and HC by diagnostic group. Prior to evaluation for classification accuracy, the bilateral mean lower left VF quadrant contrast threshold was adjusted for age at visit, gender, and years of education, while bilateral mean deviation was adjusted for gender and years of education.

Relationship between Contrast Sensitivity Performance and Cognitive Performance

FDT-2 contrast sensitivity performance was associated with performance on cognitive screening and memory measures. Impaired performance on the MMSE was significantly associated with a reduced mean contrast sensitivity threshold in the bilateral upper right VF quadrant (Figure 25A; $r=0.527$, $p<0.001$). In this association one AD participant appeared to be a significant outlier with a MMSE total score of 15. After excluding this participant the association remained, with mild attenuation (Figure 25B; $r=0.383$, $p<0.001$). Poorer memory performance on the CVLT was also significantly associated with impaired FDT-2 contrast sensitivity performance, including associations between CVLT total score and bilateral mean deviation in contrast sensitivity (Figure 25C; $r=0.471$, $p<0.001$), as well as between CVLT-SD and the mean contrast sensitivity threshold in the bilateral upper right VF quadrant (Figure 25D; $r=0.567$, $p<0.001$). The associations between memory performance and contrast sensitivity were nearly unchanged when the AD participant discussed above was excluded, so all participants were included in Figures 25C and 25D.

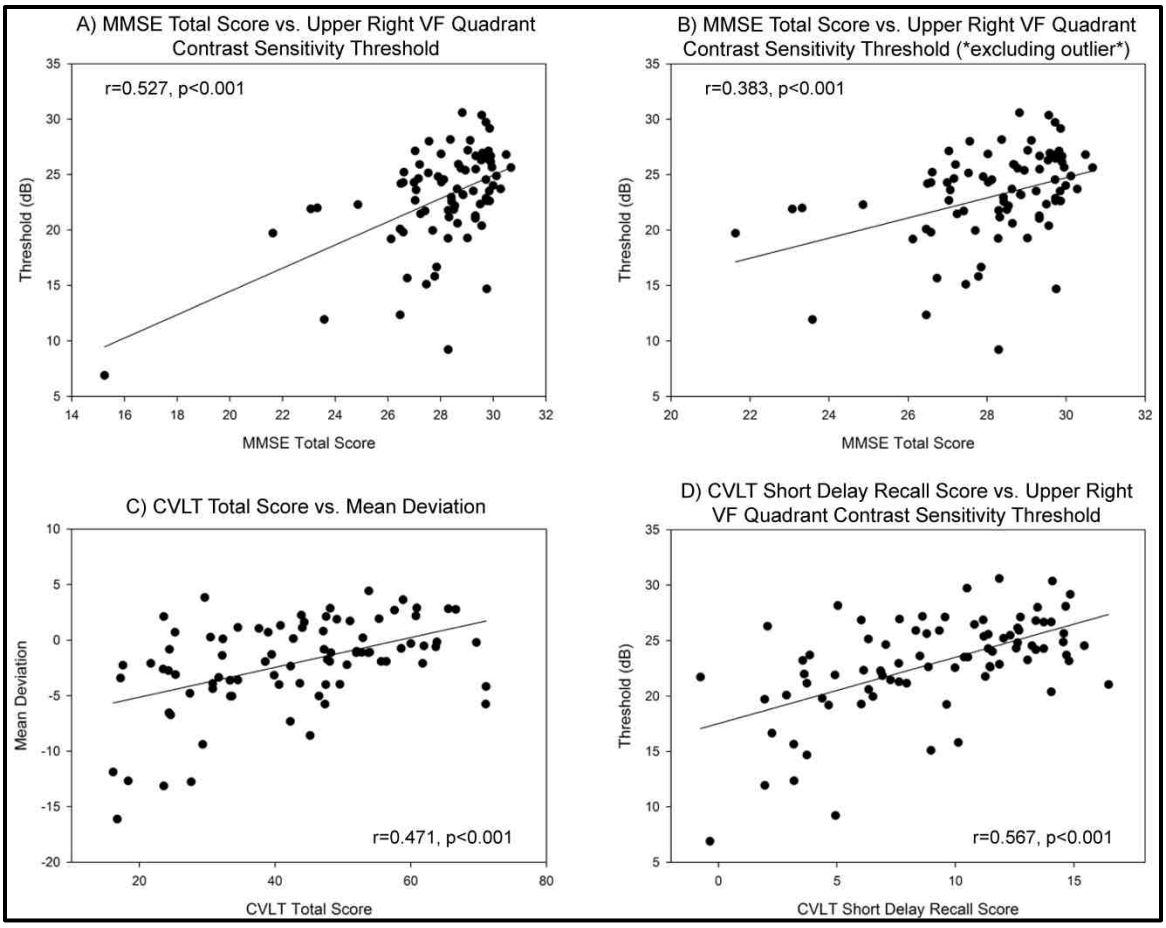

Figure 25. Relationship between Visual Contrast Sensitivity and Cognition

Significant associations between FDT-2 measures of visual contrast sensitivity and cognitive performance were observed. (A) Impaired general cognition (MMSE total score) was significantly associated with reduced mean bilateral contrast threshold of the upper right visual field (VF) quadrant. Upon visual inspection, one AD participant appeared to be a significant outlier, with an MMSE total score well below all other participants. However, when this participant was excluded (B), MMSE total score was still significantly associated with contrast sensitivity as measured by the mean bilateral contrast threshold of the upper right VF quadrant. Impaired memory performance was also significantly associated with reduced contrast sensitivity performance, including a significant association between CVLT total score and bilateral mean deviation in contrast sensitivity (C) and between CVLT short delay recall score and the mean bilateral contrast threshold of the upper right VF quadrant (D). All participants (n=84; 9 AD, 27 MCI, 19 CC, 29 HC) were included in panels A, C, and D, while 1 AD participant was

excluded (due to low MMSE total score) from panel B (n=83; 8 AD, 27 MCI, 19 CC, 29 HC). Exclusion of the AD outlier did not significantly affect the results in panels C and D. All psychometric and contrast sensitivity performance variables were pre-adjusted for age at visit (all variables except for mean deviation), gender (all variables), and years of education (all variables).

Relationship between Contrast Sensitivity Performance and Grey Matter Density

Significant associations between mean deviation and GM density (Figure 26A), between pattern standard deviation and GM density (Figure 26C), and between the mean contrast threshold in the upper right VF quadrant and GM density (Figure 26E) were found in the medial temporal lobe, including significant clusters in the left and right hippocampi. Other significant clusters were observed in the left and right striatum for all associations (Figures 26B, 26D, and 26F). For these comparisons, only 79 participants were included (9 AD, 26 MCI, 16 CC, and 28 HC) due to failed MRI acquisition or processing.

Relationship between Contrast Sensitivity Performance and Selected MRI Measures

Significant associations were observed between mean deviation in contrast sensitivity and bilateral mean medial temporal lobe cortical thickness (Figure 27A; $r=0.327$, $p=0.003$) and mean temporal lobe cortical thickness (Figure 27B; $r=0.331$, $p=0.003$). Mean temporal lobe cortical thickness was also associated with mean pattern standard deviation (Figure 27C; $r=-0.380$, $p<0.001$) and mean contrast threshold of the upper right VF quadrant (Figure 27D; $r=0.382$, $p<0.001$). Only 79 participants were included (9 AD, 26 MCI, 16 CC, and 28 HC) in these comparisons due to failed MRI acquisition or processing.

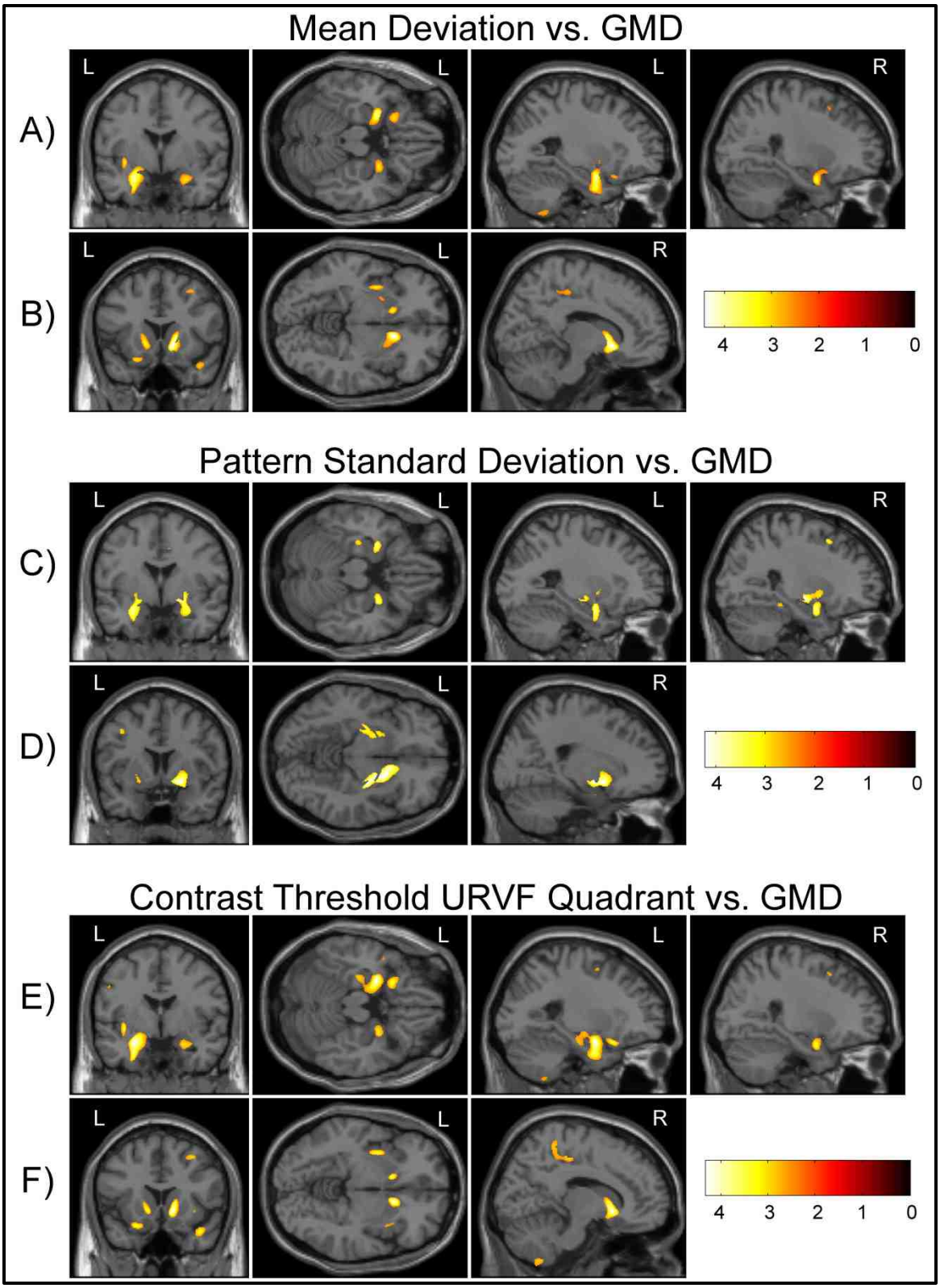
Mean Deviation vs. GMD
A)
B)
Pattern Standard Deviation vs. GMD
C)
D)
Contrast Threshold URVF Quadrant vs. GMD
E)
F)
L
R
4 3 2 1 0

Figure 26. Relationship between Visual Contrast Sensitivity and Grey Matter Density

Significant associations between impaired contrast sensitivity (reduced mean deviation) and decreased GM density were observed in the (A) medial temporal lobe and (B) striatum. Significant associations between increased pattern standard deviation in contrast sensitivity and reduced GM density were also observed in the (C) medial temporal lobe and (D) striatum. Reductions in the mean contrast threshold in the upper right visual field quadrant were significantly associated with reduced GM density in the (E) medial temporal lobe and (F) striatum, as well as a small cluster in the (F) medial parietal lobe. Age at visit, gender, years of education, MRI type and total ICV were included as covariates as appropriate. All images displayed at $p<0.005$ (uncorrected for multiple comparisons), minimum cluster size (k) = 100 voxels. (*Note:* n=79, 9 AD, 26 MCI, 16 CC, 28 HC due to failed MRI acquisition or processing; GMD=grey matter density, URVF=upper right visual field)

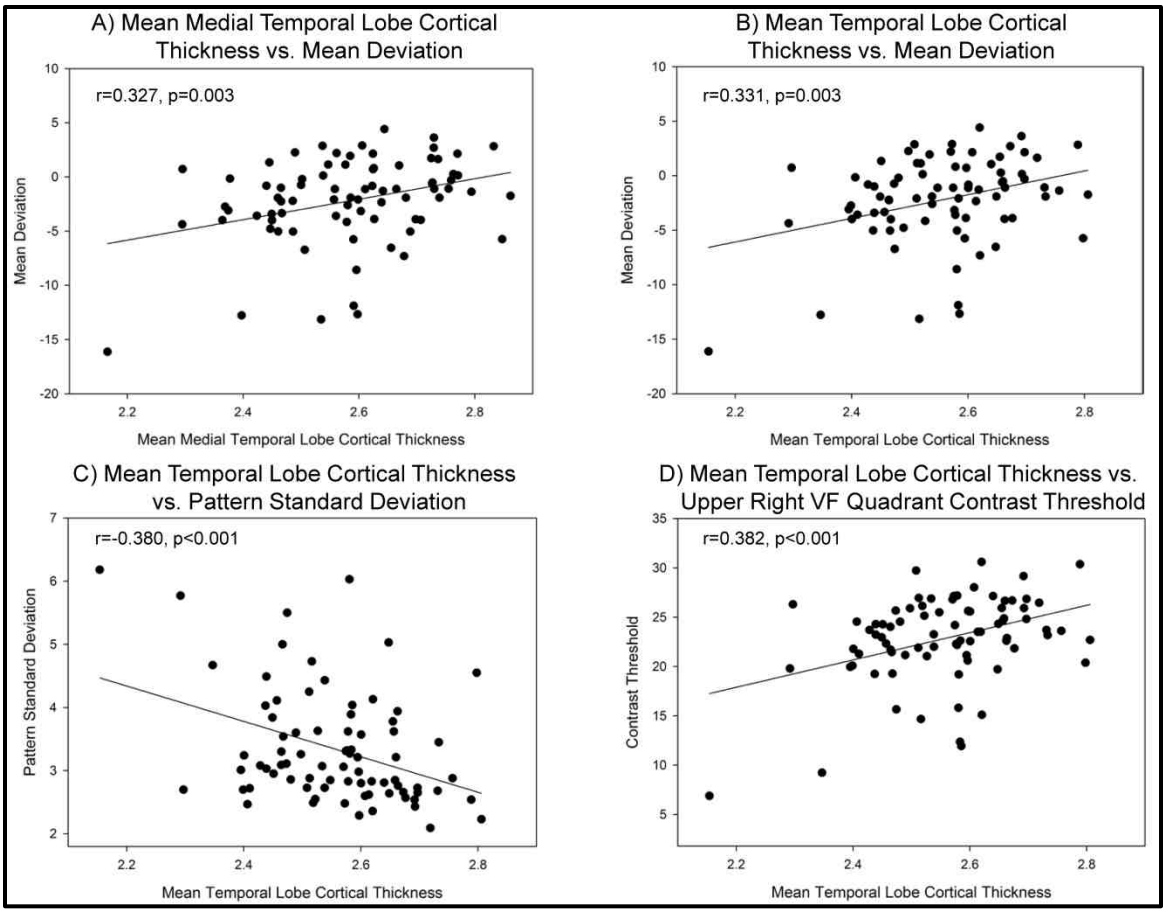

Figure 27. Relationship between Visual Contrast Sensitivity and Temporal Lobe Atrophy

Significant relationships were observed between mean medial temporal lobe cortical thickness and mean deviation in contrast sensitivity (A; r=0.327, p=0.003), as well as between mean temporal lobe cortical thickness and mean deviation in contrast sensitivity (B; r=0.331, p=0.003), pattern standard deviation in contrast sensitivity (C; r= -0.380, p<0.001), and the mean contrast threshold in the upper right visual field quadrant (D; r=0.382, p<0.001). All variables were pre-adjusted for age at visit, gender, and years of education as appropriate. (*Note:* n=79, 9 AD, 26 MCI, 16 CC, and 28 HC due to failed MRI acquisition or processing; VF=visual field)

Discussion

The present study was designed to evaluate visual contrast sensitivity in patients with MCI and AD, as well as in older adults with cognitive complaints. The results demonstrated that patients with both AD and MCI show marked deficits in contrast sensitivity with reduced general sensitivity (lower mean deviation) and abnormal variability (higher pattern standard deviation). Significant differences were detected in the majority of the 110 regions tested in the FDT-2 24-2 exam, with the most notable differences in the upper right VF quadrant. In a preliminary assessment using the available data set, measures of contrast sensitivity demonstrated significant capability to classify MCI and HC by diagnostic group. In addition to detected differences among diagnostic groups, contrast sensitivity deficits were associated with impaired cognitive performance, including in global functioning (MMSE total score) and memory performance (CVLT total score and short delay recall score). Finally, significant associations between contrast sensitivity deficits and reduced GM density and cortical thickness in the medial and lateral temporal lobes were observed.

These results suggest that contrast sensitivity deficits are a feature of AD and AD-related changes, even in early prodromal stages of the disease (i.e., CC and MCI). However, the biological and/or neuropathological basis of this deficit in contrast sensitivity is currently unknown. These deficits could result from a number of pathological changes in the visual system of AD patients, including (but not limited to): (1) sub-threshold glaucomatous damage; (2) performance deficits due to cognitive inability to complete the task; (3) degeneration and/or dysfunction of retinal ganglion cells (RGC); and/or, (4) degeneration and/or dysfunction of visual pathways within the brain. However, our findings are unlikely to result from either of the first two explanations. Although previous reports have shown a high co-occurrence of glaucoma and AD [399-401], as well as an association between the primary genetic predictor of late-onset AD (apolipoprotein E ε4 genotype) and glaucoma [402-404], participants in our cohort who showed even mild glaucoma symptoms were excluded. Additionally, no significant differences among diagnostic groups in cup-to-disc ratio or

intraocular pressure (IOP) were observed (Table 6), suggesting that glaucomatous symptoms do not likely underlie the differences among groups. In addition, it is unlikely that impaired contrast sensitivity was due solely to impaired cognition, as participants in the present study show relatively mild cognitive deficits and showed minimal errors on the FDT-2 24-2 exam (Table 6 and Figure 21).

Therefore, the observed deficits in contrast sensitivity are most likely reflecting changes associated with neuropathological and/or functional changes in the retina and/or central visual processing pathways. Patients with AD have previously been shown to have extensive retinal and optic nerve degeneration with loss of RGC, measured as thinning of the retinal nerve fiber layer using optical coherence tomography (OCT) and other techniques [376-377, 380, 405-406], as well as RGC loss noted in post-mortem retinal tissues [373-374, 378, 407-409], changes in retinal vasculature [410], and functional changes in retinal activation [366, 377, 411-412]. In addition, MCI patients have also been shown to have intermediate thinning of the nerve fiber layer using OCT [376].

RGC loss in AD and MCI may result from amyloid pathology in the eye and/or retina. Both amyloid-beta (Aβ) plaques and oligomers have been reported in post-mortem retinal tissue from patients with AD and a mouse model of AD [413], as well as *in vivo* human retinal tissue (vitreous humor) from patients with glaucoma [414-416]. In addition, amyloid has been shown to be associated with degeneration of RGC in a mouse model of glaucoma [417]. Amyloid-beta has also been shown to be present in the lenses of patients with AD, at levels comparable to the brain [418]. Therefore, in AD patients, amyloid accumulation in the eye and/or retina may result in degeneration of RGC in parallel to amyloid accumulation and Aβ-related neurodegeneration in the brain. In fact, in a mouse model of AD, plaque accumulation in the retina was not only significantly associated with amyloid plaques in the brain, but actually preceded extensive brain amyloid deposition [413].

Degeneration of RGC and/or impairment in contrast sensitivity may also result from AD pathology in the central visual pathways. AD patients show

degeneration of the primary and secondary visual cortex [366, 368-369, 371-372], as well as degeneration of subcortical regions comprising parts of the visual pathway (e.g., LGN) [370]. Previous studies have also reported that magnocellular visual pathways appear to be particularly vulnerable to degeneration in AD, with magnocellular cortical layers showing more degeneration than neighboring regions [369-370]. Interestingly, FDT contrast sensitivity performance has been shown to heavily involve the magnocellular visual pathway [381-382]. Thus, degeneration of RGC and/or visual pathways in the brain may individually affect or combine to underlie the functional deficits in contrast sensitivity seen in patients with AD and MCI, as well as CC, in this study.

The potential importance of neurodegeneration in the brain underlying the observed contrast sensitivity deficits is also supported by the observed associations with MRI measures of neurodegeneration, particularly in the reduced GM density and cortical thickness in the medial temporal lobe. These associations suggest that neurodegeneration near or in magnocellular pathways in the MTL and thalamus may partially explain the observed deficits. Furthermore, associations between impaired visual contrast sensitivity performance and reduced GM density in the striatum were also observed. The striatum is known to be important in visual processing and perception, particularly in sensory gating, attention, and visual discrimination [419]. Degeneration and dysfunction of striatal dopaminergic pathways are thought to contribute to the visual perceptual deficits associated with Huntington's and Parkinson's diseases, as well as visual hallucinations in schizophrenia [419]. Furthermore, the striatum is thought to be involved with sensory-motor tasks [420-421]. The FDT exam involves responding to a visual signal by clicking a button and therefore, FDT responses may be partially coordinated through the striatum. Thus, neurodegeneration in striatal regions may also affect the contrast sensitivity performance as measured using FDT in the present study.

The observation that the upper right visual field quadrant shows the greatest differences between groups may also support the role of central

degeneration in the observed deficits. The right visual field is processed by the left hemisphere of the brain and signals are sent along the optic tract through the left thalamus (i.e., LGN) and near the left MTL. Although neurodegeneration associated with AD occurs bilaterally, the left hippocampus has been reported to show slightly more degeneration than the right hippocampus [213]. Furthermore, in the present study, GM density changes in left MTL showed a greater association with contrast sensitivity performance than changes in the right MTL. Future studies utilizing advanced neuroimaging techniques, including amyloid PET imaging, diffusion tensor imaging of white matter tracts, and potentially functional neuroimaging of contrast sensitivity paradigms, may also help to identify the neurobiological basis for the observed deficits.

Despite the strong effects and novel observations, the present study has several limitations. We did not assess RGC loss or nerve fiber layer changes directly using OCT or other techniques. The association of RGC loss to contrast sensitivity performance would be beneficial in elucidating the neurobiological substrates of the observed contrast sensitivity deficits (i.e., retinal and/or central basis). Future studies utilizing both FDT-2 measures of retinal function and OCT measures of retinal morphology would be ideal. Second, in the present report our group of patients with AD was small relative to the other groups. This shortcoming is not surprising and somewhat unavoidable due to our exclusion of patients with glaucoma and the high co-occurrence of glaucoma and AD [399-401]. In addition, the focus of our study was to evaluate contrast sensitivity in prodromal stages of AD. Finally, the cross-sectional nature of the study design precludes assessment of the ability of FDT-2 contrast sensitivity deficits to predict and/or monitor disease progression. Future studies designed to determine the sensitivity of FDT-2 to longitudinal change and clinical outcome, as well as those including larger AD cohorts, will be informative.

The presence of contrast sensitivity deficits in patients with MCI and even some individuals who show normal cognitive function but have complaints about their cognition is noteworthy and warrants additional investigation. The results of this cross-sectional design study suggest that visual contrast sensitivity

performance, as measured by FDT-2, may represent a novel biomarker for early detection of AD and AD-related changes. However, the ability of impaired contrast sensitivity to predict future progression to AD in patients in early stages of disease or even in cognitively normal elders at-risk for progression to AD due to genetics or high amyloid accumulation is presently unknown. Future studies to determine whether contrast sensitivity can be used effectively as a biomarker for differential diagnosis and prediction of disease progression are needed. In particular, studies evaluating longitudinal contrast sensitivity performance monitoring as a screening tool or outcome variable would be particularly beneficial. FDT-2 measures of contrast sensitivity performance have previously been shown to be relatively stable, despite a learning effect, in healthy adults [422]. If proven to be dynamically sensitive to changes associated to disease progression, contrast sensitivity and/or other ocular biomarkers of AD would be particularly useful in early detection and disease monitoring due to the fact that they are relatively non-invasive, inexpensive, and widely available [423].

In conclusion, patients with MCI and AD show deficits in contrast sensitivity measured using FDT-2. Older adults with cognitive complaints but no clinically significant cognitive impairments also show some mild alterations in contrast sensitivity performance. The deficits in contrast sensitivity are generally distributed across the entire retina, although the greatest difference between patients with MCI and AD and HC is observed in the upper right VF quadrant. Measures of contrast sensitivity can also effectively categorize MCI patients versus HC. Impairments in contrast sensitivity are significantly associated with cognitive deficits, including general cognition and memory impairments, as well as neurodegeneration in the medial and lateral temporal lobe as measured using structural MRI. These results suggest that visual contrast sensitivity measured using FDT-2 may be a useful biomarker for AD, even in early clinical stages. Future studies are needed to help elucidate the biological basis of the observed contrast sensitivity deficits, as well as to examine their utility in detecting AD precursors and predicting disease progression to AD.

Acknowledgements

This study was supported in part by an investigator-initiated research grant from Welch Allyn, Inc. (AJS), the National Institutes of Health (R01 AG19771), Alzheimer's Association (IIRG-99-1653 from the Hedco Foundation), and Indiana Economic Development Corporation (IEDC 87884) to AJS, NIA P30 AG10133-18S1 Core Supplement to Drs. B. Ghetti and AJS, NIH CTSI Pre-doctoral Training Fellowship to SLR (Training Grant TL1 RR025759), as well as the NIH/NCRR Indiana Clinical and Translational Sciences Institute (U54 RR025761; C06-RR020128).

The authors gratefully acknowledge the help of the ophthalmology technicians at Indiana University School of Medicine (Linda Morgan, CCRC and Joni Hoop, CCRC, COA) and Dartmouth-Hitchcock Medical Center (Kimberly McQuaid, COMT) for assistance with the FDT exams; Drs. Vanessa Taler and Katherine Nutter-Upham, Laura Rabin, Nadia Paré, Alette Wessels, and Margaret Nordstrom for assistance with cognitive assessment and cohort follow-up; and Drs. Edward O'Neil and Greg Gdowski of Blue Highway, LLC, a subsidiary of Welch Allyn, Inc. Finally, we thank the participants and family members from New England and Indiana without whom this study would not have been possible.

Summary

The results of this report indicate that structural MRI measures of neurodegeneration are sensitive biomarkers for AD, even in early clinical stages such as MCI and older adults with cognitive complaints. The first chapter explores the use of cross-sectional MRI measures of brain atrophy to detect differences between patients with MCI and AD and healthy older adults in the largest sample to date, the Alzheimer's Disease Neuroimaging Initiative (ADNI). The results support previous findings in smaller samples, showing significant atrophy in patients with MCI and AD throughout the brain and most significantly in the medial temporal lobe (MTL). Furthermore, patients who converted from MCI to probable AD within one year after the MRI scan (MCI-Converters (MCI-C) showed significantly more MTL atrophy at baseline than participants who were stable for the subsequent year (MCI-Stables (MCI-S)). In fact, MCI-C had nearly equivalent atrophy in the hippocampus and MTL to patients already diagnosed with AD up to one year before clinical conversion. These results suggest that the neurodegeneration observed with MRI measures of atrophy is an antecedent marker of future clinical decline to dementia. Finally, the results of the effect size calculation for selected MRI regions of interest (ROIs) indicate that hippocampal and other MTL atrophy measures are the most sensitive biomarkers for detecting differences between patients who convert from MCI to probable AD during the subsequent year and those who have a stable MCI diagnosis. In sum, Chapter 1 confirms the sensitivity of cross-sectional MRI measures as biomarkers for detecting neurodegeneration associated with AD and for predicting future progression of patients with MCI to probable AD.

The second chapter of this report explores the use of dynamic MRI measures of brain atrophy rate as biomarkers for AD. In particular, the change in brain volume, cortical thickness, and grey matter (GM) density and GM volume between two MRI scans spaced 1-2 years apart was assessed either as an absolute change (Figure 8, Table 4) or as an annualized percent change (APC) in a target ROI (Figures 9-14 and Figures 16-20). In Chapter 2a, the change in whole brain GM density over one year on a voxel-wise level and APC in target

ROIs were assessed for differences among patients with AD and MCI and HC in the ADNI cohort. Similar to the analyses in Chapter 1, the differences in longitudinal atrophy and target region atrophy rates between patients who converted from MCI to probable AD over the first year of the study (MCI-C) and patients with a stable MCI diagnosis (MCI-S) were evaluated. We observed a significantly greater decline in GM density across the whole brain, as well as a faster rate of atrophy in the medial and lateral temporal, frontal, and parietal lobes, in patients with AD relative to HC. In addition, MCI-C showed greater GM atrophy and a faster rate of atrophy in all evaluated ROIs than MCI-S participants. In fact, MCI-C participants showed nearly equivalent atrophy rates in many target ROIs to AD participants, suggesting that MCI-C patients show AD-like rates of neurodegeneration during, at minimum, the year preceding clinical conversion.

The effect sizes for baseline and APC MRI measures were also calculated for all group comparisons (AD vs. HC, MCI-C vs. MCI-S, MCI-C vs. HC, MCI-S vs. HC, AD vs. MCI-S, AD vs. MCI-C). Interestingly, the effect sizes of baseline measures were greater than those of atrophy rate measures for the comparison of AD vs. HC participants. The greater sensitivity of baseline measures relative to APC measures in the comparison of AD vs. HC may be due to the fact that baseline differences developed over multiple years while the APC metrics are calculated from changes occurring over a single year. However, the effect sizes of atrophy rate measures were greater than those of baseline measures for the comparison of MCI-C vs. MCI-S. This result suggests that dynamic measures of brain atrophy rate are most sensitive to detecting neurodegeneration in participants undergoing significant clinical decline relative to those who are more clinically stable. Finally, the relationship between apolipoprotein E (*APOE*) ε4 genotype (presence or absence of 1 or 2 ε4 alleles), the most commonly reported genetic factor associated with late-onset AD, and APC in target MTL ROIs was evaluated. The results showed that *APOE* ε4 positive participants showed a higher rate of atrophy relative to *APOE* ε4 negative participants within each diagnostic group. These results support a relationship between the presence of

an *APOE* ε4 allele and AD-related neurodegeneration. Furthermore, these findings suggest that *APOE* ε4 positive AD and MCI patients show more severe disease-related neurodegeneration and that *APOE* ε4 positive HC participants may be at higher risk for cognitive decline.

Chapter 2b examines the role of longitudinal MRI measures of brain atrophy rate as biomarkers in a pre-MCI stage of disease, specifically, older adults with cognitive complaints (CC) but no significant cognitive impairment. Baseline atrophy and APC in temporal lobe ROIs over two years were evaluated for differences among patients with a stable AD diagnosis, MCI to probable AD converters, stable MCI patients, older adults with CC at baseline who progressed to a diagnosis of MCI over the two-year follow-up period, older adults with a stable CC diagnosis, and stable HC without cognitive complaints. Similar to results from previous studies and Chapters 1 and 2a, patients with AD and MCI showed greater atrophy at baseline and faster annualized atrophy rate in the temporal lobe relative to HC participants. In addition, MCI-C had greater atrophy at baseline and a faster annualized atrophy rate than MCI-S participants. However, the novel finding in this chapter concerns the CC participants. Participants who converted from CC to MCI over the course of the two-year follow-up period had slightly more atrophy at baseline and faster rates of atrophy in the temporal lobe than participants with a stable CC diagnosis. This result suggests that MRI measures of neurodegeneration are sensitive to AD-like pathological changes in older adults who are progressing towards MCI and AD in preclinical stages without significant cognitive deficits. Similar to previous chapters (Chapters 1 and 2a), effect sizes of baseline atrophy measures and APC in target ROIs for the comparison between converters and stable participants were calculated. Measures of APC in medial and lateral temporal lobe ROIs were most sensitive to the differences between MCI-C and MCI-S participants, as well as between CC-C and CC-S participants. These results support the previous finding (Chapter 2a) that dynamic measures of atrophy rate are most sensitive to the differences between patients who are declining clinically relative to those who are clinically stable. Furthermore, these results suggest that

measures of temporal lobe atrophy rate effectively detect neurodegeneration associated with clinical decline even before patients show marked cognitive impairment. Finally, the relationship between hippocampal atrophy rate and two-year change in clinical dementia severity and memory performance was evaluated for the full cohort and in the sub-group of patients who had a CC diagnosis at baseline (CC-C and CC-S). The results demonstrated that hippocampal atrophy rate was significantly associated with two-year change in clinical dementia severity across the full sample only, likely due to the differences between diagnostic groups (particularly between AD patients and all other groups). Hippocampal atrophy rate was also significantly associated with two-year change in memory performance in both the full sample and the CC at baseline only sub-group. In fact, the relationship between hippocampal atrophy rate and two-year change in memory performance was more significant in the CC at baseline sub-group ($p=0.004$) than in the full sample ($p=0.014$). These results suggest that a higher rate of hippocampal atrophy is more closely linked to memory decline in the earliest stages of disease (i.e., CC participants) and more closely linked to clinical dementia severity and impaired activities of daily living in the later stages of disease (AD and MCI). Overall, the results of this chapter support the role of MRI as a biomarker for AD and suggest that MRI measures can detect and monitor AD-related neurodegeneration even in very early pre-clinical stages (i.e., CC).

The final chapter of this report explores a novel biomarker for AD, visual contrast sensitivity. In addition, the relationships between MRI biomarkers of neurodegeneration and measures of visual contrast sensitivity were assessed. In order to establish the ability of this novel marker to detect changes associated with AD, visual contrast sensitivity, as measured by frequency doubling technology (FDT-2, Welch Allyn Inc.), was compared among a cohort of participants that included older adults with AD, MCI, and CC, as well as HC. Patients with MCI and AD showed significant impairments in contrast sensitivity, with general deficits and abnormal variability across the visual field (VF). In addition, CC participants showed notable contrast sensitivity impairments, with a

performance level intermediate between MCI and HC participants. Although general deficits were observed across the entire VF, the most severe contrast sensitivity impairment in patients with AD and MCI relative to HC was in the upper right VF quadrant. Measures of contrast sensitivity also showed accurate classification of MCI vs. HC, with an overall accuracy of 75-80%. Next, the relationship between contrast sensitivity and cognition was assessed, including relationships between contrast sensitivity and general cognition (MMSE total score) and between contrast sensitivity and memory performance (CVLT total score, short delay recall score). The results demonstrated significant associations between contrast sensitivity and both general cognition and memory performance. Finally, the relationship between contrast sensitivity and MRI markers of neurodegeneration was evaluated. First, the relationship between contrast sensitivity and GM density across the entire brain was assessed on a voxel-wise basis. The results indicated that contrast sensitivity impairment is associated with reduced GM density in the MTL, including the hippocampus, the striatum, as well as temporal and parietal lobar cortical regions. The relationship between contrast sensitivity and regional cortical thickness estimates was also examined. Similar to the whole brain analyses, impaired contrast sensitivity was associated with reductions in medial and lateral temporal lobe cortical thickness. These results suggest that impairments in contrast sensitivity observed in patients with MCI and AD may be partially mediated by neurodegeneration in the brain, particularly in the medial and lateral temporal lobes. Overall, the results in Chapter 3 indicated that visual contrast sensitivity may be a useful biomarker for detecting changes associated with AD, even in early stages of disease. Future studies designed to evaluate the ability of these measures to predict and monitor clinical progression will further elucidate the potential utility of visual contrast sensitivity as a biomarker for AD.

In summary, this report highlights the important role that MRI measures of neurodegeneration can play in studies of patients with AD, as well as in patients at earlier stages of disease (i.e., MCI, CC). The ability of MRI to detect AD-related neurodegeneration in preclinical stages, as well as to predict future

disease progression, suggests that these markers would be particularly useful in therapeutic intervention studies. For example, enriching the treatment group with patients showing significant atrophy at baseline may lead to a cleaner cohort which would be more amenable to effective intervention. Additionally, MRI measures of atrophy rate could also be used as outcome measures in a pharmaceutical trial to assess the mechanisms of a treatment (i.e., whether the treatment promotes neuronal viability and/or prevents AD-related neurodegeneration) and evaluate treatment efficacy. As discussed in Chapter 2a, the use of MRI as an outcome measure in clinical trials would require a smaller sample size to detect a reduction in neurodegeneration than changes in psychometric test performance or clinical dementia severity. Finally, MRI measures of neurodegeneration could also be utilized in the clinical diagnosis and treatment of AD to effectively detect and diagnose patients likely to progress to AD in early preclinical stages. Many scientists and clinicians now believe that an effective treatment for AD will likely involve disease prevention rather than amelioration of symptoms once a patient is already diagnosed with AD. Thus, sensitive biomarkers to detect patients most likely to degenerate will be essential for any interventional treatment to be effective. Given the sensitivity demonstrated in this report, MRI measures of neurodegeneration may be one of the biomarkers utilized in the future once an effective interventional treatment is developed to prevent AD. Furthermore, the development of new biomarkers for AD (i.e., visual contrast sensitivity) may also assist in future clinical diagnosis and therapeutic trials. The use of established biomarkers to measure known changes associated with AD will help identify the underlying pathology associated with new markers, as well as help confirm the utility of newly developed techniques.

Future Directions

The results of this report, as well as those of other researchers, present a number of future directions for continued exploration of the role of MRI and other biomarkers in diagnosis, monitoring, and predicting progression of AD. With the availability of increasing amounts of long-term longitudinal cohorts with advanced neuroimaging and protein biomarker data, a more comprehensive analysis of multiple biomarkers together (i.e., not just MRI measures) and a longer follow-up of patients with MCI, as well as CC and even HC participants, will provide important information. In particular, I would like to pursue the following future directions: (1) an extension of the longitudinal studies with a 3-5 year follow-up time to evaluate the ability of MRI markers to detect and monitor ongoing neurodegeneration, as well as to predict future progression; (2) longitudinal follow-up and monitoring with MRI biomarkers of HC participants, in particular those who show progression towards dementia (i.e., to CC, MCI and/or AD); (3) evaluation of other imaging measures as biomarkers of AD, specifically amyloid PET imaging and functional MRI of task-related brain activation; and, (4) further investigate visual contrast sensitivity as a biomarker for AD, especially for utility in monitoring disease progression in a longitudinal study with multiple contrast sensitivity tests over a 1-2 year period. I believe these additional research directions will further elucidate the role of MRI and other neuroimaging measures as biomarkers of AD and the ability of these measures to function as an important part of AD research, clinical diagnosis, and treatment.

Briefly, the first extension of the current work would be a longer-term follow-up (3-5 years) of the cohorts studied in Chapters 2a and 2b to evaluate cross-sectional atrophy and longitudinal rates of atrophy. Assessing the role of MRI measures over a more extensive follow-up period would establish the sensitivity of these markers to detecting changes more than two years before MCI to probable AD conversion, as well as CC to MCI conversion. Furthermore, a longer study period would likely allow for more participants who were classified as stable in the current study (Chapters 2a and 2b) to convert. Finally, a longer follow-up window may also allow for more HC participants to begin to progress

towards dementia. An assessment of MRI biomarkers in these participants (HC progressors) would help clarify the sensitivity of these markers to detect neurodegeneration in stages before CC and MCI, as well as to elucidate the pathological processes that initiate clinical decline.

Next, the role of other selected imaging measures as biomarkers for AD would be evaluated. Specifically, studies to evaluate amyloid deposition measured using [^{11}C]PiB or [^{18}F]florbetapir PET [100, 120, 122, 424-425] and functional MRI measures of brain activity [229, 241] in early clinical and preclinical stages of AD (e.g., MCI, CC) would provide evidence as to the utility of these measures as biomarkers of AD. In addition, a study to evaluate the relationship between measures of amyloid deposition, functional MRI measures of brain activation, and neurodegeneration measured using structural MRI at different stages of disease would provide interesting information about the associations between these neurobiological processes. In fact, studies have suggested that some of these measures are only minimally related, and thus provide independent information about disease pathology (i.e., amyloid PET and MRI measures) [17, 90]. Assessment of the independent and combined ability of measures of amyloid deposition, brain activation, and neurodegeneration to monitor and predict clinical course would also be informative. Previous studies have already shown an added benefit of combining multiple imaging biomarkers for the detection and monitoring of AD relative to a single measure [314, 426]. To date, the use of multiple combined biomarkers for disease detection, monitoring, and prediction of clinical progression has not been evaluated in older adults with cognitive complaints. Therefore, future studies assessing multiple imaging biomarkers in pre-MCI stages of disease and even in longitudinal studies of declining HC participants would provide valuable insight into the underlying mechanisms at these early stages of disease, as well as an estimate of the added benefit of multiple measures of AD-related pathology.

Finally, the analyses in Chapter 3 showed that visual contrast sensitivity is impaired in patients with AD and MCI and demonstrated a significant association of these measures with known clinical and biological markers of AD. However,

additional studies of visual contrast sensitivity measures are needed to fully characterize its utility as a biomarker for AD. In particular, longitudinal studies to assess change in visual contrast sensitivity over time (1-2 years) from 2 or more visits would provide needed information about the longitudinal stability of the measure, as well as the sensitivity of these measures to monitoring disease progression. Furthermore, these studies would be essential for determining whether visual contrast sensitivity would be a useful outcome measures for clinical therapeutic trials. In addition, the ability of visual contrast sensitivity measures to predict future decline to AD in patients with MCI as well as in earlier stages of disease should be assessed. Similar to the studies in Chapters 1 and 2, visual contrast sensitivity at baseline and/or change in visual contrast sensitivity would be compared between patients who are known to subsequently progress clinically and those who are clinically stable. The predictive ability of contrast sensitivity measures for future conversion to AD from MCI and/or CC would also be assessed. Finally, future studies in an expanded sample of participants and eventually a second independent cohort would be necessary to confirm visual contrast sensitivity as a valid biomarker for AD.

In summary, the findings of the present report support the role of MRI measures of neurodegeneration as a biomarker for AD.

Conclusions

In conclusion, the present report explored the role of MRI measures of neurodegeneration as biomarkers for AD. The results confirmed that both cross-sectional and longitudinal MRI measures are sensitive to detection of AD-related neurodegenerative changes, able to monitor disease progression, and predictive of future clinical decline. In addition, MRI measures appear to be useful for measuring neurodegeneration in not only AD patients, but also patients in earlier clinical stages, such as MCI and CC. MRI measures are also useful for evaluating novel biomarkers for AD, including visual contrast sensitivity. Thus, MRI measures of neurodegeneration are likely to be useful in therapeutic trials of potential disease-modifying treatments and potentially in the clinical diagnosis of AD.

References

1. Wimo, A., et al., *The magnitude of dementia occurrence in the world.* Alzheimer Dis Assoc Disord, 2003. **17**(2): p. 63-7.
2. Newcomer, R.J., P.J. Fox, and C.A. Harrington, *Health and long-term care for people with Alzheimer's disease and related dementias: policy research issues.* Aging Ment Health, 2001. **5 Suppl 1**: p. S124-37.
3. Bertram, L. and R.E. Tanzi, *Thirty years of Alzheimer's disease genetics: the implications of systematic meta-analyses.* Nat Rev Neurosci, 2008. **9**(10): p. 768-78.
4. Corder, E.H., et al., *Gene dose of apolipoprotein E type 4 allele and the risk of Alzheimer's disease in late onset families.* Science, 1993. **261**(5123): p. 921-3.
5. Mayeux, R., et al., *Utility of the apolipoprotein E genotype in the diagnosis of Alzheimer's disease. Alzheimer's Disease Centers Consortium on Apolipoprotein E and Alzheimer's Disease.* N Engl J Med, 1998. **338**(8): p. 506-11.
6. Corder, E.H., et al., *Protective effect of apolipoprotein E type 2 allele for late onset Alzheimer disease.* Nat Genet, 1994. **7**(2): p. 180-4.
7. Klein, W.L., W.B. Stine, Jr., and D.B. Teplow, *Small assemblies of unmodified amyloid beta-protein are the proximate neurotoxin in Alzheimer's disease.* Neurobiol Aging, 2004. **25**(5): p. 569-80.
8. Walsh, D.M. and D.J. Selkoe, *A beta oligomers - a decade of discovery.* J Neurochem, 2007. **101**(5): p. 1172-84.
9. Haass, C. and D.J. Selkoe, *Soluble protein oligomers in neurodegeneration: lessons from the Alzheimer's amyloid beta-peptide.* Nat Rev Mol Cell Biol, 2007. **8**(2): p. 101-12.
10. Masters, C.L., et al., *Molecular mechanisms for Alzheimer's disease: implications for neuroimaging and therapeutics.* J Neurochem, 2006. **97**(6): p. 1700-25.
11. Minati, L., et al., *Current concepts in Alzheimer's disease: a multidisciplinary review.* Am J Alzheimers Dis Other Demen, 2009. **24**(2): p. 95-121.
12. Nathalie, P. and O. Jean-Noel, *Processing of amyloid precursor protein and amyloid peptide neurotoxicity.* Current Alzheimer Research, 2008. **5**(2): p. 92-9.
13. Mawuenyega, K.G., et al., *Decreased clearance of CNS beta-amyloid in Alzheimer's disease.* Science, 2010. **330**(6012): p. 1774.
14. Sperling, R.A., et al., *Toward defining the preclinical stages of Alzheimer's disease: recommendations from the National Institute on Aging-Alzheimer's Association workgroups on diagnostic guidelines for Alzheimer's disease.* Alzheimers Dement, 2011. **7**(3): p. 280-92.

15. Deane, R., et al., *apoE isoform-specific disruption of amyloid beta peptide clearance from mouse brain.* J Clin Invest, 2008. **118**(12): p. 4002-13.

16. Iqbal, K. and I. Grundke-Iqbal, *Alzheimer neurofibrillary degeneration: significance, etiopathogenesis, therapeutics and prevention.* J Cell Mol Med, 2008. **12**(1): p. 38-55.

17. Jack, C.R., Jr., et al., *Hypothetical model of dynamic biomarkers of the Alzheimer's pathological cascade.* Lancet Neurol, 2010. **9**(1): p. 119-28.

18. Gomez-Isla, T., et al., *Neuronal loss correlates with but exceeds neurofibrillary tangles in Alzheimer's disease.* Ann Neurol, 1997. **41**(1): p. 17-24.

19. Bennett, D.A., et al., *Neurofibrillary tangles mediate the association of amyloid load with clinical Alzheimer disease and level of cognitive function.* Arch Neurol, 2004. **61**(3): p. 378-84.

20. Arriagada, P.V., et al., *Neurofibrillary tangles but not senile plaques parallel duration and severity of Alzheimer's disease.* Neurology, 1992. **42**(3 Pt 1): p. 631-9.

21. Oddo, S., et al., *Temporal profile of amyloid-beta (Abeta) oligomerization in an in vivo model of Alzheimer disease. A link between Abeta and tau pathology.* J Biol Chem, 2006. **281**(3): p. 1599-604.

22. Brion, J.P., *Neurofibrillary tangles and Alzheimer's disease.* Eur Neurol, 1998. **40**(3): p. 130-40.

23. Sorrentino, G. and V. Bonavita, *Neurodegeneration and Alzheimer's disease: the lesson from tauopathies.* Neurol Sci, 2007. **28**(2): p. 63-71.

24. Crews, L. and E. Masliah, *Molecular mechanisms of neurodegeneration in Alzheimer's disease.* Hum Mol Genet, 2010. **19**(R1): p. R12-20.

25. McGeer, E.G. and P.L. McGeer, *Neuroinflammation in Alzheimer's disease and mild cognitive impairment: a field in its infancy.* J Alzheimers Dis, 2010. **19**(1): p. 355-61.

26. Swerdlow, R.H., J.M. Burns, and S.M. Khan, *The Alzheimer's disease mitochondrial cascade hypothesis.* J Alzheimers Dis, 2010. **20 Suppl 2**: p. S265-79.

27. Hoozemans, J.J., et al., *Neuroinflammation and regeneration in the early stages of Alzheimer's disease pathology.* Int J Dev Neurosci, 2006. **24**(2-3): p. 157-65.

28. Schwab, C. and P.L. McGeer, *Inflammatory aspects of Alzheimer disease and other neurodegenerative disorders.* J Alzheimers Dis, 2008. **13**(4): p. 359-69.

29. Zhu, Y., et al., *Blueberry opposes beta-amyloid peptide-induced microglial activation via inhibition of p44/42 mitogen-activation protein kinase.* Rejuvenation Res, 2008. **11**(5): p. 891-901.

30. McGeer, P.L., J. Rogers, and E.G. McGeer, *Inflammation, anti-inflammatory agents and Alzheimer disease: the last 12 years.* J Alzheimers Dis, 2006. **9**(3 Suppl): p. 271-6.

31. Good, P.F., et al., *Evidence of neuronal oxidative damage in Alzheimer's disease.* Am J Pathol, 1996. **149**(1): p. 21-8.

32. Mecocci, P., U. MacGarvey, and M.F. Beal, *Oxidative damage to mitochondrial DNA is increased in Alzheimer's disease.* Ann Neurol, 1994. **36**(5): p. 747-51.

33. Schippling, S., et al., *Increased lipoprotein oxidation in Alzheimer's disease.* Free Radic Biol Med, 2000. **28**(3): p. 351-60.

34. Lovell, M.A., et al., *Elevated thiobarbituric acid-reactive substances and antioxidant enzyme activity in the brain in Alzheimer's disease.* Neurology, 1995. **45**(8): p. 1594-601.

35. Mattson, M.P. and S.L. Chan, *Neuronal and glial calcium signaling in Alzheimer's disease.* Cell Calcium, 2003. **34**(4-5): p. 385-97.

36. Parks, J.K., et al., *Neurotoxic Abeta peptides increase oxidative stress in vivo through NMDA-receptor and nitric-oxide-synthase mechanisms, and inhibit complex IV activity and induce a mitochondrial permeability transition in vitro.* J Neurochem, 2001. **76**(4): p. 1050-6.

37. Bush, A.I., C.L. Masters, and R.E. Tanzi, *Copper, beta-amyloid, and Alzheimer's disease: tapping a sensitive connection.* Proc Natl Acad Sci U S A, 2003. **100**(20): p. 11193-4.

38. Lovell, M.A., et al., *Copper, iron and zinc in Alzheimer's disease senile plaques.* Journal of the Neurological Sciences, 1998. **158**(1): p. 47-52.

39. Atwood, C.S., et al., *Dramatic aggregation of Alzheimer abeta by Cu(II) is induced by conditions representing physiological acidosis.* J Biol Chem, 1998. **273**(21): p. 12817-26.

40. Opazo, C., et al., *Metalloenzyme-like activity of Alzheimer's disease beta-amyloid. Cu-dependent catalytic conversion of dopamine, cholesterol, and biological reducing agents to neurotoxic H(2)O(2).* J Biol Chem, 2002. **277**(43): p. 40302-8.

41. Sayre, L.M., et al., *In situ oxidative catalysis by neurofibrillary tangles and senile plaques in Alzheimer's disease: a central role for bound transition metals.* J Neurochem, 2000. **74**(1): p. 270-9.

42. Huang, X., et al., *Zinc-induced Alzheimer's Abeta1-40 aggregation is mediated by conformational factors.* J Biol Chem, 1997. **272**(42): p. 26464-70.

43. Curtain, C.C., et al., *Alzheimer's disease amyloid-beta binds copper and zinc to generate an allosterically ordered membrane-penetrating structure containing superoxide dismutase-like subunits.* J Biol Chem, 2001. **276**(23): p. 20466-73.

44. Boekhoorn, K., M. Joels, and P.J. Lucassen, *Increased proliferation reflects glial and vascular-associated changes, but not neurogenesis in the presenile Alzheimer hippocampus.* Neurobiol Dis, 2006. **24**(1): p. 1-14.

45. Li, B., et al., *Failure of neuronal maturation in Alzheimer disease dentate gyrus.* J Neuropathol Exp Neurol, 2008. **67**(1): p. 78-84.

46. Haughey, N.J., et al., *Disruption of neurogenesis by amyloid beta-peptide, and perturbed neural progenitor cell homeostasis, in models of Alzheimer's disease.* J Neurochem, 2002. **83**(6): p. 1509-24.

47. Haughey, N.J., et al., *Disruption of neurogenesis in the subventricular zone of adult mice, and in human cortical neuronal precursor cells in culture, by amyloid beta-peptide: implications for the pathogenesis of Alzheimer's disease.* Neuromolecular Med, 2002. **1**(2): p. 125-35.

48. Cruz, J.C. and L.H. Tsai, *Cdk5 deregulation in the pathogenesis of Alzheimer's disease.* Trends Mol Med, 2004. **10**(9): p. 452-8.

49. Kish, S.J., et al., *Brain cytochrome oxidase in Alzheimer's disease.* J Neurochem, 1992. **59**(2): p. 776-9.

50. Sorbi, S., E.D. Bird, and J.P. Blass, *Decreased pyruvate dehydrogenase complex activity in Huntington and Alzheimer brain.* Ann Neurol, 1983. **13**(1): p. 72-8.

51. Swerdlow, R.H. and S.J. Kish, *Mitochondria in Alzheimer's disease.* Int Rev Neurobiol, 2002. **53**: p. 341-85.

52. Gabuzda, D., et al., *Inhibition of energy metabolism alters the processing of amyloid precursor protein and induces a potentially amyloidogenic derivative.* J Biol Chem, 1994. **269**(18): p. 13623-8.

53. Szabados, T., et al., *A chronic Alzheimer's model evoked by mitochondrial poison sodium azide for pharmacological investigations.* Behav Brain Res, 2004. **154**(1): p. 31-40.

54. Jagust, W., *Positron emission tomography and magnetic resonance imaging in the diagnosis and prediction of dementia.* Alzheimers Dement, 2006. **2**(1): p. 36-42.

55. Burns, J.M., et al., *Cardiorespiratory fitness and brain atrophy in early Alzheimer disease.* Neurology, 2008. **71**(3): p. 210-6.

56. Burns, J.M., et al., *Cardiorespiratory fitness in early-stage Alzheimer disease.* Alzheimer Dis Assoc Disord, 2008. **22**(1): p. 39-46.

57. Craft, S., et al., *Cerebrospinal fluid and plasma insulin levels in Alzheimer's disease: relationship to severity of dementia and apolipoprotein E genotype.* Neurology, 1998. **50**(1): p. 164-8.

58. Gasparini, L., et al., *Does insulin dysfunction play a role in Alzheimer's disease?* Trends Pharmacol Sci, 2002. **23**(6): p. 288-93.

59. Braak, H., E. Braak, and J. Bohl, *Staging of Alzheimer-related cortical destruction.* Eur Neurol, 1993. **33**(6): p. 403-8.

60. Whitehouse, P.J., et al., *Alzheimer disease: evidence for selective loss of cholinergic neurons in the nucleus basalis.* Ann Neurol, 1981. **10**(2): p. 122-6.

61. Braak, H. and E. Braak, *Evolution of the neuropathology of Alzheimer's disease.* Acta Neurol Scand Suppl, 1996. **165**: p. 3-12.

62. Storey, E., G.J. Kinsella, and M.J. Slavin, *The neuropsychological diagnosis of Alzheimer's disease.* J Alzheimers Dis, 2001. **3**(3): p. 261-285.

63. McKhann, G.M., et al., *The diagnosis of dementia due to Alzheimer's disease: recommendations from the National Institute on Aging-Alzheimer's Association workgroups on diagnostic guidelines for Alzheimer's disease.* Alzheimers Dement, 2011. **7**(3): p. 263-9.

64. Petersen, R.C., *Mild cognitive impairment as a diagnostic entity.* J Intern Med, 2004. **256**(3): p. 183-94.

65. Petersen, R.C., *Mild cognitive impairment: Current research and clinical implications.* Seminars in Neurology, 2007. **27**: p. 22-31.

66. Petersen, R.C. and D. Bennett, *Mild cognitive impairment: is it Alzheimer's disease or not?* J Alzheimers Dis, 2005. **7**(3): p. 241-5; discussion 255-62.

67. Petersen, R.C., et al., *Mild cognitive impairment: clinical characterization and outcome.* Arch Neurol, 1999. **56**(3): p. 303-8.

68. Albert, M.S., et al., *The diagnosis of mild cognitive impairment due to Alzheimer's disease: recommendations from the National Institute on Aging-Alzheimer's Association workgroups on diagnostic guidelines for Alzheimer's disease.* Alzheimers Dement, 2011. **7**(3): p. 270-9.

69. Kelley, B.J. and R.C. Petersen, *Alzheimer's disease and mild cognitive impairment.* Neurol Clin, 2007. **25**(3): p. 577-609, v.

70. Arriagada, P.V., K. Marzloff, and B.T. Hyman, *Distribution of Alzheimer-type pathologic changes in nondemented elderly individuals matches the pattern in Alzheimer's disease.* Neurology, 1992. **42**(9): p. 1681-8.

71. Mintun, M.A., et al., *[11C]PIB in a nondemented population: potential antecedent marker of Alzheimer disease.* Neurology, 2006. **67**(3): p. 446-52.

72. Morris, J.C., et al., *Cerebral amyloid deposition and diffuse plaques in "normal" aging: Evidence for presymptomatic and very mild Alzheimer's disease.* Neurology, 1996. **46**(3): p. 707-19.

73. Ahmed, S., et al., *Memory complaints in mild cognitive impairment, worried well, and semantic dementia patients.* Alzheimer Dis Assoc Disord, 2008. **22**(3): p. 227-35.

74. Dik, M.G., et al., *Memory complaints and APOE-epsilon4 accelerate cognitive decline in cognitively normal elderly.* Neurology, 2001. **57**(12): p. 2217-22.

75. Kliegel, M., D. Zimprich, and A. Eschen, *What do subjective cognitive complaints in persons with aging-associated cognitive decline reflect?* Int Psychogeriatr, 2005. **17**(3): p. 499-512.

76. Nunes, T., et al., *The Outcome of Elderly Patients with Cognitive Complaints but Normal Neuropsychological Tests.* J Alzheimers Dis, 2009.

77. Saykin, A.J., et al., *Older adults with cognitive complaints show brain atrophy similar to that of amnestic MCI.* Neurology, 2006. **67**(5): p. 834-42.

78. Gallassi, R., et al., *Are subjective cognitive complaints a risk factor for dementia?* Neurol Sci, 2010. **31**(3): p. 327-36.

79. Jonker, C., M.I. Geerlings, and B. Schmand, *Are memory complaints predictive for dementia? A review of clinical and population-based studies.* Int J Geriatr Psychiatry, 2000. **15**(11): p. 983-91.

80. Devi, G., et al., *Familial aggregation of Alzheimer disease among whites, African Americans, and Caribbean Hispanics in northern Manhattan.* Arch Neurol, 2000. **57**(1): p. 72-7.

81. de Leon, M.J., et al., *MRI and CSF studies in the early diagnosis of Alzheimer's disease.* J Intern Med, 2004. **256**(3): p. 205-23.

82. de Leon, M.J., et al., *Imaging and CSF studies in the preclinical diagnosis of Alzheimer's disease.* Annals of the New York Academy of Sciences, 2007. **1097**: p. 114-45.

83. Shaw, L.M., et al., *Cerebrospinal fluid biomarker signature in Alzheimer's disease neuroimaging initiative subjects.* Ann Neurol, 2009. **65**(4): p. 403-13.

84. DeCarli, C., *The role of neuroimaging in dementia.* Clin Geriatr Med, 2001. **17**(2): p. 255-79.

85. Ewers, M., et al., *Staging Alzheimer's disease progression with multimodality neuroimaging.* Prog Neurobiol, 2011.

86. Ewers, M., et al., *Neuroimaging markers for the prediction and early diagnosis of Alzheimer's disease dementia.* Trends Neurosci, 2011. **34**(8): p. 430-42.

87. Frisoni, G.B., et al., *The clinical use of structural MRI in Alzheimer disease.* Nat Rev Neurol, 2010. **6**(2): p. 67-77.

88. Hampel, H., et al., *Core candidate neurochemical and imaging biomarkers of Alzheimer's disease.* Alzheimers Dement, 2008. **4**(1): p. 38-48.

89. Hampel, H., et al., *Biomarkers for Alzheimer's disease: academic, industry and regulatory perspectives.* Nat Rev Drug Discov, 2010. **9**(7): p. 560-74.

90. Jagust, W.J., et al., *Relationships between biomarkers in aging and dementia.* Neurology, 2009. **73**(15): p. 1193-9.

91. Kantarci, K., et al., *Comparative diagnostic utility of different MR modalities in mild cognitive impairment and Alzheimer's disease.* Dement Geriatr Cogn Disord, 2002. **14**(4): p. 198-207.

92. Modrego, P.J., *Predictors of conversion to dementia of probable Alzheimer type in patients with mild cognitive impairment.* Current Alzheimer Research, 2006. **3**(2): p. 161-70.

93. Risacher, S.L. and A.J. Saykin, *Neuroimaging of Alzheimer's Disease, Mild Cognitive Impairment and Other Dementias*, in *Brain Imaging in Behavioral Medicine and Neuropsychology*, L.H. Sweet and R.A. Cohen, Editors. 2010, Springer: New York.

94. Sperling, R. and K. Johnson, *Pro: Can biomarkers be gold standards in Alzheimer's disease?* Alzheimers Res Ther, 2010. **2**(3): p. 17.

95. Vemuri, P. and C.R. Jack, Jr., *Role of structural MRI in Alzheimer's disease.* Alzheimers Res Ther, 2010. **2**(4): p. 23.

96. Weiner, M.W., *Imaging and biomarkers will be used for detection and monitoring progression of early Alzheimer's disease.* The Journal of Nutrition, Health & Aging, 2009. **13**: p. 332.

97. Whitwell, J.L. and C.R. Jack, Jr., *Neuroimaging in dementia.* Neurol Clin, 2007. **25**(3): p. 843-57, viii.

98. Wolf, H., et al., *Structural correlates of mild cognitive impairment.* Neurobiol Aging, 2004. **25**(7): p. 913-24.

99. Wolf, H., et al., *A critical discussion of the role of neuroimaging in mild cognitive impairment.* Acta Neurologica Scandinavica. Supplementum, 2003. **179**: p. 52-76.

100. Klunk, W.E., et al., *Imaging brain amyloid in Alzheimer's disease with Pittsburgh Compound-B.* Ann Neurol, 2004. **55**(3): p. 306-19.

101. Herholz, K., *FDG PET and differential diagnosis of dementia.* Alzheimer Dis Assoc Disord, 1995. **9**(1): p. 6-16.

102. Herholz, K., *PET studies in dementia.* Ann Nucl Med, 2003. **17**(2): p. 79-89.

103. Herholz, K., et al., *Discrimination between Alzheimer dementia and controls by automated analysis of multicenter FDG PET.* Neuroimage, 2002. **17**(1): p. 302-16.

104. Silverman, D.H., *Brain 18F-FDG PET in the diagnosis of neurodegenerative dementias: comparison with perfusion SPECT and with clinical evaluations lacking nuclear imaging.* J Nucl Med, 2004. **45**(4): p. 594-607.

105. Chetelat, G., et al., *Mild cognitive impairment: Can FDG-PET predict who is to rapidly convert to Alzheimer's disease?* Neurology, 2003. **60**(8): p. 1374-7.

106. Devanand, D.P., et al., *PET network abnormalities and cognitive decline in patients with mild cognitive impairment.* Neuropsychopharmacology, 2006. **31**(6): p. 1327-34.

107. Drzezga, A., et al., *Prediction of individual clinical outcome in MCI by means of genetic assessment and (18)F-FDG PET.* J Nucl Med, 2005. **46**(10): p. 1625-32.

108. Drzezga, A., et al., *Cerebral metabolic changes accompanying conversion of mild cognitive impairment into Alzheimer's disease: a PET follow-up study.* Eur J Nucl Med Mol Imaging, 2003. **30**(8): p. 1104-13.

109. Mosconi, L., *Brain glucose metabolism in the early and specific diagnosis of Alzheimer's disease. FDG-PET studies in MCI and AD.* Eur J Nucl Med Mol Imaging, 2005. **32**(4): p. 486-510.

110. Mosconi, L., et al., *MCI conversion to dementia and the APOE genotype: a prediction study with FDG-PET.* Neurology, 2004. **63**(12): p. 2332-40.

111. Nishi, H., et al., *Correlation between Cognitive Deficits and Glucose Hypometabolism in Mild Cognitive Impairment.* J Neuroimaging, 2008.

112. Rocher, A.B., et al., *Resting-state brain glucose utilization as measured by PET is directly related to regional synaptophysin levels: a study in baboons.* Neuroimage, 2003. **20**(3): p. 1894-8.

113. Mielke, R. and W.D. Heiss, *Positron emission tomography for diagnosis of Alzheimer's disease and vascular dementia.* J Neural Transm Suppl, 1998. **53**: p. 237-50.

114. Magistretti, P.J. and L. Pellerin, *The contribution of astrocytes to the 18F-2-deoxyglucose signal in PET activation studies.* Mol Psychiatry, 1996. **1**(6): p. 445-52.

115. Ikonomovic, M.D., et al., *Post-mortem correlates of in vivo PiB-PET amyloid imaging in a typical case of Alzheimer's disease.* Brain, 2008. **131**(Pt 6): p. 1630-45.

116. Klunk, W.E., et al., *Binding of the positron emission tomography tracer Pittsburgh compound-B reflects the amount of amyloid-beta in Alzheimer's disease brain but not in transgenic mouse brain.* J Neurosci, 2005. **25**(46): p. 10598-606.

117. Jack, C.R., Jr., et al., *11C PiB and structural MRI provide complementary information in imaging of Alzheimer's disease and amnestic mild cognitive impairment.* Brain, 2008. **131**(Pt 3): p. 665-80.

118. Okello, A., et al., *Conversion of amyloid positive and negative MCI to AD over 3 years: an 11C-PIB PET study.* Neurology, 2009. **73**(10): p. 754-60.

119. Pike, K.E., et al., *Beta-amyloid imaging and memory in non-demented individuals: evidence for preclinical Alzheimer's disease.* Brain, 2007. **130**(Pt 11): p. 2837-44.

120. Quigley, H., S.J. Colloby, and J.T. O'Brien, *PET imaging of brain amyloid in dementia: a review.* Int J Geriatr Psychiatry, 2011. **26**(10): p. 991-9.

121. Villemagne, V.L., et al., *Abeta deposits in older non-demented individuals with cognitive decline are indicative of preclinical Alzheimer's disease.* Neuropsychologia, 2008. **46**(6): p. 1688-97.

122. Wolk, D.A. and W. Klunk, *Update on amyloid imaging: from healthy aging to Alzheimer's disease.* Curr Neurol Neurosci Rep, 2009. **9**(5): p. 345-52.

123. Forsberg, A., et al., *High PIB retention in Alzheimer's disease is an early event with complex relationship with CSF biomarkers and functional parameters.* Curr Alzheimer Res, 2010. **7**(1): p. 56-66.

124. Jagust, W.J., *Amyloid imaging: coming to a PET scanner near you.* Ann Neurol, 2010. **68**(3): p. 277-8.

125. Rowe, C.C., et al., *Amyloid imaging results from the Australian Imaging, Biomarkers and Lifestyle (AIBL) study of aging.* Neurobiol Aging, 2010. **31**(8): p. 1275-83.

126. Engler, H., et al., *Two-year follow-up of amyloid deposition in patients with Alzheimer's disease.* Brain, 2006. **129**(Pt 11): p. 2856-66.

127. Jack, C.R., Jr., et al., *Serial PIB and MRI in normal, mild cognitive impairment and Alzheimer's disease: implications for sequence of pathological events in Alzheimer's disease.* Brain, 2009. **132**(Pt 5): p. 1355-65.

128. Forsberg, A., et al., *PET imaging of amyloid deposition in patients with mild cognitive impairment.* Neurobiol Aging, 2008. **29**(10): p. 1456-65.

129. Kemppainen, N.M., et al., *PET amyloid ligand [11C]PIB uptake is increased in mild cognitive impairment.* Neurology, 2007. **68**(19): p. 1603-6.

130. Koivunen, J., et al., *PET amyloid ligand [11C]PIB uptake and cerebrospinal fluid beta-amyloid in mild cognitive impairment.* Dement Geriatr Cogn Disord, 2008. **26**(4): p. 378-83.

131. Li, Y., et al., *Regional analysis of FDG and PIB-PET images in normal aging, mild cognitive impairment, and Alzheimer's disease.* Eur J Nucl Med Mol Imaging, 2008. **35**(12): p. 2169-81.

132. Koivunen, J., et al., *Amyloid PET imaging in patients with mild cognitive impairment: a 2-year follow-up study.* Neurology, 2011. **76**(12): p. 1085-90.

133. Aizenstein, H.J., et al., *Frequent amyloid deposition without significant cognitive impairment among the elderly.* Arch Neurol, 2008. **65**(11): p. 1509-17.

134. Rowe, C.C., et al., *Imaging beta-amyloid burden in aging and dementia.* Neurology, 2007. **68**(20): p. 1718-25.

135. Sperling, R.A., et al., *Amyloid deposition is associated with impaired default network function in older persons without dementia.* Neuron, 2009. **63**(2): p. 178-88.

136. Mormino, E.C., et al., *Episodic memory loss is related to hippocampal-mediated beta-amyloid deposition in elderly subjects.* Brain, 2009. **132**(Pt 5): p. 1310-23.

137. Resnick, S.M., et al., *Longitudinal cognitive decline is associated with fibrillar amyloid-beta measured by [11C]PiB.* Neurology, 2010. **74**(10): p. 807-15.

138. Jack, C.R., Jr., et al., *MR-based hippocampal volumetry in the diagnosis of Alzheimer's disease.* Neurology, 1992. **42**(1): p. 183-8.

139. Jack, C.R., Jr., et al., *Medial temporal atrophy on MRI in normal aging and very mild Alzheimer's disease.* Neurology, 1997. **49**(3): p. 786-94.

140. Korf, E.S., et al., *Medial temporal lobe atrophy on MRI predicts dementia in patients with mild cognitive impairment.* Neurology, 2004. **63**(1): p. 94-100.

141. Scheltens, P., et al., *Qualitative assessment of cerebral atrophy on MRI: inter- and intra-observer reproducibility in dementia and normal aging.* Eur Neurol, 1997. **37**(2): p. 95-9.

142. Dale, A., B. Fischl, and M. Sereno, *Cortical surface-based analysis. I. Segmentation and surface reconstruction.* Neuroimage, 1999. **9**(2): p. 179-94.

143. Fischl, B. and A.M. Dale, *Measuring the thickness of the human cerebral cortex from magnetic resonance images.* Proc Natl Acad Sci U S A, 2000. **97**(20): p. 11050-5.

144. Fischl, B., et al., *Whole brain segmentation: automated labeling of neuroanatomical structures in the human brain.* Neuron, 2002. **33**(3): p. 341-55.

145. Ashburner, J. and K.J. Friston, *Voxel-based morphometry--the methods.* Neuroimage, 2000. **11**(6 Pt 1): p. 805-21.

146. Good, C.D., et al., *A voxel-based morphometric study of ageing in 465 normal adult human brains.* Neuroimage, 2001. **14**(1 Pt 1): p. 21-36.

147. Fan, Y., et al., *Structural and functional biomarkers of prodromal Alzheimer's disease: a high-dimensional pattern classification study.* Neuroimage, 2008. **41**(2): p. 277-85.

148. Hua, X., et al., *Tensor-based morphometry as a neuroimaging biomarker for Alzheimer's disease: an MRI study of 676 AD, MCI, and normal subjects.* Neuroimage, 2008. **43**(3): p. 458-69.

149. Jack, C.R., Jr., et al., *Antemortem MRI findings correlate with hippocampal neuropathology in typical aging and dementia.* Neurology, 2002. **58**(5): p. 750-7.

150. Henneman, W.J., et al., *Hippocampal atrophy rates in Alzheimer disease: added value over whole brain volume measures.* Neurology, 2009. **72**(11): p. 999-1007.

151. Convit, A., et al., *Hippocampal atrophy in early Alzheimer's disease: anatomic specificity and validation.* Psychiatr Q, 1993. **64**(4): p. 371-87.

152. de Leon, M.J., et al., *The hippocampus in aging and Alzheimer's disease.* Neuroimaging Clin N Am, 1995. **5**(1): p. 1-17.

153. Laakso, M.P., et al., *Hippocampus in Alzheimer's disease: a 3-year follow-up MRI study.* Biol Psychiatry, 2000. **47**(6): p. 557-61.

154. Bobinski, M., et al., *MRI of entorhinal cortex in mild Alzheimer's disease.* Lancet, 1999. **353**(9146): p. 38-40.

155. De Toledo-Morrell, L., et al., *From healthy aging to early Alzheimer's disease: in vivo detection of entorhinal cortex atrophy.* Ann N Y Acad Sci, 2000. **911**: p. 240-53.

156. Dickerson, B.C., et al., *MRI-derived entorhinal and hippocampal atrophy in incipient and very mild Alzheimer's disease.* Neurobiology of Aging, 2001. **22**(5): p. 747-54.

157. Killiany, R.J., et al., *MRI measures of entorhinal cortex vs hippocampus in preclinical AD.* Neurology, 2002. **58**(8): p. 1188-96.

158. Laakso, M.P., et al., *Volumes of hippocampus, amygdala and frontal lobes in the MRI-based diagnosis of early Alzheimer's disease: correlation with memory functions.* J Neural Transm Park Dis Dement Sect, 1995. **9**(1): p. 73-86.

159. Lehericy, S., et al., *Amygdalohippocampal MR volume measurements in the early stages of Alzheimer disease.* AJNR Am J Neuroradiol, 1994. **15**(5): p. 929-37.

160. Teipel, S.J., et al., *Comprehensive dissection of the medial temporal lobe in AD: measurement of hippocampus, amygdala, entorhinal, perirhinal and parahippocampal cortices using MRI.* J Neurol, 2006. **253**(6): p. 794-800.

161. Carmichael, O.T., et al., *Ventricular volume and dementia progression in the Cardiovascular Health Study.* Neurobiol Aging, 2007. **28**(3): p. 389-97.

162. Tanna, N.K., et al., *Analysis of brain and cerebrospinal fluid volumes with MR imaging: impact on PET data correction for atrophy. Part II. Aging and Alzheimer dementia.* Radiology, 1991. **178**(1): p. 123-30.

163. Giesel, F.L., et al., *Temporal horn index and volume of medial temporal lobe atrophy using a new semiautomated method for rapid and precise assessment.* AJNR Am J Neuroradiol, 2006. **27**(7): p. 1454-8.

164. Bottino, C.M., et al., *Volumetric MRI measurements can differentiate Alzheimer's disease, mild cognitive impairment, and normal aging.* Int Psychogeriatr, 2002. **14**(1): p. 59-72.

165. Du, A.T., et al., *Magnetic resonance imaging of the entorhinal cortex and hippocampus in mild cognitive impairment and Alzheimer's disease.* J Neurol Neurosurg Psychiatry, 2001. **71**(4): p. 441-7.

166. Jack, C.R., Jr., et al., *Prediction of AD with MRI-based hippocampal volume in mild cognitive impairment.* Neurology, 1999. **52**(7): p. 1397-403.

167. Killiany, R.J., et al., *Use of structural magnetic resonance imaging to predict who will get Alzheimer's disease.* Ann Neurol, 2000. **47**(4): p. 430-9.

168. Pennanen, C., et al., *Hippocampus and entorhinal cortex in mild cognitive impairment and early AD.* Neurobiol Aging, 2004. **25**(3): p. 303-10.

169. Xu, Y., et al., *Usefulness of MRI measures of entorhinal cortex versus hippocampus in AD.* Neurology, 2000. **54**(9): p. 1760-7.

170. Convit, A., et al., *Specific hippocampal volume reductions in individuals at risk for Alzheimer's disease.* Neurobiol Aging, 1997. **18**(2): p. 131-8.

171. Apostolova, L.G., et al., *3D comparison of hippocampal atrophy in amnestic mild cognitive impairment and Alzheimer's disease.* Brain, 2006. **129**(Pt 11): p. 2867-73.

172. Ballmaier, M., et al., *Comparing gray matter loss profiles between dementia with Lewy bodies and Alzheimer's disease using cortical pattern matching: diagnosis and gender effects.* Neuroimage, 2004. **23**(1): p. 325-35.

173. Becker, J.T., et al., *Three-dimensional patterns of hippocampal atrophy in mild cognitive impairment.* Arch Neurol, 2006. **63**(1): p. 97-101.

174. Kaye, J.A., et al., *Volume loss of the hippocampus and temporal lobe in healthy elderly persons destined to develop dementia.* Neurology, 1997. **48**(5): p. 1297-304.

175. Thompson, P.M., et al., *Dynamics of gray matter loss in Alzheimer's disease.* J Neurosci, 2003. **23**(3): p. 994-1005.

176. Du, A.T., et al., *Higher atrophy rate of entorhinal cortex than hippocampus in AD.* Neurology, 2004. **62**(3): p. 422-7.

177. Frisoni, G.B., et al., *Hippocampal and entorhinal cortex atrophy in frontotemporal dementia and Alzheimer's disease.* Neurology, 1999. **52**(1): p. 91-100.

178. Juottonen, K., et al., *Volumes of the entorhinal and perirhinal cortices in Alzheimer's disease.* Neurobiol Aging, 1998. **19**(1): p. 15-22.

179. Juottonen, K., et al., *Comparative MR analysis of the entorhinal cortex and hippocampus in diagnosing Alzheimer disease.* AJNR Am J Neuroradiol, 1999. **20**(1): p. 139-44.

180. Convit, A., et al., *Age-related changes in brain: I. Magnetic resonance imaging measures of temporal lobe volumes in normal subjects.* Psychiatr Q, 1995. **66**(4): p. 343-55.

181. De Santi, S., et al., *Hippocampal formation glucose metabolism and volume losses in MCI and AD.* Neurobiol Aging, 2001. **22**(4): p. 529-39.

182. Wolf, H., et al., *Hippocampal volume discriminates between normal cognition; questionable and mild dementia in the elderly.* Neurobiol Aging, 2001. **22**(2): p. 177-86.

183. Baron, J.C., et al., *In vivo mapping of gray matter loss with voxel-based morphometry in mild Alzheimer's disease.* Neuroimage, 2001. **14**(2): p. 298-309.

184. Bozzali, M., et al., *The contribution of voxel-based morphometry in staging patients with mild cognitive impairment.* Neurology, 2006. **67**(3): p. 453-60.

185. Busatto, G.F., et al., *A voxel-based morphometry study of temporal lobe gray matter reductions in Alzheimer's disease.* Neurobiol Aging, 2003. **24**(2): p. 221-31.

186. Chetelat, G., et al., *Mapping gray matter loss with voxel-based morphometry in mild cognitive impairment.* Neuroreport, 2002. **13**(15): p. 1939-43.

187. Frisoni, G.B., et al., *Detection of grey matter loss in mild Alzheimer's disease with voxel based morphometry.* J Neurol Neurosurg Psychiatry, 2002. **73**(6): p. 657-64.

188. Hirata, Y., et al., *Voxel-based morphometry to discriminate early Alzheimer's disease from controls.* Neurosci Lett, 2005. **382**(3): p. 269-74.

189. Karas, G.B., et al., *A comprehensive study of gray matter loss in patients with Alzheimer's disease using optimized voxel-based morphometry.* Neuroimage, 2003. **18**(4): p. 895-907.

190. Karas, G.B., et al., *Global and local gray matter loss in mild cognitive impairment and Alzheimer's disease.* Neuroimage, 2004. **23**(2): p. 708-16.

191. Hamalainen, A., et al., *Voxel-based morphometry to detect brain atrophy in progressive mild cognitive impairment.* Neuroimage, 2007. **37**(4): p. 1122-31.

192. Trivedi, M.A., et al., *Structural MRI discriminates individuals with Mild Cognitive Impairment from age-matched controls: A combined neuropsychological and voxel based morphometry study.* Alzheimer's & Dementia, 2006. **2**: p. 296-302.

193. Whitwell, J.L., et al., *MRI patterns of atrophy associated with progression to AD in amnestic mild cognitive impairment.* Neurology, 2008. **70**(7): p. 512-20.

194. Whitwell, J.L., et al., *3D maps from multiple MRI illustrate changing atrophy patterns as subjects progress from mild cognitive impairment to Alzheimer's disease.* Brain, 2007. **130**(Pt 7): p. 1777-86.

195. Cardenas, V.A., et al., *Comparison of methods for measuring longitudinal brain change in cognitive impairment and dementia.* Neurobiol Aging, 2003. **24**(4): p. 537-44.

196. Fox, N.C. and P.A. Freeborough, *Brain atrophy progression measured from registered serial MRI: validation and application to Alzheimer's disease.* J Magn Reson Imaging, 1997. **7**(6): p. 1069-75.

197. Jack, C.R., Jr., et al., *Comparison of different MRI brain atrophy rate measures with clinical disease progression in AD.* Neurology, 2004. **62**(4): p. 591-600.

198. Barnes, J., et al., *Automated measurement of hippocampal atrophy using fluid-registered serial MRI in AD and controls.* J Comput Assist Tomogr, 2007. **31**(4): p. 581-7.

199. Mungas, D., et al., *Longitudinal volumetric MRI change and rate of cognitive decline.* Neurology, 2005. **65**(4): p. 565-71.

200. Stoub, T.R., et al., *Rate of entorhinal and hippocampal atrophy in incipient and mild AD: Relation to memory function.* Neurobiol Aging, 2008.

201. Barnes, J., et al., *A meta-analysis of hippocampal atrophy rates in Alzheimer's disease.* Neurobiol Aging, 2009. **30**(11): p. 1711-23.

202. Jack, C.R., Jr., et al., *Rate of medial temporal lobe atrophy in typical aging and Alzheimer's disease.* Neurology, 1998. **51**(4): p. 993-9.

203. Scahill, R.I., et al., *Mapping the evolution of regional atrophy in Alzheimer's disease: unbiased analysis of fluid-registered serial MRI.* Proc Natl Acad Sci U S A, 2002. **99**(7): p. 4703-7.

204. Thompson, P.M., et al., *Mapping hippocampal and ventricular change in Alzheimer disease.* Neuroimage, 2004. **22**(4): p. 1754-66.

205. Thompson, P.M., et al., *Mapping cortical change in Alzheimer's disease, brain development, and schizophrenia.* Neuroimage, 2004. **23 Suppl 1**: p. S2-18.

206. Whitwell, J.L., et al., *Rates of brain atrophy over time in autopsy-proven frontotemporal dementia and Alzheimer disease.* Neuroimage, 2008. **39**(3): p. 1034-40.

207. deToledo-Morrell, L., et al., *MRI-derived entorhinal volume is a good predictor of conversion from MCI to AD.* Neurobiology of Aging, 2004. **25**(9): p. 1197-203.

208. Devanand, D.P., et al., *Combining Early Markers Strongly Predicts Conversion from Mild Cognitive Impairment to Alzheimer's Disease.* Biol Psychiatry, 2008.

209. Devanand, D.P., et al., *Hippocampal and entorhinal atrophy in mild cognitive impairment: prediction of Alzheimer disease.* Neurology, 2007. **68**(11): p. 828-36.

210. Eckerstrom, C., et al., *Small baseline volume of left hippocampus is associated with subsequent conversion of MCI into dementia: the Goteborg MCI study.* Journal of the Neurological Sciences, 2008. **272**(1-2): p. 48-59.

211. Visser, P.J., et al., *Medial temporal lobe atrophy predicts Alzheimer's disease in patients with minor cognitive impairment.* Journal of Neurology, Neurosurgery & Psychiatry, 2002. **72**(4): p. 491-7.

212. Convit, A., et al., *Atrophy of the medial occipitotemporal, inferior, and middle temporal gyri in non-demented elderly predict decline to Alzheimer's disease.* Neurobiol Aging, 2000. **21**(1): p. 19-26.

213. Risacher, S.L., et al., *Baseline MRI predictors of conversion from MCI to probable AD in the ADNI cohort.* Curr Alzheimer Res, 2009. **6**(4): p. 347-61.

214. Teipel, S.J., et al., *Multivariate deformation-based analysis of brain atrophy to predict Alzheimer's disease in mild cognitive impairment.* Neuroimage, 2007. **38**(1): p. 13-24.

215. Wolf, H., et al., *The prognosis of mild cognitive impairment in the elderly.* J Neural Transm Suppl, 1998. **54**: p. 31-50.

216. Chetelat, G., et al., *Using voxel-based morphometry to map the structural changes associated with rapid conversion in MCI: a longitudinal MRI study.* Neuroimage, 2005. **27**(4): p. 934-46.

217. Karas, G., et al., *Amnestic mild cognitive impairment: structural MR imaging findings predictive of conversion to Alzheimer disease.* AJNR Am J Neuroradiol, 2008. **29**(5): p. 944-9.

218. Erten-Lyons, D., et al., *Brain volume loss in MCI predicts dementia.* Neurology, 2006. **66**(2): p. 233-5.

219. Jack, C.R., Jr., et al., *Rates of hippocampal atrophy correlate with change in clinical status in aging and AD.* Neurology, 2000. **55**(4): p. 484-89.

220. Jack, C.R., Jr., et al., *Brain atrophy rates predict subsequent clinical conversion in normal elderly and amnestic MCI.* Neurology, 2005. **65**(8): p. 1227-31.

221. Sluimer, J.D., et al., *Whole-brain atrophy rate and cognitive decline: longitudinal MR study of memory clinic patients.* Radiology, 2008. **248**(2): p. 590-8.

222. Tapiola, T., et al., *MRI of hippocampus and entorhinal cortex in mild cognitive impairment: a follow-up study.* Neurobiol Aging, 2008. **29**(1): p. 31-8.

223. Wang, P.N., et al., *Prediction of Alzheimer's disease in mild cognitive impairment: a prospective study in Taiwan.* Neurobiology of Aging, 2006. **27**(12): p. 1797-806.

224. Friese, U., et al., *Diagnostic utility of novel MRI-based biomarkers for Alzheimer's disease: diffusion tensor imaging and deformation-based morphometry.* J Alzheimers Dis, 2010. **20**(2): p. 477-90.

225. Chua, T.C., et al., *Diffusion tensor imaging in mild cognitive impairment and Alzheimer's disease: a review.* Curr Opin Neurol, 2008. **21**(1): p. 83-92.

226. Naggara, O., et al., *Diffusion tensor imaging in early Alzheimer's disease.* Psychiatry Res, 2006. **146**(3): p. 243-9.

227. Stebbins, G.T. and C.M. Murphy, *Diffusion tensor imaging in Alzheimer's disease and mild cognitive impairment.* Behav Neurol, 2009. **21**(1): p. 39-49.

228. Kantarci, K., et al., *DWI predicts future progression to Alzheimer disease in amnestic mild cognitive impairment.* Neurology, 2005. **64**(5): p. 902-4.

229. Risacher, S.L., H.A. Wishart, and A.J. Saykin, *Functional MRI Studies of Memory in Aging, Mild Cognitive Impairment, and Alzheimer's Disease*, in *Functional MRI: Basic Principles and Clinical Applications*, S.H. Faro and F.B. Mohamed, Editors. 2011, Springer: New York, NY.

230. Dickerson, B.C., et al., *Increased hippocampal activation in mild cognitive impairment compared to normal aging and AD.* Neurology, 2005. **65**(3): p. 404-11.

231. Golby, A., et al., *Memory encoding in Alzheimer's disease: an fMRI study of explicit and implicit memory.* Brain, 2005. **128**(Pt 4): p. 773-87.

232. Johnson, S.C., et al., *The relationship between fMRI activation and cerebral atrophy: comparison of normal aging and Alzheimer disease.* NeuroImage, 2000. **11**: p. 179-187.

233. Machulda, M.M., et al., *Comparison of memory fMRI response among normal, MCI, and Alzheimer's patients.* Neurology, 2003. **61**(4): p. 500-6.

234. Prvulovic, D., et al., *Functional activation imaging in aging and dementia.* Psychiatry Res, 2005. **140**(2): p. 97-113.

235. Rombouts, S.A., et al., *Functional MR imaging in Alzheimer's disease during memory encoding.* AJNR Am J Neuroradiol, 2000. **21**(10): p. 1869-75.

236. Sperling, R.A., et al., *fMRI studies of associative encoding in young and elderly controls and mild Alzheimer's disease.* J Neurol Neurosurg Psychiatry, 2003. **74**(1): p. 44-50.

237. Celone, K.A., et al., *Alterations in memory networks in mild cognitive impairment and Alzheimer's disease: an independent component analysis.* J Neurosci, 2006. **26**(40): p. 10222-31.

238. Greicius, M.D., et al., *Default-mode network activity distinguishes Alzheimer's disease from healthy aging: evidence from functional MRI.* Proc Natl Acad Sci U S A, 2004. **101**(13): p. 4637-42.

239. Koch, W., et al., *Diagnostic power of default mode network resting state fMRI in the detection of Alzheimer's disease.* Neurobiol Aging, 2010.

240. Rombouts, S.A., et al., *Altered resting state networks in mild cognitive impairment and mild Alzheimer's disease: an fMRI study.* Hum Brain Mapp, 2005. **26**(4): p. 231-9.

241. Sperling, R.A., et al., *Functional alterations in memory networks in early Alzheimer's disease.* Neuromolecular Med, 2010. **12**(1): p. 27-43.

242. Wang, L., et al., *Changes in hippocampal connectivity in the early stages of Alzheimer's disease: evidence from resting state fMRI.* Neuroimage, 2006. **31**(2): p. 496-504.

243. Dickerson, B.C., et al., *Medial temporal lobe function and structure in mild cognitive impairment.* Ann Neurol, 2004. **56**(1): p. 27-35.

244. Hamalainen, A., et al., *Increased fMRI responses during encoding in mild cognitive impairment.* Neurobiol Aging, 2007. **28**(12): p. 1889-903.

245. Trivedi, M.A., et al., *fMRI activation changes during successful episodic memory encoding and recognition in amnestic mild cognitive impairment relative to cognitively healthy older adults.* Dement Geriatr Cogn Disord, 2008. **26**(2): p. 123-37.

246. Johnson, S.C., et al., *Activation of brain regions vulnerable to Alzheimer's disease: the effect of mild cognitive impairment.* Neurobiol Aging, 2006. **27**(11): p. 1604-12.

247. Miller, S.L., et al., *Hippocampal activation in adults with mild cognitive impairment predicts subsequent cognitive decline.* J Neurol Neurosurg Psychiatry, 2008. **79**(6): p. 630-5.

248. O'Brien, J.L., et al., *Longitudinal fMRI in elderly reveals loss of hippocampal activation with clinical decline.* Neurology, 2010. **74**(24): p. 1969-76.

249. Ferri, C.P., et al., *Global prevalence of dementia: a Delphi consensus study.* Lancet, 2005. **366**(9503): p. 2112-7.

250. Jack, C.R., Jr., et al., *The Alzheimer's Disease Neuroimaging Initiative (ADNI): MRI methods.* J Magn Reson Imaging, 2008. **27**(4): p. 685-91.

251. Mueller, S.G., et al., *The Alzheimer's disease neuroimaging initiative.* Neuroimaging Clin N Am, 2005. **15**(4): p. 869-77, xi-xii.

252. Mueller, S.G., et al., *Ways toward an early diagnosis in Alzheimer's disease: The Alzheimer's Disease Neuroimaging Initiative (ADNI).* Alzheimers Dement, 2005. **1**(1): p. 55-66.

253. Mechelli, A.P., CJ; Friston, KJ; Ashburner, J, *Voxel-Based Morphometry of the Human Brain: Methods and Applications.* Current Medical Imaging Reviews, 2005. **I**(1): p. 1-9.

254. Good, C.D., et al., *Automatic differentiation of anatomical patterns in the human brain: validation with studies of degenerative dementias.* Neuroimage, 2002. **17**(1): p. 29-46.

255. Grossman, M., et al., *What's in a name: voxel-based morphometric analyses of MRI and naming difficulty in Alzheimer's disease, frontotemporal dementia and corticobasal degeneration.* Brain, 2004. **127**(Pt 3): p. 628-49.

256. Hamalainen, A., et al., *Apolipoprotein E epsilon4 allele is associated with increased atrophy in progressive mild cognitive impairment: a voxel-based morphometric study.* Neurodegenerative Diseases, 2008. **5**(3-4): p. 186-9.

257. Kinkingnehun, S., et al., *VBM anticipates the rate of progression of Alzheimer disease: a 3-year longitudinal study.* Neurology, 2008. **70**(23): p. 2201-11.

258. Pennanen, C., et al., *A voxel based morphometry study on mild cognitive impairment.* Journal of Neurology, Neurosurgery & Psychiatry, 2005. **76**(1): p. 11-4.

259. Fleisher, A.S., et al., *Volumetric MRI vs clinical predictors of Alzheimer disease in mild cognitive impairment.* Neurology, 2008. **70**(3): p. 191-9.

260. Stoub, T.R., et al., *MRI predictors of risk of incident Alzheimer disease: a longitudinal study.* Neurology, 2005. **64**(9): p. 1520-4.

261. Bouwman, F.H., et al., *CSF biomarkers and medial temporal lobe atrophy predict dementia in mild cognitive impairment.* Neurobiology of Aging, 2007. **28**(7): p. 1070-4.

262. Jack, C.R., Jr., et al., *MRI as a biomarker of disease progression in a therapeutic trial of milameline for AD.* Neurology, 2003. **60**(2): p. 253-60.

263. Colliot, O., et al., *Discrimination between Alzheimer disease, mild cognitive impairment, and normal aging by using automated segmentation of the hippocampus.* Radiology, 2008. **248**(1): p. 194-201.

264. Khan, A.R., L. Wang, and M.F. Beg, *FreeSurfer-initiated fully-automated subcortical brain segmentation in MRI using Large Deformation Diffeomorphic Metric Mapping.* Neuroimage, 2008. **41**(3): p. 735-46.

265. Klauschen, F., B.R. Angermann, and M. Meier-Schellersheim, *Understanding diseases by mouse click: the promise and potential of computational approaches in Systems Biology.* Clin Exp Immunol, 2007. **149**(3): p. 424-9.

266. Du, A.T., et al., *Different regional patterns of cortical thinning in Alzheimer's disease and frontotemporal dementia.* Brain, 2007. **130**(Pt 4): p. 1159-66.

267. McHugh, T., et al., *Hippocampal volume and shape analysis in an older adult population.* Clin Neuropsychol, 2007. **21**(1): p. 130-45.

268. Fischl, B., M. Sereno, and A. Dale, *Cortical surface-based analysis. II: Inflation, flattening, and a surface-based coordinate system.* Neuroimage, 1999. **9**(2): p. 195-207.

269. Shen, L., et al., *Comparison of manual and automated determination of hippocampal volumes in MCI and older adults with cognitive complaints.* Alzheimer's & Dementia, 2008. **4**(4 (Suppl 2)): p. T29-30.

270. Shen, L., et al., *Comparison of manual and automated determination of hippocampal volumes in MCI and early AD.* Brain Imaging Behav, 2010. **4**(1): p. 86-95.

271. Sheikh, J. and J. Yesavage, *Geriatric Depression Scale (GDS): Recent evidence and development of a shorter version.*, in *Clinical Gerontology : A Guide to Assessment and Intervention*. 1986, The Haworth Press: New York. p. 165-173.

272. Kaufer, D., et al., *Validation of the NPI-Q, a brief clinical form of the Neuropsychiatric Inventory.* J Neuropsychiatry Clin Neurosci, 2000. **12**(2): p. 233-9.

273. Rosen, W., et al., *Pathological verification of ischemic score in differentiation of dementias.* Ann Neurol, 1980. **7**(5): p. 486-8.

274. Cockrell, J.R. and M.F. Folstein, *Mini-Mental State Examination (MMSE).* Psychopharmacol Bull, 1988. **24**(4): p. 689-92.

275. Folstein, M.F., S.E. Folstein, and P.R. McHugh, *"Mini-mental state". A practical method for grading the cognitive state of patients for the clinician.* J Psychiatr Res, 1975. **12**(3): p. 189-98.

276. Morris, J.C., *The Clinical Dementia Rating (CDR): current version and scoring rules.* Neurology, 1993. **43**(11): p. 2412-4.

277. Pfeffer, R., et al., *Measurement of functional activities in older adults in the community.* J Gerontol, 1982. **37**(3): p. 323-9.

278. Rey, A., *L'examen clinique en psychologie.* 1964, Paris: Presses Universitaires de France.

279. Kaplan, E., H. Goodglass, and S. Weintraub, *The Boston Naming Test*. 1983, Philadelphia: Lea and Febiger.

280. Morris, J., et al., *The Consortium to Establish a Registry for Alzheimer's Disease (CERAD). Part I. Clinical and neuropsychological assessment of Alzheimer's disease.* Neurology, 1989. **39**(9): p. 1159-65.

281. Fan, Y., et al., *Spatial patterns of brain atrophy in MCI patients, identified via high-dimensional pattern classification, predict subsequent cognitive decline.* Neuroimage, 2008. **39**(4): p. 1731-43.

282. Misra, C., Y. Fan, and C. Davatzikos, *Baseline and longitudinal patterns of brain atrophy in MCI patients, and their use in prediction of short-term conversion to AD: results from ADNI.* Neuroimage, 2009. **44**(4): p. 1415-22.

283. Ridha, B.H., et al., *Volumetric MRI and cognitive measures in Alzheimer disease : comparison of markers of progression.* J Neurol, 2008. **255**(4): p. 567-74.

284. Apostolova, L.G., et al., *Conversion of mild cognitive impairment to Alzheimer disease predicted by hippocampal atrophy maps.* Arch Neurol, 2006. **63**(5): p. 693-9.

285. Morra, J.H., et al., *Validation of a fully automated 3D hippocampal segmentation method using subjects with Alzheimer's disease mild cognitive impairment, and elderly controls.* Neuroimage, 2008. **43**(1): p. 59-68.

286. Hansen, R.A., et al., *Efficacy and safety of donepezil, galantamine, and rivastigmine for the treatment of Alzheimer's disease: a systematic review and meta-analysis.* Clin Interv Aging, 2008. **3**(2): p. 211-25.

287. Petersen, R.C., et al., *Vitamin E and donepezil for the treatment of mild cognitive impairment.* N Engl J Med, 2005. **352**(23): p. 2379-88.

288. Sabbagh, M.N., S. Richardson, and N. Relkin, *Disease-modifying approaches to Alzheimer's disease: challenges and opportunities-Lessons from donepezil therapy.* Alzheimers Dement, 2008. **4**(1 Suppl 1): p. S109-18.

289. Salloway, S., et al., *Efficacy of donepezil in mild cognitive impairment: a randomized placebo-controlled trial.* Neurology, 2004. **63**(4): p. 651-7.

290. Thal, L.J., et al., *A randomized, double-blind, study of rofecoxib in patients with mild cognitive impairment.* Neuropsychopharmacology, 2005. **30**(6): p. 1204-15.

291. Risacher, S.L., et al., *Longitudinal MRI atrophy biomarkers: relationship to conversion in the ADNI cohort.* Neurobiol Aging, 2010. **31**(8): p. 1401-18.

292. Petersen, R.C., et al., *Current concepts in mild cognitive impairment.* Arch Neurol, 2001. **58**(12): p. 1985-92.

293. Petersen, R.C. and S. Negash, *Mild cognitive impairment: an overview.* CNS Spectr, 2008. **13**(1): p. 45-53.

294. Petersen, R.C., *Mild cognitive impairment: transition between aging and Alzheimer's disease.* Neurologia, 2000. **15**(3): p. 93-101.

295. Sluimer, J.D., et al., *Whole-brain atrophy rate in Alzheimer disease: identifying fast progressors.* Neurology, 2008. **70**(19 Pt 2): p. 1836-41.

296. Gatz, M., et al., *Role of genes and environments for explaining Alzheimer disease.* Arch Gen Psychiatry, 2006. **63**(2): p. 168-74.

297. Farrer, L.A., et al., *Effects of age, sex, and ethnicity on the association between apolipoprotein E genotype and Alzheimer disease. A meta-analysis. APOE and Alzheimer Disease Meta Analysis Consortium.* JAMA, 1997. **278**(16): p. 1349-56.

298. Cohen, R.M., et al., *Effect of apolipoprotein E genotype on hippocampal volume loss in aging healthy women.* Neurology, 2001. **57**(12): p. 2223-8.

299. Fleisher, A., et al., *Sex, apolipoprotein E epsilon 4 status, and hippocampal volume in mild cognitive impairment.* Arch Neurol, 2005. **62**(6): p. 953-7.

300. Jack, C.R., Jr., et al., *Longitudinal MRI findings from the vitamin E and donepezil treatment study for MCI.* Neurobiol Aging, 2008. **29**(9): p. 1285-95.

301. Jack, C.R., Jr., et al., *Atrophy rates accelerate in amnestic mild cognitive impairment.* Neurology, 2008. **70**(19 Pt 2): p. 1740-52.

302. Mori, E., et al., *Accelerated hippocampal atrophy in Alzheimer's disease with apolipoprotein E epsilon4 allele.* Ann Neurol, 2002. **51**(2): p. 209-14.

303. Fjell, A.M., et al., *Brain Atrophy in Healthy Aging Is Related to CSF Levels of A{beta}1-42.* Cereb Cortex, 2010.

304. Morra, J.H., et al., *Automated mapping of hippocampal atrophy in 1-year repeat MRI data from 490 subjects with Alzheimer's disease, mild cognitive impairment, and elderly controls.* Neuroimage, 2009. **45**(1 Suppl): p. S3-15.

305. Schuff, N., et al., *MRI of hippocampal volume loss in early Alzheimer's disease in relation to ApoE genotype and biomarkers.* Brain, 2009. **132**(Pt 4): p. 1067-77.

306. Du, A.T., et al., *Age effects on atrophy rates of entorhinal cortex and hippocampus.* Neurobiol Aging, 2006. **27**(5): p. 733-40.

307. Wang, P.N., et al., *Accelerated hippocampal atrophy rates in stable and progressive amnestic mild cognitive impairment.* Psychiatry Res, 2009. **171**(3): p. 221-31.

308. Chou, Y.Y., et al., *Mapping correlations between ventricular expansion and CSF amyloid and tau biomarkers in 240 subjects with Alzheimer's disease, mild cognitive impairment and elderly controls.* Neuroimage, 2009. **46**(2): p. 394-410.

309. Chupin, M., et al., *Fully automatic hippocampus segmentation and classification in Alzheimer's disease and mild cognitive impairment applied on data from ADNI.* Hippocampus, 2009. **19**(6): p. 579-87.

310. Fennema-Notestine, C., et al., *Structural MRI biomarkers for preclinical and mild Alzheimer's disease.* Hum Brain Mapp, 2009. **30**(10): p. 3238-53.

311. Nestor, S.M., et al., *Ventricular enlargement as a possible measure of Alzheimer's disease progression validated using the Alzheimer's disease neuroimaging initiative database.* Brain, 2008. **131**(Pt 9): p. 2443-54.

312. Querbes, O., et al., *Early diagnosis of Alzheimer's disease using cortical thickness: impact of cognitive reserve.* Brain, 2009. **132**(Pt 8): p. 2036-47.

313. Vemuri, P., et al., *MRI and CSF biomarkers in normal, MCI, and AD subjects: diagnostic discrimination and cognitive correlations.* Neurology, 2009. **73**(4): p. 287-93.

314. Walhovd, K.B., et al., *Multi-modal imaging predicts memory performance in normal aging and cognitive decline.* Neurobiol Aging, 2008.

315. Calvini, P., et al., *Automatic analysis of medial temporal lobe atrophy from structural MRIs for the early assessment of Alzheimer disease.* Med Phys, 2009. **36**(8): p. 3737-47.

316. McEvoy, L.K., et al., *Alzheimer disease: quantitative structural neuroimaging for detection and prediction of clinical and structural changes in mild cognitive impairment.* Radiology, 2009. **251**(1): p. 195-205.

317. Evans, M.C., et al., *Volume changes in Alzheimer's disease and mild cognitive impairment: cognitive associations.* Eur Radiol, 2009.

318. Ho, A.J., et al., *Comparing 3 T and 1.5 T MRI for tracking Alzheimer's disease progression with tensor-based morphometry.* Hum Brain Mapp, 2009.

319. Fjell, A.M., et al., *CSF Biomarkers in Prediction of Cerebral and Clinical Change in Mild Cognitive Impairment and Alzheimer's Disease.* Journal of Neuroscience, 2010. **30**(6): p. 2088-2101.

320. Holland, D., et al., *Subregional neuroanatomical change as a biomarker for Alzheimer's disease.* Proc Natl Acad Sci U S A, 2009. **106**(49): p. 20954-20959.

321. Hua, X., et al., *Optimizing power to track brain degeneration in Alzheimer's disease and mild cognitive impairment with tensor-based morphometry: an ADNI study of 515 subjects.* Neuroimage, 2009. **48**(4): p. 668-81.

322. Leow, A.D., et al., *Alzheimer's Disease Neuroimaging Initiative: A one-year follow up study using Tensor-Based Morphometry correlating degenerative rates, biomarkers and cognition.* Neuroimage, 2009.

323. McDonald, C.R., et al., *Regional rates of neocortical atrophy from normal aging to early Alzheimer disease.* Neurology, 2009. **73**(6): p. 457-65.

324. Petersen, R.C., et al., *Alzheimer's Disease Neuroimaging Initiative (ADNI): clinical characterization.* Neurology, 2010. **74**(3): p. 201-9.

325. Brett, M., et al., *Region of interest analysis using an SPM toolbox [abstract]*, in *Presented at the 8th International Conference on Functional Mapping of the Human Brain, June 2-6, 2002*. 2002: Sendai, Japan.

326. Rosner, B., *Fundamentals of Biostatistics*. 1990, Boston: PWS-Kent Publishing Company.

327. Cohen, J., *Statistical Power Analysis for the Behavioral Sciences*. 2nd ed. 1988, Hillsdale, NJ: Lawrence Erlbaum Associates, Inc.

328. Saykin, A.J., et al., *Alzheimer's Disease Neuroimaging Initiative biomarkers as quantitative phenotypes: Genetics core aims, progress, and plans.* Alzheimer's & Dementia, 2010: p. 1-9.

329. Barnes, J., et al., *Automatic calculation of hippocampal atrophy rates using a hippocampal template and the boundary shift integral.* Neurobiol Aging, 2007. **28**(11): p. 1657-63.

330. Saykin, A.J., et al., *Genetic predictors of 12 month change in MRI hippocampal volume in the Alzheimer's Disease Neuroimaging Initiative cohort: Analysis of leading candidates from the AlzGene database.* Alzheimer's & Dementia, 2009. **5**(4 Supplement): p. P3.

331. Association, A.s., *2011 Alzheimer's disease facts and figures.* Alzheimers Dement, 2011. **7**(2): p. 208-44.

332. den Heijer, T., et al., *Hippocampal, amygdalar, and global brain atrophy in different apolipoprotein E genotypes.* Neurology, 2002. **59**(5): p. 746-8.

333. Mosconi, L., et al., *Maternal family history of Alzheimer's disease predisposes to reduced brain glucose metabolism.* Proceedings of the National Academy of Sciences, 2007. **104**: p. 19067-19072.

334. Reiman, E.M., et al., *Preclinical evidence of Alzheimer's disease in persons homozygous for the epsilon 4 allele for apolipoprotein E.* New England Journal of Medicine, 1996. **334**: p. 752-758.

335. Small, G.W., et al., *Early detection of Alzheimer's disease by combining apolipoprotein E and neuroimaging.* Annals of the New York Academy of Sciences, 1996. **802**: p. 70-78.

336. Smith, C.D., et al., *Women at risk for AD show increased parietal activation during a fluency task.* Neurology, 2002. **58**(8): p. 1197-202.

337. Hohman, T.J., et al., *Subjective cognitive complaints and longitudinal changes in memory and brain function.* Neuropsychology, 2011. **25**(1): p. 125-30.

338. Prichep, L.S., et al., *Prediction of longitudinal cognitive decline in normal elderly with subjective complaints using electrophysiological imaging.* Neurobiol Aging, 2006. **27**(3): p. 471-81.

339. Ramakers, I.H., et al., *Symptoms of preclinical dementia in general practice up to five years before dementia diagnosis.* Dement Geriatr Cogn Disord, 2007. **24**(4): p. 300-6.

340. Reid, L.M. and A.M. Maclullich, *Subjective memory complaints and cognitive impairment in older people.* Dement Geriatr Cogn Disord, 2006. **22**(5-6): p. 471-85.

341. Storandt, M., et al., *Longitudinal course and neuropathologic outcomes in original vs revised MCI and in pre-MCI.* Neurology, 2006. **67**(3): p. 467-73.

342. Chao, L.L., et al., *Evidence of neurodegeneration in brains of older adults who do not yet fulfill MCI criteria.* Neurobiol Aging, 2010. **31**(3): p. 368-77.

343. Stewart, R., et al., *Longitudinal neuroimaging correlates of subjective memory impairment: 4-year prospective community study.* Br J Psychiatry, 2011. **198**(3): p. 199-205.

344. Wang, P.J., et al., *Regionally specific atrophy of the corpus callosum in AD, MCI and cognitive complaints.* Neurobiology of Aging, 2006. **27**: p. 1613-1617.

345. Wang, Y., et al., *Selective changes in white matter integrity in MCI and older adults with cognitive complaints.* Biochim Biophys Acta, 2011.

346. Mosconi, L., et al., *Hypometabolism and altered cerebrospinal fluid markers in normal apolipoprotein E E4 carriers with subjective memory complaints.* Biol Psychiatry, 2008. **63**(6): p. 609-18.

347. Nutter-Upham, K.E., et al., *Verbal fluency performance in amnestic MCI and older adults with cognitive complaints.* Arch Clin Neuropsychol, 2008. **23**(3): p. 229-41.

348. Rabin, L.A., et al., *Self- and informant reports of executive function on the BRIEF-A in MCI and older adults with cognitive complaints.* Arch Clin Neuropsychol, 2006. **21**(7): p. 721-32.

349. Jurica, P., C. Leitten, and S. Mattis, *Dementia Rating Scale - 2*. 2001, Lutz, FL: Psychological Assessment Resources, Inc.

350. Delis, D., et al., *California Verbal Learning Test: adult version research edition manual*. 1987, San Antonio, TX: The Psychological Corporation.

351. Delis, D., et al., *California Verbal Learning Test-second edition: adult version manual*. 2000, San Antonio, TX: The Psychological Corporation.

352. Wechsler, D., *Wechsler Memory Scale – Revised*. 1987, New York: Psychological Association.

353. Wechsler, D., *Wechsler Memory Scale-third edition, WMS-III administration and scoring manual.* 3rd ed. 1997, San Antonio, TX: The Psychological Corporation.

354. Schmand, B., et al., *Subjective memory complaints may announce dementia.* Neurology, 1996. **46**(1): p. 121-5.

355. McKhann, G., et al., *Clinical diagnosis of Alzheimer's disease: report of the NINCDS-ADRDA Work Group under the auspices of Department of Health and Human Services Task Force on Alzheimer's Disease.* Neurology, 1984. **34**(7): p. 939-44.

356. Cronin-Golomb, A., *Vision in Alzheimer's disease.* Gerontologist, 1995. **35**(3): p. 370-6.

357. Jackson, G.R. and C. Owsley, *Visual dysfunction, neurodegenerative diseases, and aging.* Neurol Clin, 2003. **21**(3): p. 709-28.

358. Valenti, D.A., *Alzheimer's disease: visual system review.* Optometry, 2010. **81**(1): p. 12-21.

359. Idrizbegovic, E., et al., *Central auditory function in early Alzheimer's disease and in mild cognitive impairment.* Age Ageing, 2011. **40**(2): p. 249-54.

360. Iliadou, V. and S. Kaprinis, *Clinical psychoacoustics in Alzheimer's disease central auditory processing disorders and speech deterioration.* Ann Gen Hosp Psychiatry, 2003. **2**(1): p. 12.

361. Djordjevic, J., et al., *Olfaction in patients with mild cognitive impairment and Alzheimer's disease.* Neurobiol Aging, 2008. **29**(5): p. 693-706.

362. Schiffman, S.S., *Taste and smell losses in normal aging and disease.* JAMA, 1997. **278**(16): p. 1357-62.

363. Cronin-Golomb, A., et al., *Visual dysfunction in Alzheimer's disease: relation to normal aging.* Ann Neurol, 1991. **29**(1): p. 41-52.

364. Cronin-Golomb, A., et al., *Visual function in Alzheimer's disease and normal aging.* Ann N Y Acad Sci, 1991. **640**: p. 28-35.

365. Gilmore, G.C., et al., *Motion perception and Alzheimer's disease.* J Gerontol, 1994. **49**(2): p. P52-7.

366. Katz, B. and S. Rimmer, *Ophthalmologic manifestations of Alzheimer's disease.* Surv Ophthalmol, 1989. **34**(1): p. 31-43.

367. Pache, M., et al., *Colour vision deficiencies in Alzheimer's disease.* Age Ageing, 2003. **32**(4): p. 422-6.

368. Armstrong, R.A., *Visual field defects in Alzheimer's disease patients may reflect differential pathology in the primary visual cortex.* Optom Vis Sci, 1996. **73**(11): p. 677-82.

369. Hof, P.R. and J.H. Morrison, *Quantitative analysis of a vulnerable subset of pyramidal neurons in Alzheimer's disease: II. Primary and secondary visual cortex.* J Comp Neurol, 1990. **301**(1): p. 55-64.

370. Leuba, G. and K. Saini, *Pathology of subcortical visual centres in relation to cortical degeneration in Alzheimer's disease.* Neuropathol Appl Neurobiol, 1995. **21**(5): p. 410-22.

371. McKee, A.C., et al., *Visual association pathology in preclinical Alzheimer disease.* J Neuropathol Exp Neurol, 2006. **65**(6): p. 621-30.

372. Mielke, R., et al., *Dysfunction of visual cortex contributes to disturbed processing of visual information in Alzheimer's disease.* Int J Neurosci, 1995. **82**(1-2): p. 1-9.

373. Blanks, J.C., et al., *Retinal ganglion cell degeneration in Alzheimer's disease.* Brain Res, 1989. **501**(2): p. 364-72.

374. Curcio, C.A. and D.N. Drucker, *Retinal ganglion cells in Alzheimer's disease and aging.* Ann Neurol, 1993. **33**(3): p. 248-57.

375. Hinton, D.R., et al., *Optic-nerve degeneration in Alzheimer's disease.* N Engl J Med, 1986. **315**(8): p. 485-7.

376. Paquet, C., et al., *Abnormal retinal thickness in patients with mild cognitive impairment and Alzheimer's disease.* Neurosci Lett, 2007. **420**(2): p. 97-9.

377. Parisi, V., et al., *Morphological and functional retinal impairment in Alzheimer's disease patients.* Clin Neurophysiol, 2001. **112**(10): p. 1860-7.

378. Sadun, A.A. and C.J. Bassi, *Optic nerve damage in Alzheimer's disease.* Ophthalmology, 1990. **97**(1): p. 9-17.

379. Tsai, C.S., et al., *Optic nerve head and nerve fiber layer in Alzheimer's disease.* Arch Ophthalmol, 1991. **109**(2): p. 199-204.

380. Valenti, D.A., *Neuroimaging of retinal nerve fiber layer in AD using optical coherence tomography.* Neurology, 2007. **69**(10): p. 1060.

381. Anderson, A.J. and C.A. Johnson, *Frequency-doubling technology perimetry.* Ophthalmol Clin North Am, 2003. **16**(2): p. 213-25.

382. Zeppieri, M. and C.A. Johnson (2008) *Frequency Doubling Techology (FDT) Perimetry*.

383. Tatemichi, M., et al., *Performance of glaucoma mass screening with only a visual field test using frequency-doubling technology perimetry.* Am J Ophthalmol, 2002. **134**(4): p. 529-37.

384. Cello, K.E., J.M. Nelson-Quigg, and C.A. Johnson, *Frequency doubling technology perimetry for detection of glaucomatous visual field loss.* Am J Ophthalmol, 2000. **129**(3): p. 314-22.

385. Kelly, D.H., *Nonlinear visual responses to flickering sinusoidal gratings.* J Opt Soc Am, 1981. **71**(9): p. 1051-5.

386. Richards, W. and T.B. Felton, *Spatial frequency doubling: retinal or central?* Vision Res, 1973. **13**(11): p. 2129-37.

387. White, A.J., et al., *An examination of physiological mechanisms underlying the frequency-doubling illusion.* Invest Ophthalmol Vis Sci, 2002. **43**(11): p. 3590-9.

388. Scarmeas, N. and Y. Stern, *Imaging studies and APOE genotype in persons at risk for Alzheimer's disease.* Curr Psychiatry Rep, 2006. **8**(1): p. 11-7.

389. Fox, N.C., et al., *Correlation between rates of brain atrophy and cognitive decline in AD.* Neurology, 1999. **52**(8): p. 1687-9.

390. Anderson, A.J., et al., *Characteristics of the normative database for the Humphrey matrix perimeter.* Invest Ophthalmol Vis Sci, 2005. **46**(4): p. 1540-8.

391. McKendrick, A.M. and A. Turpin, *Advantages of terminating Zippy Estimation by Sequential Testing (ZEST) with dynamic criteria for white-on-white perimetry.* Optom Vis Sci, 2005. **82**(11): p. 981-7.

392. Turpin, A., et al., *Properties of perimetric threshold estimates from full threshold, ZEST, and SITA-like strategies, as determined by computer simulation.* Invest Ophthalmol Vis Sci, 2003. **44**(11): p. 4787-95.

393. Heaton, R., et al., *Wisconsin Card SortingTest manual revised and expanded*. 1993, Odessa, FL: Psychological Assessment Resources.

394. Elliott, D.B., *Evaluating visual function in cataract.* Optom Vis Sci, 1993. **70**(11): p. 896-902.

395. Elliott, D.B., J. Gilchrist, and D. Whitaker, *Contrast sensitivity and glare sensitivity changes with three types of cataract morphology: are these techniques necessary in a clinical evaluation of cataract?* Ophthalmic Physiol Opt, 1989. **9**(1): p. 25-30.

396. Neargarder, S.A., et al., *The impact of acuity on performance of four clinical measures of contrast sensitivity in Alzheimer's disease.* J Gerontol B Psychol Sci Soc Sci, 2003. **58**(1): p. P54-62.

397. Johnson, C.A. and S.J. Samuels, *Screening for glaucomatous visual field loss with frequency-doubling perimetry.* Invest Ophthalmol Vis Sci, 1997. **38**(2): p. 413-25.

398. Sponsel, W.E., et al., *Frequency doubling perimetry.* Am J Ophthalmol, 1998. **126**(1): p. 155-6.

399. Bayer, A.U., F. Ferrari, and C. Erb, *High occurrence rate of glaucoma among patients with Alzheimer's disease.* Eur Neurol, 2002. **47**(3): p. 165-8.

400. Tamura, H., et al., *High frequency of open-angle glaucoma in Japanese patients with Alzheimer's disease.* J Neurol Sci, 2006. **246**(1-2): p. 79-83.

401. Wostyn, P., K. Audenaert, and P.P. De Deyn, *Alzheimer's disease and glaucoma: is there a causal relationship?* Br J Ophthalmol, 2009. **93**(12): p. 1557-9.

402. Al-Dabbagh, N.M., et al., *Apolipoprotein E polymorphisms and primary glaucoma in Saudis.* Mol Vis, 2009. **15**: p. 912-9.

403. Mabuchi, F., et al., *The apolipoprotein E gene polymorphism is associated with open angle glaucoma in the Japanese population.* Mol Vis, 2005. **11**: p. 609-12.

404. Vickers, J.C., et al., *The apolipoprotein epsilon4 gene is associated with elevated risk of normal tension glaucoma.* Mol Vis, 2002. **8**: p. 389-93.

405. Iseri, P.K., et al., *Relationship between cognitive impairment and retinal morphological and visual functional abnormalities in Alzheimer disease.* J Neuroophthalmol, 2006. **26**(1): p. 18-24.

406. Kergoat, H., et al., *An evaluation of the retinal nerve fiber layer thickness by scanning laser polarimetry in individuals with dementia of the Alzheimer type.* Acta Ophthalmol Scand, 2001. **79**(2): p. 187-91.

407. Blanks, J.C., et al., *Retinal pathology in Alzheimer's disease. II. Regional neuron loss and glial changes in GCL.* Neurobiol Aging, 1996. **17**(3): p. 385-95.

408. Blanks, J.C., et al., *Retinal pathology in Alzheimer's disease. I. Ganglion cell loss in foveal/parafoveal retina.* Neurobiol Aging, 1996. **17**(3): p. 377-84.

409. Sadun, A.A., *The optic neuropathy of Alzheimer's disease.* Metab Pediatr Syst Ophthalmol, 1989. **12**(1-3): p. 64-8.

410. Berisha, F., et al., *Retinal abnormalities in early Alzheimer's disease.* Invest Ophthalmol Vis Sci, 2007. **48**(5): p. 2285-9.

411. Katz, B., et al., *Abnormal pattern electroretinogram in Alzheimer's disease: evidence for retinal ganglion cell degeneration?* Ann Neurol, 1989. **26**(2): p. 221-5.

412. Martinelli, V., et al., *Pattern visual evoked potential mapping in Alzheimer's disease: correlations with visuospatial impairment.* Dementia, 1996. **7**(2): p. 63-8.

413. Koronyo-Hamaoui, M., et al., *Identification of amyloid plaques in retinas from Alzheimer's patients and noninvasive in vivo optical imaging of retinal plaques in a mouse model.* Neuroimage, 2011. **54 Suppl 1**: p. S204-17.

414. Janciauskiene, S. and T. Krakau, *Alzheimer's peptide: a possible link between glaucoma, exfoliation syndrome and Alzheimer's disease.* Acta Ophthalmol Scand, 2001. **79**(3): p. 328-9.

415. Yin, H., et al., *Soluble amyloid beta oligomers may contribute to apoptosis of retinal ganglion cells in glaucoma.* Med Hypotheses, 2008. **71**(1): p. 77-80.

416. Yoneda, S., et al., *Vitreous fluid levels of beta-amyloid((1-42)) and tau in patients with retinal diseases.* Jpn J Ophthalmol, 2005. **49**(2): p. 106-8.

417. Guo, L., et al., *Targeting amyloid-beta in glaucoma treatment.* Proc Natl Acad Sci U S A, 2007. **104**(33): p. 13444-9.

418. Goldstein, L.E., et al., *Cytosolic beta-amyloid deposition and supranuclear cataracts in lenses from people with Alzheimer's disease.* Lancet, 2003. **361**(9365): p. 1258-65.

419. Brown, L.L., J.S. Schneider, and T.I. Lidsky, *Sensory and cognitive functions of the basal ganglia.* Curr Opin Neurobiol, 1997. **7**(2): p. 157-63.

420. Boussaoud, D. and I. Kermadi, *The primate striatum: neuronal activity in relation to spatial attention versus motor preparation.* Eur J Neurosci, 1997. **9**(10): p. 2152-68.

421. Kermadi, I. and D. Boussaoud, *Role of the primate striatum in attention and sensorimotor processes: comparison with premotor cortex.* Neuroreport, 1995. **6**(8): p. 1177-81.

422. Iester, M., et al., *Learning effect, short-term fluctuation, and long-term fluctuation in frequency doubling technique.* Am J Ophthalmol, 2000. **130**(2): p. 160-4.

423. Frost, S., R.N. Martins, and Y. Kanagasingam, *Ocular biomarkers for early detection of Alzheimer's disease.* J Alzheimers Dis, 2010. **22**(1): p. 1-16.

424. Clark, C.M., et al., *Use of florbetapir-PET for imaging beta-amyloid pathology.* JAMA, 2011. **305**(3): p. 275-83.

425. Okamura, N. and K. Yanai, *Florbetapir (18F), a PET imaging agent that binds to amyloid plaques for the potential detection of Alzheimer's disease.* IDrugs, 2010. **13**(12): p. 890-9.

426. Walhovd, K.B., et al., *Combining MR Imaging, Positron-Emission Tomography, and CSF Biomarkers in the Diagnosis and Prognosis of Alzheimer Disease.* AJNR Am J Neuroradiol, 2010.

Curriculum Vitae

Shannon Leigh Risacher

Educational Background

2006-2011 Indiana University (Indianapolis, IN)
Medical Neuroscience, Ph.D.

2002-2006 Purdue University (Indianapolis, IN)
Bachelor of Science, Psychology, Chemistry Minor
With Distinction

2000-2002 Earlham College (Richmond, IN)
Biology Major

Awards and Fellowships

2010-2011 Indiana Clinical and Translational Sciences Institute (CTSI)
Pre-doctoral Fellowship in Translational Research

2011 Travel Fellowship, 2011 International Conference on Alzheimer's Disease (Paris, France)

2010 Stark Neuroscience Kays Fellowship Award

2009 Travel Fellowship, 2009 International Conference on Alzheimer's Disease (Vienna, Austria)

2008 Best Poster Award, Society for Neuroscience, Local Chapter

2006-2008 Dean's Fellowship, Indiana University School of Medicine, Medical Neuroscience Graduate Program

2002-2006 Dean's List Honors

Research Experience

2008-2011 *Graduate Research,* Indiana University School of Medicine, Indiana University Center for Neuroimaging

- Graduate research on the utility of neuroimaging and genetic biomarkers in identifying and predicting the progression of Alzheimer's disease.

2007-2008 *Graduate Research Rotation,* Indiana University School of Medicine, Medical Neuroscience Program

- Graduate research rotation contributing to PET study of the striatal dopamine response to drugs of abuse in normal and alcohol-preferring rats.

2007 *Graduate Research Rotation,* Indiana University School of Medicine, Medical Neuroscience Program

- Graduate research rotation contributing to a study to examine locomotor sensitization to nicotine in a rat model of schizophrenia.

2007 *Graduate Research Rotation,* Indiana University School of Medicine, Medical Neuroscience Program

- Graduate research rotation contributing to an fMRI study of responses of alcoholics to the smell of alcoholic beverages.

2004-2006 *Undergraduate Researcher*, Purdue School of Science, IUPUI, Capstone Honors Research

- Undergraduate research project focusing on the underlying neural mechanisms associated with fetal alcohol syndrome in a neonatal rat model.

Publications and Presentations

Original Manuscripts

Risacher SL, WuDunn D, Pepin SM, MaGee TR, McDonald BC, Flashman LA, Wishart HA, Pixley HS, Rabin LA, Paré N, Englert JJ, Schwartz E, Curtain JR, West JD, O'Neill DP, Santulli RB, Newman RW, Saykin AJ (*submitted*). Visual contrast sensitivity in AD, MCI, and older adults with cognitive complaints.

Conroy SK, Nho K, McDonald BC, **Risacher SL**, Kim S, Foroud T, Jack CR Jr., Weiner MW, Shen L, Saykin AJ, and the Alzheimer's Disease Neuroimaging Initiative (ADNI) (*submitted*). *ESR1* genetic variation and brain structure in cognitively normal older adults: differential effects of sex and brain region.

Swaminathan S, Shen L, **Risacher SL**, Yoder KK, West JD, Kim S, Nho K, Foroud T, Inlow M, Potkin SG, Huentelman MJ, Craig DW, Jagust WJ, Koeppe RA, Mathis CA, Jack CR Jr., Weiner MW, Saykin AJ, and the Alzheimer's Disease Neuroimaging Initiative (ADNI) (*in press*). Amyloid pathway-based candidate gene analysis of [^{11}C]PiB-PET in the Alzheimer's Disease Neuroimaging Initiative (ADNI) cohort. *Brain Imaging and Behavior.*

Swaminathan S, Kim S, Shen L, **Risacher SL**, Foroud T, Pankratz N, Potkin SG, Huentelman MJ, Craig DW, Weiner MW, Saykin AJ, and the Alzheimer's Disease Neuroimaging Initiative (*in press)*. Genomic copy number analysis in Alzheimer's disease and mild cognitive impairment: An ADNI study. *International Journal of Alzheimer's Disease*.

Kim S, Swaminathan S, Shen L, **Risacher SL**, Nho K, Foroud T, Shaw LM, Trojanowski JQ, Potkin SG, Huentelman MJ, Craig DW, DeChairo BM, Aisen PS, Petersen RC, Weiner MW, Saykin AJ and the Alzheimer's Disease Neuroimaging Initiative (2011). Genome-wide association study of CSF biomarkers Abeta1-42, t-tau, and p-tau181p in the ADNI cohort. *Neurology*, 76(1): 69-79.

Sullivan JM, **Risacher SL**, Normandin MD, Yoder KK, Froehlich JC, Morris ED (2011). Imaging of alcohol-induced dopamine release in rats: preliminary findings with [11C]raclopride PET. *Synapse,* 65(9): 929-37.

Nho K, Shen L, Kim S, **Risacher SL**, West JD, Foroud T, Jack CR, Weiner MW, Saykin AJ (2010). Automatic prediction of conversion from Mild Cognitive Impairment to probable Alzheimer's Disease using structural magnetic resonance imaging. *AMIA Annu Symp Proc*: 542-6.

Shen L, Qi Y, Kim S, Nho K, Wan J, **Risacher SL**, Saykin AJ, and the Alzheimer's Disease Neuroimaging Initiative (2010). Sparse bayesian learning for identifying imaging biomarkers in AD prediction. *Med Image Comput Comput Assist Interv,* 13(Pt 3): 611-8.

Epstein NU, Saykin AJ, **Risacher SL**, Gao S, Farlow MR, and the Alzheimer's Disease Neuroimaging Initiative (2010). Differences in medication use in the Alzheimer's Disease Neuroimaging Initiative: analysis of baseline characteristics. *Drugs and Aging,* 27(8): 677-86.

Risacher SL, Shen L, West JD, Kim S, McDonald BC, Beckett LA, Harvey DJ, Jack CR Jr, Weiner MW, Saykin AJ, and the Alzheimer's Disease Neuroimaging Initiative (2010). Longitudinal MRI atrophy biomarkers: relationship to conversion in the ADNI cohort. *Neurobiology of Aging,* 31(8): 1401-18.

Saykin AJ, Shen L, Foroud TM, Potkin SG, Swaminathan S, Kim S, **Risacher SL**, Nho K, Huentelman MJ, Craig DW, Thompson PM, Stein JL, Moore JH, Farrer LA, Green RC, Bertram L, Jack CR Jr, Weiner MW, and the Alzheimer's Disease Neuroimaging Initiative (2010). Alzheimer's Disease Neuroimaging Initiative biomarkers as quantitative phenotypes: Genetics core aims, progress and plans. *Alzheimer's & Dementia*, 6(3): 265-73.

Shen L, Kim S, **Risacher SL**, Nho K, Swaminathan S, West JD, Foroud T, Pankratz N, Huentelman MJ, Craig DW, DeChairo BM, Potkin SG, Jack C, Weiner M, Saykin AJ, and the Alzheimer's Disease Neuroimaging Initiative (ADNI). Whole genome association study of brain-wide imaging phenotypes for identifying quantitative trait loci in MCI and AD: A study of the ADNI cohort. *Neuroimage,* 53(3): 1051-63.

Shen L, Saykin AJ, Kim S, Firpi H, West J, **Risacher SL**, McDonald BC, McHugh TL, Wishart HA, Flashman LA (2010). Comparison of manual and automated determination of hippocampal volumes in MCI and older adults with cognitive complaints*. Brain Imaging and Behavior,* 4(1): 86-95.

Risacher SL, Saykin AJ, West JD, Shen L, Firpi HA, McDonald BC, and the Alzheimer's Disease Neuroimaging Initiative (2009). Baseline MRI predictors of conversion from MCI to probable AD in the ADNI cohort. *Current Alzheimer Research*, 6(4): 347-361.

Cheng TE, Yoder KK, Normandin MD, **Risacher SL**, Converse AK, Hampel JA, Miller MA, Morris ED (2009). "A rat head holder for simultaneous scanning of two rats in small animal PET scanners: design, construction, feasibility testing and kinetic validation." *Journal of Neuroscience Methods*, 176(1): 24-33.

Other Publications

Risacher SL, Wishart HA, Saykin AJ. Functional MRI studies of memory in aging, Mild Cognitive Impairment, and Alzheimer's disease. In S.H. Faro & F.B. Mohamed (Eds.), *Functional Neuroradiology, Second Edition*. New York: Springer, 2011.

Risacher SL and Saykin AJ. Neuroimaging of Alzheimer's disease, Mild Cognitive Impairment and other dementias. In L. H. Sweet & R. A. Cohen (Eds.), *Brain Imaging in Behavioral Medicine and Clinical Neuroscience*. New York: Springer, 2010.

Abstracts and Poster Presentations

Risacher SL, Yoder KK, West JD, WuDunn D, MaGee TR, McDonald BC, Hutchins GD, Zheng QH, Saykin AJ. Relationship of visual contrast sensitivity to amyloid deposition assessed by [11C] PiB PET. *Accepted for poster presentation at the Human Amyloid Imaging Conference, January 12-13, 2012.*

Wang H, Nie F, Huang H, **Risacher SL**, Ding C, Saykin AJ, Shen L, and the Alzheimer's Disease Neuroimaging Initiative (ADNI). Sparse multi-task regression and feature selection to identify brain imaging predictors for memory performance. *Accepted for poster presentation at the International Conference on Computer Vision, November 6-13, 2011.*

Nho K, Shen L, Kim S, Swaminathan S, **Risacher SL**, Saykin AJ, and the Alzheimer's Disease Neuroimaging Initiative (ADNI). The effect of reference panels and software tools on genotype imputation. *Presented at the 2011 American Medical Informatics Association Annual Symposium, October 22-25, 2011.*

Shen L, Kim S, Qi Y, Inlow M, Swaminathan S, Nho K, Wan J, **Risacher SL**, Shaw LM, Trojanowski JQ, Weiner MW, Saykin AJ, and the Alzheimer's Disease Neuroimaging Initiative (ADNI). Identifying neuroimaging and proteomic biomarkers for MCI and AD via the Elastic Net. *Oral presentation at the 14th International Conference on Medical Image Computing and Computer Assisted Intervention, September 18-22, 2011.*

Risacher SL, Shen L, West JD, Flashman LA, Wishart HA, Rabin LA, Paré N, Englert JJ, Schwartz ES, Kim S, McDonald BC, Curtain JR, Pixley HS, Santulli RB, Saykin AJ. Longitudinal structural MRI changes in Alzheimer's disease, Mild Cognitive Impairment, and older adults with cognitive complaints: Relationship to conversion status. *Presented at the 2011 International Conference on Alzheimer's Disease, July 16-21, 2011.*

Hemond CC, Nho K, Shen L, **Risacher SL**, Kim S, Saykin AJ, Greicius MD, and the Alzheimer's Disease Neuroimaging Initiative. Dissecting pathogenic ApoE pathways with the ADNI dataset: The case for Reelin. *Presented at the 2011 International Conference on Alzheimer's Disease, July 16-21, 2011.*

Kim S, Swaminathan S, Inlow M, **Risacher SL**, Shen L, Foroud T, Shaw LM, Trojanowski JQ, Soares H, Weiner MW, Saykin AJ, and the Alzheimer's Disease Neuroimaging Initiative (ADNI). Influence of genetic variation on plasma proteomics in AD, MCI and controls: Pairwise gene-protein analysis in the ADNI-1 cohort. *Presented at the 2011 International Conference on Alzheimer's Disease, July 16-21, 2011.*

Swaminathan S, **Risacher SL**, Yoder KK, West JD, Shen L, Kim S, Inlow M, Foroud T, Jagust WJ, Koeppe RA, Mathis CA, Shaw LM, Trojanowski JQ, Soares H, Aisen PS, Petersen RC, Weiner MW, Saykin AJ, and the Alzheimer's Disease Neuroimaging Initiative (ADNI). *APOE* ε4 status modulates the association of plasma and cortical Aβ: Relationship of plasma Aβ and [^{11}C]PiB PET in the ADNI cohort. *Presented at the 2011 International Conference on Alzheimer's Disease, July 16-21, 2011.*

Wang Y, West JD, Magee TR, McDonald BC, **Risacher SL**, Farlow MR, Saykin AJ. Patterns of resting-state fMRI indicates compensatory effects in prodromal Alzheimer's disease. *Presented at the 2011 International Conference on Alzheimer's Disease, July 16-21, 2011.*

Swaminathan S, Shen L, **Risacher SL**, Kim S, Nho K, West JD, Foroud T, Yoder KK, Potkin SG, Huentelman MJ, Craig DW, Jagust WJ, Koeppe RA, Mathis CA, Weiner MW, Saykin AJ, and the Alzheimer's Disease Neuroimaging Initiative. Amyloid pathway-based candidate gene analysis of [^{11}C]PiB-PET in the Alzheimer's Disease Neuroimaging Initiative (ADNI) cohort. *Presented at the 60th Annual Meeting of the American Society of Human Genetics in November 2010.*

Deters K, Nho K, Swaminathan S, **Risacher SL**, Kim S, Foroud T, Shen L, Saykin AJ, and the Alzheimer's Disease Neuroimaging Initiative. Association of haplotypes of the *MAPT* gene with Alzheimer's disease and quantitative neuroimaging phenotypes. *Presented at the Annual Biomedical Research Conference for Minority Students in November 2010.*

Nho K, Shen L, Kim S, **Risacher SL**, West JD, Foroud T, Jack CR, Weiner MW, Saykin AJ (2010). Automatic prediction of conversion from mild cognitive impairment to probable Alzheimer's disease using structural magnetic resonance imaging. *AIMA Annual Symposium Proceedings*, 2010 Nov 13: 542-6.

Shen L, Qi Y, Kim S, Nho K, Wan J, **Risacher SL**, Saykin AJ, and the Alzheimer's Disease Neuroimaging Initiative. Sparse bayesian learning for identifying imaging biomarkers in AD prediction. *Presented at the 13th International Conference on Medical Image Computing and Computer Assisted Intervention in September 2010.*

Newell KL, Murrell JR, Saykin AJ, Epperson F, Gouvion C, Hineman E, Yoder KK, **Risacher SL**, Vidal RG, Farlow MR, Unverzagt FW, Ghetti B. Parieto-Occipital lobe atrophy, cotton wool plaques, and corticospinal tract degeneration associated with I229F mutation in the *Presenilin 1 g*ene. *Presented at the 17th International Congress of Neuropathology in September 2010.*

Risacher SL, Saykin AJ, Pepin S, WuDunn D, Magee TR, Englert J, Flashman LA, Pixley HS, Wishart WA, Shen L, West JD, McDonald BC, O'Neill DP, Santulli RB, Newman RW. Visual contrast sensitivity as a novel biomarker for neurodegeneration in early Alzheimer's disease, mild cognitive impairment, and older adults with cognitive complaints. *Presented at the International Conference on Alzheimer's Disease in July 2010.*

Kim S, Swaminathan S, Shen L, **Risacher SL**, Nho K, Foroud T, Shaw LM, Trojanowski JQ, Potkin SG, Huentelman MJ, Craig DW, DeChairo BM, Weiner MW, Saykin AJ, and the Alzheimer's Disease Neuroimaging Initiative. Genome-wide association study of CSF biomarkers amyloid beta 1-42, tau and tau phosphorylated at threonine 181 in the ADNI cohort. *Presented at the International Conference on Alzheimer's Disease in July 2010.*

Saykin AJ, Yoder KK, **Risacher SL**, Magee TR, McDonald BC, Zheng QH, Mock BH, Shen L, West JD, Fletcher JW, Farlow MR, Hutchins GD. Neuroinflammation and Amyloid Deposition: Concurrent [11C]PBR28 and [11C]PiB PET in patients with Alzheimer's disease, mild cognitive impairment, and older adults with cognitive complaints. *Presented at the International Conference on Alzheimer's Disease in July 2010.*

Swaminathan S, Kim S, Shen L, **Risacher SL**, Foroud T, Pankratz N, Potkin SG, Huentelman MJ, Craig DW, Weiner MW, Saykin AJ, and the Alzheimer's Disease Neuroimaging Initiative. Preliminary analysis of copy number variation in the ADNI cohort. *Presented at the International Conference on Alzheimer's Disease in July 2010.*

Unverzagt FW, Farlow MR, Gao S, Saykin AJ, Murrell JR, **Risacher SL**, Lane KA, West JD, Matthews BR, Piccardo P, Miravalle L, Vidal RG, Ghetti B. Cognition and brain structure in Gerstmann-Straussler-Scheinker disease (PRNP F198S). *Presented at the International Conference on Alzheimer's Disease in July 2010.*

Yoder KK, **Risacher SL**, Magee TR, McDonald BC, Zheng QH, Wang M, Mock BH, West JD, Shen L, Hutchins GD, Saykin AJ. Age-Related neuroinflammation in non-demented elderly adults: Preliminary findings with the TSPO ligand [^{11}C]PBR28. *Presented at the 8th International Symposium on Functional Neuroreceptor Mapping of the Living Brain in July 2010.*

Risacher SL, Shen L, Saykin AJ, West JD, Kim S, McDonald BC, and the Alzheimer's Disease Neuroimaging Initiative (2009). Volumetric, cortical thickness, and grey matter density changes on MRI over 12 months." *Alzheimer's & Dementia, 5*(4), *Supplement,* P26-27*.*

Saykin AJ, Shen L, **Risacher SL**, Kim S, Nho K, West JD, Foroud TM, and the Alzheimer's Disease Neuroimaging Initiative (2009). Genetic predictors of 12 month change in MRI hippocampal volume in the Alzheimer's Disease Neuroimaging Initiative cohort: Analysis of leading candidates from the AlzGene database. *Alzheimer's & Dementia, 5*(4), *Supplement:* P3.

Risacher SL, Sullivan J, Normandin MD, Cheng TE, Morris ED (2008). Positional repeatability of rat stereotactic head holder for small animal PET studies. *Journal of Nuclear Medicine Meeting Abstracts*. 49: 402P-b.

Saykin AJ, West JD, Shen L, Firpi HA, Wessels AM, Cannon A, **Risacher SL**, McDonald BC, and the Alzheimer's Disease Neuroimaging Initiative (2008). Hippocampal and distributed gray matter abnormalities in MCI and early AD in the ADNI baseline 1.5T MRI scans: Cross-sectional analysis and relation to verbal learning. *Alzheimer's & Dementia*, 4(4), *Suppl. 2*: T59.